

MODELLING OF THE TUBULAR FILTER PRESS PROCESS

David James Mullan

BScEng(Natal)

Submitted in fulfilment of the academic
requirements for the degree of
MScEng
in the
School of Chemical Engineering,
University of Natal, Durban.

February 2000

Abstract

The objective of this project was to develop a suitable procedure for the design, control and optimisation of the Tubular Filter Press. To this end, the following objectives were defined for this study :

- To extend or improve upon the constant pressure compressible cake filtration model, predictive solution procedure, and standard laboratory characterisation techniques required to obtain the empirical model parameters, presented in Rencken (1992).

A new generalised area contact constant pressure compressible cake filtration model was developed for both the internal cylindrical and planar filtration geometries. The model utilises a heuristically developed area contact function which relates the interparticle contact area to the solids compressive pressure within the cake. If the area contact is zero, the model reduces to the conventional point contact model as presented in Rencken (1992). The sludge used in this investigation was found to exhibit a negligible degree of area contact.

A new pseudo variable pressure solution procedure was developed, that is an extension of the constant pressure solution procedure, to account for the initial variable pressure stage of the Tubular Filter Press operation. The pseudo variable pressure solution procedure was found to account accurately for the initial filtration behaviour observed during the pressurisation period of the Tubular Filter Press. However for the normal operation of the Tubular Filter Press, the difference between the output of the pseudo variable pressure and constant pressure solution procedures, was found to be insignificant.

Wall friction in compression-permeability (C-P) cell tests was identified as a main source of error. The significance of wall friction was investigated using a specially constructed C-P cell, that enabled the transmitted pressure through the cake sample to be measured. The accuracy of the characterisation which had been corrected for the effects of wall friction, was found to improve the prediction of the filtration behaviour of the sludge significantly.

The direct shear test was identified and documented as a feasible experimental procedure to determine the coefficient of earth pressure at rest. The coefficient of earth pressure is unique to the non-planar filtration geometries. The coefficient of earth pressure at rest was determined for the sludge used in this investigation.

- To incorporate the constant pressure compressible cake filtration model and the associated predictive solution procedures into a user-friendly computer programme that will facilitate the design and optimisation of full-scale plants.

The predictive solution procedures were incorporated into the Windows 95 computer programme, COMPRESS, that can be used for any constant pressure compressible cake dead-end filtration application where the filtration geometry is planar or internal cylindrical.

A control and optimisation strategy for the continuous operation of the Tubular Filter Press has been proposed.

- To develop a regressive solution procedure, and incorporate this procedure into a user-friendly computer programme, that will enable the empirical model parameters, normally obtained from standard laboratory-scale tests, to be obtained from actual filtration data.

A regressive solution procedure was developed that utilises a direct search optimisation technique that is an extension of the COMPLEX method. The regressive solution procedure was incorporated into the Windows 95 program, REGRESS. The program utilises filtration data from any dead-end constant pressure filtration application of either planar or internal cylindrical geometry. REGRESS provides an effective means for determining the true physical or plant specific filtration characteristics of the sludge. The regressive solution procedure also enables the parameters specific to the new area contact model to be determined. The sludge characterisation obtained from regressing on filtration data was found to be a significant improvement in predicting the filtration behaviour, than the characterisation obtained from the standard non-filtration laboratory-scale methods, even after the C-P cell data had been corrected for the effects of wall friction.

The programs COMPRESS and REGRESS should greatly assist in the design, control and optimisation of the Tubular Filter Press process.

Preface

I, David James Mullan, declare that unless indicated, this dissertation is my own work and that it has not been submitted, in whole or in part, for a degree at another University or Institution.

David James Mullan

July 1999

Acknowledgements

I would like to express my thanks and appreciation to the following people and organisations for their contributions towards this investigation:

The Water Research Commission, for helping to fund this investigation.

Martin Pryor at Umgeni Water, and Theo Nyawose for his assistance during the tests on the Tubular Filter Press at Wiggins Water Works.

The workshop staff at the Department of Chemical Engineering, particularly Kelly Robertson for the construction of compression-permeability cell and planar filtration apparatus.

The head of the Department of Civil Engineering, Dr Schreiner, for permission to use the direct shear apparatus, and the workshop staff for their assistance during the direct shear tests.

My supervisor, Prof. Chris Buckley, for his advice and not worrying where I was most of the time (including Monday morning meetings), or if I would ever actually finish this investigation.

Mr C. Brouckaert for his advice and assistance.

Eden Kempthorne, for generously allowing me to use his computer, even though he needed it. Without which, this investigation would never have been completed.

My parents, for feeding me and giving me a place to stay during the final stages of this investigation.

Table of Contents

List of Figures	xii
List of Tables	xx
Nomenclature	xxiv
Chapter 1 : Introduction	1-1
1.1 Background	1-1
1.2 Project Objective	1-2
1.3 Thesis Outline	1-3
Chapter 2 : Literature Review	2-1
2.1 Advances in the Current Filtration Model	2-1
2.2 Weaknesses in the Current Filtration Model	2-1
2.3 Alternative Filtration Models	2-4
2.3.1 Two Resistance Filtration Theory	2-4
2.3.2 Single Resistance Filtration Theory	2-7
Chapter 3 : Theory for Constant Pressure Compressible Cake Filtration	3-1
3.1 Empirical Permeability and Porosity Correlations	3-1
3.2 Development of a New Generalised Area Contact Model	3-4
3.2.1 Area Contact Function	3-4
3.2.2 Relationship between Liquid and Solids Compressive Pressure	3-8
3.2.2.1 Planar Filtration	3-8
3.2.2.2 Internal Cylindrical Filtration	3-10
3.2.3 Solids Compressive Pressure and Liquid Pressure Gradients	3-12
3.2.3.1 Planar Filtration	3-13
3.2.3.2 Internal Cylindrical Filtration	3-15
3.2.4 Point-Area Compressive Pressure	3-18
3.2.4.1 Planar Filtration	3-18
3.2.4.2 Internal Cylindrical Filtration	3-19
3.2.4.3 Multiple Porosity Correlation Data	3-20
3.3 Predictive Solution Procedure	3-21
3.3.1 Constant Pressure Solution Procedure	3-21
3.3.1.1 Solids Compressive Pressure and Liquid Pressure Profiles	3-22
3.3.1.2 Mass Balances	3-24
3.3.1.3 Time Relationships	3-25
3.3.2 Development of a New Pseudo Variable Pressure Solution Procedure	3-26
3.3.2.1 Cake Growth Phase	3-27

3.3.2.2	Cake Compression Phase	3-29
3.4	Development of a Regressive Solution Procedure	3-30
3.4.1	Direct Search Technique	3-31
3.4.2	Objective Function	3-37
3.4.2.1	Time Independent Analysis	3-38
3.4.2.2	Time Dependent Analysis	3-39
3.4.3	Explicit Constraints	3-39
3.4.4	Implicit Constraints	3-40
3.4.4.1	Parameter: β	3-40
3.4.4.2	Parameter: B	3-40
3.4.4.2.1	Multiple Porosity Correlation Data	3-41
3.4.4.3	Parameter: p_{sl}	3-42
3.4.4.4	Parameter: F	3-43
3.4.4.4.1	Single Permeability Correlation Data Set	3-43
3.4.4.4.2	Multiple Permeability Correlation Data Sets	3-47
3.4.4.5	Parameter: A_0	3-47
3.4.4.6	Parameter: p_{sa}	3-47
3.5	Coefficient of Earth Pressure at Rest	3-47
3.6	Determination of Empirical Permeability and Porosity Correlation Data	3-50
3.6.1	Compression-Permeability Cell Tests	3-50
3.6.1.1	Determining Correlation Data	3-52
3.6.1.2	Approximate Correction for Side Wall Friction	3-53
3.6.2	Settling Tests	3-55
3.6.2.1	Porosity Correlation Data	3-55
3.6.2.2	Permeability Correlation Data	3-56
3.7	Aspects of Modelling Specific to the Tubular Filter Press	3-60
3.7.1	Dynamic Dead-End Internal Cylindrical Filtration	3-60
3.7.1.1	Dead-End Shear Model	3-60
3.7.1.2	Axial Pressure Profiles	3-61
3.7.1.3	Axial Feed Solids Concentration Profiles	3-62
3.7.2	Cake Recovery	3-62
3.7.2.1	Recovery due to the Action of Rollers or Hydraulic Conveyance	3-63
3.7.2.2	Recovery Function	3-63
3.8	Model Implementation	3-63
3.8.1	Predictive Solution Procedure (COMPRESS)	3-64
3.8.2	Regression Procedure (REGRESS)	3-66

Chapter 4 : Experimental Study of Compressible Cake Filtration	4-1
4.1 Determination of Solids Density	4-1
4.2 Compression - Permeability Cell Tests	4-2
4.2.1 Experimental System	4-2
4.2.2 Experimental Procedure	4-4
4.2.2.1 Assembly	4-4
4.2.2.2 Compression	4-5
4.3 Settling Tests	4-5
4.3.1 Experimental Procedure	4-6
4.3.1.1 Determination of Porosity at Low Solids Compressive Pressures	4-6
4.3.1.2 Determination of Permeability at Low Solids Compressive Pressures	4-6
4.4 Direct Shear Tests	4-6
4.4.1 Experimental System	4-6
4.4.2 Experimental Procedure	4-7
4.5 Planar Filtration Tests	4-8
4.5.1 Experimental System	4-8
4.5.2 Experimental Procedure	4-9
4.5.3 Determination of Medium Resistance	4-10
4.6 Full-Scale Plant Tests - Wiggins Water Works	4-10
4.6.1 Experimental System	4-10
4.6.2 Experimental Procedure	4-13
4.6.3 Determination of Medium Resistance	4-14
Chapter 5 : Results and Discussion	5-1
5.1 Determination of Solids Density	5-1
5.2 Results of Compression - Permeability Cell Tests	5-1
5.2.1 Standard Analysis	5-1
5.2.2 Approximate Correction for Side Wall Friction	5-3
5.2.3 Common Experimental Problems	5-7
5.3 Results of Settling Tests	5-7
5.3.1 Determination of Porosity at Low Solids Compressive Pressures	5-7
5.3.2 Determination of Permeability at Low Solids Compressive Pressures	5-8
5.4 Results of Direct Shear Tests	5-10
5.5 Results of Planar Filtration Tests	5-13
5.5.1 Determination of Medium Resistance	5-17
5.6 Result of Full-Scale Tubular Filter Press Experiments	5-17
5.6.1 Cake Recovery	5-27
5.6.2 Determination of Medium Resistance	5-31
5.7 Permeability and Porosity Correlations : Standard Laboratory Sludge Characterisation	5-32

5.7.1	Wall Friction in C-P Cell Tests Neglected	5-33
5.7.2	Wall Friction in C-P Cell Tests Accounted	5-33
5.8	Comparison between Filtration Model and Filtration Experiments : Standard Laboratory Characterisation	5-33
5.8.1	Planar Filtration Experiments	5-34
5.8.2	Tubular Filter Press Experiments	5-47
5.9	Regression Analysis	5-61
5.9.1	Evaluation of the Regressive Solution Procedure	5-61
5.9.1.1	Time Independent Analysis	5-62
5.9.1.2	Time Dependent Analysis	5-62
5.9.1.3	Combined Analysis	5-62
5.9.2	Experimental Data	5-63
5.9.3	The Effect of Inaccuracies in Experimental Data	5-64
5.9.3.1	Cake Loss	5-64
5.9.3.1.1	Time Independent Analysis	5-65
5.9.3.1.2	Time Dependent Analysis	5-68
5.9.3.2	Filtrate Flow Rate	5-69
5.9.3.3	Cake Compressibility	5-71
5.9.3.4	Miscellaneous Factors	5-72
5.9.4	Results of Regression Analysis	5-72
5.9.4.1	Planar Filtration Experiments	5-73
5.9.4.2	Tubular Filter Press	5-81
5.10	Optimisation and Control of the Tubular Filter Press	5-91
5.11	Evaluation of New Area Contact Model	5-92
5.12	Effects of Instantaneous Cake Equilibrium Assumption	5-96
Chapter 6 : Conclusion		6-1
References		
Appendices		
Appendix A : Physical Properties of Solid-Liquid System		A-1
A.1	Solids Density	A-1
A.2	Liquid Density	A-1
A.3	liquid Viscosity	A-1
Appendix B : Results of Compression-Permeability Cell Tests		B-1
B.1	Result of C-P Cell Test B.1	B-1
B.2	Result of C-P Cell Test B.2	B-2

Appendix C : Results of Settling Tests	C-1
C.1 Results of Settling Tests to determine Porosity at Low Solids Compressive Pressure	C-1
C.1.1 Result of Settling Test C.1	C-1
C.1.2 Result of Settling Test C.2	C-2
C.1.3 Result of Settling Test C.3	C-2
C.2 Results of Settling Tests to determine Permeability at Low Solids Compressive Pressure	C-3
C.2.1 Result of Settling Test C.4	C-3
C.2.2 Result of Settling Test C.5	C-4
C.2.3 Result of Settling Test C.6	C-4
C.2.4 Result of Settling Test C.7	C-5
C.2.5 Result of Settling Test C.8	C-5
C.2.6 Result of Settling Test C.9	C-6
C.2.7 Result of Settling Test C.10	C-6
C.2.8 Result of Settling Test C.11	C-7
C.2.9 Result of Settling Test C.12	C-7
C.2.10 Combined Results of Settling Tests	C-8
Appendix D : Results of Direct Shear Tests	D-1
D.1 Results of Direct Shear Test D.1	D-1
D.2 Results of Direct Shear Test D.2	D-4
D.3 Results of Direct Shear Test D.3	D-7
Appendix E : Results of Planar Filtration Experiments	E-1
E.1 Results of Planar Filtration Experiments at an Applied Pressure of 100 kpa	E-1
E.1.1 Experiment E.1.1	E-1
E.1.2 Experiment E.1.2	E-2
E.1.3 Experiment E.1.3	E-3
E.1.4 Experiment E.1.4	E-5
E.1.5 Experiment E.1.5	E-7
E.1.6 Experiment E.1.6	E-9
E.2 Results of Planar Filtration Experiments at an Applied Pressure of 200 kpa	E-11
E.2.1 Experiment E.2.1	E-11
E.2.2 Experiment E.2.2	E-12
E.2.3 Experiment E.2.3	E-13
E.2.4 Experiment E.2.4	E-15
E.2.5 Experiment E.2.5	E-17
E.2.6 Experiment E.2.6	E-19
E.3 Results of Planar Filtration Experiments at an Applied Pressure of 300 kpa	E-21
E.3.1 Experiment E.3.1	E-21

H.1.1.2 Plant Specifications	H-1
H.1.1.3 Sludge Characterisation	H-1
H.1.1.4 Calculation Parameters	H-2
H.1.1.5 Operating Conditions	H-2
H.1.2 Programme Output : COMPRESS	H-2
H.1.2.1 100 kPa, 600 s	H-2
H.1.2.2 100 kPa, 1200 s	H-2
H.1.2.3 300 kPa, 600 s	H-2
H.1.2.4 300 kPa, 1200 s	H-2
H.2 Regression Analysis	H-4
H.2.1 Programme Input : REGRESS	H-4
H.2.1.1 Search Specifications	H-4
H.2.1.2 Correlation Data	H-4
H.2.1.3 Explicit Parameter Bounds	H-4
H.2.1.4 Experimental Data	H-5
H.3 Results of Regression Analysis	H-5
H.3.1 Time Independent Analysis	H-6
H.3.2 Time Dependent Analysis	H-8
H.3.3 Combined Analysis	H-10
Appendix I : Results of Regression Analysis on Planar and Tubular Filter Press Filtration Data	I-1
I.1 Programme Input : REGRESS	I-1
I.1.1 Search Specifications	I-1
I.1.2 Correlation Data	I-1
I.1.3 Explicit Parameter Bounds	I-1
I.1.3.1 Planar Filtration	I-2
I.1.3.2 Tubular Filter Press	I-2
I.1.4 Experimental Data	I-2
I.1.4.1 Planar Filtration	I-2
I.1.4.2 Tubular Filter Press	I-3
I.1.5 Calculation Parameters	I-3
I.2 Results of Regression Analysis	I-4
I.2.1 Planar Filtration	I-4
I.2.2 Tubular Filter Press	I-4

List of Figures

FIGURE 3.1	: Representation of Contact Between Particles in a Filter Cake	3-4
FIGURE 3.2	: Relationship between the Porosity, Particle Orientation and Interparticle Contact Area in a Filter Cake	3-7
FIGURE 3.3	: Force Balance on a Planar Differential Element of Cake	3-9
FIGURE 3.4	: Force Balance on an Internal Cylindrical Differential Element of Cake	3-11
FIGURE 3.5	: Lateral Force on Internal Cylindrical Differential Element of Cake Resolved into Components	3-11
FIGURE 3.6	: Intersection of Porosity Correlation Data Showing an Inconsistency with Regard to the Applicability of the Area Contact Model	3-21
FIGURE 3.7	: Flow Chart of Modified Complex Method	3-32
FIGURE 3.8	: Force Balance on Differential Element of Cake inside the C-P Cell	3-53
FIGURE 3.9	: Relationship Between Height of Sediment and Volume of Dry Solids per Unit Area	3-55
FIGURE 3.10	: Settling Regimes for a Slurry	3-57
FIGURE 3.11	: Up-Flow of Liquid through Differential Element of Slurry due to Liquid Pressure Gradient	3-58
FIGURE 3.12	: Forces Exerted on Differential Element of Slurry	3-59
FIGURE 4.1	: Schematic Diagram of Compression-Permeability Cell	4-2
FIGURE 4.2	: Process Schematic of Compression-Permeability Cell	4-3
FIGURE 4.3	: Schematic Diagram of Direct Shear Box	4-7
FIGURE 4.4	: Schematic Diagram of Planar Filtration Cell	4-9
FIGURE 4.5	: Schematic Diagram of Tubular Filter Press at Wiggins Water Works	4-10
FIGURE 5.1	: Permeability versus Solids Compressive Pressure for the C-P Cell Experiments	5-2
FIGURE 5.2	: Solids Volume Fraction versus Solids Compressive Pressure the for C-P Experiments	5-2
FIGURE 5.3	: Results of Wall Friction Analysis for Experiment B.1	5-4
FIGURE 5.4	: Results of Wall Friction Analysis for Experiment B.2	5-4
FIGURE 5.5	: Permeability versus Corrected Solids Compressive Pressure for C-P Cell Experiments	5-5
FIGURE 5.6	: Solids Volume Fraction versus Corrected Solids Compressive Pressure for C-P Cell Experiments	5-6
FIGURE 5.7	: Equilibrium Settling Heights of Sediment versus Volume of Solids per Unit Area	5-8
FIGURE 5.8	: Initial Settling Velocity of the Sediment Surface versus Initial Porosity of the Suspension	5-9

FIGURE 5.9	: Permeability versus Solids Compressive Pressure for Settling Experiments	5-9
FIGURE 5.10	: Horizontal Shear Force versus Horizontal Shear Displacement for Direct Shear Test D.1	5-10
FIGURE 5.11	: Horizontal Shear Force versus Horizontal Shear Displacement for Direct Shear Test D.2	5-11
FIGURE 5.12	: Horizontal Shear Force versus Horizontal Shear Displacement for Direct Shear Test D.3	5-11
FIGURE 5.13	: Relationship between Maximum Horizontal Shear Stress and Normal Stress for Direct Shear Tests	5-12
FIGURE 5.14	: Effect of Filtration Pressure on Filtrate Volume for Planar Filtration Experiments E.1.6, E.2.6, E.3.6 and E.4.6	5-13
FIGURE 5.15	: Filtrate Volume versus Time for Planar Filtration Experiments at an Applied Pressure of 100 kPa	5-14
FIGURE 5.16	: Filtrate Volume versus Time for Planar Filtration Experiments at an Applied Pressure of 200 kPa	5-14
FIGURE 5.17	: Filtrate Volume versus Time for Planar Filtration Experiments at an Applied Pressure of 300 kPa	5-15
FIGURE 5.18	: Filtrate Volume versus Time for Planar Filtration Experiments at an Applied Pressure of 400 kPa	5-15
FIGURE 5.19	: Effect of Filtration Pressure on Average Cake Dry Solids Concentration for Planar Filtration Experiments	5-16
FIGURE 5.20	: Effect of Filtration Pressure on Calculated Cake Thickness for Planar Filtration Experiments	5-17
FIGURE 5.21	: Gauge Pressure Readings for Experiment F.2	5-18
FIGURE 5.22	: Feed Volume Readings for Experiment F.2	5-18
FIGURE 5.23	: Feed Flow Rate Profile for Experiment F.2	5-19
FIGURE 5.24	: Vertical Orientation of the Tube Curtain with respect to the Feed Pump	5-21
FIGURE 5.25	: Pressurisation Profiles for Experiments Conducted at Operating Pressures of Approximately 200 kPa	5-22
FIGURE 5.26	: Pressurisation Profiles for Experiments Conducted at Operating Pressures of Approximately 300 kPa	5-23
FIGURE 5.27	: Pressurisation Profiles for Experiments Conducted at Operating Pressures of Approximately 400 kPa	5-23
FIGURE 5.28	: Filtrate Volume Profiles for Experiments Conducted at Operating Pressures of Approximately 200 kPa	5-22
FIGURE 5.29	: Filtrate Volume Profiles for Experiments Conducted at Operating Pressures of Approximately 300 kPa	5-24
FIGURE 5.30	: Filtrate Volume Profiles for Experiments Conducted at Operating Pressures of Approximately 400 kPa	5-25

FIGURE 5.31	: Average Cake Dry Solids Concentration Profiles for Experiments Conducted at Operating Pressures of Approximately 200 kPa	5-26
FIGURE 5.32	: Average Cake Dry Solids Concentration Profiles for Experiments Conducted at Operating Pressures of Approximately 300 kPa	5-26
FIGURE 5.33	: Average Cake Dry Solids Concentration Profiles for Experiments Conducted at Operating Pressures of Approximately 400 kPa	5-27
FIGURE 5.34	: Average Cake Dry Solids Concentration of Screened Cake Samples	5-27
FIGURE 5.35	: Effect of Feed Solids Concentration on Cake Recovery	5-28
FIGURE 5.36	: Effect of Final Filtration Time on Cake Recovery	5-29
FIGURE 5.37	: Effect of Filtration Pressure on Cake Recovery	5-29
FIGURE 5.38	: Effect of Approximate Total Mass Wet Cake on Cake Recovery	5-30
FIGURE 5.39	: Comparison between Experimental and Predicted Filtrate Volumes for Planar Filtration at 100 kPa using the Laboratory Sludge Characterisation	5-34
FIGURE 5.40	: Comparison between Experimental and Predicted Filtrate Volumes for Planar Filtration at 200 kPa using the Laboratory Sludge Characterisation	5-35
FIGURE 5.41	: Comparison between Experimental and Predicted Filtrate Volumes for Planar Filtration at 300 kPa using the Laboratory Sludge Characterisation	5-35
FIGURE 5.42	: Comparison between Experimental and Predicted Filtrate Volumes for Planar Filtration at 400 kPa using the Laboratory Sludge Characterisation	5-36
FIGURE 5.43	: Comparison between Experimental and Predicted Average Cake Dry Solids Concentrations for Planar Filtration at 100 kPa using the Laboratory Sludge Characterisation	5-36
FIGURE 5.44	: Comparison between Experimental and Predicted Average Cake Dry Solids Concentrations for Planar Filtration at 200 kPa using the Laboratory Sludge Characterisation	5-37
FIGURE 5.45	: Comparison between Experimental and Predicted Average Cake Dry Solids Concentrations for Planar Filtration at 300 kPa using the Laboratory Sludge Characterisation	5-37
FIGURE 5.46	: Comparison between Experimental and Predicted Average Cake Dry Solids Concentrations for Planar Filtration at 400 kPa using the Laboratory Sludge Characterisation	5-38
FIGURE 5.47	: Comparison between Experimental and Predicted Cake Thickness for Planar Filtration at 100 kPa using the Laboratory Sludge Characterisation	5-38
FIGURE 5.48	: Comparison between Experimental and Predicted Cake Thickness for Planar Filtration at 200 kPa using the Laboratory Sludge Characterisation	5-39
FIGURE 5.49	: Comparison between Experimental and Predicted Cake Thickness for Planar Filtration at 300 kPa using the Laboratory Sludge Characterisation	5-39
FIGURE 5.50	: Comparison between Experimental and Predicted Cake Thickness for Planar Filtration at 400 kPa using the Laboratory Sludge Characterisation	5-40

FIGURE 5.51	: Calculated Solids Compressive Pressure Profile through Planar Filtration Cake Characterised by Equations 5.7	5-41
FIGURE 5.52	: Calculated Cake Solids Concentration and Porosity Profile through Planar Filtration Cake Characterised by Equations 5.7	5-42
FIGURE 5.53	: Rheological Property Profiles through Planar Filtration Cake Characterised by Equations 5.7	5-45
FIGURE 5.54	: Effect of Cake Loss on Predicted Average Cake Dry Solids Concentration for Planar Filtration Cake Characterised by Equations 5.7	5-46
FIGURE 5.55	: Effect of Cake Loss on Predicted Cake Thickness for Planar Filtration Cake Characterised by Equations 5.7	5-46
FIGURE 5.56	: Comparison between Experimental and Predicted Filtrate Volume Profiles for the Tubular Filter Press Experiment F.1 using Laboratory Sludge Characterisation	5-48
FIGURE 5.57	: Comparison between Experimental and Predicted Filtrate Volume Profiles for the Tubular Filter Press Experiment F.2 using Laboratory Sludge Characterisation	5-48
FIGURE 5.58	: Comparison between Experimental and Predicted Filtrate Volume Profiles for the Tubular Filter Press Experiment F.3 using Laboratory Sludge Characterisation	5-49
FIGURE 5.59	: Comparison between Experimental and Predicted Filtrate Volume Profiles for the Tubular Filter Press Experiment F.4 using Laboratory Sludge Characterisation	5-49
FIGURE 5.60	: Comparison between Experimental and Predicted Filtrate Volume Profiles for the Tubular Filter Press Experiment F.5 using Laboratory Sludge Characterisation	5-50
FIGURE 5.61	: Comparison between Experimental and Predicted Filtrate Volume Profiles for the Tubular Filter Press Experiment F.6 using Laboratory Sludge Characterisation	5-50
FIGURE 5.62	: Comparison between Experimental and Predicted Filtrate Volume Profiles for the Tubular Filter Press Experiment F.7 using Laboratory Sludge Characterisation	5-51
FIGURE 5.63	: Comparison between Experimental and Predicted Filtrate Volume Profiles for the Tubular Filter Press Experiment F.8 using Laboratory Sludge Characterisation	5-51
FIGURE 5.64	: Comparison between Experimental and Predicted Filtrate Volume Profiles for the Tubular Filter Press Experiment F.9 using Laboratory Sludge Characterisation	5-52

FIGURE 5.65	: Comparison between Experimental and Predicted Filtrate Volume Profiles for the Tubular Filter Press Experiment F.10 using Laboratory Sludge Characterisation	5-52
FIGURE 5.66	: Predicted Cake Thickness Profiles for Experiment F.2	5-54
FIGURE 5.67	: Comparison between Experimental and Predicted Average Cake Dry Solids Concentration for the Tubular Filter Press Experiment F.1 using the Laboratory Sludge Characterisation	5-56
FIGURE 5.68	: Comparison between Experimental and Predicted Average Cake Dry Solids Concentration for the Tubular Filter Press Experiment F.2 and Experiment F.3 using the Laboratory Sludge Characterisation	5-57
FIGURE 5.69	: Comparison between Experimental and Predicted Average Cake Dry Solids Concentration for the Tubular Filter Press Experiment F.4 and Experiment F.5 using the Laboratory Sludge Characterisation	5-57
FIGURE 5.70	: Comparison between Experimental and Predicted Average Cake Dry Solids Concentration for the Tubular Filter Press Experiment F.6 using the Laboratory Sludge Characterisation	5-58
FIGURE 5.71	: Comparison between Experimental and Predicted Average Cake Dry Solids Concentration for the Tubular Filter Press Experiment F.7 and Experiment F.8 using the Laboratory Sludge Characterisation	5-58
FIGURE 5.72	: Comparison between Experimental and Predicted Average Cake Dry Solids Concentration for the Tubular Filter Press Experiment F.9 and Experiment F.10 using the Laboratory Sludge Characterisation	5-59
FIGURE 5.73	: Solids Compressive Pressure Profile through Dimensionless Internal Cylindrical Cake Thickness	5-60
FIGURE 5.74	: Calculated Solids Compressive Pressure Profile through Cake Thickness resulting from Cake Loss	5-65
FIGURE 5.75	: Calculated Porosity Profile Through Cake Thickness resulting from Cake Loss	5-66
FIGURE 5.76	: Effect of Filtrate Flow Rate on Calculated Cake Pressure Drop	5-69
FIGURE 5.77	: Effect of Filtrate Flow Rate on Calculated Porosity Profile	5-70
FIGURE 5.78	: Comparison between Incompressible and Highly Compressible Solids Compressive Pressure Profiles	5-71
FIGURE 5.79	: Comparison between Experimental and Predicted Filtrate Volumes for Planar Filtration at 100 kPa using the Regression Sludge Characterisation	5-74
FIGURE 5.80	: Comparison between Experimental and Predicted Filtrate Volumes for Planar Filtration at 200 kPa using the Regression Sludge Characterisation	5-75
FIGURE 5.81	: Comparison between Experimental and Predicted Filtrate Volumes for Planar Filtration at 300 kPa using the Regression Sludge Characterisation	5-75

FIGURE 5.82	: Comparison between Experimental and Predicted Filtrate Volumes for Planar Filtration at 400 kPa using the Regression Sludge Characterisation	5-76
FIGURE 5.83	: Comparison between Experimental and Predicted Average Cake Dry Solids Concentrations for Planar Filtration at 100 kPa using the Regression Sludge Characterisation	5-76
FIGURE 5.84	: Comparison between Experimental and Predicted Average Cake Dry Solids Concentrations for Planar Filtration at 200 kPa using the Regression Sludge Characterisation	5-77
FIGURE 5.85	: Comparison between Experimental and Predicted Average Cake Dry Solids Concentrations for Planar Filtration at 300 kPa using the Regression Sludge Characterisation	5-77
FIGURE 5.86	: Comparison between Experimental and Predicted Average Cake Dry Solids Concentrations for Planar Filtration at 400 kPa using the Regression Sludge Characterisation	5-78
FIGURE 5.87	: Comparison between Experimental and Predicted Cake Thickness for Planar Filtration at 100 kPa using the Regression Characterisation	5-78
FIGURE 5.88	: Comparison between Experimental and Predicted Cake Thickness for Planar Filtration at 200 kPa using the Regression Characterisation	5-79
FIGURE 5.89	: Comparison between Experimental and Predicted Cake Thickness for Planar Filtration at 300 kPa using the Regression Characterisation	5-79
FIGURE 5.90	: Comparison between Experimental and Predicted Cake Thickness for Planar Filtration at 400 kPa using the Regression Characterisation	5-80
FIGURE 5.91	: Comparison between Experimental and Predicted Filtrate Volume Profiles for the Tubular Filter Press for Experiment F.1 using the Plant Specific Characterisation	5-83
FIGURE 5.92	: Comparison between Experimental and Predicted Filtrate Volume Profiles for the Tubular Filter Press for Experiment F.2 using the Plant Specific Characterisation	5-83
FIGURE 5.93	: Comparison between Experimental and Predicted Filtrate Volume Profiles for the Tubular Filter Press for Experiment F.3 using the Plant Specific Characterisation	5-84
FIGURE 5.94	: Comparison between Experimental and Predicted Filtrate Volume Profiles for the Tubular Filter Press for Experiment F.4 using the Plant Specific Characterisation	5-84
FIGURE 5.95	: Comparison between Experimental and Predicted Filtrate Volume Profiles for the Tubular Filter Press for Experiment F.5 using the Plant Specific Characterisation	5-85

FIGURE 5.96	: Comparison between Experimental and Predicted Filtrate Volume Profiles for the Tubular Filter Press for Experiment F.6 using the Plant Specific Characterisation	5-85
FIGURE 5.97	: Comparison between Experimental and Predicted Filtrate Volume Profiles for the Tubular Filter Press for Experiment F.7 using the Plant Specific Characterisation	5-86
FIGURE 5.98	: Comparison between Experimental and Predicted Filtrate Volume Profiles for the Tubular Filter Press for Experiment F.8 using the Plant Specific Characterisation	5-86
FIGURE 5.99	: Comparison between Experimental and Predicted Filtrate Volume Profiles for the Tubular Filter Press for Experiment F.9 using the Plant Specific Characterisation	5-87
FIGURE 5.100	: Comparison between Experimental and Predicted Filtrate Volume Profiles for the Tubular Filter Press for Experiment F.10 using the Plant Specific Characterisation	5-87
FIGURE 5.101	: Comparison between Experimental and Predicted Average Cake Dry Solids Concentration for the Tubular Filter Press Experiment F.1 using the Plant Specific Characterisation	5-88
FIGURE 5.102	: Comparison between Experimental and Predicted Average Cake Dry Solids Concentration for the Tubular Filter Press Experiment F.2 and Experiment F.3 using the Plant Specific Characterisation	5-89
FIGURE 5.103	: Comparison between Experimental and Predicted Average Cake Dry Solids Concentration for the Tubular Filter Press Experiment F.4 and Experiment F.5 using the Plant Specific Characterisation	5-89
FIGURE 5.104	: Comparison between Experimental and Predicted Average Cake Dry Solids Concentration for the Tubular Filter Press Experiment F.6 using the Plant Specific Characterisation	5-90
FIGURE 5.105	: Comparison between Experimental and Predicted Average Cake Dry Solids Concentration for the Tubular Filter Press Experiment F.7 and Experiment F.8 using the Plant Specific Characterisation	5-90
FIGURE 5.106	: Comparison between Experimental and Predicted Average Cake Dry Solids Concentration for the Tubular Filter Press Experiment F.9 and Experiment F.10 using the Plant Specific Characterisation	5-91
FIGURE 5.107	: Schematic Diagram of the Continuous Tubular Filter Press Process at Wiggins Water Works	5-92
FIGURE 5.108	: Comparison between output of Point Contact and Area Contact Filtration Models using Sludge Characterisation given by Equations 5.7	5-93

FIGURE 5.109	: Comparison between Calculated Solids Compressive Pressure Profiles using the Point Contact and Area Contact Filtration Models and the Sludge Characterisation given by Equations 5.7	5-94
FIGURE 5.110	: Comparison between Calculated Porosity Profiles using the Point Contact and Area Contact Filtration Models and the Sludge Characterisation given by Equations 5.7	5-95
FIGURE 5.111	: Area Contact through Cake Characterised by Equations 5.7	5-95

List of Tables

TABLE 5.1	: Linear Regression Analysis on Permeability Data for C-P Cell Experiments B.1 and B.2 Combined	5-3
TABLE 5.2	: Linear Regression Analysis on Porosity Data for C-P Cell Experiments B.1 and B.2 Combined	5-3
TABLE 5.3	: Wall Friction Model Parameters for C-P Cell Experiments B.1 and B.2	5-4
TABLE 5.4	: Linear Regression Analysis on Permeability Data for C-P Cell Experiments B.1 and B.2 Combined and the Corrected Solids Compressive Pressure	5-6
TABLE 5.5	: Linear Regression Analysis on Porosity Data for C-P Cell Experiments B.1 and B.2 Combined and the Corrected Solids Compressive Pressure	5-6
TABLE 5.6	: Maximum Horizontal Shear Stress and Normal Stress Data for Direct Shear Tests	5-12
TABLE 5.7	: Average Values of the Average Cake Dry Solids Concentrations at each Applied Pressure for the Constant Pressure Planar Filtration Experiments	5-16
TABLE 5.8	: Tube Filling Time and Tube Filling Volume and Average Initial Feed Flow Rate for Tubular Filter Press Experiments	5-20
TABLE 5.9	: Relationship between Recovery and Key Operational Variables	5-31
TABLE 5.10	: Quantitative Assessment of the Agreement between the Planar Filtration Experiments and the Model Output using Equations 5.6	5-40
TABLE 5.11	: Quantitative Assessment of the Agreement between the Planar Filtration Experiments and the Model Output using Equations 5.7	5-41
TABLE 5.12	: Maximum Limiting Cake Loss with respect to Filtration Pressure	5-47
TABLE 5.13	: Quantitative Assessment of the Agreement between the Tubular Filter Press Experiments and the Model Output using Equations 5.6	5-54
TABLE 5.14	: Quantitative Assessment of the Agreement between the Tubular Filter Press Experiments and the Model Output using Equations 5.7	5-55
TABLE 5.15	: Results of Time Independent Regression Analysis on Planar Filtration Experimental Data	5-67
TABLE 5.16	: Variation of Calculated Cake Pressure Drop the Average Porosity and the Time Independent Components of the Objective Function with Filtrate Flow Rate	5-71
TABLE A.1	: Results of Experiments to determine the Solids Density	A-1
TABLE B.1	: Results of C-P Cell Test B.1	B-1
TABLE B.2	: Results of Wall Friction Analysis for C-P Cell Test B.1	B-2
TABLE B.3	: Result of C-P Cell Test B.2	B-2
TABLE B.4	: Result of Wall Friction Analysis for C-P Cell Test B.2	B-3
TABLE C.1	: Result of Porosity Settling Test C.1	C-1

TABLE C.2	: Result of Porosity Settling Test C.2	C-2
TABLE C.3	: Result of Porosity Settling Test C.3	C-2
TABLE C.4	: Result of Permeability Settling Test C.4	C-3
TABLE C.5	: Result of Permeability Settling Test C.5	C-4
TABLE C.6	: Result of Permeability Settling Test C.6	C-4
TABLE C.7	: Result of Permeability Settling Test C.7	C-5
TABLE C.8	: Result of Permeability Settling Test C.8	C-5
TABLE C.9	: Result of Permeability Settling Test C.9	C-6
TABLE C.10	: Result of Permeability Settling Test C.10	C-6
TABLE C.11	: Result of Permeability Settling Test C.11	C-7
TABLE C.12	: Result of Permeability Settling Test C.12	C-7
TABLE C.13	: Combined Results of Permeability Settling Tests to determine the Settling Regimes of the Slurry	C-8
TABLE C.14	: Relationship between Permeability, Initial Slurry Porosity and Solids Compressive Pressure for Slurry in the Consolidation Settling Regime	C-8
TABLE D.1	: Result of Day 1 of Direct Shear Test D.1	D-1
TABLE D.2	: Result of Day 2 of Direct Shear Test D.1	D-2
TABLE D.3	: Result of Day 3 of Direct Shear Test D.1	D-2
TABLE D.4	: Result of Day 4 of Direct Shear Test D.1	D-3
TABLE D.5	: Result of Day 5 of Direct Shear Test D.1	D-3
TABLE D.6	: Result of Day 6 of Direct Shear Test D.1	D-4
TABLE D.7	: Result of Day 1 of Direct Shear Test D.2	D-4
TABLE D.8	: Result of Day 2 of Direct Shear Test D.2	D-5
TABLE D.9	: Result of Day 3 of Direct Shear Test D.2	D-5
TABLE D.10	: Result of Day 4 of Direct Shear Test D.2	D-6
TABLE D.11	: Result of Day 5 of Direct Shear Test D.2	D-6
TABLE D.12	: Result of Day 6 of Direct Shear Test D.2	D-7
TABLE D.13	: Result of Day 1 of Direct Shear Test D.3	D-7
TABLE D.14	: Result of Day 2 of Direct Shear Test D.3	D-8
TABLE D.15	: Result of Day 3 of Direct Shear Test D.3	D-8
TABLE D.16	: Result of Day 4 of Direct Shear Test D.3	D-9
TABLE D.17	: Result of Day 5 of Direct Shear Test D.3	D-9
TABLE D.18	: Result of Day 6 of Direct Shear Test D.3	D-10
TABLE E.1	: Result of Planar Filtration Experiment E.1.1	E-1
TABLE E.2	: Result of Planar Filtration Experiment E.1.2	E-2
TABLE E.3	: Result of Planar Filtration Experiment E.1.3	E-3
TABLE E.4	: Result of Planar Filtration Experiment E.1.4	E-5
TABLE E.5	: Result of Planar Filtration Experiment E.1.5	E-7
TABLE E.6	: Result of Planar Filtration Experiment E.1.6	E-9

TABLE E.7	: Result of Planar Filtration Experiment E.2.1	E-11
TABLE E.8	: Result of Planar Filtration Experiment E.2.2	E-12
TABLE E.9	: Result of Planar Filtration Experiment E.2.3	E-13
TABLE E.10	: Result of Planar Filtration Experiment E.2.4	E-15
TABLE E.11	: Result of Planar Filtration Experiment E.2.5	E-17
TABLE E.12	: Result of Planar Filtration Experiment E.2.6	E-19
TABLE E.13	: Result of Planar Filtration Experiment E.3.1	E-21
TABLE E.14	: Result of Planar Filtration Experiment E.3.2	E-22
TABLE E.15	: Result of Planar Filtration Experiment E.3.3	E-23
TABLE E.16	: Result of Planar Filtration Experiment E.3.4	E-25
TABLE E.17	: Result of Planar Filtration Experiment E.3.5	E-27
TABLE E.18	: Result of Planar Filtration Experiment E.3.6	E-29
TABLE E.19	: Result of Planar Filtration Experiment E.4.1	E-31
TABLE E.20	: Result of Planar Filtration Experiment E.4.2	E-32
TABLE E.21	: Result of Planar Filtration Experiment E.4.3	E-33
TABLE E.22	: Result of Planar Filtration Experiment E.4.4	E-35
TABLE E.23	: Result of Planar Filtration Experiment E.4.5	E-37
TABLE E.24	: Result of Planar Filtration Experiment E.4.6	E-39
TABLE F.1	: Result of Tubular Filter Press Experiment F.1	F-1
TABLE F.2	: Result of Tubular Filter Press Experiment F.2	F-5
TABLE F.3	: Result of Tubular Filter Press Experiment F.3	F-6
TABLE F.4	: Result of Tubular Filter Press Experiment F.4	F-10
TABLE F.5	: Result of Tubular Filter Press Experiment F.5	F-12
TABLE F.6	: Result of Tubular Filter Press Experiment F.6	F-16
TABLE F.7	: Result of Tubular Filter Press Experiment F.7	F-18
TABLE F.8	: Result of Tubular Filter Press Experiment F.8	F-22
TABLE F.9	: Result of Tubular Filter Press Experiment F.9	F-24
TABLE F.10	: Result of Tubular Filter Press Experiment F.10	F-28
TABLE F.11	: Result of Test F.11 to determine Medium Resistance	F-31
TABLE F.12	: Result of Test F.12 to determine Medium Resistance	F-32
TABLE H.1	: Filtrate Volume versus Time Data for Pseudo Experimental Data	H-3
TABLE H.2	: Explicit Bounds of Objective Function Variables for Regression Analysis on Pseudo Experimental Data	H-5
TABLE H.3	: Results of Regression Analysis H.1	H-6
TABLE H.4	: Results of Regression Analysis H.2	H-6
TABLE H.5	: Results of Regression Analysis H.3	H-7
TABLE H.6	: Results of Regression Analysis H.4	H-7
TABLE H.7	: Results of Regression Analysis H.5	H-7
TABLE H.8	: Results of Regression Analysis H.6	H-8

TABLE H.9	: Results of Regression Analysis H.7	H-8
TABLE H.10	: Results of Regression Analysis H.8	H-9
TABLE H.11	: Reduced Objective Function Variable Space for Regression H.9	H-9
TABLE H.12	: Results of Regression Analysis H.9	H-9
TABLE H.13	: Results of Regression Analysis H.10	H-10
TABLE H.14	: Results of Regression Analysis H.11	H-10
TABLE H.15	: Results of Regression Analysis H.12	H-10
TABLE H.16	: Results of Regression Analysis H.13	H-11
TABLE I.1	: Explicit Bounds of Objective Function Variables for Regression Analysis on Planar Filtration Data	I-2
TABLE I.2	: Explicit Bounds of Objective Function Variables for Regression Analysis on Tubular Filter Press Filtration Data	I-2
TABLE I.3	: Results of Regression Analysis I.1	I-4
TABLE I.4	: Results of Regression Analysis I.2	I-4
TABLE I.5	: Results of Regression Analysis I.3	I-4
TABLE I.6	: Results of Regression Analysis I.4	I-4
TABLE I.7	: Results of Regression Analysis I.5	I-5
TABLE I.8	: Results of Regression Analysis I.6	I-5
TABLE I.9	: Results of Regression Analysis I.7	I-5

Nomenclature

<i>A</i>	= area of plane perpendicular to the direction of filtrate flow, (m ²)
<i>A_c</i>	= interparticle contact area in the plane perpendicular to the direction of filtrate flow, (m ²)
<i>A_{cell}</i>	= area of cake in C-P cell, (m ²)
<i>A₀</i>	= coefficient of area contact, (-)
<i>a</i>	= empirical constant, (-)
<i>B</i>	= empirical constant, (-)
<i>b</i>	= empirical constant, (-)
<i>C_f</i>	= average dry solids concentration of flush fluid, (m/m)
<i>C_r</i>	= average dry solids concentration of recovered cake, (m/m)
<i>C_s</i>	= average dry solids concentration of screened cake, (m/m)
<i>c</i>	= cohesive force between the side wall and the compressed cake, (Pa)
<i>D</i>	= inside diameter of the cell, (m)
<i>D_m</i>	= maximum distance between two points in the complex, (-)
<i>(D_m)_{min}</i>	= terminating condition for the maximum distance between two points in the complex, (-)
<i>d</i>	= integer number of objective function variables, (-)
<i>d_f</i>	= mean diameter of particle aggregates, (m)
<i>e</i>	= integer number of implicit constraints, (-)
<i>F</i>	= empirical constant, (-)
<i>F_s</i>	= accumulated frictional drag force on particles, (N)
<i>f</i>	= coefficient of friction, (-)
<i>f_A(...)</i>	= function, (-)
<i>f_A(...)</i>	= area contact function, (-)
<i>f_p(...)</i>	= applied variable pressure function, (Pa)
<i>G</i>	= integer number of experimental observations with endpoint data, (-)
<i>g</i>	= constant of gravitational acceleration, (m/s ²)
<i>g_i(...)</i>	= functional form of implicit constraint, (-)
<i>H</i>	= integer number of experimental observations including time dependent data, (-)
<i>H_∞</i>	= final height of sediment, (m)
<i>I</i>	= the number of experimental observations, (-)
<i>i</i>	= integer number, (-)
<i>J</i>	= integer number of time dependent data points within single experimental observation, (-)
<i>j</i>	= integer number, (-)
<i>K</i>	= permeability, (m ²)

K_i	= permeability of cake when $p_s \leq p_{si}$, (m^2)
K_0	= permeability at $p_s = 0$, (m^2)
k_0	= the coefficient of earth pressure at rest, (-)
L	= compressed equilibrium thickness of the cake, (m)
L_i	= assumed immediate cake thickness, (m)
l	= tube length or axial length of cake, (m)
l_j	= lower bound of objective function variable w_j , (-)
M	= the number of permeability correlation parameter sets, (-)
m	= mass fraction of moisture in cake, (-)
m_w	= mass wet cake, (kg)
N	= number of particles in the plane perpendicular to the direction of filtrate flow, (-)
N_a	= specified total number of attempts to replace points in complex, (-)
N_f	= feasible loop exit number, (-)
N_i	= improvement loop exit number, (-)
N_r	= required total number of points to replace in complex, (-)
n	= integer number, (-)
n_a	= current number of attempts to replace points in complex, (-)
n_f	= integer number of loops as a result of a reflected point not being feasible, (-)
n_i	= integer number of loops as a result of a reflected point not being an improvement over worst point in complex, (-)
n_r	= current number of replaced points in complex, (-)
P_{avg}	= average applied pressure over variable pressure time step, (Pa)
ΔP_c	= cake pressure drop, (Pa)
ΔP_H	= hydrostatic pressure difference between top and bottom of vertical tube, (Pa)
ΔP_m	= medium pressure drop, (Pa)
P_v	= applied pressure during pressurisation period, (Pa)
P_0	= operating pressure, (Pa)
p_A	= the applied pressure at the top of the cake, (Pa)
p_L	= liquid pressure, (Pa)
p_p	= percentage local proximity, (%)
p_s	= solids compressive pressure, (Pa)
p_{sa}	= packing orientation yield compressive pressure, (Pa)
p_{si}	= solids compressive pressure below which the permeability and porosity are assumed constant, (Pa)
p_{sf}	= solids compressive pressure corresponding to the porosity of the feed sludge, (Pa)
p_T	= transmitted pressure through the cake, (Pa)
p_v	= vertical solids pressure in the cake, (Pa)

p_a	= empirical constants, (-)
Δp_c	= hydrostatic pressure drop across cake in C-P cell, (Pa)
Q_c	= compressed filtrate flow rate, (m ³ /s)
Q_f	= volumetric flow rate of filtrate, (m ³ /s)
Q_t	= total combined filtrate flow rate, (m ³ /s)
R	= recovery, (%)
R_i	= recovery index, (kg.s ³ /m ²)
R_m	= medium resistance, (m ⁻¹)
R_r	= randomly generated number in the range [-1, 1], (-)
r	= radius, (m)
r_i	= radius at which $p_s = p_{si}$ in filter cake, (m)
r_1	= internal tube radius, (m)
r_2	= internal radius of the cake, (m)
r^2	= correlation coefficient in linear regression
s_f	= slurry feed solids concentration, (kg/m ³)
T	= the number of porosity correlation parameter sets, (-)
t	= filtration time, (s)
t_f	= final filtration time, (s)
Δt	= variable pressure time step, (s)
Δt_c	= thickness of cake in C-P cell, (m)
t_p	= pressurisation time, (s)
u_j	= upper bound of objective function variable w_j , (-)
u_l	= apparent liquid velocity relative to solids, (m/s)
V_c	= compressed filtrate volume, (m ³)
V_f	= volume of filtrate, (m ³)
V'_f	= volume of filtrate that would yield compressed representative cake structure, (m ³)
$V_l(\dots)$	= volume of liquid as a function of radius, (m ³)
V_t	= total filtrate volume, (m ³)
V_0	= initial settling velocity of surface of sediment, (m/s)
v	= volume filtrate per unit medium area, (m ³ /m ²)
W_1	= weighting factor of cake pressure drop component, (-)
W_2	= weighting factor of average porosity component, (-)
W_3	= weighting factor of filtrate volume profile component, (-)
W_4	= weighting factor of cake thickness component, (-)
\bar{w}	= vector of objective function variables, (-)
\bar{w}_h	= point in complex with the highest objective function result, (-)
\bar{w}_r	= reflected point, (-)

\overline{w}_l	= point in complex with lowest objective function value, (-)
\overline{w}_p	= point generated randomly within local percentage proximity of \overline{w}_l , (-)
\overline{w}_i	= randomly generated point within total allowable variable space, (-)
\overline{w}_0	= centroid of remaining $(k-1)$ points in complex, (-)
X	= thickness of filter cake (planar filtration), (m)
x	= distance from medium in planar filtration, (m)
x_i	= distance from filter medium to position in cake where $p_s = p_{si}$, (m)
y	= distance measured from bottom of cylinder, (m)
z	= distance from the top of the cake, (m)

Greek Symbols

a^*	= local specific cake resistance, (m/kg)
\bar{a}_{av}	= average specific cake resistance, (m/kg)
$a(\dots)$	= objective function result, (-)
β	= empirical constant, (-)
γ	= empirical constant, (-)
δ	= empirical constant, (-)
ε	= porosity, (-)
ε_{av}	= average porosity of the cake
ε'_{av}	= average porosity of compressed representative cake structure, (-)
ε_i	= porosity of cake when $p_s \leq p_{si}$, (-)
ε_{if}	= internal porosity of particle aggregates, (-)
ε_{in}	= initial porosity of suspension
ε_f	= porosity of the feed sludge, (-)
ε_0	= porosity at $p_s = 0$, (-)
ζ	= reflection coefficient, (-)
θ	= cylindrical co-ordinate, (radians)
ϑ	= cake thickness, (m)
ϑ'	= cake thickness of compressed representative cake structure, (m)
κ	= cohesion, (Pa)
λ	= empirical constant, (-)
μ_f	= liquid viscosity, (Pa.s)
ω	= boundary approach limit, (-)
ρ_{av}	= average density of sludge, (kg/m ³)
ρ_l	= liquid density, (kg/m ³)
ρ_s	= solids density, (kg/m ³)

σ	=	root-mean-squared deviation, (-)
σ_h	=	horizontal effective stress, (Pa)
σ_n	=	normal stress acting on shear plane, (Pa)
σ_v	=	vertical effective stress, (Pa)
τ	=	horizontal shear stress, (Pa)
ζ	=	standard deviation of objective function values in the complex, (-)
$(\zeta^2)_{\min}$	=	terminating condition for the standard deviation squared of objective function values within the complex, (-)
ϕ	=	angle of shearing resistance, (radians)
ϕ_s	=	volume fraction solids in feed sludge, (-)
φ	=	temperature, (°C)
ω	=	volume of dry solids per unit cross-sectional area, measured from bottom of cylinder, (m ³ /m ²)
ω_c	=	volume of cake dry solids per unit medium area, (m ³ /m ²)
ω_0	=	total volume of dry solids per unit cross sectional area, (m ²)
ρ	=	mass dry solids in cake, (kg)
ρ'	=	mass dry solids of compressed representative cake structure, (kg)
ρ^*	=	mass dry solids of a filter cake at the uncompressed cake thickness but produced at a higher applied pressure, (kg)
$\Pi_{density}$	=	local particulate density, (m ⁻³)
$\Pi_{orientation}$	=	local particle orientation, (-)
Ψ_{shape}	=	local particle shape distribution, (-)
Ψ_{size}	=	local particle size distribution, (-)

Chapter 1

Introduction

The Tubular Filter Press is a tubular configured filter press for the filtration of sludges. The operation of the Tubular Filter Press is continuous and cyclic, each cycle consisting of a filtration stage, followed by a cleaning stage. During the filtration stage, a filter cake is formed on the inside of a curtain of porous woven fabric tubes, at a constant applied pressure and dead-end filtration mode. During the cleaning stage, the applied pressure is relieved, the tubes partially collapse, and the cake is hydraulically removed from the tubes by pumping the feed sludge through the tubes, at a high flow rate. Cake removal is further facilitated by a roller cleaning carriage that constricts the tubes, whilst moving down the length of the tube curtain, and increases the local shear forces as the feed sludge is pumped through the tubes. The flakes of cake are deposited onto a porous conveyor belt, where the excess sludge is drained, before being conveyed to a cake collection bin. A full process description of the vertical Tubular Filter Press at the Umgeni Water Wiggins Water Works is given in Section 4.6.

1.1 BACKGROUND

The first application of the Tubular Filter Press was at the Umgeni Water H.D. Hill Water Works in Pietermaritzburg, which was commissioned in January 1987. The prototype unit was designed to dewater thickened clarifier waste sludge resulting from the treatment of surface water at the water treatment plant. The orientation of the tube curtain for the prototype unit was horizontal. Despite the fact that the plant operated regularly, the prototype unit at H.D. Hill was found not to be commercially viable, due to various design and operational problems. The prototype unit was part of an operating water works and not readily available for research purposes. As a result, adequate research could not be performed to optimise the process and design. The exact details and nature of the design and operational problems associated with the prototype unit are available elsewhere (Pryor and Mullan, 1998), but the main problems were due to cloth splits, tube blockages, low cake recovery, inadequate conveyor drainage, and the lack of an optimal control strategy for continuous operation.

The publication of Rencken (1992), yielded a large body of knowledge on the Tubular Filter Press. Rencken (1992), developed a model for constant pressure compressible cake filtration inside a horizontal porous tube, investigated cake recovery during the cake removal cycle of the Tubular Filter Press, and developed an unsteady-state internal cylindrical axial convection shear model for cross-flow filtration of the water works clarifier sludge. The work provided a greater understanding of the cake deposition and removal processes of the Tubular Filter Press, to assist in finding solutions to the two main problems experienced on the prototype Tubular

Filter Press, namely, tube blockages during the filtration stage, and low cake recoveries during the cleaning stage. The work however, was not applied to a full-scale plant.

In the light of difficulties experienced on the prototype unit, in order to produce a marketable product and obtain effective technology transfer, a full-scale pilot plant was needed for experimental and developmental purposes. The weaknesses that were identified in the design of the prototype unit at H.D. Hill were addressed in the design of the new pilot plant (Pryor and Mullan, 1998). The most significant difference in the new design, was a vertically mounted tube curtain, with tubes of shorter length and larger internal diameter, in order to reduce the potential for tube blockages and to assist in the cake recovery. The pilot plant was built at the Umgeni Water Wiggins Water Works in Durban, and was used to treat the combined sludge from the clarifiers and sand filter backwash. The pilot plant was commissioned in September 1995, and the technology demonstrated at the International Water Supply Association Conference. The performance of new design was also assessed (Pryor and Mullan, 1998). Tube blockages were completely eliminated in the new design, and the performance of the filter was found to be reasonable, producing cake concentrations of 20 to 32 % solids (m/m), and cake recoveries of up to 75 %. It remains to be demonstrated that the pilot-plant can be operated on a continuous basis, and effectively controlled and optimised.

1.2 PROJECT OBJECTIVE

An impediment to the exploitation and commercialisation of the Tubular Filter Press technology, is the lack of a suitable design procedure. The key mechanisms of the process have been identified (Rencken, 1992), however, due to the complexity of the mathematical model, and the rigorous numerical calculations required by the solution procedure, the filtration model has been essentially inaccessible. The filtration model must be therefore be presented in a format so that it can be easily utilised in the development of a suitable design procedure, and so that control and optimisation strategies can be developed for the continuous operation of the Tubular Filter Press, and other constant pressure compressible cake filtration applications.

Rencken (1992), documents standard laboratory characterisation techniques required to obtain the empirical parameters necessary for the filtration model. Although these tests are standard, they still require specialised equipment, are difficult to perform, lengthy, and often prone to failure. In addition, there is doubt as to the accuracy and applicability of characterisations obtained from the non-filtration standard laboratory techniques. A more immediate, reliable and accurate method for determining the empirical parameters is therefore essential to complement the design procedure, and assist in the control and optimisation of the Tubular Filter Press, particularly if the quality of the feed sludge is variable.

The objectives of this project were to :

- Extend or improve upon the constant pressure compressible cake filtration model, predictive solution procedure, and standard laboratory characterisation techniques required to obtain the empirical model parameters, presented in Rencken (1992).
- Incorporate the constant pressure compressible cake filtration model and the associated predictive solution procedure into a user-friendly computer programme that will facilitate the design and optimisation of full-scale plants.
- Develop a regressive solution procedure, and incorporate this procedure into a user-friendly computer programme, that will enable the empirical model parameters, normally obtained from standard laboratory-scale tests, to be obtained from actual filtration data.

1.3 THESIS OUTLINE

The project is introduced in **Chapter 1**, and the objectives for the project are defined. The main findings of the literature survey conducted on constant pressure compressible cake filtration, are summarised in **Chapter 2**. The mathematical filtration model and associated solution procedures are developed, and the experimental theory for constant pressure compressible cake filtration is presented, in **Chapter 3**, along with the relevant literature, which discussed in more detail. The experimental equipment and techniques for the study of compressible cake filtration are detailed in **Chapter 4**. The results of the experimental study are presented and discussed in **Chapter 5**, and the mathematical filtration model and associated solution procedures are evaluated. Conclusions and recommendations are presented in **Chapter 6**.

Chapter 2

Literature Review

The Tubular Filter Press is a novel process and with the exception of the work performed by Rencken (1992), no other comprehensive body of work exists specifically on this subject. One of the objectives of this study was to extend and/or improve upon, where necessary, the theoretical filtration model and experimental techniques for determining the empirical porosity and permeability correlation parameters, documented in Rencken (1992), for internal cylindrical constant pressure compressible cake filtration. To this end, a literature review was conducted in order to:

- determine if there had been any subsequent advances or significant improvements to the existing models and techniques documented by Rencken (1992),
- identify any weaknesses in the theoretical model or experimental techniques proposed by Rencken (1992), and
- identify and assess any alternative filtration theories that could be used to model the Tubular Filter Press.

Most of the relevant literature is not reviewed in this chapter, but presented and discussed in more detail in Chapter 3, in context and in conjunction with the development of the new generalised area contact compressible cake filtration model. In this chapter, a general overview of the results of the literature survey is presented.

2.1 ADVANCES IN THE CURRENT FILTRATION MODEL

No subsequent improvements in the constant pressure compressible cake filtration modelling techniques or the experimental techniques to determine the empirical model parameters in the permeability and porosity correlations, utilised by Rencken (1992), were identified in the literature.

2.2 WEAKNESSES IN THE CURRENT FILTRATION MODEL

A number of assumptions are made in the development of the conventional modern filtration theory which could possibly lead to problems in the wide-scale application of the filtration model developed by Rencken (1992) (i.e. solid/liquid systems other than the solid/liquid system studied by Rencken (1992)).

Equilibrium porosities and hence equilibrium cake structures are assumed to be attained instantaneously with changing solids compressive pressure during filtration. This assumption may not be valid for cohesive materials, where the solids in the cake are secondary particles.

In addition to the compression of the external interstices, there is simultaneous compression or deformation of the interfloc voids. The latter, is not only time dependent, but also affected by floc strength. No models were identified in the literature, and it seems impossible to develop a *dynamic* filtration model that can account for consolidation of filter cake structures during filtration. The effects of this assumption are discussed in Section 3.11.

The solid particles of the filter cake are assumed to be in point contact with one another. As such, the liquid pressure is effective over the entire cross-sectional area of the cake. All models identified in the literature use this assumption. The only attempt to model area contact identified in the literature was by Tiller and Huang (1961). From a force balance over a differential element of cake, they proposed the following equation relating the solids compressive pressure and liquid pressure, for the planar filtration geometry:

$$dp_s + (1 - A_c/A)dp_L = 0 \quad (2.1)$$

where A = area of plane perpendicular to the direction of filtrate flow, (m²)
 A_c = interparticle contact area in the plane perpendicular to the direction of filtrate flow, (m²)
 p_L = liquid pressure, (Pa)
 p_s = solids compressive pressure, (Pa)

In the development of the compressible cake filtration model of Tiller and Huang (1961), Equation 2.1 was not included, and the model developed further into an area contact model. The model development followed the conventional point contact assumption, $A_c/A = 0$. In the derivation of Equation 2.1, the area contact is also assumed to be constant across the differential element, this is extremely unlikely for compressible cakes where the cake structure is dependent on the solids compressive pressure through the cake. A novel, generalised area contact model is developed in Chapter 3, that can account for any area contact that may exist in filter cakes.

In conventional modern filtration theory, it is also assumed that the overall cake structure, and hence porosity and permeability, obtained in a compression-permeability cell test under a given mechanical load, is representative of the local porosity and permeability, at a point in a filter cake where the local solids compressive pressure, is equal to the mechanical load. Certain inadequacies in compression-permeability cell testing are identified and discussed in Section 3.6.1.

For incompressible cake filtration, the cake structure remains constant and the solid particles, once deposited in the cake structure, remain stationary relative to the medium. In compressible

cake filtration, as the cake thickness increases, the local cake structure at a fixed distance from the medium, begins to consolidate under an increasing local solids compressive pressure. As a result, the solid particles in a compressible cake, move towards the medium as the local porosity changes, and the cake is compressed. Shirato et al. (1969), modified D'Arcy's law (D'Arcy, 1856) for planar filtration (see Equation 3.28), to account for the relative velocity of the liquid phase with respect to the solids particles.

$$\frac{dp_L}{dx} = \frac{\mu_f \varepsilon}{K} (u_L - u_s) \quad (2.2)$$

where K = permeability, (m²)
 u_L = average pore velocity of liquid, (m/s)
 u_s = average solids velocity, (m/s)
 x = distance from medium for planar filtration, (m)
 ε = porosity, (-)
 μ_f = liquid viscosity (Pa.s)

According to Shirato et al. (1969), Equation 2.2 should be used for filtration of highly concentrated slurries where the rate of cake growth is rapid and the total filtration times are measured in tens of seconds. In terms of this definition, the slurry types used in practical applications of the Tubular Filter Press, and in this investigation, are relatively dilute and the final filtration times are well in excess of being measured in tens of seconds. The solids velocity term has therefore been excluded from the filtration model developed by Rencken (1992), and in the development of the novel generalised area contact model in Chapter 3.

In addition to the solids velocity that results from compression of the local cake structure in compressible filtration, the liquid which is initially deposited in the cake, is *squeezed* out as the porosity decreases. This will result in an increase in the liquid flow rate towards the medium. For internal cylindrical filtration, the liquid contained in an internal portion of the cake between an arbitrary radius and the internal radius of the tube, is given by:

$$V_l(r) = 2\pi l \int_r^{r_1} \varepsilon r dr \quad (2.3)$$

where l = tube length or axial length of cake, (m)
 r = radius, (m)
 r_1 = internal tube radius, (m)
 $V_l(\dots)$ = volume of liquid as a function of cake radius, (m³)

The liquid flow rate at the medium, minus the liquid flow rate into the internal portion of cake at an arbitrary radius, is equal to the rate of accumulation of liquid as is given by:

$$(Q_f)_i - (Q_f)_r = \frac{\partial V_f(r)}{\partial t} \quad (2.4)$$

where Q_f = volumetric flow rate of filtrate, (m³/s)
 t = filtration time, (s)

Differentiating Equation 2.4 with respect to radius yields:

$$\frac{\partial Q_f}{\partial r} = -2\pi r l \frac{\partial \varepsilon}{\partial t} \quad (2.5)$$

Equation 2.3 to Equation 2.5 were derived by Tiller and Yeh (1985), for external cylindrical filtration, and modified for internal cylindrical filtration by Rencken (1992). Tiller and Yeh (1985), and Rencken (1992), assumed that $\partial \varepsilon / \partial t$ is small, and therefore the liquid flow rate through the cake is independent of the radius. The assumption of a constant filtrate flow rate through the cake at any time leads to ordinary rather than complex partial differential equations in the development of the filtration model, and greatly simplifies the numerical calculations required by the solution procedure. Leu (1981), derived the full partial differential continuity equations for planar compressible cake filtration, however had difficulty in solving the full equations and had to make various simplifications.

2.3 ALTERNATIVE FILTRATION MODELS

The sludge type investigated by Rencken (1992), was found to be super-compressible, and is therefore representative of the extreme case of cake compressibility. The applicability of the internal cylindrical compressible cake filtration model developed by Rencken (1992), was found to be very good for the water works sludge he investigated. The model is general enough to successfully account for a wide range of cake compressibilities, that are likely to find application for the Tubular Filter Press. There is therefore no immediate need to find an alternative theoretical platform to model the Tubular Filter Press. However, for sake of completeness, a brief literature review of alternative modelling strategies was conducted.

2.3.1 Two Resistance Filtration Theory

Most of the models identified in the literature, including the model developed by Rencken (1992), belong the same family of *Two Resistance* models. The theory is developed in analogy with Ohm's law for two electrical resistors in series in an electrical circuit. The filter medium and the filter cake, are analogous to the two resistors in series, and the filtration pressure and filtrate flow rate are analogous to the electrical potential and current respectively.

Most filtration models identified in the literature incorporate an average specific resistance term, which is defined as follows:

$$\frac{1}{a_{av}^*} = \frac{1}{\Delta P_c} \int_0^{\Delta P_c} \frac{dp_s}{a^*} \quad (2.6)$$

where ΔP_c = cake pressure drop, (Pa)
 a^* = local specific cake resistance, (m/kg)
 a_{av}^* = average specific cake resistance, (m/kg)

The specific cake resistance is a function of the solids compressive pressure and is defined as follows:

$$a^* = \frac{1}{\rho_s(1-\varepsilon)K} \quad (2.7)$$

where ρ_s = solids density, (kg/m³)

The porosity and permeability are functions of the solids compressive pressure (see Section 3.1). Doubt has been expressed as to the validity of Equation 2.6, and it has been modified to include the effects of filtration rate (Tiller and Copper, 1960), and internal variations in liquid velocity (Tiller and Shirato, 1964). The value of the average specific cake resistance calculated from Equation 2.6, utilising compression-permeability cell data, seldom agrees with values derived from actual filtration data. The form of Equation 2.6 is also mathematically inconsistent since generally, $1/(a_{av}^*) \neq (1/a^*)_{av}$. It has also been shown (Tosun and Willis, 1982), that the specific cake resistance is not a linear transformation of porosity and permeability as given by Equation 2.7, particularly for compressible cakes. Filtration models that incorporate the average specific cake resistance term have therefore been ignored as possible theoretical alternatives for modelling the Tubular Filter Press.

Another filter press process identified in the literature, that employs the principle of filtering sludges on the inside of a vertical collapsible porous woven tube, is the Uni-flow filter (Henry et al., 1976). Henry et al. (1976), developed a model for the filtration stage of the Uni-flow filter that accounted for both the applied axial pressure distribution in the tube, due to the hydrostatic pressure head, and the compressible nature of the sludge. The model accurately predicted the axial variation in cake thickness and filtrate flux for a neutralised acid mine slurry. The orientation of the Tubular Filter Press studied by Rencken (1992), was horizontal, and as such the model developed by Henry et al. (1976), was not applicable to the horizontal Tubular Filter Press. The Uni-flow filter differs not only in the orientation of the filter tubes, but also in the cake removal and separation mechanism. The cake is removed from the tubes by

a pressure shock wave, generated by the sudden release in the tube pressure as the inlet valve at the top of the tube is closed, and the discharge valve at the bottom of the tube is opened. The cake and remaining slurry in the tubes, is dumped into a thickener and allowed to settle. Cake is drawn from the bottom of the thickener, whilst the remaining slurry is decanted and recycled with the feed sludge. For the vertical orientation of the Tubular Filter Press, there is no longer any significant difference between the filtration stage of the Tubular Filter Press, and the Uni-flow filter, and the model developed by Henry et al. (1976), could therefore be applied to the Tubular Filter Press.

The mathematical basis for the model developed by Henry et al. (1976), is the simple parabolic filtration equation developed by Ruth (1935), which is based on the concept of an average specific cake resistance in the integrated form of Equation 2.6. The model neglects the medium resistance term, and the conventional Ruth equation is given by:

$$\frac{dV_f}{dt} = \frac{A^2 P_0}{\mu_f \alpha_c^* v \rho} \quad (2.8)$$

Where P_0 = operating pressure, (kPa)
 V_f = filtrate volume, (m³)
 ρ = mass dry solids in cake, (kg)

Although not immediately applicable to the Tubular Filter Press, as the cake removal mechanism differs, the model assumes that the medium resistance is negligible. Due to the nature of the cake removal mechanism of the Uni-flow filter, it cannot be guaranteed that all of the cake will be removed by the pressure shock wave. In which case the tube may be *blinded* by residual cake, and the initial medium resistance of the tube may be significant, and perhaps variable for each subsequent filtration stage.

In the development of the model developed by Henry et al. (1976), it was assumed that the cake thickness is small compared to the internal tube radius, as a result, planar, and not internal cylindrical theory, was utilised. In addition, the porosity of cake at a fixed point along the tube, is assumed to remain constant with respect to time. As shown in Section 5.8.2, this is not true for internal cylindrical filtration. The only advantage the filtration model developed by Henry et al. (1976), has over the model developed by Rencken (1992), is that it can account for the axial pressure distribution in the tubes. As discussed in Section 3.7.1.2, provided the applied pressure is not too small, and the tubes are not very long, as is the case for practical applications of the Tubular Filter Press, the difference in the applied pressure between the top and the bottom of the tube will not be significant, and the filtration behaviour may adequately be modelled assuming a constant applied pressure equal to the average of the applied pressure along the tube. If however, the axial pressure distribution is found to be significant, the solution

procedure for the constant pressure compressible cake filtration model developed by Rencken (1992), can be extended to account for the axial pressure distribution in the tubes. The model developed by Henry et al. (1976), will not be considered for this study.

2.3.2 Single Resistance Filtration Theory

A relatively new filtration theory based upon the multiphase equations of change has been identified in the literature. Due to the mathematical complexity of this *Multiphase* theory, the exact details of this theory will not be presented here, but the basic differences in terms of the theoretical development and experimental techniques required, will be highlighted. Exact details of the theoretical development and differences between conventional filtration theory are available elsewhere (Willis and Tosun, 1980); (Willis, Collins et al., 1983); (Willis, 1983); (Tosun and Willis, 1985); (Willis, Tosun et al., 1985); (Tosun and Sahioglu, 1987); (Tosun and Willis, 1989); (Willis, Tosun et al., 1989); (Tosun, Yetis et al., 1993). The new *Single Resistance* model differs considerably from the conventional *Two Resistance* model utilised by Rencken (1992).

Generalised multiphase equations of change are developed from the fundamental concepts of the conservation of mass and momentum, using volume averaging techniques to shift from the unmeasurable microscopic local property level (i.e. within the pores of the filter cake) to the mathematically smooth, volume averaged level. These generalised expressions are then simplified by a series of assumptions that are most likely to be encountered in filtration practice, e.g. that the process is isothermal, that a single solid particulate phase is non-deformable and insoluble in a single Newtonian liquid phase etc. to obtain the set of four multiphase equations of change (a continuity and motion equation for each phase) that describe the filtration process. Once the four governing multiphase equations of change have been reduced to the one dimensional (planar) geometry, they contain six unknown functions. A determinate system requires two more equations or equivalent experimental information. Only two of the six unknown functions can be measured, the porosity profile and liquid pressure profile through the cake. These profiles are normally measured by pressure taps and electroconductive porosity probes within the filter cake, the pressure taps are connected to pressure transducers for local fluid pressure measurement and the porosity probes are designed to measure local electrical conductivity which is correlated to local porosity.

It was concluded that the new multiphase filtration theory would not be suitable as an alternative theory to model the Tubular Filter Press. No application of the theory to the internal cylindrical geometry was found in the literature, the model is mathematically rigorous and extending the model to the internal cylindrical geometry would not be trivial. The experimental techniques and equipment required in order to solve the multiphase equations of change are far more sophisticated than those required by the conventional *Two Resistance* model. The theory

is still in its infancy, and the wide-scale practical applicability of this theory still has to be proven.

The result of the literature survey indicated that there would be no immediate advantage obtained from using any alternative filtration models for the Tubular Filter Press. Various weaknesses have been identified in the filtration model and experimental techniques documented in Rencken (1992), and where possible these have been addressed in Chapter 3.

Chapter 3

Theory for Constant Pressure Compressible Cake Filtration

In this chapter a mathematical model for constant pressure compressible cake filtration is presented and the experimental techniques required to obtain the empirical parameters for the model are documented. A new generalised *area contact* model is developed that is an extension of the model used by Rencken (1992), which was based on the model developed by Tiller and Yeh (1985). A novel *pseudo variable pressure* solution procedure is developed that is an extension of the constant pressure solution procedure. The pseudo variable pressure solution procedure can account for the initial variable pressure stage experienced during full-scale constant pressure filtration applications such as the Tubular Filter Press. A novel *regressive* solution procedure is developed that can obtain the empirical permeability and porosity correlation parameters that would normally be obtained from laboratory-scale tests, and the parameters specific to the new area contact model, from filtration data. In addition, some aspects unique to the modelling of the Tubular Filter Press are discussed.

3.1 EMPIRICAL PERMEABILITY AND POROSITY CORRELATIONS

The local permeability and porosity in compressible cakes are functions of the local solids compressive pressure within the cake. In order to model compressible cake filtration, the behaviour of the local permeability and porosity with respect to solids compressive pressure must be known. The solids compressive pressure arises from the frictional drag force on the solid particles in the cake, as the filtrate flows through the cake. The solids compressive pressure is defined as the cumulative frictional drag force divided by the cake cross-sectional area perpendicular to the direction of filtrate flow. In order to *characterise* the behaviour of local permeability and porosity, empirical correlations are proposed. It is observed (Tiller and Cooper, 1962); (Tiller and Leu, 1980), that the functional relationship of the local porosity and permeability is exponential with respect to the solids compressive pressure and the two commonly accepted correlations are presented below.

Tiller and Cooper (1962), proposed the following set of equations:

$$K = Fp_s^{-\delta} \qquad p_s \geq p_{si} \qquad (3.1.a)$$

$$K = K_i = Fp_{si}^{-\delta} \qquad p_s \leq p_{si} \qquad (3.1.b)$$

$$(1 - \varepsilon) = B p_s^\beta \quad p_s \geq p_{si} \quad (3.1.c)$$

$$(1 - \varepsilon_i) = B p_{si}^\beta \quad p_s \leq p_{si} \quad (3.1.d)$$

where F, δ, B, β = empirical constants, (-)
 K = permeability, (m²)
 ε = porosity, (-)
 p_s = solids compressive pressure, (Pa)
 K_i = permeability of cake when $p_s \leq p_{si}$, (m²)
 ε_i = porosity of cake when $p_s \leq p_{si}$, (-)
 p_{si} = solids compressive pressure below which the permeability and porosity are assumed constant, (Pa)

and Tiller and Leu (1980), presented an alternative set of equations:

$$K = K_0 \left(1 - \frac{p_s}{p_a}\right)^{-\gamma} \quad (3.2.a)$$

$$(1 - \varepsilon) = (1 - \varepsilon_0) \left(1 - \frac{p_s}{p_a}\right)^\lambda \quad (3.2.b)$$

where γ, λ, p_a = empirical constants, (-)
 K_0 = permeability at $p_s = 0$, (m²)
 ε_0 = porosity at $p_s = 0$, (-)

Various standard laboratory-scale tests are performed to obtain permeability and porosity data over a range of solids compressive pressures and the parameters in the above equations are obtained by numerical regression on the data. Both the correlations above have the same number of empirical parameters.

Compression-Permeability cell (C-P cell) tests are conducted to obtain permeability and porosity data in the high solids compressive range, approximately 50 to 500 kPa. Although these tests have been used at lower pressures, reservations have been expressed on the accuracy of the data at low pressures mainly due to wall friction effects. Murase et al. (1989), proposed a centrifuge method for the determination of porosity data in the intermediate solids compressive pressure range, approximately 1 to 100 kPa. Rencken (1992), found that when the results from centrifuge tests were incorporated into the filtration model, the accuracy of the model output decreased. As such, for the purposes of this study, centrifuge tests will not be considered as an important method for obtaining data for the correlations. Shirato et al. (1983), proposed a batch settling test for the determination of permeability and porosity data in the

low solids compressive pressure range, typically below 1 kPa. These settling tests require simple and inexpensive testing equipment.

Equations 3.1 assume that the permeability and porosity are constant below some low solids compressive pressure, p_{si} . Caution should be exercised in determining the value of p_{si} since relatively small variations in the value can have marked effects on the filtrate volume versus time predictions of the filtration model. According to Tiller and Leu (1980), the location of p_{si} is entirely empirical and relatively arbitrary, since C-P cell tests are not sufficiently accurate at low solids compressive pressures to accurately determine its value. Tiller and Leu (1980), introduced Equations 3.2 to overcome this problem, by defining a permeability and porosity at a solids compressive pressure of zero. However, Shirato et al. (1983), subsequently introduced the settling method for determining permeability and porosity data at very low solids compressive pressures, which enables the location of p_{si} to be determined more accurately.

Equations 3.2 are restricted in that they are intended to be fitted over the entire range of permeability and porosity data. Equations 3.1, however, can be extended to include multiple empirical parameter sets which are valid over sections of the solids compressive pressure range. This is important because various authors (Tiller et al., 1987), have expressed reservations about the validity of these correlations for highly compressible cakes as the range over which these equations apply decreases with increasing compressibility. Rencken (1992), found that the fit between Equations 3.2 and experimental data were not good and when the regressed parameters were incorporated into the internal cylindrical filtration model the agreement between experimental data and the model predictions were poor.

The extended form of Equations 3.1 for multiple correlation parameter sets is as follows:

$$K = K_i = F_1 p_{si}^{-\delta_1} = F_1 p_{s1}^{-\delta_1} \quad p_s \leq p_{s1} \quad (3.3.a)$$

$$K = F_n p_s^{-\delta_n} \quad p_{sn} \leq p_s < p_{s(n+1)} \quad (3.3.b)$$

$$K = F_{(n+1)} p_s^{-\delta_{(n+1)}} \quad p_s \geq p_{s(n+1)} \quad (3.3.c)$$

$$(1 - \varepsilon_i) = B_1 p_{si}^{\beta_1} = B_1 p_{s1}^{\beta_1} \quad p_s \leq p_{s1} \quad (3.3.d)$$

$$(1 - \varepsilon) = B_j p_s^{\beta_j} \quad p_{sj} \leq p_s < p_{s(j+1)} \quad (3.3.e)$$

$$(1 - \varepsilon) = B_{(j+1)} p_s^{\beta_{(j+1)}} \quad p_s \geq p_{s(j+1)} \quad (3.3.f)$$

$$n \in [1, (M-1)]$$

$$j \in [1, (T-1)]$$

where $M \geq 2$ = the number of permeability correlation parameter sets, (-)
 $T \geq 2$ = the number of porosity correlation parameter sets, (-)
 n, j = integer numbers, (-)

Depending on the compressibility of the cake, there will normally be a correlation parameter set for each test type utilised, or if a test type covers a large solids compressive pressure range, the data within a test type may be subdivided and parameter sets obtained in each region. Equations 3.3 will be the basis for the constant pressure compressible cake filtration model.

3.2 DEVELOPMENT OF A NEW GENERALISED AREA CONTACT MODEL

Previously, the development of filtration models assumed that the particles of the filter cake are in *point contact* with one another and as such, the liquid pressure is effective over the entire cross-sectional area of the cake (Tiller, 1966); (Tiller and Yeh, 1985); (Rencken, 1992). The *point contact* model is however idealistic and in actual filter cakes there will be area contact between the particles, see Figure 3.1.

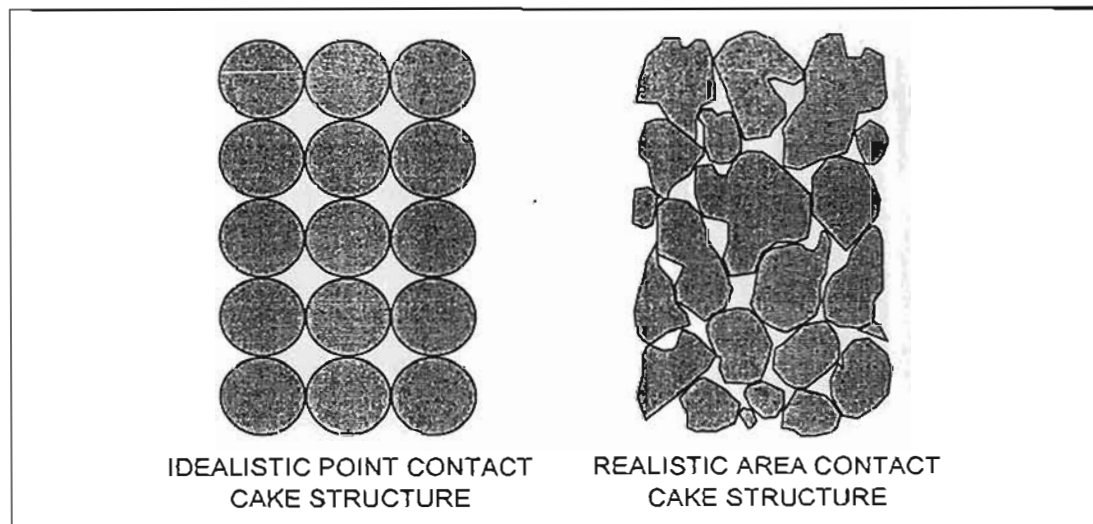


FIGURE 3.1 : Representation of Contact Between Particles in a Filter Cake

A new generalised filtration model that can account for any area contact that may exist between the solid particles in a filter cake is presented below.

3.2.1 Area Contact Function

The local interparticle contact area is a function of the local cake structure or packing of the particles within the cake. An area contact function describing the relationship between the

interparticle contact area in the plane perpendicular to the direction of filtrate flow and the cake structure is developed heuristically.

The cake structure is a function of the particle shape distribution, particle size distribution, particulate density (the number of particles present in a given volume), and the orientation of the particles with respect to one another. The interparticle contact area in the plane perpendicular to the filtrate flow direction through the cake is assumed to be given by the product of the area of this plane, and an area contact function:

$$A_c = A \times f_A(\Psi_{shape}, \Psi_{size}, \Pi_{density}, \Pi_{orientation}) \quad (3.4)$$

where

- A = area of plane perpendicular to the direction of filtrate flow, (m²)
- A_c = interparticle contact area in the plane perpendicular to the direction of filtrate flow, (m²)
- $f_A(\dots)$ = area contact function, (-)
- $\Pi_{density}$ = local particulate density, (m⁻³)
- $\Pi_{orientation}$ = local particle orientation, (-)
- Ψ_{shape} = local particle shape distribution, (-)
- Ψ_{size} = local particle size distribution, (-)

For a given particle shape and size distribution, the local particulate density is directly related to the local solids volume fraction within the cake and hence the local cake porosity. Its effect can therefore be separated from the area contact function. It is assumed that the interparticle contact area is directly proportional to the local solids volume fraction within the cake. For compressible cakes the porosity is a function of the solids compressive pressure within the cake.

$$f_A(\dots) = f'_A(\Psi_{shape}, \Psi_{size}, \Pi_{orientation}) \times [1 - \varepsilon(p_s)] \quad (3.5)$$

The direct proportionality between interparticle contact area and the local solids volume fraction, is only expected to hold for relatively high solids compressive pressures where the changes in porosity with respect to solids compressive pressure are not as pronounced, due to the more consolidated nature cake structure. At lower solids compressive pressures, small changes in solids compressive pressure can result in relatively large changes in cake porosity (and hence cake structure) and the relationship between cake porosity and area contact will be difficult to determine, but it is unlikely that it will behave proportionally as shown in Equation 3.5.

The particle shape and size distributions will have a direct and strong influence on the area contact function. Particles may be in the shape of spheres, fibres, flakes etc. or more complex shapes due to particle association (flocculation and coagulation) to form particle structures. For example, flake-like particles will exhibit greater area contact behaviour than spherical particles, and systems with a broad particle size distribution may exhibit greater area contact behaviour because the smaller particles occupy the interstices between the larger particles. For a given slurry type (ignoring the effects of small-scale solids migration), the particle shape and size distributions are assumed to be constant with respect to filtration time and distance through the cake, the area contact function can now be written as:

$$f_A(\dots) = f_A''(\Pi_{orientation}) \times [1 - \epsilon(p_s)] \quad (3.6)$$

For particles which are not symmetrical about a point (a sphere is an example of a particle that displays point symmetry), the orientation of the particles with respect to one another and the plane perpendicular to the filtrate flow direction within the cake will affect the cake structure and hence the interparticle contact area. It is assumed that the particle orientation is a function of the solids compressive pressure.

$$\Pi_{orientation} = f(p_s) \quad (3.7)$$

At the cake surface, the particles are deposited with a random orientation and the resulting cake structure is therefore random and unstable. As subsequent layers of cake are deposited, the solids compressive pressure increases. The increasing solids compressive pressure will begin to stress the underlying random cake structure and the particles will begin to realign and re-orientate themselves in such a way as to form a more uniform and stable cake structure (this includes the deformation of associated particle structures such as flocs). Substituting Equation 3.7 into Equation 3.6 yields:

$$f_A(\dots) = f_A'''(p_s) \times [1 - \epsilon(p_s)] \quad (3.8)$$

The region of the cake near the cake surface where the solids compressive pressure is low, is characterised by a cake structure which is very porous and composed of randomly orientated particles. The particles in this region will be assumed to be in point contact with one another. Only as the solids compressive pressure increases towards the septum, and the cake structure becomes more compact and the particles begin to orientate themselves will they begin to be in area contact with one another, see Figure 3.2.

For a given system, the area contact function is composed of two principle parts, the particulate density component and the particle orientation component, both of which are

functions of solids compressive pressure. The cross over from *point contact* to *area contact* may be gradual or sudden depending on the behaviour of these two components with respect to solids compressive pressure. The behaviour of the particulate density component is characterised by the functional dependence of the cake porosity, however, it is not expected to hold for low solids compressive pressures. The behaviour of the particle orientation component is difficult to ascertain and is assumed that it behaves as a step function i.e. as if the packing orientation exhibits a yield compressive stress.

$$f_A'''(p_s) = 0 \quad 0 \leq p_s \leq p_{sa} \quad (3.9.a)$$

$$f_A'''(p_s) = A_0 \quad p_s > p_{sa} \quad (3.9.b)$$

where p_{sa} = packing orientation yield compressive pressure, (Pa)

A_0 = coefficient of area contact, (-)

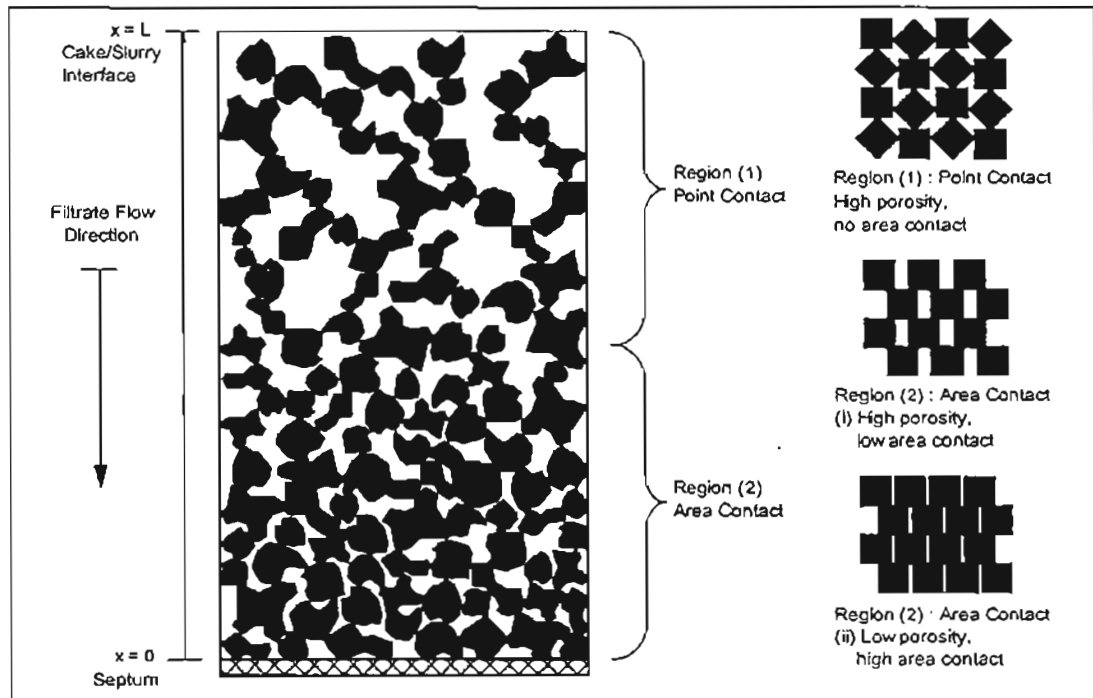


FIGURE 3.2 : Relationship between the Porosity, Particle Orientation and Interparticle Contact Area in a Filter Cake

It is also assumed that the particle density component of the area contact function holds for solids compressive pressures greater than the packing orientation yield compressive pressure, as the behaviour of the cake structure with respect to solids compressive pressure will be more predictable. As a result the packing orientation yield compressive pressure can be redefined as the *point-area* compressive pressure, and represents the solids compressive pressure at which the interparticle contact changes from point contact to area contact.

The coefficient of area contact, A_0 , is assumed to be constant for a given system. The area contact in the plane perpendicular to the direction of filtrate flow can be determined from the following set of equations:

$$A_c = 0 \qquad 0 \leq p_s \leq p_{sa} \qquad (3.10.a)$$

$$A_c = A[A_0[1 - \varepsilon(p_s)]] \qquad p_s > p_{sa} \qquad (3.10.b)$$

The area contact function states that below the point-area compressive pressure, the particles in the filter cake are in point contact with one another. Above the point-area compressive pressure, the particles begin to experience area contact, the extent of this area contact is given by the product of the local solids volume fraction and a constant area contact coefficient.

The ratio of the interparticle contact area to the area of the plane perpendicular to the filtrate flow direction is zero if the particles are in point contact with one another and has maximum possible value of 1. Since the porosity ranges from 0 to 1, the coefficient of area contact has a minimum value of 0 and a maximum value of 1.

$$A_0 = A_c/A \times 1/(1 - \varepsilon) \qquad A_0 \in [0, 1] \qquad (3.11)$$

3.2.2 Relationship between Liquid and Solids Compressive Pressure

In filtration, drag stresses arise from the interfacial transfer of momentum from the liquid to the solid particles as the liquid flows around the solid particles towards the medium in the direction of decreasing liquid pressure. The viscous drag occurs only if there is relative motion between the liquid and solids particles and is therefore zero within the slurry and at the cake-slurry interface. Since the particles are in contact with one another, the frictional drag force on the solid particles is cumulative and reaches a maximum at the medium.

The theoretical relationships between the liquid and solids compressive pressures are derived from a force balance over a differential element of cake.

3.2.2.1 Planar Filtration

For one-dimensional filtration, the plane perpendicular to the direction of filtrate flow is any plane parallel to the septum. Summing the individual particle properties over the number of particles in the plane perpendicular to the direction of filtrate flow yields (see Figure 3.3):

$$\sum_{i=1}^N A_i = A \qquad (3.12)$$

$$\sum_{i=1}^N (A_c)_i = A_c \quad (3.13)$$

$$\sum_{i=1}^N (A_c + dA_c)_i = A_c + dA_c \quad (3.14)$$

$$\sum_{i=1}^N (F_s)_i = F_s \quad (3.15)$$

$$\sum_{i=1}^N (F_s + dF_s)_i = F_s + dF_s \quad (3.16)$$

where F_s = accumulated frictional drag force on particles, (N)
 N = number of particles in the plane perpendicular to the direction of filtrate flow, (-)

A force balance over a planar differential element of cake neglecting inertial and accelerative effects, Figure 3.3, yields:

$$p_L(A - A_c) + F_s = (p_L + dp_L)(A - (A_c + dA_c)) + (F_s + dF_s) \quad (3.17)$$

where p_L = liquid pressure, (Pa)

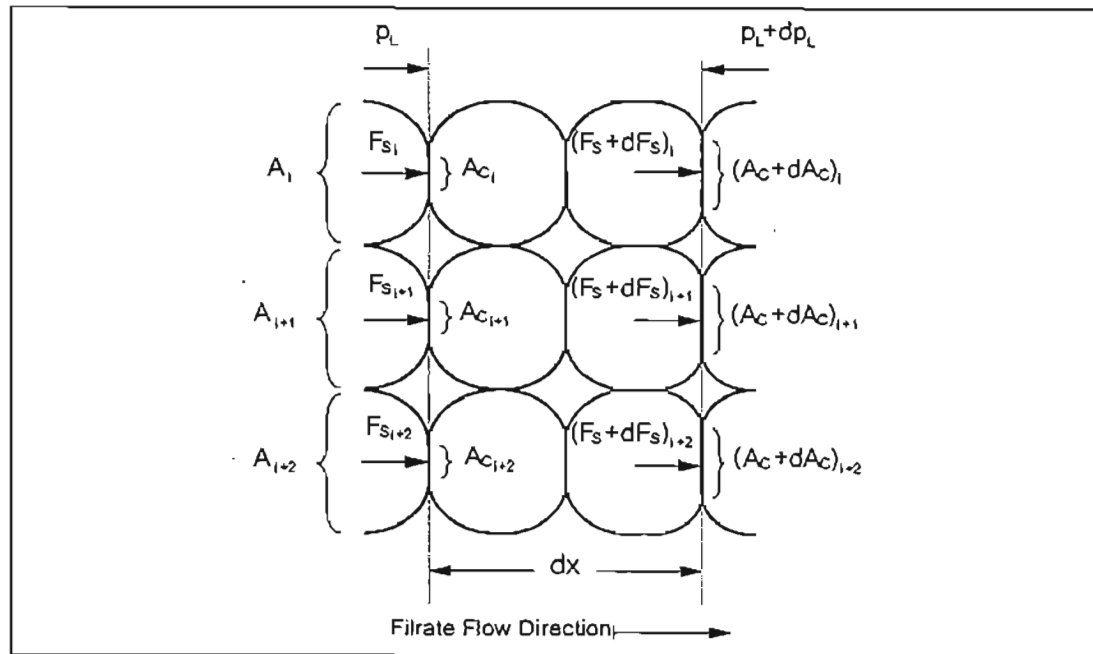


FIGURE 3.3 : Force Balance on a Planar Differential Element of Cake

The solids compressive pressure, which for planar filtration is given by the accumulated frictional drag force, divided by the cake cross-sectional area perpendicular to the direction of the filtrate flow, is defined as:

$$p_s = F_s/A \quad (3.18)$$

Combining Equation 3.18 with Equation 3.17 and simplifying, leads to:

$$dp_L(1 - A_c/A) - (p_L + dp_L)dA_c/A + dp_s = 0 \quad (3.19)$$

From Equation 3.10.b, for $p_s > p_{sa}$ we have:

$$dA_c/A = -A_0 d\epsilon \quad (3.20)$$

Substituting Equations 3.10.b and Equation 3.20 into Equation 3.19 leads to:

$$(1 - A_0 + A_0\epsilon)dp_L + A_0 p_L d\epsilon + dp_s = 0 \quad (3.21)$$

Equation 3.21 is novel. For $0 \leq p_s \leq p_{sa}$ and $A_0 = 0$ (i.e. point contact), Equation 3.21 reduces to the familiar expression relating solids compressive pressure to liquid pressure for planar filtration.

$$dp_L + dp_s = 0 \quad (3.22)$$

3.2.2.2 Internal Cylindrical Filtration

For internal cylindrical filtration, the plane perpendicular to the filtrate flow direction, is a cylindrical surface of constant radius. The set of Equations 3.12 to 3.16 are valid over this surface. Figure 3.4 shows the forces acting on a differential element of cake.

In addition to the forces acting in the radial direction, there are forces acting laterally on the sides of the element of cake. These forces arise from the liquid pressure acting on the sides of the element of cake and an effective solids force resulting from the accumulated frictional force acting on the element of cake in the radial direction (see Section 3.5). In planar filtration these forces are antagonistic and have no component acting in the direction of filtrate flow and are ignored in the force balance. In cylindrical filtration however, the geometry is such that these forces have a component acting in the radial direction that must be taken into account. Figure 3.5 shows how these forces may be resolved into components.

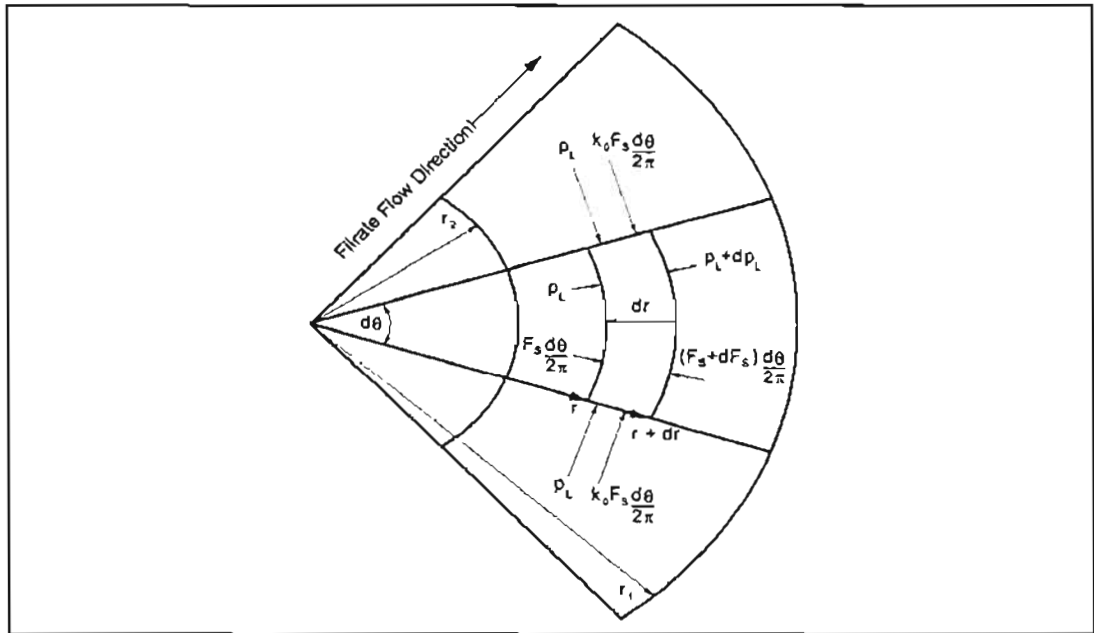


FIGURE 3.4 : Force Balance on an Internal Cylindrical Differential Element of Cake

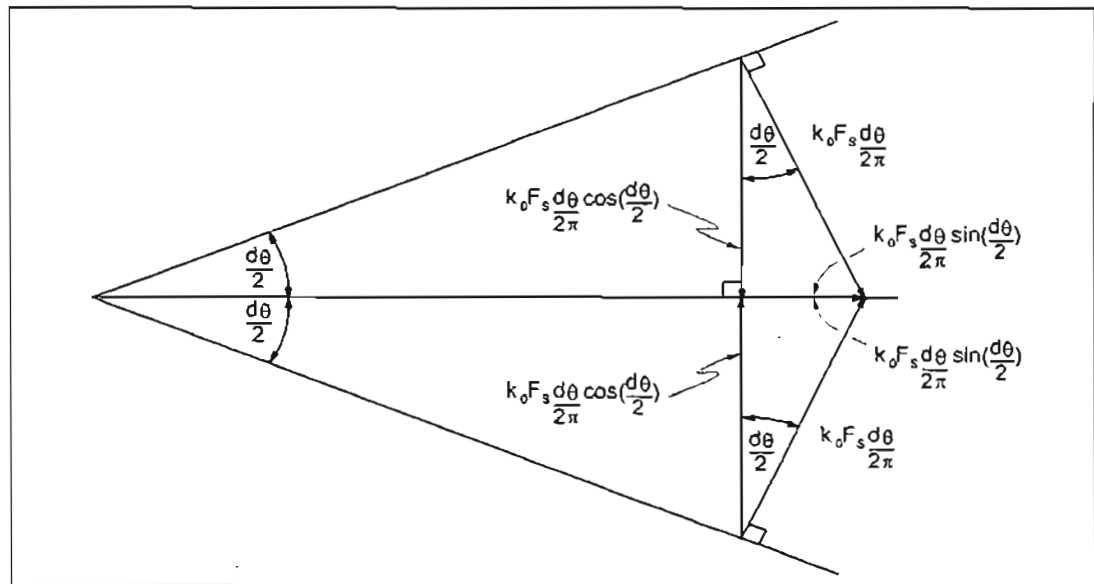


FIGURE 3.5 : Lateral Force on Internal Cylindrical Differential Element of Cake Resolved into Components

Despite the fact that the area of the sides of the differential element of cake are parallel, and not perpendicular to the direction of filtrate flow, it is assumed that the interparticle contact area in these surfaces can be approximated by the area contact function.

A force balance on the cylindrical differential element of cake, neglecting inertial and accelerative effects, yields:

$$\begin{aligned}
& p_L(r d\theta l) \left[1 - \frac{A_c}{A} \right] + F_s \frac{d\theta}{2\pi} + 2 \sin\left(\frac{d\theta}{2}\right) \left[k_0 F_s \frac{d\theta}{2\pi} + p_L(l dr) \left[1 - \frac{A_c}{A} \right] \right] \quad (3.23) \\
& = (p_L + dp_L)(r + dr) d\theta l \left[1 - \left(\frac{A_c}{A} + \frac{dA_c}{A} \right) \right] + (F_s + dF_s) \frac{d\theta}{2\pi}
\end{aligned}$$

where k_0 = coefficient of earth pressure at rest, (-)
 l = axial length of cake or tube length, (m)
 r = radius, (m)
 θ = cylindrical co-ordinate, (radians)

Defining the solids compressive pressure as the solids force acting perpendicularly on a superficial area of cake divided by that superficial area of cake, Equation 3.23 becomes:

$$\begin{aligned}
& p_L(r d\theta l) \left[1 - \frac{A_c}{A} \right] + p_s(r d\theta l) + 2 \sin\left(\frac{d\theta}{2}\right) \left[k_0 p_s(l dr) + p_L(l dr) \left[1 - \frac{A_c}{A} \right] \right] \quad (3.24) \\
& = (p_L + dp_L)(r + dr) d\theta l \left[1 - \left(\frac{A_c}{A} + \frac{dA_c}{A} \right) \right] + (p_s + dp_s)(r + dr) d\theta l
\end{aligned}$$

For $p_s > p_{sa}$, substituting Equations 3.10.b and Equation 3.20 into Equation 3.24 and simplifying, leads to:

$$\begin{aligned}
& 2 \sin\left(\frac{d\theta}{2}\right) (k_0 + [1 - A_0(1 - \varepsilon)] p_L) dr \quad (3.25) \\
& = d(rp_s) d\theta + [1 - A_0(1 - \varepsilon)] d(rp_L) d\theta + [A_0 d\varepsilon] (rp_L) d\theta
\end{aligned}$$

Now as $d\theta \rightarrow 0$, $\sin(d\theta/2) \rightarrow d\theta/2$, so Equation 3.25 reduces to:

$$[1 - A_0(1 - \varepsilon)] \frac{dp_L}{dr} + A_0 p_L \frac{d\varepsilon}{dr} + \frac{dp_s}{dr} = (k_0 - 1) \frac{p_s}{r} \quad (3.26)$$

Equation 3.26 is novel. For $0 \leq p_s \leq p_{sa}$ and $A_0 = 0$ (i.e. point contact), Equation 3.26 reduces to Equation 3.27, which is the same expression derived by (Rencken, 1992), relating solids compressive to liquid pressure for internal cylindrical filtration.

$$\frac{dp_L}{dr} + \frac{dp_s}{dr} = (k_0 - 1) \frac{p_s}{r} \quad (3.27)$$

Equation 3.26 is equally valid for external cylindrical filtration and can be derived in an analogous way as presented above.

3.2.3 Solids Compressive Pressure and Liquid Pressure Gradients

In the determination of the solids compressive pressure and liquid pressure gradients through the cake, and hence the overall solids compressive pressure and liquid pressure profiles, the cake can be thought to exist of a number of distinct hypothetical regions. The cake structure, and hence the behaviour of the cake properties, is different in each region.

Previously, with the use of point contact models and the assumed functional relationship of permeability and porosity with solids compressive pressure, as described by the correlations given in Section 3.1, the cake could be thought to exist of two distinct hypothetical regions.

The first region extends from the cake surface where $p_s = 0$, to the point within the cake where $p_s = p_{si}$. In this region, the particles of the cake are in point contact with one another in a fixed cake structure that consequently exhibits a constant porosity and permeability independent of the solids compressive pressure.

The second region extends from the point where $p_s = p_{si}$, to the filter medium. In this region the cake structure is no longer fixed but compressible, and the porosity and permeability are functions of the solids compressive pressure. The particles in the cake are still assumed to be in point contact with one another.

With the introduction of the area contact model, a third hypothetical region of cake can be thought to exist. The second region described above is now restricted from $p_s = p_{si}$ to a point within the cake where the point-area compressive pressure is reached, $p_s = p_{sa}$. The third region of cake now extends from the point-area compressive pressure to the filter medium. In this region the porosity and permeability are functions of the solids compressive pressure as before, except now the particles in the cake are assumed to be in area contact with one another, and this area contact is also a function of the solids compressive pressure.

Since the first hypothetical region given by $0 < p_s \leq p_{si}$ represents a *mandatory* region of constant porosity and permeability and hence a constant, fixed cake structure, the crossover from point contact to area contact cannot occur in this region. So generally, $p_{sa} \geq p_{si}$. Equality represents an extreme case where the second hypothetical region is excluded altogether.

A fourth hypothetical region can exist for internal cylindrical compressible filtration. This region is in addition to the three regions which have been discussed. This region will be discussed in more detail in Section 3.2.3.2 below.

3.2.3.1 Planar Filtration

For planar filtration the expression describing the liquid pressure gradient for a fluid flowing through a porous medium is given as follows (D'Arcy, 1856):

$$\frac{dp_L}{dx} = \frac{\mu_f Q_f}{AK} \quad (3.28)$$

where μ_f = liquid viscosity, (Pa.s)
 Q_f = volumetric flow rate of filtrate, (m³/s)
 x = distance from medium, (m)

The corresponding equations relating the solids compressive pressure and liquid pressure, are given by **Equations 3.21** and **Equation 3.22** respectively:

$$\frac{dp_s}{dx} = [A_0(1 - \epsilon) - 1] \frac{dp_L}{dx} - A_0 p_L \frac{d\epsilon}{dx} \quad p_s > p_{sa} \quad (3.29.a)$$

$$\frac{dp_s}{dx} = -\frac{dp_L}{dx} \quad 0 \leq p_s \leq p_{sa} \quad (3.29.b)$$

Both the porosity and permeability are functions of the solids compressive pressure and their assumed functional relationships are described by **Equations 3.3** in **Section 3.1**. The solids compressive pressure and liquid pressure gradients can now be determined in each of the hypothetical cake regions.

REGION 1: $0 \leq p_s \leq p_{s1}$

$$\frac{dp_s}{dx} = -\frac{dp_L}{dx} \quad (3.30.a)$$

$$\frac{dp_L}{dx} = \frac{\mu_f Q_f}{AK_i} \quad (3.30.b)$$

REGION 2: $p_{s1} < p_s \leq p_{sa}$

$$\frac{dp_s}{dx} = -\frac{dp_L}{dx} \quad (3.31.a)$$

$$\frac{dp_L}{dx} = \frac{\mu_f Q_f p_s^\beta}{AF} \quad (3.31.b)$$

REGION 3: $p_s > p_{sa}$

From **Equation 3.3.e** the following is obtained:

$$\frac{d\epsilon}{dx} = \frac{d\epsilon}{dp_s} \frac{dp_s}{dx} = -B\beta p_s^{(\beta-1)} \frac{dp_s}{dx} \quad (3.32)$$

Substituting Equation 3.32 into Equation 3.29.a, yields:

$$\frac{dp_s}{dx} = \frac{[A_0 B p_s^\beta - 1]}{[1 - A_0 p_L B \beta p_s^{\beta-1}]} \frac{dp_L}{dx} \quad (3.33.a)$$

with:
$$\frac{dp_L}{dx} = \frac{\mu_f Q_f p_s^\delta}{A F} \quad (3.33.b)$$

3.2.3.2 Internal Cylindrical Filtration

For internal cylindrical filtration the expression describing the liquid pressure gradient for a fluid flowing through a porous medium is given as follows (Rencken 1992):

$$\frac{dp_L}{dr} = -\frac{\mu_f Q_f}{2\pi r l K} \quad (3.34)$$

The corresponding equations relating the solids compressive pressure and liquid pressure, are Equations 3.26 and 3.27 respectively:

$$\frac{dp_s}{dr} = (k_0 - 1) \frac{p_s}{r} - A_0 p_L \frac{d\varepsilon}{dr} - [1 - A_0(1 - \varepsilon)] \frac{dp_L}{dr} \quad p_s > p_{sa} \quad (3.35.a)$$

$$\frac{dp_s}{dr} = (k_0 - 1) \frac{p_s}{r} - \frac{dp_L}{dr} \quad 0 \leq p_s \leq p_{sa} \quad (3.35.b)$$

Again, both the porosity and permeability are functions of the solids compressive pressure and their assumed functional relationships are described by Equations 3.3 in Section 3.1. The solids compressive pressure and liquid pressure gradients can now be determined in each of the hypothetical cake regions.

REGION 1: $0 \leq p_s \leq p_{s1}$

$$\frac{dp_s}{dr} = (k_0 - 1) \frac{p_s}{r} - \frac{dp_L}{dr} \quad (3.36.a)$$

$$\frac{dp_L}{dr} = -\frac{\mu_f Q_f}{2\pi r l K_i} \quad (3.36.b)$$

REGION 2: $p_{s1} < p_s \leq p_{sa}$

$$\frac{dp_s}{dr} = (k_0 - 1) \frac{p_s}{r} - \frac{dp_L}{dr} \quad (3.37.a)$$

$$\frac{dp_L}{dr} = -\frac{\mu_f Q_f p_s^\delta}{2\pi r l F} \quad (3.37.b)$$

REGION 3: $p_s > p_{sa}$

From Equation 3.3.e the following is obtained:

$$\frac{d\varepsilon}{dr} = \frac{d\varepsilon}{dp_s} \frac{dp_s}{dr} = -B\beta p_s^{(\beta-1)} \frac{dp_s}{dr} \quad (3.38)$$

Substituting Equation 3.38 into Equation 3.35.a, yields:

$$\frac{dp_s}{dr} = \frac{\left[(k_0 - 1) \frac{p_s}{r} - [1 - A_0 B p_s^\beta] \frac{dp_L}{dr} \right]}{[1 - A_0 p_L B \beta p_s^{(\beta-1)}]} \quad (3.39.a)$$

with
$$\frac{dp_L}{dr} = -\frac{\mu_f Q p_s^\delta}{2\pi r l F} \quad (3.39.b)$$

REGION 4: disassociated region

Rencken (1992), observed that for internal cylindrical filtration, as the cake thickness increases, it is possible for the solids compressive pressure at the medium and in cake layers close to the medium to decrease. This effect was found to be a strong function of the coefficient of earth pressure at rest. For $k_0 = 0$, the effect was at its maximum, whilst for $k_0 = 1$, the effect was not observed.

A similar effect can be observed in external cylindrical filtration (Tiller and Yeh, 1985), where the solids compressive pressure at the medium can increase above the applied filtration pressure as the cake thickness increases.

Both the above effects can be explained as follows: The frictional drag force over a layer of cake particles in the plane perpendicular to the direction of filtrate flow is transmitted in the direction of the filtrate flow to the subsequent layer of cake particles together with the accumulated frictional drag force from the previous layers. Since the frictional drag force over the cake layer is equal to the sum of frictional drag forces experienced by each individual particle in that layer, the amount by which the accumulated frictional drag force is incremented across a layer of particles, is proportional to the number of particles in that layer. In planar filtration the average number of particles in each cake layer is constant, however, for cylindrical filtration the average number of particles in the cake layer is a function of the radial distance through the cake. For a thin cake, the ratio of the cake thickness to the radius of the medium is small and the filtration behaves similar to a planar filtration. As the cake thickness increases, the filtration becomes more cylindrical in nature and the above effect becomes exaggerated. For internal cylindrical filtration, as the cake thickness increases, each

subsequent deposited layer of cake has a reduced area and hence the solids compressive pressure transmitted through to the medium will decrease as the cake thickness increases. The opposite is true for external cylindrical filtration where each newly deposited layer of cake has an increased area, and so the solids compressive pressure at the medium can increase above the applied filtration pressure as the cake thickness increases. For planar filtration where each deposited layer of cake has a constant area and hence the solids compressive pressure at the medium remains essentially constant (note: this is not true for the early stages of the filtration where the effect of the medium resistance predominates).

To a degree, the above effect is compensated for by the radial component of the effective solids force acting laterally on the sides of the cylindrical element of cake. This effective solids force is directly proportional to the value of the coefficient of earth pressure at rest. For external cylindrical filtration the radial component of this force acts outwardly against the direction of filtrate flow and hence against the accumulated frictional drag force. For internal cylindrical filtration it acts inwardly with the accumulated frictional drag force. For planar filtration this force has no component that acts in the direction of filtrate flow.

For both internal and external cylindrical filtration, for $k_0 = 1$, the effect is no longer observed and like planar filtration, the solids compressive pressure at the medium remains relatively constant (ignoring the effects of the medium resistance). For $k_0 = 1$, the equation relating solids compressive pressure to liquid pressure (Equation 3.26), reduces to the corresponding equation for planar filtration (Equation 3.21) and cylindrical filtration begins to imitate planar filtration behaviour in terms of the solids compressive pressure and liquid pressure profiles through the cake. This is because the radial component of the effective solids force acting laterally on the sides of the cylindrical element of cake becomes sufficiently large so as to fully compensate for the radial dependence of the frictional drag force.

For external cylindrical filtration, the effect of increasing solids compressive pressure at the medium does not present a problem with regard to modelling the pressure profiles through the cake, however, for internal cylindrical filtration this is not the case. As the cake thickness increases, there will come into being a small region of cake extending from the medium that experiences a reduced solids compressive pressure. This region of cake will increase with increasing cake thickness.

It is unlikely that the cake structure in this region, and hence the cake properties such as permeability, porosity and area contact, once stressed at a higher solids compressive pressure profile, will *relax* to a new state as determined by the current solids compressive pressure profile (Pillay, 1991). This would only occur, for example, if the cake particles themselves are deformable and exhibit an elastic behaviour (as would be the case for latex beads or very

strongly associated particle structures). It is more likely that the porosity and permeability profiles in this region will remain at their minimum values, and the area contact profile at its maximum, as determined by the previous higher solids compressive pressure profile. As a result the porosity, permeability and area contact, in this region become *disassociated* from their functional dependence on solids compressive pressure and rather become a *pseudo-function* of the cake radius in this region. The solids compressive pressure and liquid pressure gradients in this region can therefore be calculated as follows:

$$\frac{dp_s}{dr} = (k_0 - 1) \frac{p_s}{r} - A_0 p_L \frac{d\epsilon(r)}{dr} - [1 - A_0(1 - \epsilon(r))] \frac{dp_L}{dr} \quad (3.40.a)$$

$$\frac{dp_L}{dr} = - \frac{\mu_f Q_f}{2\pi r l K(r)} \quad (3.40.b)$$

If $\epsilon(r)$ and $K(r)$ are known from a previous calculation history, the correct solids compressive and liquid pressure profiles can be calculated in this disassociated region.

3.2.4 Point-Area Compressive Pressure

As a result of various assumptions made in the development of the area contact function it became necessary to define a point-area compressive pressure, which is the solids compressive pressure above which the interparticle contact changes from point contact to area contact.

The point-area compressive pressure as well as the coefficient of area contact, are empirically determined parameters. At this stage there is no documented experimental procedure to determine these parameters directly (except for regressing for model parameters from actual filtration data). However, in context of the area contact model, a minimum feasible point-area compressive pressure can be identified in addition to the required model constraint:

$$P_{sa} \geq p_{st} \quad (3.41)$$

3.2.4.1 Planar Filtration

During planar filtration the solids compressive pressure increases towards the medium.

$$\frac{dp_s}{dx} < 0 \quad (3.42)$$

For low solids compressive pressures (and hence relatively high liquid pressures) the term:

$$\left[1 - A_0 p_L B \beta p_s^{(\beta-1)} \right]$$

in Equation 3.33.a can become less than zero, resulting in solids compressive pressure profiles which are not physically realisable (gradients which are greater than zero). To ensure physically realisable pressure profiles, a lower limit for solids compressive pressure needs to be determined for which Equation 3.33.a and the hence area contact model is valid.

Equation 3.31.a describing the solids compressive pressure gradient in the point contact region, results in solids compressive pressure gradients which are always less than zero. For the purposes of identifying a safe lower bound for the point-area compressive pressure, continuity of the solids compressive pressure profiles at the crossover from point contact to area contact is assumed. By equating Equation 3.31.a and Equation 3.33.a, it can be shown that:

$$\frac{p_s}{p_L} = \beta \quad (3.43)$$

Therefore, provided the ratio of the solids compressive pressure to the liquid pressure is greater than the exponential component of the porosity correlation, β , the area contact model will be valid and the pressure profiles physically realisable.

$$\frac{p_s}{p_L} > \beta \quad (3.44)$$

Equation 3.44 is a necessary condition for the area contact model. Equation 3.44 also provides a means of estimating the lower limit for the point-area compressive pressure. The integrated form of Equation 3.22 is:

$$p_s + p_L = P_0 \quad (3.45)$$

where P_0 = operating pressure, (Pa)

Equation 3.45 will still be valid at the crossover point from point to area contact, substituting Equation 3.44 into Equation 3.45 and solving for the solids compressive pressure gives the lower limit for the point-area compressive pressure.

$$p_{sa} > P_0 \left(\frac{\beta}{1 + \beta} \right) \quad (3.46)$$

3.2.4.2 Internal Cylindrical Filtration

For internal cylindrical filtration, at low solids compressive pressures (and hence relatively high liquid pressures), Equation 3.39.a can also describe solids compressive pressure gradients that are not physically realisable.

By assuming continuity of the solids compressive pressure profiles at the crossover from point contact to area contact (equating the solids compressive pressure gradients of Equation 3.37.a and Equation 3.39.a respectively) it can be shown that:

$$\frac{p_s}{p_L} = \beta \left[\frac{(k_0 - 1)2\pi l F + \mu_f Q_f p_s^{(\beta-1)}}{\mu_f Q_f p_s^{(\beta-1)}} \right] \quad (3.47)$$

For $k_0 = 1$, Equation 3.47 reduces to Equation 3.43, for $0 \leq k_0 < 1$, the term in brackets in Equation 3.47 will always be positive and therefore less than unity. Therefore, provided the ratio of the solids compressive pressure to liquid pressure is greater than the exponential component of the porosity correlation, the area contact model will be valid and the pressure profiles will be physically realisable.

For $k_0 = 1$, Equation 3.45 is also valid for internal cylindrical filtration, and hence, Equation 3.45 can be used to determine the lower limit of the point-area compressive pressure. For $0 \leq k_0 < 1$, Equation 3.45 does not hold, but can be considered a sufficiently accurate approximation so that Equation 3.46 can be used to estimate the lower limit of the point-area compressive pressure.

3.2.4.3 Multiple Porosity Correlation Data

A problem arises when estimating the lower limit for the point-area compressive pressure when there are multiple porosity correlation parameter sets. Once the condition given by Equation 3.44 becomes true, and Equation 3.46 used to estimate the point-area compressive pressure, it must hold for all subsequent porosity correlation data sets. If not, the lower limit of the point-area compressive pressure must be increased beyond the value of the solids compressive pressure where the condition is violated, so that all subsequent correlation data sets are consistent in this manner.

Consider Equations 3.3, if point A in Figure 3.6 represents the point where $p_s = p_{s(n+1)}$ and is a point where the above mentioned inconsistency holds, then the following expressions must be true:

$$\frac{p_{s(n+1)}}{p_0 - p_{s(n+1)}} > \beta_n \quad (3.48.a)$$

$$\frac{p_{s(n+1)}}{P_0 - p_{s(n+1)}} < \beta_{n+1} \quad (3.48.b)$$

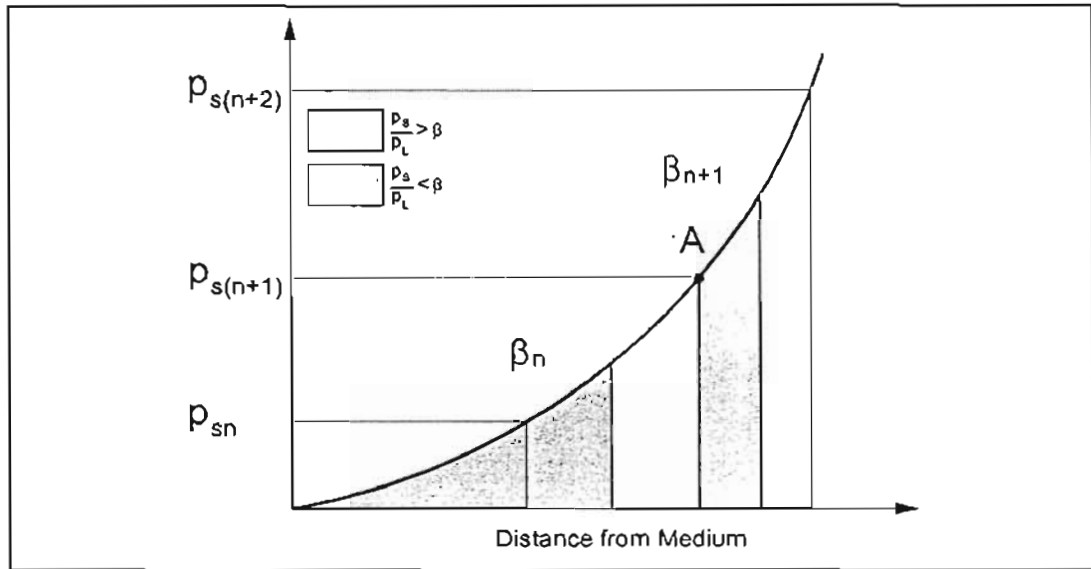


FIGURE 3.6 : Intersection of Porosity Correlation Data Showing an Inconsistency with Regard to the Applicability of the Area Contact Model

Therefore if Equations 3.48.a and Equations 3.48.b hold, the minimum of the point-area compressive pressure will have to increased beyond $p_{s(n+1)}$, as determined by:

$$p_{sa} = P_0 \left(\frac{\beta_{n+1}}{1 + \beta_{n+1}} \right) \quad (3.49)$$

This procedure is repeated for subsequent correlation data sets until the consistency of the condition given in Equation 3.44 can be ensured.

3.3 PREDICTIVE SOLUTION PROCEDURE

The constant pressure compressible filtration model described above is used in conjunction with the empirical permeability and porosity correlation parameters obtained from C-P cell experiments, settling experiments, or from regressing on actual filtration data, to predict the filtration performance. The constant pressure solution procedure is described below, then a new *pseudo variable pressure* solution procedure is developed.

3.3.1 Constant Pressure Solution Procedure

In constant pressure filtration the applied filtration pressure is constant throughout the duration of the filtration process. The constant pressure operating condition is easy to achieve under small-scale laboratory conditions, however, in full-scale industrial applications there may be a

pressurisation period before the constant pressure condition is met. The implications of this are discussed in Section 3.3.2 below.

3.3.1.1 Solids Compressive Pressure and Liquid Pressure Profiles

Equation 3.30, Equation 3.31 and Equation 3.33 for planar filtration and Equation 3.36, Equation 3.37 and Equation 3.39 for internal cylindrical Filtration, which describe the solids compressive and liquid pressure gradients, together with Equations 3.3, represent a system of two simultaneous ordinary differential equations. The initial conditions for planar filtration are as follows:

$$p_s(X) = 0 \quad (3.50)$$

$$p_L(X) = P_0 \quad (3.51)$$

where X = thickness of filter cake (planar filtration), (m)

and the initial conditions for internal cylindrical filtration are:

$$p_s(r_2) = 0 \quad (3.52)$$

$$p_L(r_2) = P_0 \quad (3.53)$$

where r_2 = internal radius of the cake, (m)

The solids compressive pressure is zero at the cake slurry interface and the liquid pressure is equal to the applied operating pressure. The system of two simultaneous ordinary differential equations is too complex to obtain a full analytic solution. Partial analytic solutions can be obtained, however, these solutions are cumbersome and not general since special cases exist for $k_0 = 1$, $\delta = 1$ and cases where multiple correlation data sets exist.

The solids compressive pressure and liquid pressure profiles for a given cake thickness can however, be easily obtained by numerical integration. The numerical integration technique used for this study was the fourth-order Runge-Kutta technique.

The pressure drop across the medium for planar filtration is given by (Leu, 1981):

$$\Delta P_m = \frac{\mu_f Q_f R_m}{A} \quad (3.54)$$

where ΔP_m = medium pressure drop, (Pa)

$$R_m = \text{medium resistance, (m}^{-1}\text{)}$$

The pressure drop across the medium for internal cylindrical filtration is given by (Rencken, 1992):

$$\Delta P_m = \frac{\mu_f Q_f R_m}{2\pi r_1 l} \quad (3.55)$$

where r_1 = internal tube radius, (m)

The cake pressure drop is given by the difference between the applied operating pressure and the liquid pressure at the medium, for example, for internal cylindrical filtration, is given by the following expression:

$$\Delta P_c = P_0 - p_L(r_1) \quad (3.56)$$

The liquid pressure drop at the medium is obtained from the numerically integrated liquid pressure profile. Both the cake and medium pressure drops are functions of the filtrate flow rate and the sum is the total liquid pressure drop, which should be equal to the applied operating pressure.

$$P_0(Q_f) = \Delta P_m(Q_f) + \Delta P_c(Q_f) \quad (3.57)$$

For a given cake thickness, the correct filtrate flow rate, and hence also the correct liquid pressure and solids compressive pressure profiles through the cake, can be determined using any numerical technique for solving non-linear equations, such as the method of interval halving, so that Equation 3.57 holds. The upper bound of the filtrate flow rate on the interval can be obtained from the initial filtrate flow rate. The initial filtrate flow rate is found by solving for Q_f in Equation 3.54 or Equation 3.55, initially there is no filter cake and the medium pressure drop is given by the applied operating pressure. In a sequential calculation, where the filtration properties are being calculated at increments of cake thickness, the upper bound can be obtained from the calculated filtrate flow rate at the previous cake thickness.

For internal cylindrical filtration, as described in Section 3.2.3.2, Equations 3.40.a and 3.40.b should be used in the disassociated region whilst calculating the pressure profiles through the cake. In the disassociated region, the porosity and permeability functions have become pseudo functions of the distance through the cake. The pseudo functions can be approximated by the series of point values based on the previous calculation history. Since the porosity and permeability are no longer pure functions, it is no longer possible to properly implement the

fourth-order Runge-Kutta technique. In the disassociated region, the simpler but less accurate Euler numerical integration technique is used.

Under normal operation of internal cylindrical filtration applications, where the cake thickness to internal tube radius ratio at the end of the filtration cycle is small, the effect of the disassociated region on predicting filtration performance will not be observed. For cases where the disassociated region does come into being, it will still only represents a lesser portion of the total cake thickness, and therefore, provided the cake thickness does not become comparable to the internal tube radius, its effect will not be significant. In terms of the calculation methodology, the change to the use of less accurate numerical techniques for solving differential equations, such as the Euler technique for the latter part of the numerical integration, will not impact significantly on the accuracy of the overall integration.

3.3.1.2 Mass Balances

Once the correct filtrate flow rate has been determined and the correct solids compressive pressure profile calculated, the porosity profile through the cake can be calculated using the porosity correlations, Equations 3.3.d, e, f. The average porosity of the cake is then given by,

$$\text{planar:} \quad \varepsilon_{av} = \frac{1}{X} \int_0^X \varepsilon dx \quad (3.58)$$

$$\text{internal cylindrical:} \quad \varepsilon_{av} = \frac{2\pi \int_{r_2}^{r_1} \varepsilon r dr}{\pi(r_1^2 - r_2^2)} \quad (3.59)$$

where ε_{av} = average porosity of the cake

Since the solids and the liquid are individually incompressible, a mass balance on a volumetric basis gives:

$$\left[\begin{array}{c} \text{Volume of} \\ \text{slurry per unit} \\ \text{medium area} \end{array} \right] = \left[\begin{array}{c} \text{Volume of} \\ \text{cake per unit} \\ \text{medium area} \end{array} \right] + \left[\begin{array}{c} \text{Volume of} \\ \text{filtrate per unit} \\ \text{medium area} \end{array} \right] \quad (3.60.a)$$

or

$$\frac{\omega_c}{\phi_s} = \frac{\omega_c}{(1 - \varepsilon_{av})} + v \quad (3.60.b)$$

where ω_c = volume of cake dry solids per unit medium area, (m³/m²)
 ϕ_s = volume fraction solids in feed sludge, (-)

v = volume filtrate per unit medium area, (m³/m²)

The volume of cake dry solids per unit medium area is given by,

planar: $\omega_c = (1 - \varepsilon_{av})X$ (3.61)

internal cylindrical: $\omega_c = \frac{(1 - \varepsilon_{av})(r_1^2 - r_2^2)}{2r_1}$ (3.62)

Solving for v using Equation 3.60.b and Equation 3.61 for planar filtration and Equation 3.60.b and Equation 3.62 for internal cylindrical filtration gives,

planar: $v = \frac{X(1 - \varepsilon_{av} - \phi_s)}{\phi_s}$ (3.63)

internal cylindrical: $v = \frac{(1 - \varepsilon_{av} - \phi_s)(r_1^2 - r_2^2)}{\phi_s 2r_1}$ (3.64)

3.3.1.3 Time Relationships

For constant pressure filtration, the filtration time can be calculated as follows:

$$t = \int_0^{V_f} \frac{dV_f}{Q_f} \quad (3.65)$$

where V_f = volume of filtrate, (m³)
 t = filtration time, (s)

The volume of filtrate can be determined for planar filtration from Equation 3.63 and for internal cylindrical filtration from Equation 3.64, and is given by,

planar: $V_f = \frac{AX(1 - \varepsilon_{av} - \phi_s)}{\phi_s}$ (3.66)

internal cylindrical: $V_f = \frac{(1 - \varepsilon_{av} - \phi_s)(r_1^2 - r_2^2)\pi l}{\phi_s}$ (3.67)

The filtrate flow rate and filtrate volume are calculated for each successive positive increment of the cake thickness and the filtration time calculated at each increment is calculated by numerical integration of Equation 3.65. In so doing the cumulative and instantaneous filtration properties are obtained with respect to the filtration time. The Trapezoidal numerical

integration technique was found to be suitable the numerical integration of Equation 3.65 as it can be used for both an even and odd number of integration panels.

3.3.2 Development of a New Pseudo Variable Pressure Solution Procedure

Often in the case of practical applications of constant pressure filtration, and in the case of the Tubular Filter Press, there is a period of time before the actual final filtration pressure is attained. If this *pressurisation* time is significant, the solution procedure will have to be modified to account for the *pseudo variable pressure* stage of the filtration.

The solution procedure is considered a pseudo variable pressure methodology as it does not follow the methodology of conventional variable pressure filtration models. Instead, the constant pressure solution procedure described above, is adapted to account for the variable pressure stage of the calculation. This variable pressure stage of the calculation only accounts for the initial period of the calculation, thereafter, the solution methodology reverts to the conventional constant pressure solution procedure. If the variable pressure stage of the calculation represents the greater portion of the filtration time, then the use of conventional variable pressure methodologies, should be considered.

For the calculation of the cumulative and instantaneous filtration properties during the pseudo variable pressure stage of the filtration, the applied variable pressure profile must be known with respect to time. It is assumed that the applied variable pressure profile will increase or remain constant with respect to time. The applied variable pressure profile is given by the following applied variable pressure function:

$$P_v = f_p(t) \qquad \frac{df_p(t)}{dt} \geq 0 \qquad (3.68)$$

where P_v = applied pressure during pressurisation period, (Pa)
 $f_p(\dots)$ = applied variable pressure function, (Pa)

At the pressurisation time, the applied variable pressure equals the constant operating pressure, and thereafter the pressure remains constant at this value.

$$P_v = P_0 = f_p(t_p) \qquad (3.69)$$

where t_p = pressurisation time, (s)

The equations and techniques described in Section 3.3.1 remain valid, except the overall approach of the calculation differs. Instead of calculating the change in filtration time for a

given change of cake thickness at a known constant applied pressure, the change in cake thickness is calculated for a known change in filtration time at the average applied pressure over that time interval.

If the cake is incompressible, the thickness of the previously deposited cake layer would remain constant during the subsequent growth of cake at higher applied pressures. This is not the case for compressible cakes. In reality, cake growth and compression occur simultaneously, for the purposes of the modified solution methodology it is assumed that cake growth and compression occur independently. The calculation is treated as a series of constant pressure cake growth phases over a given time interval, followed by a cake compression phase at the increased average pressure over the following time interval. The principal assumption is that any compression of the previously deposited cake layers takes place during, and is completed, over the growth of the cake at the higher average pressure over the next time interval. Provided the calculation time intervals are small, the calculation should approximate simultaneous cake growth and compression. The assumption that compression is completed during the growth of the subsequent cake layer may under certain circumstances not be true, especially where cake growth is extremely rapid.

3.3.2.1 Cake Growth Phase

During the variable pressure stage of the calculation, $t < t_p$, a constant variable pressure time step is set, and the filter cake is grown until the calculated filtration time is equal to the time at the end of the interval given by:

$$t_{i+1} = t_i + \Delta t \quad (3.70)$$

where Δt = variable pressure time step, (s)

The filter cake is grown at the average pressure over the time interval given by;

$$(P_{avg})_{i+1} = [f_p(t_i) + f_p(t_{i+1})]/2 \quad (3.71)$$

where P_{avg} = average applied pressure over variable pressure time step, (Pa)

Cake growth is achieved by sequentially incrementing the cake thickness and calculating the filtration properties and filtration time as described in Section 3.3.1. Once the calculated filtration time exceeds t_{i+1} , the correct cake thickness can be found using a numerical technique for solving non-linear equations such as the method of interval halving, such that the calculated filtration time equals t_{i+1} .

At the completion of the growth phase at $t = t_{i+1}$, the following standard constant pressure filtration properties are known:

$$\begin{array}{ll} (\varepsilon_{av})_{i+1} & (V_f)_{i+1} \\ \vartheta_{i+1} & (Q_f)_{i+1} \\ \rho_{i+1} & \end{array}$$

where ρ = mass dry solids in cake, (kg)
 ϑ = cake thickness, (m)

In addition to the standard constant pressure filtration properties, the following properties specific to the variable pressure portion of the calculation are known,

$$(Q_t)_{i+1} = (Q_f)_{i+1} + (Q_c)_{i+1} \quad (3.72)$$

where Q_c = compressed filtrate flow rate, (m³/s)
 Q_t = total combined filtrate flow rate, (m³/s)

and,

$$(V_t)_{i+1} = (V_f)_{i+1} + (V_c)_{i+1} \quad (3.73)$$

where V_c = compressed filtrate volume, (m³)
 V_t = total filtrate volume, (m³)

Prior to the calculation of the first growth phase there existed no previous filter cake that could be compressed, hence at the completion of the growth phase over the first time interval the compressed filtrate volume and the compressed filtrate flow rate are zero. It should be noted, that since the cake growth is assumed to occur simultaneously yet independently of cake compression, filtration times calculated during the cake growth phase should use standard constant pressure filtrate volumes and flow rates as given by Equation 3.65.

During a constant pressure filtration, the filtrate flow rate has a maximum value at the start of the filtration when there is no filter cake, the initial filtrate flow rate is determined by the medium resistance and the constant applied operating pressure. As the cake thickness increases, the combined resistance of the filter medium and the cake increases, and the filtrate flow rate decreases with time. During a variable pressure calculation, the filtrate flow rate can

increase with time as the applied filtration pressure increases. Later, as the filtration pressure approaches the constant operating value, and the relative change in filtration pressure decreases, the cake resistance will begin to predominate as the cake thickness increases, and the filtrate flow rate will reach a maximum value and then begin to decrease with time. During the period where the filtrate flow rate is increasing, the upper bound of filtrate flow rate used when calculating the correct filtrate flow rate for a given cake thickness, should be determined from the maximum applied pressure and the medium resistance, thereafter, the previously calculated filtrate flow rate can be used.

3.3.2.2 Cake Compression Phase

Before the growth stage over the next time interval, the cake is compressed at the average applied pressure of the next time interval.

$$(P_{avg})_{i+2} = [f_p(t_{i+1}) + f_p(t_{i+2})]/2 \quad (3.71)$$

During the cake compression phase, the structural properties of the filter cake will change, for example, the cake length and the average porosity will decrease as the filtrate in the interstitial spaces is *squeezed* out of the cake. The mass of dry solids in the cake, Q_{i+1} , will however remain constant. Compression involves determining a representative cake structure with the same mass dry solids in the cake, but compressed at the higher average applied pressure. This new cake structure represents the basis for the next growth stage.

An equivalent representative cake structure can be obtained from a cake that was grown at a constant pressure of $(P_{avg})_{i+2}$ but has the same mass dry solids, Q_{i+1} . The properties of the representative cake structure would be:

$$\begin{array}{ll} \mathcal{G}'_{i+1} & (\varepsilon_{av})'_{i+1} \\ (V_f)'_{i+1} & Q'_{i+1} = Q_{i+1} \end{array}$$

where V_f' = volume of filtrate resulting from compressed representative cake structure, (m³)
 ε_{av}' = average porosity of compressed representative cake structure, (-)
 \mathcal{G}' = cake thickness of compressed representative cake structure, (m)
 Q' = mass dry solids of compressed representative cake structure, (kg)

The compressed representative cake structure can be obtained by performing a sequential constant pressure calculation at an applied pressure of $(P_{avg})_{i+2}$. This however can be time consuming, a very good approximation can be obtained much quicker as follows. The current

uncompressed cake thickness, \mathfrak{S}_{i+1} , will result in a higher mass dry solids if an instantaneous cake structure is calculated at this cake thickness and at an applied pressure of $(P_{avg})_{i+2}$ (note: filtration time is not being calculated so a sequential calculation is not necessary).

$$\varrho_{i+1}^* = \varrho((P_{avg})_{i+2}, \mathfrak{S}_{i+1}) \quad (3.74)$$

where ϱ^* = mass dry solids of a filter cake at the uncompressed cake thickness but produced at a higher applied pressure, (kg)

Using the assumption that the average porosity at the same cake pressure drop is constant with respect to cake thickness (this is true for planar filtration and since at the start of the filtration the cake thickness is small, is a very good approximation for internal cylindrical filtration), the cake thickness of the new representative cake structure, \mathfrak{S}'_{i+1} , at which the mass dry solids in the cake will be equal, can be determined by direct proportionality between the mass dry solids and the cake volume. For example, the cake thickness of the representative cake structure can be obtained for planar filtration as follows:

$$\mathfrak{S}'_{i+1} = \frac{\mathfrak{S}_{i+1}\varrho_{i+1}}{\varrho_{i+1}^*} \quad (3.75)$$

With \mathfrak{S}'_{i+1} and $(P_{avg})_{i+2}$ the structural properties of the representative cake structure can be calculated. The compression properties for the next interval can then be calculated as follows:

$$(V_c)_{i+2} = (V_f)_{i+1}' - (V_f)_{i+1} \quad (3.76)$$

$$(Q_c)_{i+2} = \frac{(V_c)_{i+2}}{\Delta t} \quad (3.77)$$

Once the average applied filtration pressure reaches the constant operating pressure, the calculation procedure can return to that previously described for constant pressure filtration.

3.4 DEVELOPMENT OF A REGRESSIVE SOLUTION PROCEDURE

Standard laboratory-scale tests used to obtain sludge characteristics, in addition to requiring specialised equipment, are cumbersome, time consuming and often prone to failure. In addition, there is also some question as to whether these tests can accurately determine the filtration characteristics of the sludge. These tests are therefore not feasible to perform on an ongoing basis where the characteristics of the sludge to a filtration plant are variable.

The regressive solution procedure utilises the constant pressure compressible cake filtration model in addition to data obtained from full-scale and/or laboratory-scale filtration plants to find the empirical correlation parameters that would ordinarily be obtained from C-P Cell and settling tests, and to also find model parameters specific to the new area contact model.

The regressive solution procedure finds the optimum set of model parameters such that the output of the filtration model matches as close as possible, the actual filtration data. The filtration data and the model output are compared to one another in the form of an objective function. A search strategy is employed to find the optimum set of model parameters such that the objective function is minimised.

For the regressive solution procedure to be of any practical and general use, it is important that the objective function utilises experimental data that is relatively simple to obtain and does not require expensive, sophisticated equipment. Various experimental techniques have been developed to measure filtration properties that are not under normal operational circumstances readily available. For instance, cake growth can be measured *in situ* with respect to filtration time with X-rays (Bierck et al., 1988); (Shen et al., 1994), porosity profiles through the filter cake can be measured using electroconductive probes (Wakeman, 1981); (Sirato and Aragaki, 1972), and liquid pressure profiles through the cake can be measured using hydraulic pressure probes (Sirato and Aragaki, 1972); (Wu, 1994). The information obtained from these more sophisticated experimental techniques may be better in terms of developing a more accurate regressive solution procedure, but for practical purposes will not be considered for this study.

3.4.1 Direct Search Technique

Due to the numerical complexity of the filtration model which translates into a numerically complex objective function, search strategies that require information from first and second order derivatives of the objective function will not be used. Direct search strategies require the value of the objective function only, as a result the search steps and directions are not fixed in some optimal way as determined from derivatives of the objective function, but rather heuristically by a predetermined scheme. The strength of direct search strategies lies, not in their theoretical proofs of convergence and rates of convergence, but in their simplicity and that they have proved themselves in practice.

There are a number of existing direct search techniques. The direct search technique developed for this study is an adaptation of the COMPLEX method (Box, 1965). The COMPLEX method is in turn an extension of the SIMPLEX method (Nelder and Mead, 1965 in Box, 1965), to include both implicit and explicit constraints. The steps required by the technique are detailed below and illustrated in Figure 3.7.

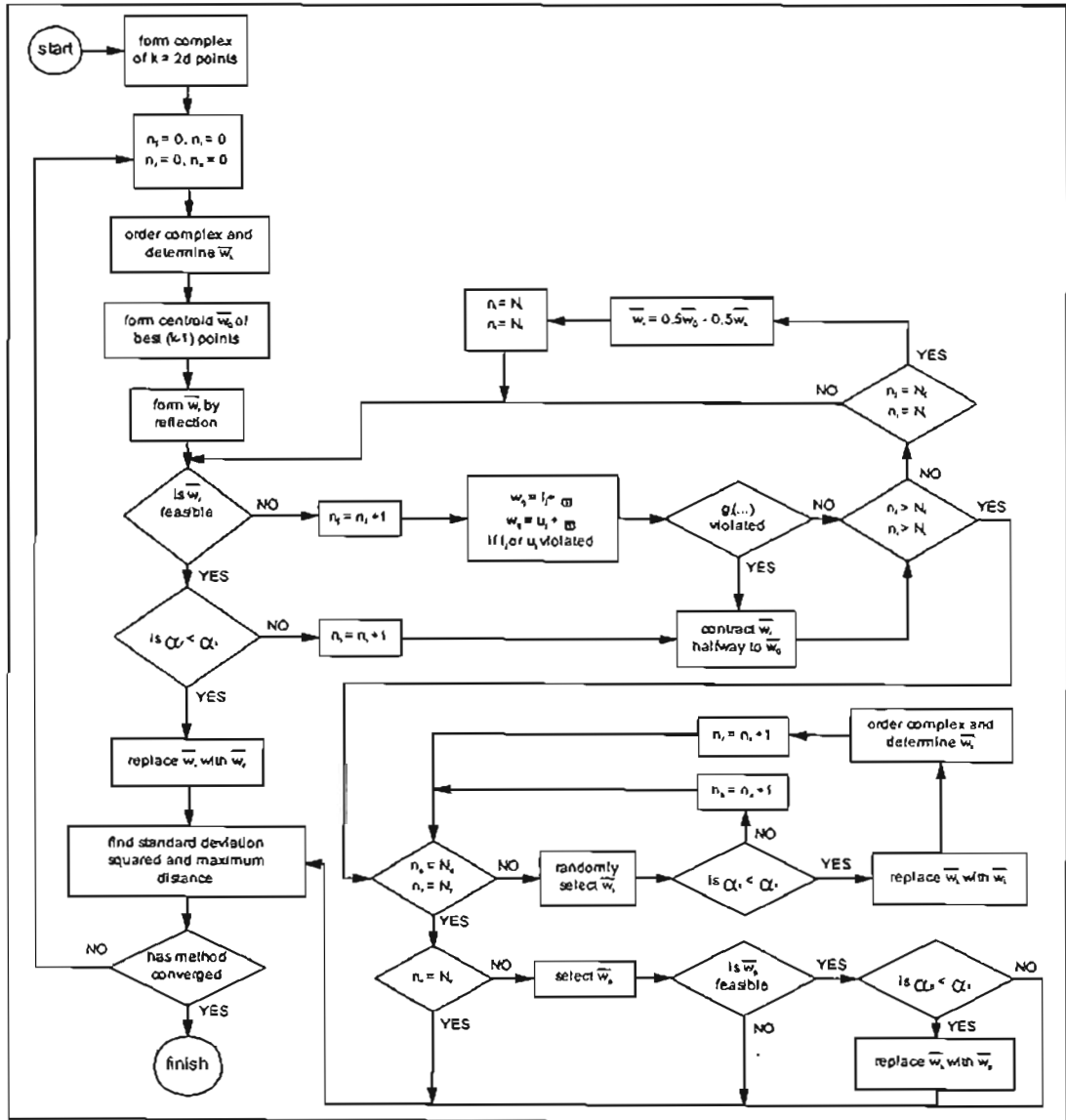


Figure 3.7 : Flow Chart of Modified Complex Method

The purpose of the direct search technique is to minimise the objective function,

$$a(\bar{w}) = a(w_1, w_2, \dots, w_d) \quad (3.79)$$

- where
- $a(\dots)$ = objective function, (-)
 - \bar{w} = vector of objective function variables, (-)
 - d = integer number of objective function variables, (-)

subject to the explicit constraints,

$$l_j \leq w_j \leq u_j \quad j \in [1, d] \quad (3.80)$$

where l_j = lower bound of objective function variable w_j , (-)
 u_j = upper bound of objective function variable w_j , (-)

and also the implicit constraints,

$$g_i(\bar{w}) \leq 0 \quad i \in [1, e] \quad (3.81)$$

where $g_i(\dots)$ = functional form of implicit constraint, (-)
 e = integer number of implicit constraints, (-)

1) Randomly generate a set of $k = 2^d$ points which satisfy both the implicit and explicit constraints and evaluate the objective function at each of the k points. This set of points is known as the complex.

2) Order the points based on the value of the objective function and find the point with the greatest objective function value, \bar{w}_k , form the centroid of the other $(k - 1)$ points.

$$\bar{w}_0 = \frac{1}{(k-1)} \sum_{i \neq k} \bar{w}_i \quad (3.82)$$

where \bar{w}_k = point in complex with the highest objective function result, (-)
 \bar{w}_0 = centroid of remaining $(k - 1)$ points in complex, (-)

3) Move away from \bar{w}_k and form point \bar{w}_r by reflecting \bar{w}_k through \bar{w}_0 using a reflection coefficient greater than unity.

$$\bar{w}_r = (1 + \zeta)\bar{w}_0 - \zeta\bar{w}_k \quad (3.83)$$

where \bar{w}_r = reflected point, (-)
 ζ = reflection coefficient, (-)

4) Test if \bar{w}_r is feasible.

- Determine if an explicit constraint is violated. If l_j is violated, set $w_{rj} = l_j + \varpi$, if u_j is violated, set $w_{rj} = u_j - \varpi$, where ϖ is the boundary approach limit. The order of magnitude of the boundary approach limit must be well below the expected order of magnitude of the objective function variables.

- If an implicit constraint is violated, the reflected point is contracted halfway towards the centroid, $\bar{w}_r = (\bar{w}_r + \bar{w}_0)/2$.

The reflected point is then tested for feasibility once again.

5) Once a feasible reflected point has been obtained, the value of the objective function at this reflected point is evaluated and compared to the worst point in the complex. If $a(\bar{w}_r) > a(\bar{w}_k)$, the reflected point is once again contracted halfway towards the centroid and the technique returns to step 4. If $a(\bar{w}_r) < a(\bar{w}_k)$, the point \bar{w}_k in the complex is replaced by the reflected point. The points of the complex are then reordered according to their objective function values, and the technique then proceeds to step 12.

6) If whilst attempting to obtain a feasible point, the number of loops back to step 4 equals the feasible loop exit number, $n_f = N_f$, proceed to step 8.

where N_f = feasible loop exit number, (-)
 n_f = integer number of loops as a result of a reflected point not being feasible, (-)

7) If whilst attempting to obtain a point whose objective function value is less than the worst point in the complex, the number of loops back to step 4 equals the improvement loop exit number, $n_i = N_i$, proceed to step 8.

where N_i = improvement loop exit number, (-)
 n_i = integer number of loops as a result of a reflected point not being an improvement over worst point in complex, (-)

8) The reflected point is set to halfway between the worst point in the complex and the centroid, $\bar{w}_r = 0.5\bar{w}_0 + 0.5\bar{w}_k$, and the technique returns to step 4.

9) If after step 8, the reflected point is either not feasible or not an improvement over the worst point in the complex, proceed to step 10.

10) The value of the objective function, for a randomly generated point within the total allowable variable space, \bar{w}_i , that satisfies both the explicit and implicit boundary conditions is evaluated. If $a(\bar{w}_i) < a(\bar{w}_k)$, the point \bar{w}_k in the complex is replaced by the randomly generated point \bar{w}_i and the points of the complex are then reordered according to their objective function values. This procedure is repeated until the number of random replacements

equals the specified replacement number, $n_r = N_r$, or the number of replacement attempts equals the specified attempt number, $n_a = N_a$.

where \bar{w}_i = randomly generated point within total allowable variable space, (-)
 N_r = required total number of points to replace in complex, (-)
 N_a = specified total number of attempts to replace points in complex, (-)
 n_r = current number of replaced points in complex, (-)
 n_a = current number of attempts to replace points in complex, (-)

If the required number of replacements has been met, proceed to step 12. If step 10 terminates before the required number of replacements, proceed to step 11.

11) A randomly generated point, \bar{w}_p , is generated within a certain local percentage proximity to the point in the complex, \bar{w}_i which gives the lowest objective function value.

$$w_{pj} = w_{ij} \left(1 + \frac{R_r p_p}{100} \right) \quad j \in [1, d] \quad (3.84)$$

$$R_r \in [-1, 1]$$

where \bar{w}_i = point in complex with lowest objective function value, (-)
 \bar{w}_p = point generated randomly within local percentage proximity of \bar{w}_i , (-)
 R_r = randomly generated number in the range $[-1, 1]$, (-)
 p_p = percentage local proximity, (%)

If \bar{w}_p is feasible, its objective function value is evaluated. If $a(\bar{w}_p) < a(\bar{w}_k)$, the point \bar{w}_k in the complex is replaced by the randomly generated point \bar{w}_p . The points of the complex are then reordered according to their objective function values and the technique proceeds to step 12. If \bar{w}_p is not feasible or does not offer an improvement over \bar{w}_k the technique proceeds directly to step 12.

12) The convergence criteria, the standard deviation squared of the objective function values in the complex and the maximum distance between two points in the complex, are calculated.

$$\zeta^2 = \left\{ \frac{1}{k} \sum_{i=1}^k a(\bar{w}_i)^2 - \left[\frac{\sum_{i=1}^k a(\bar{w}_i)}{k} \right]^2 \right\} \quad (3.85)$$

where ζ = standard deviation of objective function values in the complex, (-)

$$D_m = \max_{i=1}^d \left[\max_{j=1}^d \left[\sqrt{(w_{i1} - w_{j1})^2 + \dots + (w_{id} - w_{jd})^2} \right] \right] \quad (3.86)$$

where D_m = maximum distance between two points in the complex, (-)

13) If both the convergence criteria are sufficiently small, $\zeta^2 < (\zeta^2)_{\min}$ and $D_m < (D_m)_{\min}$, terminate the search, otherwise return to step 2.

where $(\zeta^2)_{\min}$ = terminating condition for the standard deviation squared of objective function values within the complex, (-)

$(D_m)_{\min}$ = terminating condition for the maximum distance between two points in the complex, (-)

The choice of $k = 2d$ and $\zeta = 1.3$ are empirical rules suggested by Box (1965). The large number of points in the complex is to prevent possible premature collapse of the complex. The reflection coefficient greater than unity enables the complex to expand and move in the required direction. This, in addition to the contractions of the complex, enable the complex to move around the feasible region, along a constraint and turn corners where constraints intersect, setting variables that exceed explicit constraints just inside their boundaries also assists with this.

Steps 6 to 11 are additions to the COMPLEX method of Box (1965). For the COMPLEX method, if the objective function is convex and the implicit constraints are convex, the problem will have a unique solution. These conditions may be difficult to ascertain and if the objective function is concave, or the implicit constraints not convex, the method could fail. For instance, if the objective function is concave, the centroid of feasible points may not be feasible itself and the contractions of the reflected point to the centroid may not achieve their objective of locating a feasible point. The purpose of the extensions to the COMPLEX method (steps 6 - 11) is to ensure that the method will not get stuck if the complex straddles a concave section of the objective function or implicit constraints. An example may be where some points in the complex occupy more than one local minima of the objective function. If attempting to find a feasible or improved point by contracting towards the centroid fails after a number of attempts the method breaks away from that of the standard COMPLEX method and assumes that it has located a concave region. As a last resort of the reflection-contraction phase, the feasibility of a point lying halfway between the centroid and the worst point in the complex is tested. If this fails the method then proceeds to randomly locate other minima in the total allowable variable space, and in so doing, move the complex away from the concave region. This also has the added benefit of increasing the possibility that the method finds the

global, and not a local minimum, in the objective function. If this phase is not completely successful, the method then attempts to replace points in the complex with other points within a certain percentage proximity of the point in the complex with the lowest objective function value. This procedure is more effective in relocating the complex away from the concave region and possibly into the better global minimum.

Compared to other direct search techniques, polyhedra strategies (such as the COMPLEX method) have the disadvantage that near the optimum, they converge slowly and sometimes stagnate. The initial configuration of the complex can also influence the results obtained. It is therefore recommended that several runs be made with different initial configurations of the complex to ensure consistency of the final result and that the global minimum of the objective function is indeed found.

3.4.2 Objective Function

The form of the objective function that is to be minimised is as follows:

$$a = \left[\frac{1}{W_1 + W_2 + W_3 + W_4} \right] [W_1 a(\Delta P_c) + W_2 a(\varepsilon_{av}) + W_3 a(V_f) + W_4 a(\vartheta)] \quad (3.87.a)$$

$$a(\Delta P_c) = \sqrt{\frac{1}{G} \sum \left[\frac{(\Delta P_c)_{calc} - (\Delta P_c)_{exp}}{(\Delta P_c)_{exp}} \times 100 \right]^2} \quad (3.87.b)$$

$$a(\varepsilon_{av}) = \sqrt{\frac{1}{G} \sum \left[\frac{[(\varepsilon_f)_{min} - (\varepsilon_{av})_{calc}] - [(\varepsilon_f)_{min} - (\varepsilon_{av})_{exp}]}{[(\varepsilon_f)_{min} - (\varepsilon_{av})_{exp}]} \times 100 \right]^2} \quad (3.87.c)$$

$$a(V_f) = \frac{1}{H} \sum \sqrt{\frac{1}{J} \sum \left[\frac{(V_f(t))_{calc} - (V_f(t))_{exp}}{(V_f(t))_{exp}} \times 100 \right]^2} \quad (3.87.d)$$

$$a(\vartheta) = \sqrt{\frac{1}{H} \sum \left[\frac{(\vartheta)_{calc} - (\vartheta)_{exp}}{(\vartheta)_{exp}} \times 100 \right]^2} \quad (3.87.e)$$

- where
- G = integer number of experimental observations with endpoint data, (-)
 - H = integer number of experimental observations including time dependent data, (-)
 - J = integer number of time dependent data points within single experimental observation, (-)
 - W_1 = weighting factor of cake pressure drop component, (-)
 - W_2 = weighting factor of average porosity component, (-)
 - W_3 = weighting factor of filtrate volume profile component, (-)
 - W_4 = weighting factor of cake thickness component, (-)
 - a = objective function result, (-)
 - $(\varepsilon_f)_{min}$ = minimum porosity of experimental feed sludges, (-)

The objective function is structured such that the best agreement between experimentally observed filtration properties and those evaluated by the model, results in the minimum of the objective function, which is zero.

The objective function consists of four individually weighted components. The cake pressure drop and average porosity components arise from an endpoint, time independent analysis of the experimental data, whilst the filtrate volume and cake thickness components arise from a time dependent analysis.

For instances where the calculated cake pressure drop is less than the experimentally observed cake pressure drop the form of the cake pressure drop component of the objective function becomes:

$$\sqrt{\frac{1}{G} \sum \left[\frac{(\Delta P_c)_{calc} - (\Delta P_c)_{exp}}{(\Delta P_c)_{calc}} \times 100 \right]^2}$$

Depending on the degree of cake compressibility, the calculation of pressure profiles, and hence, cake pressure drops through the cake can be very sensitive and result in extremely large cake pressure drops, and hence, very large objective function values for relatively small changes in model parameters. This subtle modification to the objective function serves to balance the cake pressure drop component of the objective function by providing higher objective function values, and hence, greater sensitivity to cases where the calculated cake pressure drop is less than the experimentally observed cake pressure drop.

3.4.2.1 Time Independent Analysis

The time independent analysis utilises endpoint data, i.e. experimental data observed at the end of the filtration process, the final filtration time is not taken into consideration. The endpoint data are namely, the final filtrate volume, the final filtrate flow rate, and the average cake porosity. The final filtrate flow rate is used with Equation 3.54 and Equation 3.55 to calculate the experimentally observed cake pressure drop.

Based on the experimentally observed final cake thickness (obtained from a mass balance), experimentally observed final filtrate flow rate and a given set of model parameters, the solids compressive pressure and liquid pressure profiles through the cake can be calculated. As a result the calculated cake pressure drop and average porosity of the cake can be determined. The calculated cake pressure drop and average porosity can then be compared to the experimentally observed cake pressure drop and average porosity for each of the experimental observations.

Since the relative changes in calculated average porosities can be relatively small for changes in model parameters, the sensitivity of this component of the objective function is increased by comparing the differences between the calculated and experimentally observed average porosities, and the maximum allowable cake porosity which is given by the minimum experimental feed sludge porosity.

3.4.2.2 Time Dependent Analysis

With the exception of the filtrate volume and filtrate flow rate, it is difficult to observe changes in other filtration properties with respect to filtration time, such as cake length, without the use of sophisticated experimental equipment. Filtrate volume and filtrate flow rate data with respect to filtration time are essentially the same since the former is merely the integral of the latter. Integrated data is by nature less affected by experimental noise and hence more reliable.

For the time dependent analysis, the calculated filtrate volume versus time profile using the given set of model parameters, is compared to the experimentally observed filtrate volume profile, by comparing each of the experimentally measured filtrate volumes, to the calculated filtrate volume, at the same time.

Although it is not practically possible, under normal operating conditions, to measure cake growth with respect to filtration time, the final cake thickness is determined by a mass balance at the end of the filtration, and is compared to the calculated cake thickness as determined by the model at the final filtration time.

3.4.3 Explicit Constraints

The total number of model parameters or objective function variables and their mandatory explicit constraints are presented below:

$$\begin{array}{ll}
 F > 0 & \delta \geq 0 \\
 B > 0 & \beta \geq 0 \\
 p_{st} > 0 & 0 \leq A_0 \leq 1 \\
 P_{sa} > 0 &
 \end{array} \tag{3.88}$$

There are a total of seven objective function variables, five resulting from the empirical porosity and permeability correlations and two specific to the area contact model. Additional artificial explicit constraints can be set within these mandatory explicit constraints to give a more realistic indication of the variables expected maxima and minima, and hence, reduce the

total variable space that needs to be searched. The total number of variables in objective function parameter set can also be reduced by fixing the value of a variable explicitly, or, if applicable, by binding the variables value to the limiting value determined by the variables implicit constraint (see Section 3.4.4).

For example, by fixing $A_0 = 0$ explicitly, the filtration model becomes a pure point contact model, and the variable, P_{sa} becomes redundant. The value of the variable p_{si} can also be bound to its minimum value as determined by its implicit constraint, Equation 3.99. The total number of objective function variables then becomes four.

The objective function variables are specific to the characterisation of the sludge or the area contact model, any other model parameters are not considered to be regressible parameters since their true values can easily be determined by some other experimental technique or, as in the case of k_0 , its effect on the output of the filtration model is too insignificant for its value to be determined accurately by regression.

3.4.4 Implicit Constraints

The sequence in which the model parameter values in a parameter set are determined whilst initialising the complex with values within the total allowable parameter space, or in which the feasibility of the parameters in a reflected parameter set are determined, is important. This is because certain parameters are subject to implicit constraints that require the values of other parameters to be known and feasible, these parameters may have in turn been subject to other implicit constraints.

Presented below is an outline of the sequence in which the various parameters are selected or their feasibility determined and the various implicit constraints governing the respective parameters.

3.4.4.1 Parameter: β

There are no implicit constraints on this parameter.

3.4.4.2 Parameter: B

From rearranging Equation 3.1.c relating porosity to solids compressive pressure we have:

$$\varepsilon = 1 - Bp_s^\beta \quad (3.89)$$

The porosity given by this equation must be greater than, or equal to zero for all practical values of solids compressive pressure.

$$\varepsilon \geq 0 \quad (3.90)$$

The lowest porosity is given by the highest value of solids compressive pressure, which is the solids compressive pressure at the medium. For planar filtration this is given by the cake pressure drop. For internal cylindrical filtration, the solids compressive pressure at the medium is less than the cake pressure drop, but provided the cake thickness is small relative to the internal tube radius, the cake pressure drop is very close and provides a good approximation of the upper bound of the solids compressive pressure. Since there may be experimental data at a number of different filtration pressures, the maximum cake pressure drop must be used. Combining Equation 3.89 with Equation 3.90 and rearranging we get the following implicit constraint for the parameter: B .

$$B \leq \frac{1}{(\Delta P_c)_{\max}^{\beta}} \quad (3.91)$$

where $(\Delta P_c)_{\max}$ = maximum cake pressure drop, (Pa)

Equation 3.91 is valid for regressions with both single and multiple porosity correlation data sets. There is an additional implicit constraint for regressions with multiple porosity correlation data sets, this is discussed further below.

3.4.4.2.1 Multiple Porosity Correlation Data

In the case of multiple correlation data sets, there is already correlation data present over the initial portion of the solids compressive pressure range. Consider Equation 3.3.d to Equation 3.3.f, the terminal data set already present which represents the second to last data set overall, is given by:

$$(1 - \varepsilon) = B_j p_s^{\beta_j} \quad p_{sj} \leq p_s < p_{s(j+1)} \quad (3.92)$$

$$j = (T - 1) \quad T \geq 2$$

The final data set which we are looking for by regression is given by:

$$(1 - \varepsilon) = B_{(j+1)} p_s^{\beta_{(j+1)}} \quad p_s \geq p_{s(j+1)} \quad (3.93)$$

$$j = (T - 1)$$

The porosity versus solids compressive pressure relationship as described by the correlation data sets given by Equation 3.3.d to Equation 3.3.f must be continuous, i.e. the functions given by Equation 3.92 and Equation 3.93 must intersect. The solids compressive pressure where they intersect is the lower bound of validity of the correlation data given in Equation 3.93, $p_s = p_{s(j+1)}$, and is given as follows:

$$p_{s(j+1)} = \exp \left\{ \frac{(\ln B_j - \ln B_{(j+1)})}{(\beta_{(j+1)} - \beta_j)} \right\} \quad (3.94)$$

The lower bound of validity of the final correlation data set given by Equation 3.94, $p_s = p_{s(j+1)}$, must lie between the lower bound of the previous data set, $p_s = p_{sj}$, and the maximum practical solids compressive pressure which is given by the maximum experimental cake pressure drop.

$$p_{sj} < p_{s(j+1)} < (\Delta P_c)_{\max} \quad (3.95)$$

Substituting Equation 3.94 into the constraint given by Equation 3.95 gives the following additional implicit constraint for the parameter: $B_{(j+1)}$

$$p_{sj} < \exp \left\{ \frac{(\ln B_j - \ln B_{(j+1)})}{(\beta_{(j+1)} - \beta_j)} \right\} < (\Delta P_c)_{\max} \quad (3.96)$$

The equivalent form of implicit constraint given by Equation 3.91 for regressions with multiple correlation data sets is as follows:

$$B_{(j+1)} \leq \frac{1}{(\Delta P_c)_{\max}^{\beta_{(j+1)}}} \quad (3.97)$$

3.4.4.3 Parameter: p_{si}

This parameter represents the solids compressive pressure below which the porosity and permeability of the cake remain constant. Within the slurry and at the cake-slurry interface there is no relative motion between the liquid and solid particles and as a result there is no viscous drag forces and the solids compressive pressure is zero. The feed slurry has a constant porosity which is related to the feed solids concentration. From the porosity correlation data, the solids compressive pressure corresponding to the porosity of the feed slurry can be determined as follows:

$$p_{sf} = \left(\frac{1 - \epsilon_f}{B} \right)^{\frac{1}{n}} \quad (3.98)$$

where p_{sf} = solids compressive pressure corresponding to the porosity of the feed sludge, (Pa)
 ϵ_f = porosity of the feed sludge, (-)

Since the feed solids concentration may vary for the experimental data, the highest p_{sf} must be used which corresponds to the lowest porosity and highest experimental feed solids concentration. The calculated p_{sf} represents the lower bound for p_{si} and hence the following implicit constraint for the parameter: p_{si}

$$p_{si} \geq \left(\frac{(s_f)_{\max}}{B\rho_s} \right)^{\frac{1}{n}} \quad (3.99)$$

where s_f = slurry feed solids concentration, (kg/m³)

3.4.4.4 Parameter: F

Two separate implicit constraints for the parameter F exist, one for the case of a single permeability correlation data set and another for the case of multiple permeability correlation data sets.

3.4.4.4.1 Single Permeability Correlation Data Set

The following analysis is for a single permeability correlation parameter set that extends over the entire range of solids compressive pressure and not for the case where there are multiple permeability correlation parameter sets.

In the region of the filter cake extending from the cake surface where $p_s = 0$, to the point within the cake where $p_s = p_{si}$, the particles of the cake are in point contact with one another, the cake has a fixed structure and the porosity and permeability of the cake are constant and independent of the solids compressive pressure.

For planar filtration, Equation 3.30.a can be integrated with the following boundary conditions:

$$p_s(X) = 0 \quad (3.100)$$

$$p_s(x_i) = p_{si} \quad (3.101)$$

where X = thickness of filter cake (planar filtration), (m)

x_i = distance from filter medium to position in cake where $p_s = p_{si}$, (m)

to give the following expression:

$$p_{si} = \frac{\mu_f Q_f}{AK_i} (X - x_i) \quad (3.102)$$

Similarly for internal cylindrical filtration, Equation 3.36.a can be integrated with the following boundary conditions:

$$p_s(r_2) = 0 \quad (3.103)$$

$$p_s(r_i) = p_{si} \quad (3.104)$$

where r_i = radius at which $p_s = p_{si}$ in filter cake, (m)

to give the following expression:

$$p_{si} = \frac{\mu_f Q_f}{2\pi l K_i (1 - k_0)} \left[1 - \left(\frac{r_2}{r_i} \right)^{(1-k_0)} \right] \quad (3.105)$$

Equation 3.105 does not however account for the unique case where $k_0 = 1$, for this case, the integrated form of Equation 3.36.a is as follows:

$$p_{si} = \frac{\mu_f Q_f}{2\pi l K_i} \ln \left(\frac{r_1}{r_2} \right) \quad (3.106)$$

Substituting Equation 3.1.b into Equation 3.102 for planar filtration and Equation 3.105 or Equation 3.106 for internal cylindrical filtration enables the parameter F to be determined provided the position of the constant permeability region is known and the filtrate flow rate that results in $p_s = p_{si}$ at this position is known as well.

For the purposes of locating an upper bound for the parameter F the region of constant permeability can be assumed to extend throughout the entire cake thickness. The position of the constant permeability region, x_i in Equation 3.102 and r_i in Equation 3.105 or Equation 3.106, is given by the cake thickness which can be evaluated from the experimental cake concentration, final filtrate volume and filtrate feed concentration. The filtrate flow rate is also known and is given by the experimental final filtrate flow rate.

Compression of the filter cake to porosities lower than the porosity of feed slurry and hence the start of filtration only occurs if the solids compressive pressure in the cake exceeds

$p_s = p_{si}$. The upper bound of the parameter F evaluated by the method described above is thus unrealistically high since filtration will not yet have commenced even at the experimental cake thicknesses. The upper bound of the parameter F can be reduced further by assuming a more realistic upper bound for the cake thickness required before filtration commences, which could be called an *immediate* cake thickness.

For planar filtration, rearranging Equation 3.102 with Equation 3.1.b and an assumed immediate cake thickness with $x_i = 0$ (the constant permeability region is assumed to occupy the entire immediate cake thickness) yields the following upper bound for the parameter F :

$$F \leq \frac{\mu_f Q_f L_i p_{si}^{(\delta-1)}}{A} \quad (3.107)$$

where L_i = assumed immediate cake thickness, (m)

For planar filtration the pressure drop across the medium is given by the following expression (Leu, 1981):

$$\Delta P_m = \frac{\mu_f Q_f R_m}{A} \quad (3.54)$$

From Equation 3.45 and Equation 3.57 we have the following:

$$\Delta P_m = P_0 - \Delta P_c = P_0 - (P_0 - p_L|_{r=0}) = P_0 - p_{si} \quad (3.108)$$

Combining Equation 3.107, Equation 3.54 and Equation 3.108 yields the following implicit constraint for planar filtration for the parameter: F

$$F \leq \frac{(P_0 - p_{si}) L_i p_{si}^{(\delta-1)}}{R_m} \quad (3.109)$$

For internal cylindrical filtration, rearranging Equation 3.105 with Equation 3.1.b and an assumed immediate cake thickness with $r_i = r_1$ (the constant permeability region is assumed to occupy the entire immediate cake thickness) yields the following upper bound for the parameter F :

$$F \leq \frac{\mu_f Q_f p_{si}^{(\delta-1)}}{2\pi l(1-k_0)} \left[1 - \left(\frac{r_1 - L_i}{r_1} \right)^{(1-k_0)} \right] \quad (3.110)$$

and similarly for the special case where $k_0 = 1$,

$$F \leq \frac{\mu_f Q_f p_{si}^{(\delta-1)}}{2\pi l} \ln\left(\frac{r_1}{r_1 - L_i}\right) \quad (3.111)$$

For internal cylindrical filtration the pressure drop across the medium is given by Equation 3.55. Equation 3.108 does not hold for internal cylindrical filtration but can be considered as a good approximation provided the cake thickness is small relative to the internal tube radius. Substituting Equation 3.108 into Equation 3.55 and rearranging yields the following estimate for the filtrate flow rate:

$$(Q_f)_{guess} = \frac{(P_0 - p_{si})2\pi r_1 l}{\mu_f R_m} \quad (3.112)$$

Substituting Equation 3.112 into Equation 3.110 gives the following estimate for the upper bound of the parameter: F

$$(F)_{guess} = \frac{(P_0 - p_{si})r_1}{R_m p_{si}^{(1-\delta)}(1 - k_0)} \left[1 - \left(\frac{r_1 - L_i}{r_1}\right)^{(1-k_0)} \right] \quad (3.113)$$

and similarly for the special case where $k_0 = 1$,

$$(F)_{guess} = \frac{(P_0 - p_{si})p_{si}^{(\delta-1)}r_1}{R_m} \ln\left(\frac{r_1}{r_1 - L_i}\right) \quad (3.114)$$

Integrating Equation 3.36.b with the following boundary condition:

$$p_L(r_2) = P_0 \quad (3.115)$$

yields:

$$p_L = P_0 + \frac{\mu_f Q_f}{2\pi l K_i} \ln\left(\frac{r_2}{r}\right) \quad (3.116)$$

Substituting Equation 3.116 and Equation 3.55 into Equation 3.57 with the immediate cake thickness and rearranging yields the following expression:

$$Q_f = P_0 \left[\frac{\mu_f}{2\pi l} \left[\frac{R_m}{r_1} - \frac{p_{si}^\delta \ln\left(\frac{r_1 - L_i}{r_1}\right)}{F} \right] \right]^{-1} \quad (3.117)$$

Substituting Equation 3.117 into Equation 3.110 or Equation 3.111, and eliminating Q_f , yields a functional relationship with the following form:

$$F \leq f(F) \quad (3.118)$$

where $f(\dots)$ = function, (-)

By substituting F_{guess} from Equation 3.113 or Equation 3.114 into the right hand side of Equation 3.115 and in turn substituting the result of the expression back into the right hand side and repeating this process, Equation 3.118 will eventually converge on the actual upper bound for internal cylindrical filtration for the parameter: F

3.4.4.4.2 Multiple Permeability Correlation Data Sets

In an analogous way as the implicit constraint for the parameter B for multiple porosity correlation data sets was obtained in Section 3.4.4.2.1, it can be shown that the implicit constraint for the parameter $F_{(n+1)}$ for multiple permeability correlation data sets is given by the following expression:

$$p_{sn} < \exp \left\{ \frac{(\ln F_{(n+1)} - \ln F_n)}{(\delta_{(n+1)} - \delta_n)} \right\} < (\Delta P_c)_{\max} \quad (3.119)$$

3.4.4.5 Parameter: A_0

There are no implicit constraints on this parameter.

3.4.4.6 Parameter: p_{sa}

The implicit constraints governing this parameter for single and multiple porosity correlation data sets have already been defined and discussed in Section 3.2.4.

3.5 COEFFICIENT OF EARTH PRESSURE AT REST

From the expressions relating solids compressive pressure to liquid pressure (Section 3.2.2), it is evident that the only difference between planar and internal cylindrical models is the term:

$$(1 - k_0) \frac{P_s}{r}$$

where k_0 = the coefficient of earth pressure at rest, (-)

For internal cylindrical filtration, as the internal tube radius increases, the cylindrical nature of the filtration becomes less significant for a given cake thickness, similarly, for a given tube radius, the cylindrical nature of the filtration decreases as the cake thickness decreases. Henry et al. (1976), modelled internal cylindrical compressible filtration inside a vertical porous tube assuming that the cake thickness is small compared to the tube radius and hence that planar theory could be used. He obtained good agreement between experimental results and predictions of the model for a compressible lime neutralised acid mine sludge.

For more compressible cakes such as the cake studied by Rencken (1992), the above effect becomes even less significant since the filtration is essentially controlled by a highly compressed thin layer of filter cake on the filter medium, and the *apparent* cake thickness is considerably less than the actual cake thickness and hence the cylindrical nature of the filtration is even further reduced. This is evident in the results obtained by Rencken (1992), who assumed a value of $k_0 = 0.34$ and found that over the practical range of internal cake diameters, as applicable to the Tubular Filter Press, the coefficient of earth pressure at rest had no significant effect on the model output when varied from 0 to 1. Provided that the ratio of cake thickness to tube radius is small and/or the cake is very compressible, internal cylindrical filtration could probably be more than adequately modelled using planar filtration theory.

Internal cylindrical filtration has been shown to be adequately be modelled using planar filtration theory. The use of planar filtration theory to model internal cylindrical filtration may also have an advantageous side-effect in light of the effect of the disassociated region. In planar filtration the solids compressive pressure at the medium and cake layers close to the medium does not decrease with increasing cake thickness as it does for internal cylindrical filtration. Hence the porosity and permeability do not become disassociated from there functional dependence on solids compressive pressure and remain at there minimum values as determined by the maximum solids compressive pressure and as calculated by the permeability and porosity correlations. This effect can be advantageous for reducing the complexity of the calculation procedure since the porosity and permeability profiles as determined by the solids compressive pressure profile through the cake should closely approximate the disassociated porosity and permeability profiles if internal cylindrical theory had been used, and as a result the overall cake porosity and permeability should be comparable.

Tiller and Yeh (1985), developed a model for external cylindrical filtration where the cake is deposited on the outside of porous cylindrical tubes and the filtrate flow direction is radially inward. The model of Tiller and Yeh (1985), predicted that for external cylindrical compressible cake filtration the effect of k_0 was also negligible. External cylindrical filtration may not however be adequately modelled using planar theory, the solids compressive pressure at the medium and cake layers close to the medium can increase with increasing cake

thickness. No advantage is obtained in using planar filtration theory since the functional dependence of the porosity and permeability on solids compressive pressure does become disassociated for external cylindrical filtration, and as a result the associated calculation complexities do not exist as they do for internal cylindrical filtration. The effect of the increasing solids compressive pressure has to be accounted for since this has immediate effects on overall cake porosities and permeabilities, which would not be accounted for if planar theory had been used.

Previously (Rencken, 1992), a value for k_0 was assumed, nonetheless if one is to utilise the cylindrical filtration model, which incorporates this term, a method for determining the coefficient of earth pressure at rest should be identified and an attempt be made to determine its true value.

The coefficient of earth pressure at rest is a concept originating from the field of soil mechanics and represents the ratio of horizontal to vertical effective stress when a mass of one-dimensionally compressed soil (or filter cake) is subjected to a vertical effective stress (Muir-Wood, 1990).

$$k_0 = \frac{\sigma_h}{\sigma_v} \quad (3.120)$$

where σ_h = horizontal effective stress, (Pa)
 σ_v = vertical effective stress, (Pa)

During monotonic one-dimensional normal compression of soils (or filter cakes) which have been deposited uniformly and only moved downwards during deposition (as is the case in the formation of filter cakes), each state of deformation is essentially similar to all the preceding states and the effective stresses have the same similarity. The value of k_0 is then found to be constant. k_0 can vary between 0 and 1, reported values vary between 0.3 and 1 (Yeh, 1985). A soil that is composed of rigid, greatly interlocked particles can support its own weight without needing to push sideways very much to prevent lateral movement, such a soil would be expected to have a low value of k_0 . A material that has no frictional strength, e.g. water, produces a lateral push equal to the overburden pressure, i.e. $k_0 = 1$.

For a one dimensionally normally compressed soil (and hence a filter cake), k_0 is given by the following expression (Jáky, 1944, in Muir-Wood, 1990):

$$k_0 = \left(1 + \frac{2}{3} \sin \phi\right) \left(\frac{1 - \sin \phi}{1 + \sin \phi}\right) \quad (3.121)$$

where ϕ = angle of shearing resistance, (radians)

The angle of shearing resistance can be determined by a number of soil testing procedures such as the triaxial compression test, direct shear test and the unconfined compression test. It was decided that the most practical test, in term of the size of sample required and the sophistication of the test, would be a method known as direct shear testing.

In a direct shear test a sample of soil (or filter cake) is subjected simultaneously to a constant normal load and a horizontal shearing force. The sample is caused to fail along a horizontal shear plane by increasing the horizontal force while the transversal strain in the plain of shear is prevented. For failure of the sample to occur, i.e. for sliding to occur on the shear plane, the horizontal shear stress must overcome both a frictional and a cohesive stress. The cohesive stress is constant and independent of the applied normal stress, however the frictional stress is dependent on the normal stress acting on the shear plane. The horizontal shear stress where failure occurs can be shown to obey the following relationship (Muir-Wood, 1990):

$$\tau = \sigma_n \tan \phi + \kappa \quad (3.122)$$

where τ = horizontal shear stress, (Pa)
 σ_n = normal stress acting on shear plane, (Pa)
 κ = cohesion, (Pa)

By performing a number direct shear tests at different horizontal shear stresses, the angle of shearing resistance can be obtained from the slope of the line obtained by plotting the maximum horizontal shear stress where the sample fails versus the normal stress.

3.6 DETERMINATION OF EMPIRICAL PERMEABILITY AND POROSITY CORRELATION DATA

The laboratory-scale tests required to find the empirical parameters for the porosity and permeability correlations given by **Equations 3.3**, and hence to characterise the filtration behaviour of the sludge, are documented.

3.6.1 Compression-Permeability Cell Tests

Compression-Permeability cell (C-P cell) testing is the primary laboratory-scale test to evaluate the empirical parameters in the correlations relating permeability and porosity to solids compressive pressure, **Equations 3.3**. The primary assumption in C-P cell testing is that the local values of porosity and permeability in the filter cake are equal to the total average

porosity and permeability of a cake sample in a C-P cell, provided the mechanical pressure in the C-P cell is equal to the local value of solids compressive pressure in the filter cake. There are however, a number of problems associated with this primary assumption, and the overall cake structure in the C-P cell may not be representative of the local cake structure in the filter cake.

The cake structure in the C-P cell, and hence the results obtained from C-P cell testing, may be affected by the testing procedure (Lu, Tiller et al. 1970). The method by which the cake in the C-P cell is initially formed from the slurry may affect the resulting cake structure. Cakes may be formed by sedimentation or slow filtration. A cake formed by sedimentation and then consolidation in a C-P cell may also not be representative of a cake formed during filtration. The method by which the cake sample is stressed mechanically to obtain data at different pressures may also affect the cake structure. Is a single cake used with successive increments of applied pressure (allowing for equilibrium to be attained between each step) or is a different, newly prepared cake used for each loading. The rate at which the cake sample is loaded and consolidated may also be a factor. If filtrate is allowed to pass through the cake for prolonged periods of time, the migration of small-scale solids could adversely affect permeability values due to *blinding* of the cake and/or filter medium (the permeability would be reduced, however the porosity would remain unaffected).

The cakes studied in C-P cells are static. After each loading, the cake in the cell is allowed to reach equilibrium, the point where cake consolidation ceases. Depending on the applied pressure and the thickness of the cake sample, this can take several hours. Cakes formed during filtration are on the other hand are dynamic, the stress on an element of cake increases continually as successive layers of cake are formed above. Cake elements are small and should therefore reach equilibrium quicker than cakes in C-P cells, however there is a question as to what extent a cake element is in equilibrium with its associated local solids compressive pressure, particularly for cakes formed very rapidly or for short filtration times.

The main problem associated with C-P cell tests is that they are not accurate at low values of solids compressive pressure, mainly due to the effects of wall friction. The properties of the cake in the C-P cell are assumed to be homogenous. Wall friction in C-P cell testing causes non-uniformity in stress distributions within the cake which in turn affect local porosity and permeability values. Previously it was assumed that provided the cake thickness to cell diameter ratio (L/D) was less than 0.6, these effects would be negligible (Grace, 1953). However it has been shown that even with (L/D) ratios as low as 0.2, the transmitted pressure in the C-P cell was less than 85 % of the applied pressure (Tiller and Lu, 1972); (Lu, Tiller et al., 1970), even for highly compressible cakes. In the absence of wall friction the stress distribution through the cake would be equal and the transmitted pressure at the bottom of the

cake would equal the applied pressure at the top. Although the effects of wall friction are reduced for smaller (L/D) ratios, it has been found that the repeatability of test results decreases for decreasing (L/D) ratios, particularly if (L/D) < 0.2 (Lu, Tiller et al., 1970).

Unless an attempt is made to correct C-P cell data for the effects of side wall friction, the data obtained from C-P cell tests could be in error and due care must be taken in all design using sludge characterisations derived from this data since there can be no guarantee that the calculated cake structures will be representative of cakes formed during actual filtration. Correction methods have been developed by Tiller and Haynes et al. (1972), who suggested relations for correcting calculated values of porosity and specific cake resistance in terms of the ratio of applied to transmitted pressure. However, the method proposed by Shirato et al. (1968), where the compressive pressure is corrected after statistically comparing calculated and experimentally determined transmitted pressures is probably more general, since adhesion between particles and the cell walls is accounted for.

3.6.1.1 Determining Correlation Data

The permeability of the cake in the C-P cell at a particular loading can be determined from D'arcy's law (D' Arcy, 1856) and is given by:

$$K = \frac{\mu_f Q_f \Delta t_c}{A_{cell} \Delta p_c} \quad (3.123)$$

where Δt_c = thickness of cake in C-P cell, (m)
 A_{cell} = area of cake in C-P cell, (m²)
 Δp_c = hydrostatic pressure drop across cake in C-P cell, (Pa)

It is assumed that the combined resistance of the porous plates and filter papers in the C-P cell is negligible.

The final porosity of the cake in the C-P cell at the end of the test can be determined from the final moisture content of the cake:

$$\varepsilon = \frac{\frac{m}{\rho_l}}{\frac{m}{\rho_l} + \frac{(1-m)}{\rho_s}} \quad (3.124)$$

where m = mass fraction of moisture in cake, (-)
 ρ_l = liquid density, (kg/m³)

3.6.1.2 Approximate Correction for Side Wall Friction

The following method for the correction of side wall friction in C-P cell testing was developed by Shirato et al. (1968).

Assuming that the vertical pressure is uniformly distributed across the cell and that there is a constant cohesive force at the wall, a force balance over a differential element of cake shown in Figure 3.8 may be written as follows:

$$\frac{\pi D^2}{4} [p_v - (p_v + dp_v)] = (k_0 f p_v + c) \pi D dz \quad (3.125)$$

- where
- f = coefficient of friction, (-)
 - D = inside diameter of the cell, (m)
 - z = distance from the top of the cake, (m)
 - c = cohesive force between the side wall and the compressed cake, (Pa)
 - p_v = vertical solids pressure in the cake, (Pa)

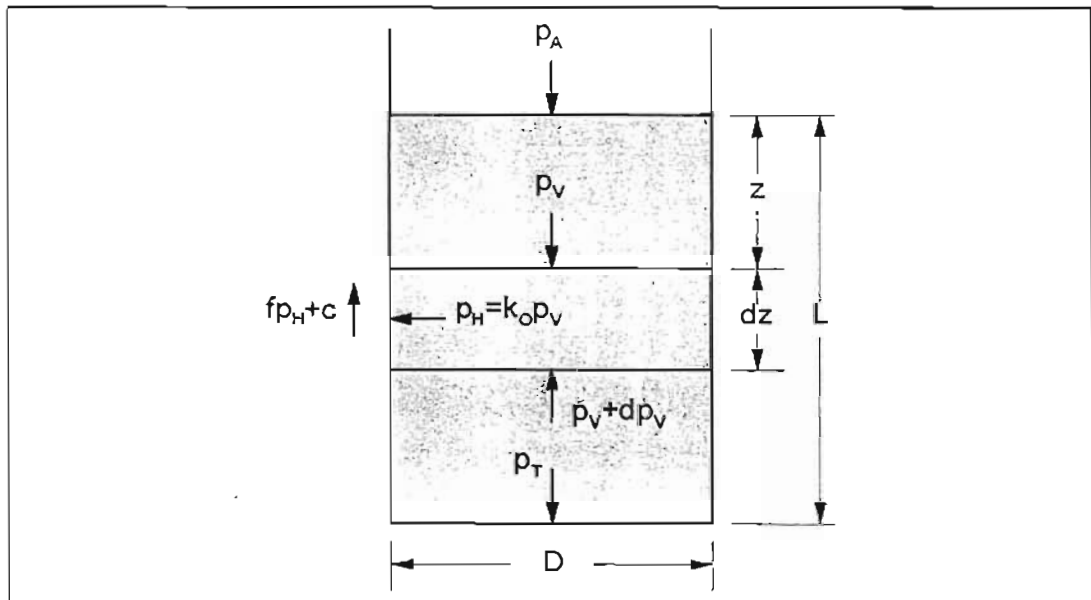


FIGURE 3.8 : Force Balance on Differential Element of Cake inside the C-P Cell

Integrating Equation 3.125, assuming that $k_0 f$ and c are constant, from the top of the cake, where the vertical pressure is equal to the applied pressure, to some point within the cake yields:

$$p_v = \frac{1}{k_0 f} \left[\frac{k_0 f p_A + c}{\exp(4 k_0 f z / D)} - c \right] \quad (3.126)$$

where p_A = the applied pressure at the top of the cake, (Pa)

Or alternatively, integrating Equation 3.125 from the top of the cake to the bottom of the cake, where the vertical pressure will be equal to the transmitted pressure, yields:

$$p_T = \frac{1}{k_{of}} \left[\frac{k_{of} p_A + c}{\exp(4k_{of}L/D)} - c \right] \quad (3.127)$$

where p_T = transmitted pressure through the cake, (Pa)
 L = compressed equilibrium thickness of the cake, (m)

The average compressive pressure through the cake is defined as:

$$p_S = \frac{1}{L} \int_0^L p_T dz \quad (3.128)$$

Substituting Equation 3.126 into Equation 3.128 yields:

$$p_S = \frac{p_A + (c/k_{of})}{4k_{of}L/D} \{1 - \exp(-4k_{of}L/D)\} - \frac{c}{k_{of}} \quad (3.129)$$

Due to the variable stress within the cake, and hence variable porosity and permeability, the data obtained from the C-P cell test would be better correlated with the solids compressive pressure obtained from Equation 3.129 as opposed to the applied pressure as in conventional C-P cell testing.

The terms k_{of} and c may be obtained by statistically comparing experimentally measured transmitted pressures to those calculated from Equation 3.127 and determining which values of k_{of} and c result in a minimum root-mean-squared deviation as given by the expression:

$$\sigma = \sqrt{\frac{1}{I} \sum \left[\frac{(p_T)_{calc} - (p_T)_{exp}}{(p_T)_{exp}} \times 100 \right]^2} \quad (3.130)$$

where σ = root-mean-squared deviation, (-)
 I = the number of experimental observations, (-)

A new C-P cell has been constructed that will enable the measurement of the transmitted pressure in the C-P cell (see Section 4.2.1) and hence the data can be corrected for the effects of wall friction.

3.6.2 Settling Tests

The following techniques for the determination of permeability and porosity data at low solids compressive pressures was developed by Shirato, Murase et al. (1983), and are the same techniques as documented by Rencken (1992).

3.6.2.1 Porosity Correlation Data

When a suspension containing a dry solids volume per unit area, ω_0 , settles in a cylinder, the final equilibrium height of the sediment is denoted by H_∞ . When the initial volume of solids is increased by $d\omega_0$, the final height of the sediment will be given by $(H_\infty + dH_\infty)$. The porosity variation of the suspension AB is identical to that of the suspension CD in Figure 3.9. As a result the total solids volume in sediment CE can be represented by:

$$\omega_0 + d\omega_0 = \omega_0 + dH_\infty(1 - \epsilon) \quad (3.131)$$

where H_∞ = final height of sediment, (m)
 ω_0 = total volume of dry solids per unit cross sectional area, (m²)

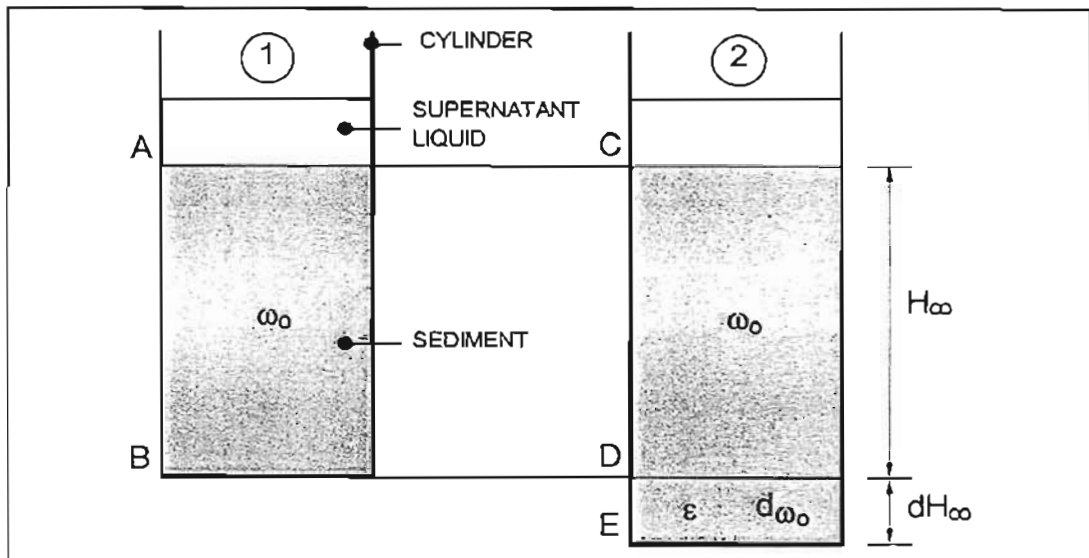


FIGURE 3.9 : Relationship Between Height of Sediment and Volume of Dry Solids per Unit Area

solving for the porosity in Equation 3.131:

$$\epsilon = 1 - \frac{d\omega_0}{dH_\infty} \quad (3.132)$$

ω_0 is related to the solids compressive pressure by the relation:

$$p_s = (\rho_s - \rho_l)g\omega_0 \quad (3.133)$$

where g = constant of gravitational acceleration, (m/s²)

Shirato, Murase et al. (1983), found that on the basis of experimental data, H_∞ could be represented in terms of ω_0 by the following equation:

$$H_\infty = a\omega_0^b \quad (3.134)$$

where a, b = empirical constants, (-)

substituting Equation 3.134 into Equation 3.132 and eliminating ω_0 by means of Equation 3.133, one obtains Equation 3.135:

$$(1 - \epsilon) = Bp_s^\beta \quad (3.135)$$

where $B = \frac{1}{ab[(\rho_s - \rho_l)g]^{(1-b)}}$ (3.136)

and $\beta = (1 - b)$ (3.137)

The empirical constants a and b may be obtained from linear regression using the experimental results of $\ln H_\infty$ and $\ln \omega_0$ and the linearised form of Equation 3.134:

$$\ln H_\infty = \ln a + b \ln \omega_0 \quad (3.138)$$

3.6.2.2 Permeability Correlation Data

Michaels and Bolger (1962), investigated the sedimentation behaviour of a flocculated suspensions of kaolin. For their sedimentation model they assumed that for flocculated suspensions, the basic flow units or settling entities are small clusters of particles or flocs. For gravity settling the flocs group into clusters called particle or floc aggregates. Michaels and Bolger (1962), found that the floc aggregates determine the sedimentation behaviour of flocculated suspensions.

Shirato, Murase et al. (1983), confirmed the results of Michaels and Bolger (1962). By using zinc oxide, Mitsukuri Gairome clay and ferric oxide slurries, they showed that sedimentation

behaviour may be classified into three general regions according to the initial porosity of the suspension, ϵ_{in} , as shown in Figure 3.10.

In the dilute concentration region, *free* or *hindered* settling of the individual particles or aggregates may occur. In the intermediate concentration region, sedimentation behaviour becomes unstable due to the partial collapse of particle aggregates. In the higher consolidation concentration region the supernatant liquid-sediment surface interface subsides slowly due to the *consolidation* or *compression* of the sediment. In order to describe the sedimentation behaviour in the dilute concentration region, Michaels and Bolger (1962), modified the equation developed by Richardson and Zaki (1954), for the hindered settling of uniform, spherical particles. According to the modified equation, for dilute suspensions, the initial settling velocity of the surface of the sediment can be related to the initial porosity by:

$$V_0^{1/4.65} = \left[\frac{gd_f^2(\rho_s - \rho_l)}{18\mu_f(1 - \epsilon_{if})^{3.65}} \right]^{1/4.65} (\epsilon_{in} - \epsilon_{if}) \quad (3.139)$$

- where d_f = mean diameter of particle aggregates, (m)
 V_0 = initial settling velocity of surface of sediment, (m/s)
 ϵ_{if} = internal porosity of particle aggregates, (-)
 ϵ_{in} = initial porosity of suspension

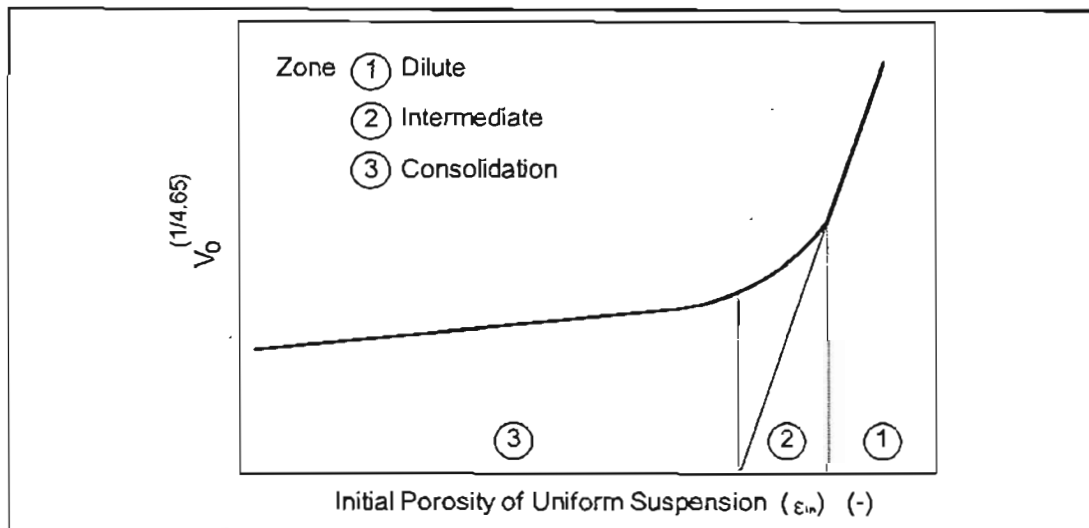


FIGURE 3.10 : Settling Regimes for a Slurry

As shown in Figure 3.10, a straight line is obtained in the dilute region in accordance with Equation 3.139.

The technique for measuring porosity and permeability at low solids compressive pressure is only applicable in the high concentration region where sedimentation takes place due to consolidation of the sediment (Shirato et al. 1983). For batch sedimentation of a concentrated suspension inside a cylinder, the liquid pressure and solids compressive pressure increase towards the bottom of the cylinder. When a differential element of suspension settles due to consolidation, liquid has to flow through the element due to the liquid pressure gradient across the element as shown on Figure 3.11. The liquid pressure gradient across the element is caused by the weight of the particles lying above the element. The D'arcy equation (D'arcy, 1856), may be used to describe the liquid flow through the element:

$$u_l = -\frac{K}{\mu_f} \frac{\delta p_L}{\delta y} \quad (3.140)$$

where u_l = apparent liquid velocity relative to solids, (m/s)
 y = distance measured from bottom of cylinder, (m)

But

$$d\omega = (1 - \epsilon)dy \quad (3.141)$$

where ω = volume of dry solids per unit cross-sectional area, measured from bottom of cylinder, (m³/m²)

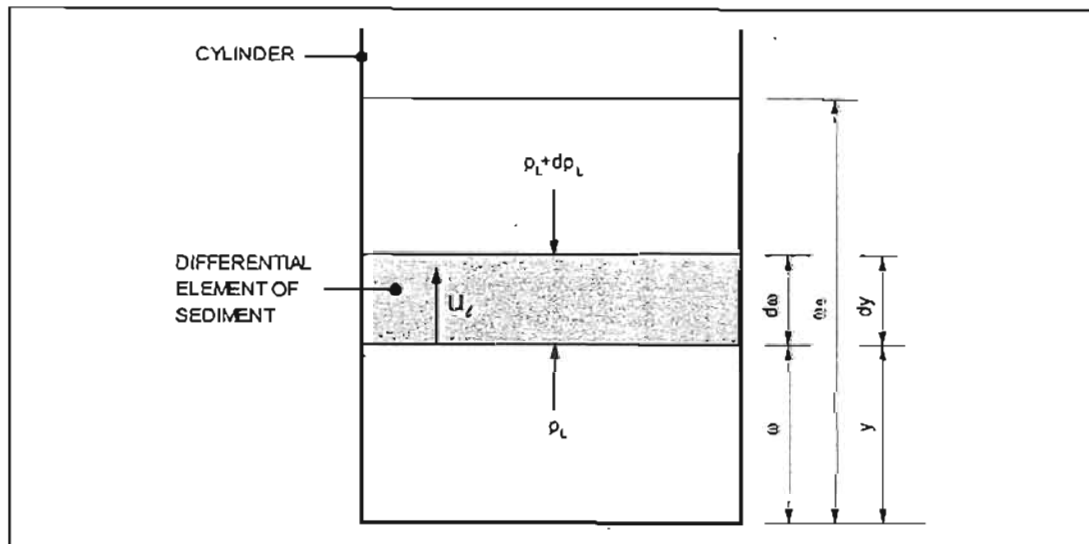


FIGURE 3.11 : Up-Flow of Liquid through Differential Element of Slurry due to Liquid Pressure Gradient

Therefore Equation 3.140 can be written in terms of ω , as follows:

$$u_l = -\frac{K(1-\epsilon)}{\mu_f} \frac{\delta p_L}{\delta \omega} \quad (3.142)$$

The forces acting on a differential element, $\delta\omega$, are shown in Figure 3.12. The following equation can be derived from Newton's second law of motion (assuming accelerative and inertial effects to be negligible):

$$\frac{\delta p_L}{\delta \omega} + \frac{\delta p_s}{\delta \omega} = -(\rho_s - \rho_l)g \quad (3.143)$$

Wall friction is assumed to be negligible.

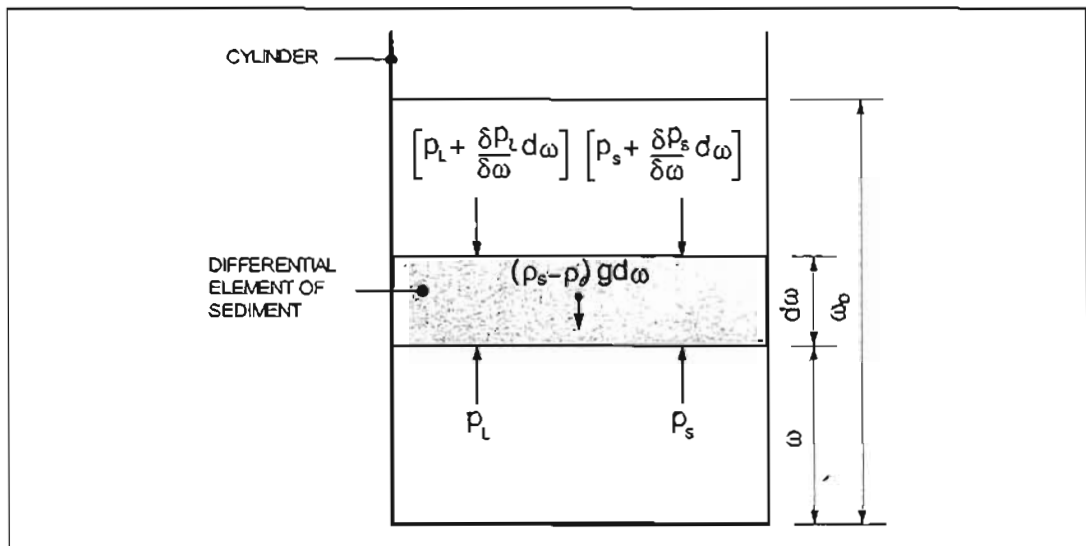


FIGURE 3.12 : Forces Exerted on Differential Element of Slurry

Since the solids compressive pressure can be assumed to be constant throughout the height of the cylinder at the beginning of a settling test, when the suspension is uniform (Shirato et al. 1983), the initial liquid pressure gradient can be obtained from Equation 3.143.

$$\left(\frac{\delta p_L}{\delta \omega} \right)_{t=0} = -(\rho_s - \rho_L)g \quad (3.144)$$

At the start of the test, u_l , in Equation 3.142 can be considered as a constant which is equal to the initial settling velocity of the sediment surface, V_0 . Combining Equation 3.142 and Equation 3.144:

$$K = \frac{V_0 \mu_f}{(\rho_s - \rho_l)(1 - \epsilon_{in})g} \quad (3.145)$$

Both Shirato et al. (1983), and Rencken (1992), found the initial height of the uniform suspension in the cylinder, had no effect on the initial settling velocity of the suspension.

3.7 ASPECTS OF MODELLING SPECIFIC TO THE TUBULAR FILTER PRESS

The full-scale application of constant pressure filtration can introduce additional operational variables that may require the revision of the filtration model and the associated solution procedures. In this section some aspects of the modelling process specific to the Tubular Filter Press are discussed. The development of pseudo variable pressure solution procedure to account for the initial variable pressure stage of the Tubular Filter Press operation, has already been discussed in Section 3.3.2.

3.7.1 Dynamic Dead-End Internal Cylindrical Filtration

During the modelling of the dead-end filtration cycle of the Tubular Filter Press the *dynamic* properties of the filter tube have been ignored, the entire tube has been treated as being uniform with respect to filtration pressure and cake thickness and dynamic effects such as the shearing of the filter cake have been ignored. In reality both the local filtration pressure and cake thickness will vary down the length of the tube. The overall filtration rate will be determined by the accumulation of the local filtration rates along the tube, which depend on the local filtration pressure and cake thickness. Hence the significance of these factors should be considered.

3.7.1.1 Dead-End Shear Model

Shearing of the filter cake has been modelled by Rencken (1992) during the cleaning cycle and during the cross-flow filtration mode of the Tubular Filter Press, but not during the dead-end filtration mode. Shearing of the cake within the tube will be a function of the local axial flow velocity and internal cake radius, both of which are dependent on the axial pressure profile within the tube. The local axial flow velocity will be a maximum at the top of the tube and zero at the bottom, hence if any shearing takes place, it will be at the top of the tube. However, unlike shearing during cross-flow mode, any sheared material will be redeposited further down the tube during dead-end mode, if this effect are significant it could lead to blockages further down the tube.

Intuitively one would expect that shearing effects will be negligible since the filtration rate and hence the axial flow rate will decrease sharply as soon as a thin layer of cake is deposited. During the initial stage of the filtration the tube internal cross-sectional area available for flow is still relatively large and hence the axial flow velocity will be low. By the time the internal

cross sectional area has decreased significantly, the axial flow rate will no longer be significant. If any shearing occurs it will probably be restricted to the tube inlet and its effects will be negligible. Shearing effects hence may only be of significance for very long tubes with a small internal diameters. For the purposes of this study, these effects have been ignored.

Henry et al. (1976), who modelled dead-end constant pressure compressible cake filtration inside a vertical porous tube, assumed that no shearing of the filter cake occurred during filtration, due to the very low shear stress at the cake surface.

3.7.1.2 Axial Pressure Profiles

The local filtration pressure in the tube will be equal to the overall applied pressure plus a hydrostatic contribution, minus the liquid pressure drop associated with the flow of the slurry down the tube. The local hydrostatic contribution will depend on the orientation of the tubes, the density of the slurry and the vertical displacement relative to the tube inlet. For filtration tubes that are vertically orientated, the hydrostatic pressure contribution will be significant. The pressure head loss due to fluid flow will depend on the internal cake radius, the axial flow profile within the tube and the physical properties of the slurry such as the viscosity. The liquid pressure drop due to the flow of the slurry down the tube, for a tube operating in dead-end mode is expected to be negligible. These factors will only be of significance for relatively low applied pressures, long filter tubes and dense, highly viscous slurries.

A predictive solution procedure can be developed for the constant pressure compressible cake filtration model to account for the axial applied pressure profile. The solution procedure would entail devising the tube into a number of discrete elements, and treating each element as a separate constant pressure filtration. The applied pressure for each element would be the average of axial pressure profile over that particular element. The filtration behaviour of the entire tube at a particular point in time can be determined by evaluating the filtration behaviour of each discrete element at the same time. The axial profiles of filtration properties such as cake thickness, could also be determined with respect to time.

At this stage, the greatly increased computational requirements do not appear to be justifiable. Provided the hydrostatic pressure over the length of the tube is small compared to the overall applied filtration pressure, it is assumed that the filtration can be adequately modelled as a constant pressure filtration, where the applied pressure is equal to the average of the axial pressure profile along the length of the tube. For typical applications of the vertical Tubular Filter Press, the difference in the applied pressure between the top and the bottom of the tube will be in the region of approximately 10 %.

Henry et al. (1976), accounted for the axial pressure profile when modelling dead-end constant pressure compressible cake filtration inside a vertical porous tube. This is discussed in more detail in Section 2.3.1.

3.7.1.3 Axial Feed Solids Concentration Profiles

For long filtration times and low applied pressures, the filtrate flow rate may be sufficiently low such that the settling rate of the solids in the sludge may be greater than the axial flow rate in the tube. As a result, a non-uniform feed solids concentration profiles may occur in the tube. It is however, unlikely that during the length of time required for the filtration cycle of the Tubular Filter Press, under normal operating conditions, that the concentration effects due to settling would become significant. In addition it would occur at the end of the filtration cycle when filtration rates are low, and as a result will have no effect on the overall filtration behaviour. It is therefore assumed that under normal operation of the Tubular Filter Press, the effect of axial feed solids concentration profiles will be negligible.

3.7.2 Cake Recovery

Rencken (1992), studied the cake recovery due to shearing of the cleaning fluid prior to the action of rollers and then due to the combined action of the rollers and hydraulic conveyance of the flakes of cake during the cake removal cycle of a horizontal laboratory-scale internal cylindrical filtration apparatus. Rencken (1992), developed a shear model, and was able to accurately predict the increase in average cake porosity and internal cake radius as the loosely consolidated layers of cake were sheared off by the cleaning fluid, but was unable to account for the combined action of the rollers and hydraulic conveyance.

For the vertical orientation of the Tubular Filter Press, the cake removal mechanism is different from the horizontal Tubular Filter Press studied by Rencken (1992). For the horizontal Tubular Filter Press the principle cake removal mechanism is due to the action of the rollers, the cake is exposed to the shearing action of the cleaning fluid *in situ*, prior to being removed by the rollers and hydraulically conveyed out of the tubes. For the vertical Tubular Filter Press the cake is removed by the combined action of the cylindrical shape of tube curtain collapsing when not pressurised in dead-end mode as during the filtration cycle, and series of flush cycles. The combined action of the flush fluid and the weight of the cake is sufficient to remove most of the cake from the tubes. The rollers are only used during the final flush cycle to remove any remaining cake (which is usually negligible). As such, cake losses are mainly due to hydraulic conveyance only and the shear model developed by Rencken (1992), is not directly applicable.

Chapter 4

Experimental Study of Compressible Cake Filtration

Water from the Inanda Dam (KwaZulu-Natal), is treated at the Wiggins Water Works. The sludge used for this investigation was obtained from clarifier and sand filter backwash water at Wiggins Water Works. At the water works, the raw water is first treated using lime to adjust the pH of the raw water just prior to coagulation. A blended polymeric coagulant consisting of poly-aluminum-chloride and di-methyl-di-allyl-ammonium-chloride is then added, bentonite is used as a coagulant aid. The flocculated particles are allowed to settle in Degremont type pulsator clarifiers which produces a sludge concentration of approximately 2 to 5 kg/m³. Rapid gravity sand filtration removes any further solids present in the water after clarification. The backwash water emanating from the sand filters is combined with the clarifier sludge and thickened to a solids concentration of approximately 10 to 30 kg/m³. The sludge used for the laboratory-scale tests was drawn from the bottom of the holding tank of the Tubular Filter Press at the Wiggins Water Works when the full-scale plant tests were being conducted on the Tubular Filter Press. This sludge was sieved at 210 µm to remove any debris.

4.1 DETERMINATION OF SOLIDS DENSITY

Five density bottles (pycnometers) were cleaned and dried using acetone, and the bottles weighed accurately. The stoppers were removed from the bottles, and the bottles were filled with distilled water, ensuring that no air was trapped on the inside. The stoppers were then replaced and the bottles immersed in a water bath set at 25 °C. After half an hour each bottle was removed from the water bath, the exterior dried rapidly yet thoroughly, and the combined mass of the bottle and distilled water determined. From the density of water at 25 °C the exact volume of each bottle with its stopper, at 25 °C, was determined.

The bottles were then thoroughly dried using acetone and the mass of each bottle determined once again. A sample of sludge was dried in an oven at 105 °C and the dry solids crushed into a fine powder using a mortar and pestle. A representative sample of the solids was added to each bottle and the mass of solids in each bottle determined by difference. The bottles were then carefully filled with distilled water, ensuring no air was trapped on the inside of the bottle or in the solids. The stoppers were inserted in the bottles and the bottles immersed in the water bath set at 25 °C. After half an hour the bottles were removed from the hot water bath, the exterior dried thoroughly, and weighed.

The volume of solids in each bottle was determined from the difference between the bottle volume and the volume of water in each bottle. The density of the solids in each bottle could then be determined from the solids mass and solids volume.

4.2 COMPRESSION - PERMEABILITY CELL TESTS

4.2.1 Experimental System

A schematic of the C-P cell used during this study is shown in Figure 4.1. The C-P cell was constructed based on the design given by Rowe et al. (1966), and used by Rencken (1992), but has been modified to include a *floating* bottom that enables the transmitted pressure to be measured.

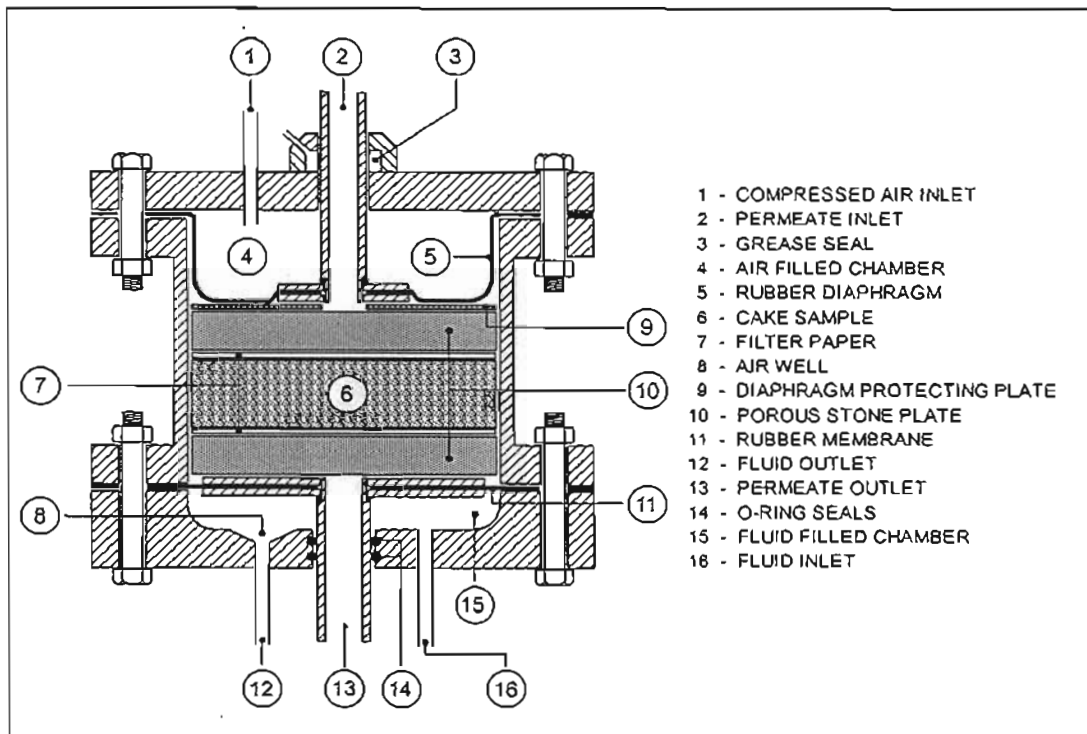


FIGURE 4.1 : Schematic Diagram of Compression-Permeability Cell

The entire cell is constructed out of 304 stainless steel which is resistant to corrosion. The base and cover are bolted to the flanges of the cell body at six positions, the top rubber diaphragm and bottom rubber membrane serving as gaskets. A uniform load is applied to the sample by increasing the air pressure in the air filled chamber. A thin plastic plate is placed on top of the top porous plate to prevent the damage to the rubber diaphragm. A grease seal enables the permeate inlet stem to move *frictionlessly* through the cover whilst still maintaining the air pressure in the air filled chamber. The grease seal also serves the secondary function of ensuring the inlet stem remains true. The rubber diaphragm is clamped tightly between two

plates which screw onto the inlet stem, an o-ring at the base of the thread completes the seal. Consolidation of the sample is measured at the centre by a dial gauge at the top of the inlet stem. The dial gauge is rigidly supported by an adjustable arm attached to the edge of the cover so that it is free from deflection due to distortion of the cover with changing pressure. A top and bottom filter paper separate the cake sample from the two porous discs. The inner wall of the cell body is polished to reduce any friction between the wall and the cake sample. The outlet stem is attached to the bottom rubber membrane by two plates in the same manner as described for the top diaphragm, providing a false bottom that *floats* on a fluid filled chamber that has been machined out of the base of the cell. Any force on the bottom porous plate will be transmitted to the fluid, the associated increase in pressure is measured with a fluid filled pressure gauge. The fluid is incompressible so no movement of the bottom plate should occur. Two o-rings complete the seal in the fluid filled chamber where the outlet stem passes through the base.

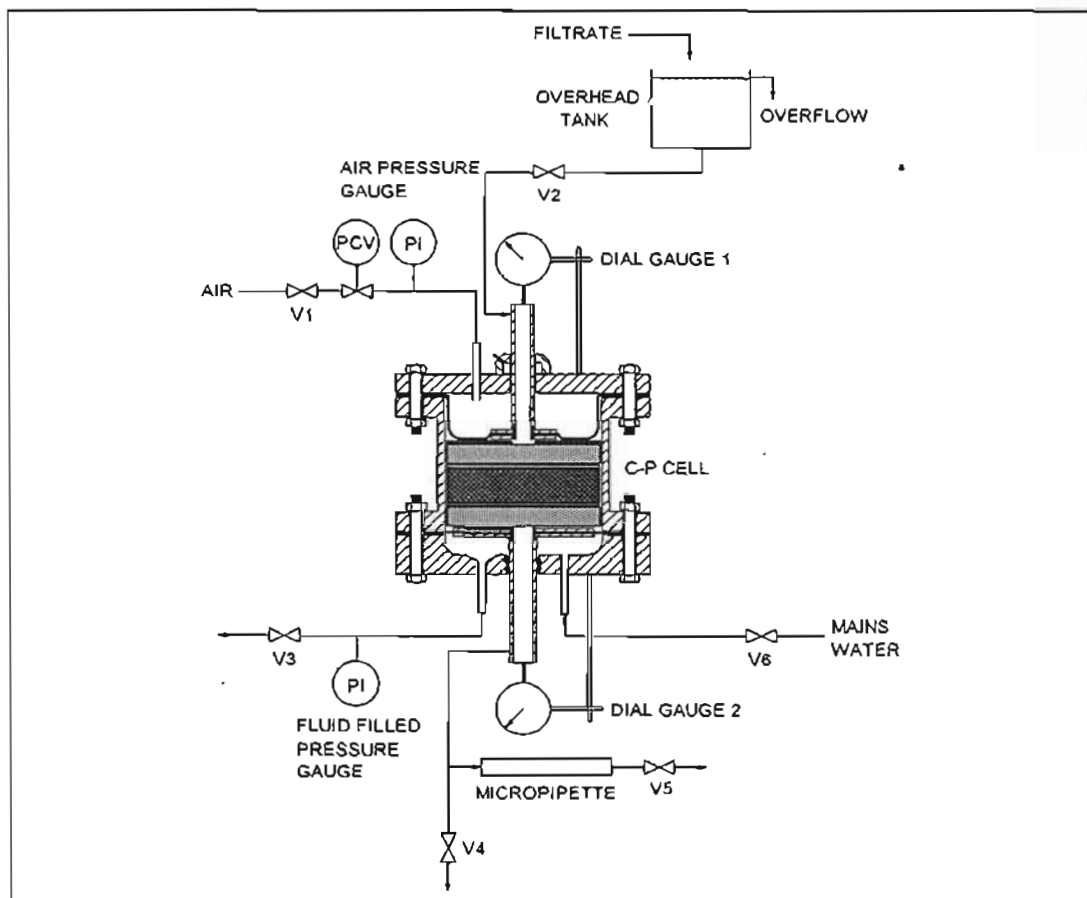


FIGURE 4.2 : Process Schematic of Compression-Permeability Cell

Once the base of the cell is assembled, air is removed from the fluid filled chamber by inverting the cell and flushing with fluid at a high flow rate, any trapped air is entrained out of the chamber. To facilitate the air clearing, all corners are machined round where possible and an air well is machined into the base at the fluid outlet. Any air that may be trapped inside the

fluid filled chamber will contract as the fluid pressure increases, the associated movement of the bottom plate, if excessive, will disrupt the cake structure which is undesirable. A dial gauge attached to the permeate outlet in the same manner as described above will measure any movement of the bottom plate.

A process schematic of the C-P cell apparatus is shown in Figure 4.2. Filtrate is stored in a header tank and allowed to flow down the inlet stem through the cake and then through a micropipette to enable the measurement of the volumetric flow rate of the permeate. The level of filtrate in the header tank, and hence the hydrostatic head, is fixed by an overflow pipe. The cake is compressed by the pressure exerted on the top porous plate by the rubber diaphragm. The air pressure is controlled with a pressure control valve. The transmitted pressure is measured by the fluid filled pressure gauge attached to the fluid filled chamber. The fluid inlet line is attached to the mains water.

4.2.2 Experimental Procedure

4.2.2.1 Assembly

The base of the cell was bolted tightly to the cell body using the bottom rubber membrane as a gasket, which in turn was tightly clamped between the two bottom plates screwed onto the permeate outlet stem. The assembled base was then inverted and valves V3 and V6 opened. The mains water was then turned on at a low flow rate and the bottom chamber was filled with water and most the air expelled. The water flow rate was then increased and any remaining trapped air entrained out of the chamber. Valves V6 and then V3 were closed in quick succession so that the fluid pressure inside the chamber was at ambient pressure and not the mains water pressure. The assembled base was then placed upright and the bottom dial gauge attached to the permeate outlet stem. The cell was then filled with filtrate and valves V4 and V5 opened so that the air in the feed line to the micropipette and the pipette by-pass line was expelled. Valves V4 and V6 were then closed. A porous disc which had been soaked in water to remove air and debris from the pores was then allowed to settle into the filtrate onto the bottom of the cell. A glass micro-fibre filter paper which had been cut to a diameter slightly larger than the diameter of the cell and soaked in water to remove any air was carefully placed onto the surface of the filtrate in the cell ensuring that no air was trapped underneath. The filter paper was then placed on top of the bottom porous disc ensuring that a proper seal was formed between the filter paper and the sides of the cell. Valve V4 was then opened and the filtrate in the cell allowed to drain to just above the bottom filter paper. The cell was then partially filled with a concentrated slurry, density approximately 86 kg/m^3 , leaving sufficient room for the top porous disc. Filtrate was then poured gently on top of the slurry through a porous disc held just above the surface of the slurry so as not to disturb it. The remainder of the cell was filled with clear filtrate in this manner. Valve V4 was then opened to ensure that the bottom seal had not

been compromised and the permeate was clear, valve V4 was then closed. A second filter paper cut to the same diameter of the cell, which had been soaked in water was then placed on the surface of the filtrate ensuring no air bubbles were trapped underneath and allowed to settle onto the slurry. The second porous disc was then placed in the cell and allowed to settle onto the filter paper. The cell was then left overnight to allow the slurry to gently consolidate under the weight of the top porous plate. Valve V2 was then opened and the supply line to the permeate inlet stem cleared of any air. The plastic diaphragm protecting plate was placed on top of the top porous plate. The entire top assembly was then carefully lowered on top of the cell whilst filtrate flowed out of the permeate inlet stem, ensuring that no air was trapped between the diaphragm and the top porous disc. The top was then tightly bolted to the cell using the rubber diaphragm as the gasket. The header tank was then filled with filtrate, the level in the header tank was fixed, and valve V4 was opened.

4.2.2.2 Compression

The pressure in the diaphragm was slowly increased in small increments to the first applied pressure of approximately 50 kPa so as not to disturb the cake in the cell. This was important as the cake at this stage was not consolidated and very unstable. The cell was then left for several hours for the cake to consolidate. The top dial gauge was then attached to the top of the permeate inlet stem. Consolidation equilibrium was determined when movement of the permeate inlet stem, as observed on the top dial gauge, had ceased. In order to measure the permeate flow rate, valve V5 was opened and the level in the micropipette allowed to drop, valve V4 was then closed and the permeate timed over a measured change in volume in the micropipette. Valve V5 was then closed and valve V4 opened. The applied and transmitted pressures and the readings on the top and bottom dial gauge were then recorded. The applied pressure was then increased in increments of approximately 50 kPa, allowing consolidation equilibrium to be reached at each pressure, up to a final pressure of 450 kPa and further readings obtained in the same manner.

At the end of the run, the applied pressure was cut-off and all valves closed. The cell was then carefully disassembled and the highly consolidated cake removed from the cell body and weighed. Any irregularities in the cake, if present, were observed. The cake was then placed in an oven at 120 °C for at least 5 hours and re-weighed to determine the mass of solids in the cake.

4.3 SETTLING TESTS

4.3.1 Experimental Procedure

4.3.1.1 Determination of Porosity at Low Solids Compressive Pressures

Different quantities of homogenised sludge were introduced into various glass and polypropylene measuring cylinders with internal diameters ranging from 60 - 90 mm. It was assumed that the internal diameter and material of the measuring cylinders would not have any significant effects on the settling behaviour of the sludge. The initial heights of the sludge in the cylinders were recorded, and ranged from approximately 60 - 900 mm. The initial solids concentration of the sludge was sufficiently high so as to be in the region where settling occurs due to consolidation and not free or hindered settling. The sludge in the cylinders was left to stand undisturbed in a controlled environment for 3 weeks, by which time settling or consolidation of the sediment had ceased, and the final equilibrium height had been attained. The final equilibrium heights were recorded.

4.3.1.2 Determination of Permeability at Low Solids Compressive Pressures

Homogenised sludge was introduced into three glass measuring cylinders, at three different initial heights. The glass cylinders had an internal diameter of 50 mm and a volume of 500 ml. The initial heights of the sludges were recorded and height of the interface between the sediment and the supernatant liquid recorded with respect to time to determine the initial settling velocity of the surface of the sediment. This procedure was repeated over a range of initial solids concentrations from approximately 40 to 80 kg/m³.

4.4 DIRECT SHEAR TESTS

4.4.1 Experimental System

A schematic diagram of the shear box that was used for the direct shear experiments is shown in Figure 4.3.

The direct shear apparatus consisted of a inner square metal shear box that was open at the top and the bottom and split horizontally across the middle into two parts. The inner shear box was held uniformly together by four aligning pins at the corners of the box (these pins were removed at the start of the shear test). The bottom half of the inner shear box fitted firmly into a square depression in the centre of the base of the larger outer metal box. The top half of the

inner shear box had a fixed arm that extended over the top of the outer box and made contact with a force transducer. The force transducer was fixed (and hence the top half of the inner shear box was fixed) and measured the horizontal shear stress on the cake sample during the course of the test. The cake sample was held between two porous stone plates, a toothed grid with drainage holes was placed between the bottom porous plate and the cake sample with the serrations of the toothed grid at right angles to the direction of shear. A metal pressure pad was placed on top of the top porous plate. A metal yoke pivoted on the centre of the pressure pad and hung over and below the direct shear box, the normal stress was applied to the cake sample by stacking metal weights onto the bottom of the hanger. The outer box sat on a carriage with ball bearings and was movable. Movement was facilitated by a chain driven pulley system, driven by an electric motor. The motor had an elaborate gear system that enabled the movement of the outer box, and hence the shear rate, to be adjusted. A dial gauge measured the horizontal shear displacement.

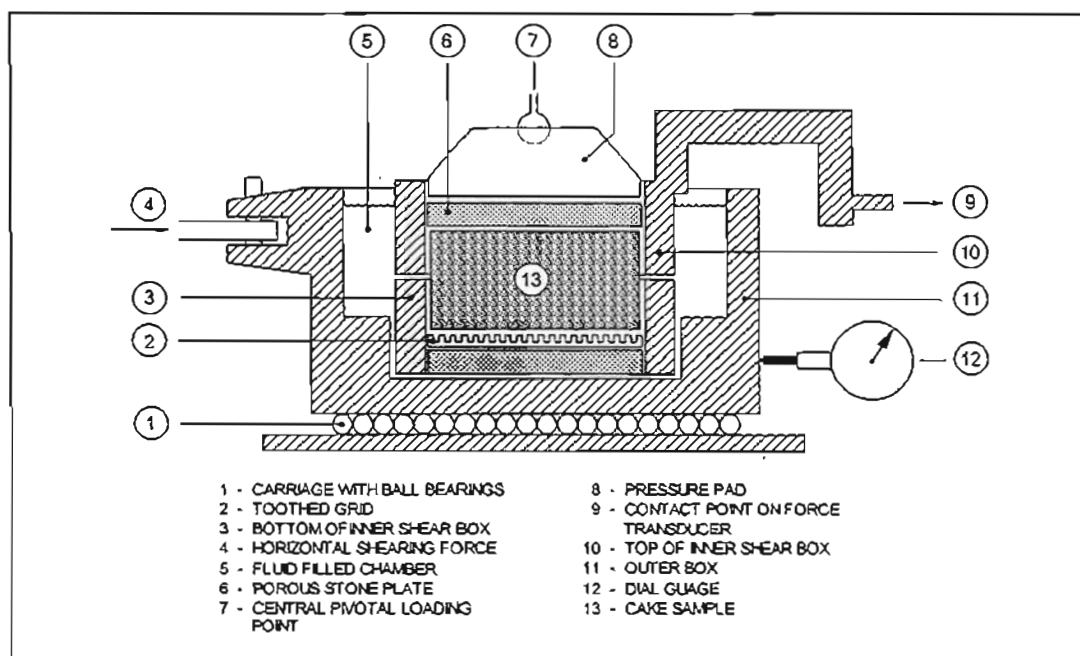


FIGURE 4.3 : Schematic Diagram of Direct Shear Box

4.4.2 Experimental Procedure

A representative sample of the filter cake obtained from the full-scale plant tests at the Wiggins Water Works was homogenised into a paste, this paste was used in the direct shear tests. The solids concentration of the paste was determined.

The inner shear box with aligning pins in place was placed into the outer box and the position of the outer box was adjusted so that the fixed arm of the top half of the shear box was in contact with the force transducer. The porous stone plate which had been soaked in water was placed in the bottom of the shear box followed by the toothed grid. The shear box was filled

uniformly with the cake sample to just below the top of the shear box. Another porous stone plate which had also been soaked was placed on top of the cake sample and the pressure pad placed on top of the stone plate. The outer box was then filled with filtrate. The hanger was placed on the top of the pressure pad and the aligning pins removed from the shear box. The sample was then loaded to the desired normal stress by adding standardised weights to the bottom of the hanger. The weights were added gradually so as not to squeeze the sample out of the inner shear box. The cake sample was allowed to consolidate overnight.

Following consolidation of the sample, the dial gauge which measures horizontal shear displacement was fixed into position and the initial reading noted. The gears on the motor were adjusted so that the horizontal shear rate was sufficiently slow so as to permit drainage in the sample and prevent the build up pore water pressure. This was verified later. The motor that controls the shear rate was started, the slack in the chain was taken up and the gap between the fixed arm of the upper half of the shear box and the force transducer closed. Readings of horizontal shear stress versus horizontal shear displacement were then taken until the shear stress remained constant indicating that shearing was complete.

Three direct shear boxes were set up in the same way as described above, but each with a different normal stress, the tests were conducted simultaneously. On completion of the tests the force transducers were calibrated using the hanger and the standardised weights.

4.5 PLANAR FILTRATION TESTS

4.5.1 Experimental System

A schematic diagram of the apparatus used for the planar filtration tests is shown in Figure 4.4.

The filter cell consisted of a stainless steel cylinder with an internal diameter of 0.145 m. The base and the cover were bolted onto the flanges of the cell body at six locations, rubber gaskets completed the seal. Pressure was applied to the sludge in the cell by means of compressed air, the compressed air inlet was in the cover of the cell. The base of the cell had been machined out so that the porous stone plate fitted neatly inside and its top surface lay flush with the top of the base. The filter paper lay across the top of the base and porous stone plate. The filtrate outlet emptied into a large beaker which was placed on an electronic mass balance.

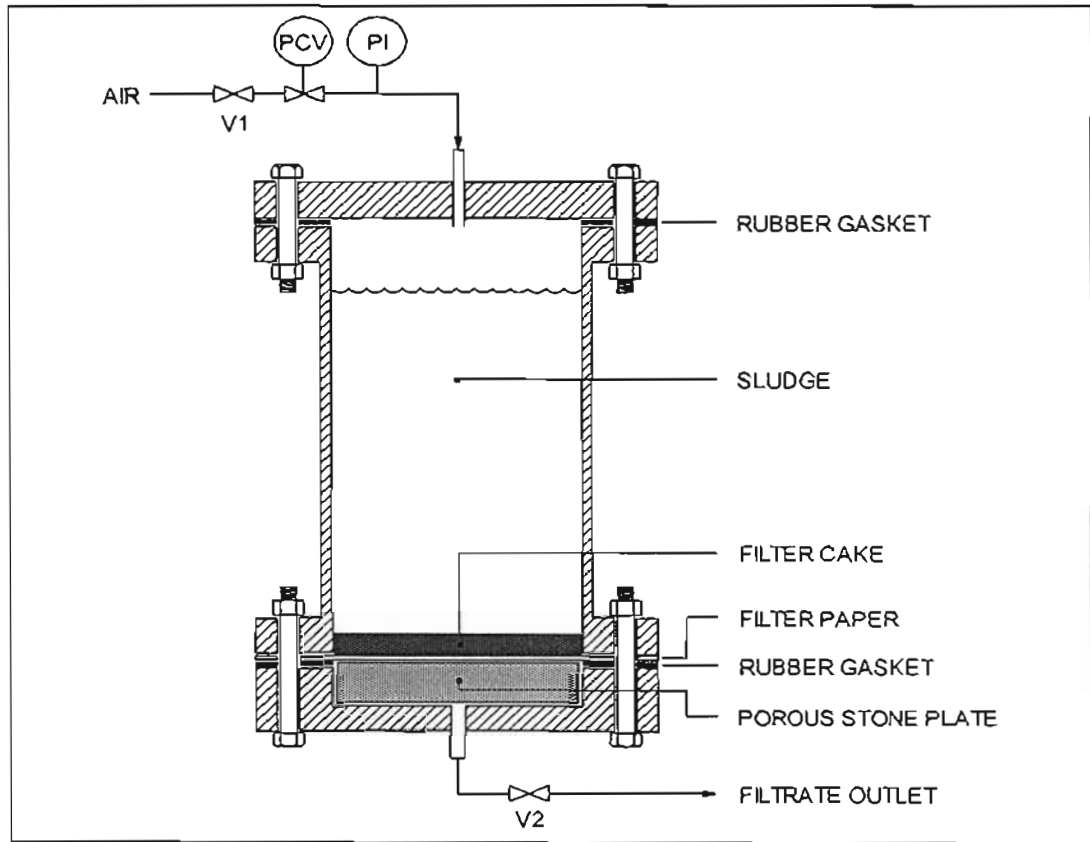


FIGURE 4.4 : Schematic Diagram of Planar Filtration Cell

4.5.2 Experimental Procedure

The porous stone was placed within the base of the cell, and with the filter paper and rubber gasket in place, the body of the cell bolted onto the base. The cell was then partially filled with water. Valve V2 was opened and the water in the cell drained to immediately below the surface of the filter paper. Valve V2 was then closed. The homogenised sludge was poured into the cell and the cover quickly bolted onto the cell body. Valve V1 was opened and the desired filtration pressure was set with the pressure control valve. Valve V2 was then opened and the mass of filtrate was recorded with respect to time.

Once the required filtration time has elapsed, valve V2 was shut and the filtration terminated. Valve V1 was shut and the filtration pressure is released via the pressure control valve. The cover was removed from the cell and the remaining sludge was carefully poured from the cell body. The cell body was then carefully removed so as not to disturb the cake, the mass of the wet filter cake was determined and the thickness of the cake measured. The cake was then placed in an oven at 120 °C for at least 5 hours and re-weighed to determine the mass of solids in the cake.

It was assumed that any effects due to settling of the sludge during the course of the filtration were negligible.

and moulded into a top and bottom manifold. The inlet manifold has an orifice restriction at the inlet of each tube to ensure an even flow distribution between the tubes whilst the tubes are filling just prior to the filtration cycle or being flushed during the cake removal cycle.

The normal operation of the Tubular Filter Press is controlled by a Programmable Logic Controller (PLC). Instrument air is provided from a compressor to control the pneumatic valves. Outputs from the PLC are wired to relays in an electrical control panel where the operation of individual components of the Tubular Filter Press such as the pneumatic valves, pumps, stirrers, cake conveyor and roller cleaning carriage can be controlled by switching the control status between automatic and manual and utilising the start and stop switches.

Prior to the initiation of the filtration cycle, the state of control of all the components of the Tubular Filter Press are switched to automatic and the stirrers in the feed and pre-feed tanks are started. The PLC program is then started by depressing the main start button on the control panel. If the level of the sludge in the feed tank is sufficiently high, as determined by the level switches in the feed tank, the feed valve (valve V2) will open, the discharge valve (valve V5) and the flush valve (valve V1), will close (if not already closed), and the MONO feed pump (pump P3) will start automatically. If the level of sludge in the feed tank on start-up is too low, or if during the course of the filtration the level in the feed tank drops and triggers level switch LS3, the raw sludge valve (valve V7) will open and the centrifugal raw sludge pump (pump P1) will start automatically. Sludge from the sludge holding tank will be pumped into the pre-feed tank and the overflow from the pre-feed tank will flow into the feed tank. If the level in the feed tank rises and triggers level switch LS1, the raw sludge pump will stop and the raw sludge valve will close automatically.

With the discharge valve closed, the tubes began to fill and filtration commenced. Once the tubes had completely filled, the pressure in the tubes rose to a constant pre-set operating pressure. The operational pressure of the Tubular Filter Press could not be set to an immediate fixed value, as the pressure response was dependent on the degree of flow resistance or *back-pressure*. The operational pressure increased as the resistance to flow increased when cake is deposited on the inside of the tubes. The maximum operating pressure was controlled by regulating the recycle flow back to the feed tank via the manually controlled pressure control valve (valve V8). During the filtration, the filtrate permeated out and ran down the sides of the porous fabric tubes, and was collected in a permeate collection tray situated immediately below the tube curtain. The overflow from the permeate collection tray flowed to the permeate tank. The flow rate and volume of the feed sludge pumped to the tube curtain was measured by an electromagnetic flow meter. In addition the electromagnetic flow meter sent an electronic pulse to the PLC for every litre of feed sludge pumped. The PLC used this pulse to determine when to terminate the filtration cycle. During the course of the filtration the cake

thickness increased, and as a result the permeate flow rate (as determined by the feed flow rate) decreased, when the time between pulses increased beyond a pre-set value, the filtration cycle was terminated. The feed pump was stopped and the discharge valve opened.

The discharge valve opened onto a porous conveyor belt which was situated above the feed tank. The sudden release in pressure and associated collapse of the porous tubes caused some of the cake to break away from the inner walls of the porous tubes and to flow out of the tubes along with the excess feed sludge. The cleaning cycle was then initiated. The cake conveyor was started and the spray valve (valve V4) was opened automatically. The centrifugal flush pump (pump P4) was started against the closed flush valve. The PLC then initiated a series of timers to open and close the flush valve, and hence initiate a predetermined number of flushes of a predetermined duration. During a flush, the feed sludge was pumped through the tubes at a high flow rate, to effect the removal of the remaining cake from the tube walls. The flow rate of the flush fluid could be regulated by the manual valve V12. Whilst the cake that was discharged onto the conveyor belt was being conveyed towards the cake collection bins, the excess feed sludge drained through the porous conveyor belt and back into the feed tank. The cake was dumped into the cake collection bins situated at the end of the conveyor belt. A jet of water was directed onto the conveyor belt to keep the conveyor belt clean in order to facilitate better draining of the excess feed sludge. The filter cake reported to cake collection bin 2, whilst mainly flush fluid that had drained through the conveyor belt as well as some cake that clung to the conveyor belt reported to cake collection bin 1 which is placed below where the conveyor extends beyond the feed tank.

Situated at opposite sides and parallel to the tube curtain, are the pair of horizontal rollers of the cleaning carriage. The rollers engage automatically at the top of the tube curtain during the last flush cycle. The rollers constrict the tubes leaving a narrow gap which dramatically increases the velocity and turbulence of the flush fluid at that point in each tube. The carriage moves down the tube curtain effectively removing any remaining cake and cleaning the inside of the tubes. The cleaning carriage utilises an electric motor with a gear and chain mechanism to move at approximately 4.5 m/min. When the carriage reaches the bottom of the tube curtain, a limit switch signals the PLC, the rollers are released, the cake conveyor stopped and the spray valve closed automatically. During normal operation, the filtration cycle was then initiated once more.

4.6.2 Experimental Procedure

During normal operation of the Tubular Filter Press, sludge from the water treatment plant is continually fed to the sludge holding tank. The filtration characteristics of the sludge fed to the Tubular Filter Press may be variable due to the variable nature of the raw water to the water

treatment plant. In order to ensure that the filtration characteristics of the sludge under investigation remained constant, the system was closed. The total amount of sludge in the sludge holding tank, pre-feed tank and feed tank was estimated to be in the region of 5 m³ and to have an average concentration of approximately 26 kg/m³.

Prior to commencing a run the sludge was *conditioned* for at least an hour. Manual valves V3, V6 and V10 were closed and V9, V11 and V12 were opened. The control state of the raw sludge valve and raw sludge pump was switched to manual, the stirrers in the feed tank and pre-feed tank were started, the raw sludge valve was opened and the raw sludge pump started. A submersible pump was placed in the feed tank and the sludge in the feed tank pumped back to the sludge holding tank. Conditioning entailed mixing the sludge thoroughly in the feed and pre-feed tank and circulating the sludge between the holding tank and the feed tank via the pre-feed tank using the submersible pump and the raw-sludge pump. The purpose of conditioning the sludge in this manner was to ensure that the solids concentration of the sludge in each tank was equal and that the filtration characteristics of the sludge remained constant for each run. The level in the feed tank was monitored and occasionally the raw sludge pump had to be turned off to avoid overflow in the feed tank. The solids concentration in each tank was monitored directly using an electronic solids concentration meter, when the solids concentration in each tank was relatively equal, a representative sample of the sludge in the feed tank was taken to accurately determine the feed solids concentration via a gravimetric method. The submersible pump was switched off and when the feed tank reached capacity the raw-sludge pump was switched off, the raw sludge valve was closed and the control state of the raw sludge valve and raw sludge pump switched from manual to automatic.

The mass of the cake collection bins were determined and the bins placed at the end of the cake conveyor. The limiting pulse time on the control panel was set. The filtration cycle was then initiated. The volume of sludge pumped and the reading on the pressure gauge was then recorded with respect to time. The filling of the tubes was observed and the time required to fill the tubes was observed and recorded. A representative sample of filtrate was collected.

The number of flushes and the flush flow rate was kept constant for all the plant runs. The tubes were flushed 3 times, during the final flush, the roller cleaning carriage was engaged. The extent of the cake recovery for each flush was observed. At the end of the cake removal cycle, the PLC program was stopped before another filtration cycle was initiated. The combined mass of the cake and cake collection bins was determined. A representative sample of cake was taken from each collection bin to determine the average cake dry solids concentration. Since it was believed that flush fluid could report to the cake collection bins if drainage on the cake conveyor was inadequate, a second representative sample of cake was taken from cake collection bin 2 was placed on a wire screen where it was allowed to drain over a period of

time. The cake samples were weighed, then placed in an oven at 120 °C for at least 5 hours and re-weighed to determine the mass of solids in the cake.

The cake was then dumped into the permeate tank. The control state of the raw sludge valve and the raw sludge pump was switched to manual. The raw sludge valve was closed (if not already closed), valves V10 and V3 were opened manually and valve V9 was closed manually. The raw sludge pump was then started and the contents of the permeate tank circulated until the cake in the permeate tank had been sufficiently redispersed. Valve V6 was opened manually and then valve V3 closed manually and the contents of the permeate tank pumped into the sludge holding tank. The level in the permeate tank was monitored and the raw sludge pump stopped when the level was just above the intake for the pump. Valves V10 and V6 were then closed and valve V9 opened manually.

Runs were performed at a high and a low feed solids concentration. To reduce the feed solids concentration of the sludge, the contents of the feed tank was purged from the system using the submersible pump. The feed tank was then filled with water. The sludge was then conditioned thoroughly until the feed solids concentration in all the tanks was constant. It was assumed that the addition of water to the system did not affect the filtration characteristics of the sludge.

4.6.3 Determination of Medium Resistance

During the process of reducing the feed solids concentration of the sludge, the feed tank was drained, rinsed thoroughly and filled with mains water. Prior to conditioning the system, the mains water in the feed tank was used to determine the resistance of the tube curtain fabric.

The control state of the raw sludge pump and raw sludge valve was switched to manual, to ensure that during the course of the test the level switches in the feed tank did not cause the PLC program to automatically start the raw sludge pump and contaminate the water in the feed tank with sludge from the pre-feed tank. The filtration cycle was then initiated and the volume of water pumped and the tube pressure was recorded with respect to time. After the pressure in the tubes had stabilised and a sufficient period of time had elapsed, the cleaning cycle was initiated manually from the electronic control panel. Two tests were conducted in this manner.

Chapter 5

Results and Discussion

The results of the experimental study on constant pressure compressible cake filtration are presented and discussed. The mathematical model for constant pressure compressible cake filtration, and the associated solution procedures that have been developed, are evaluated and discussed.

5.1 DETERMINATION OF SOLIDS DENSITY

The results of the experiments to determine the density of the solids in the sludge are tabulated in Appendix A.

The average density of the solids was found to be 2314.3 kg/m³.

5.2 RESULTS OF COMPRESSION - PERMEABILITY CELL TESTS

The purpose of these experiments was to determine the permeability and porosity characteristics of the sludge, in the higher solids compressive pressure range and to determine the effects of wall friction on the accuracy of C-P cell testing. The analysis of the results is divided into two sections. The results are initially presented assuming no wall friction effects (standard analysis), and then corrected for the effects of side wall friction.

The results of the C-P cell tests are tabulated in Appendix B.

5.2.1 Standard Analysis

Plots of permeability and solids volume fraction versus solids compressive pressure for Test B.1 and Test B.2 are shown in Figure 5.1 and Figure 5.2 respectively. For the standard analysis the solids compressive pressure is assumed to be given by the applied pressure. Over the range of solids compressive pressure for the tests, the data was subdivided into regions that showed greater individual linearity in accordance with Equations 3.3.

Linear regression analysis using the permeability versus solids compressive pressure data in each of the regions A, B and C (as shown in Figure 5.1), and over the entire data range ABC, for the two tests yielded values for F and δ in each of these regions (see Equations 3.3). The results of the linear regression analysis are shown in Table 5.1.

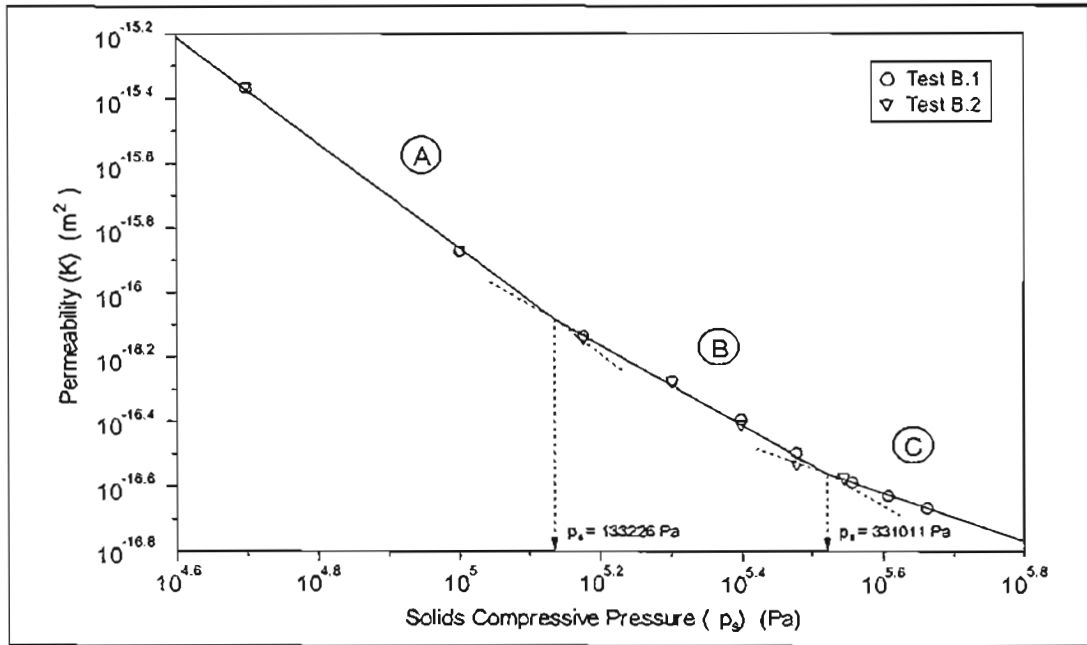


FIGURE 5.1 : Permeability versus Solids Compressive Pressure for C-P Cell Experiments

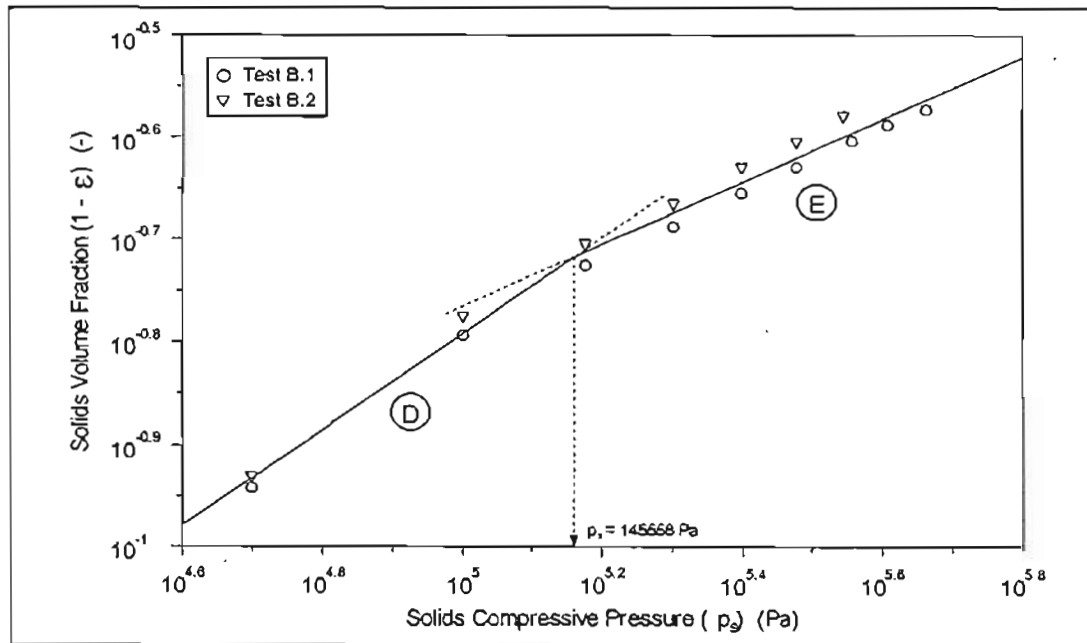


FIGURE 5.2 : Solids Volume Fraction versus Solids Compressive Pressure for C-P Cell Experiments

The intersections of each of the linear regions was calculated from the regression data and found to be at solids compressive pressures, $p_s = 133226$ Pa (region A-B), and $p_s = 331011$ Pa (region B-C).

TABLE 5.1 : Linear Regression Analysis on Permeability Data for C-P Cell Experiments B.1 and B.2 Combined

	Linear Region			
	A	B	C	ABC
F	1.911×10^{-8}	1.963×10^{-10}	4.289×10^{-13}	1.017×10^{-9}
δ	1.629	1.241	0.759	1.37
r^2	0.999	0.989	0.998	0.989

where r^2 = correlation coefficient for the linear regression analysis.

Linear regression analysis using the porosity versus solids compressive pressure data in each of the regions D and E (as shown in Figure 5.2), and over the entire data range DE, for the two tests yielded values for B and β in each of these regions (see Equations 3.3). The results of the regression analysis are shown in Table 5.2.

TABLE 5.2 : Linear Regression Analysis on Porosity Data for C-P Cell Experiments B.1 and B.2 Combined

	Linear Region		
	D	E	DE
B	7.344×10^{-4}	5.039×10^{-3}	2.001×10^{-3}
β	0.468	0.306	0.38
r^2	0.989	0.943	0.976

The intersection of the two linear regions was calculated from the regression data and is $p_s = 145557$ Pa (region D-E).

5.2.2 Approximate Correction for Side Wall Friction

A computer program, CPCELL, was written in the C programming language to analyse the C-P cell data and to determine the parameters k_{of} and c in the wall friction model described in Section 3.6.1.2 such that the objective function given by Equation 3.130 was minimised. The program employs the numerical direct search optimisation technique known as the SIMPLEX method.

The results of the analysis for the C-P cell Experiment B.1 and Experiment B.2 are shown in Figure 5.3 and Figure 5.4 respectively and given in Table 5.3.

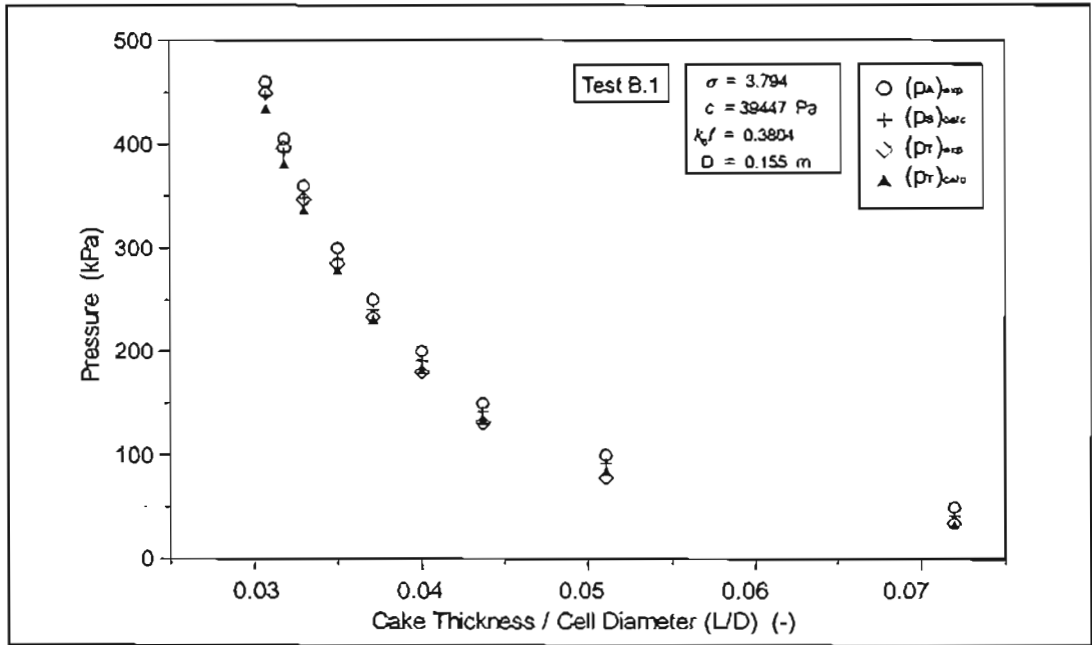


FIGURE 5.3 : Results of Wall Friction Analysis for Experiment B.1

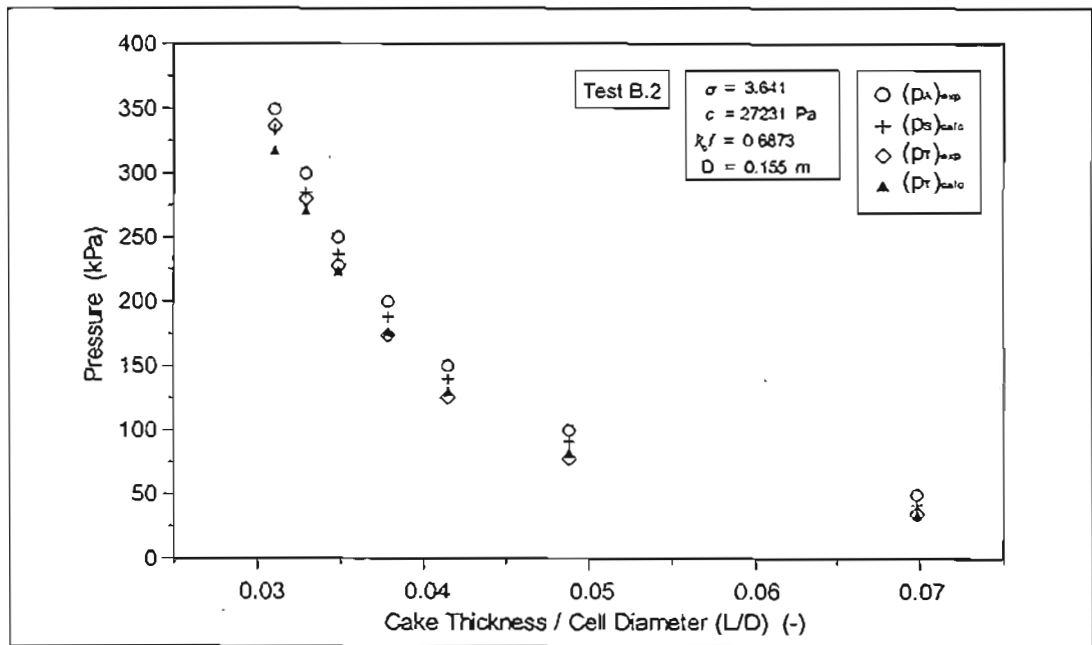


FIGURE 5.4 : Results of Wall Friction Analysis for Experiment B.2

TABLE 5.3 : Wall Friction Model Parameters for C-P Cell Experiments B.1 and B.2

	Test B.1	Test B.2
k_{0f}	0.38	0.687
c	39447 Pa	27231 Pa
σ	3.794	3.641

The accuracy of the wall friction model for predicting the transmitted pressure through the cake decreases for applied pressures greater than 250 kPa. In some cases the average solids compressive pressure through the cake as determined by Equation 3.129 is less than the experimentally measured transmitted pressure. For this reason, the corrected solids compressive pressure for the C-P cell tests for applied pressures greater than 250 kPa was determined by taking the average of the experimentally measured applied and transmitted pressures. For applied pressures of 250 kPa and less the corrected solids compressive pressure was determined from the wall friction model using Equation 3.129.

Plots of permeability and solids volume fraction versus the *corrected* solids compressive pressure for the two experiments are shown in Figure 5.5 and Figure 5.6 respectively. Over the range of solids compressive pressure for the tests, the data was subdivided into regions that showed greater individual linearity in accordance with Equations 3.3.

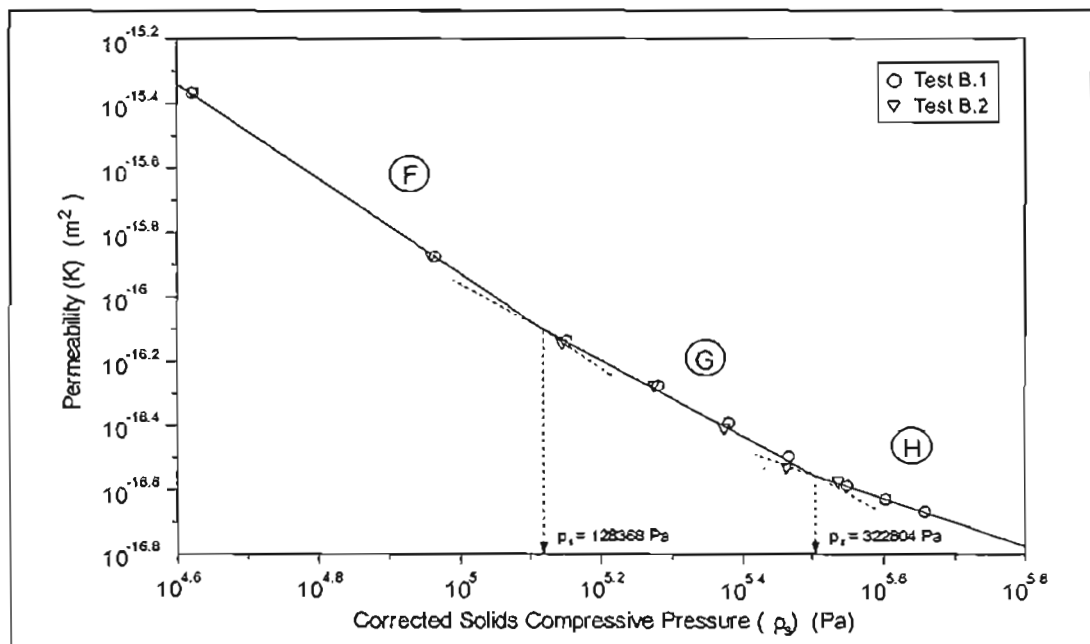


FIGURE 5.5 : Permeability versus Corrected Solids Compressive Pressure for C-P Cell Experiments

Linear regression analysis using the permeability versus *corrected* solids compressive pressure data in each of the regions F, G and H (as shown in Figure 5.5), and over the entire data range FGH, for the two tests yielded values for F and δ in each of these regions (see Equations 3.3). The results of the regression analysis are shown in Table 5.4.

The intersections of each of the linear regions was calculated from the regression data and found to be at $p_s = 128368$ Pa (region F-G) and $p_s = 322804$ Pa (region G-H).

TABLE 5.4 : Linear Regression Analysis on Permeability Data for C-P Cell Experiments B.1 and B.2 Combined and the Corrected Solids Compressive Pressure

	Linear Region			
	F	G	H	FGH
F	2.771×10^{-9}	9.145×10^{-11}	3.133×10^{-13}	3.139×10^{-10}
δ	1.474	1.184	0.736	1.28
r^2	0.999	0.987	0.999	0.991

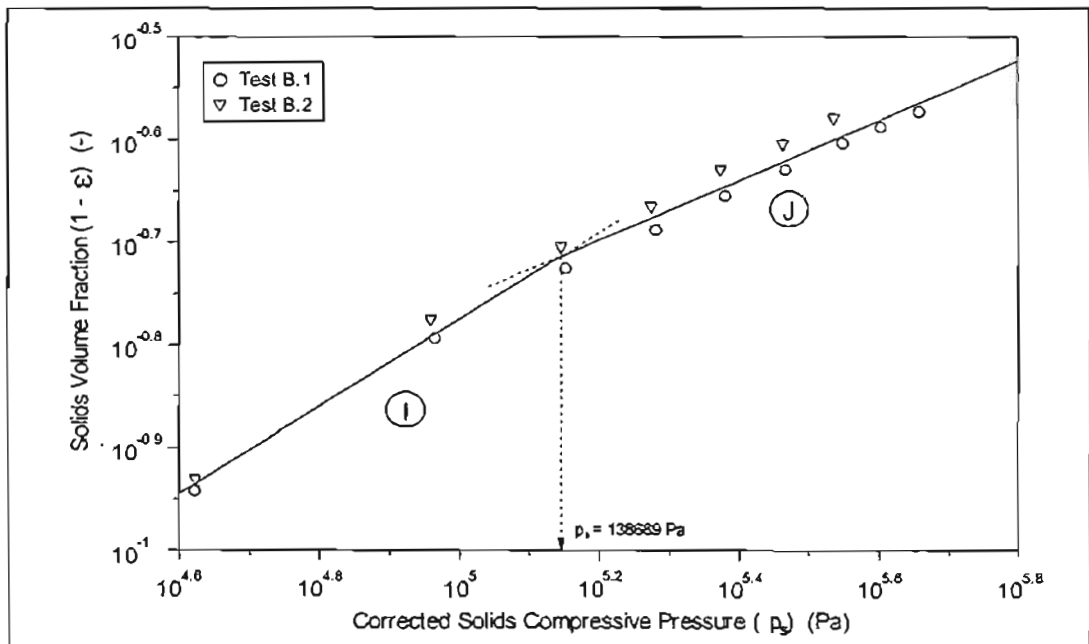


FIGURE 5.6 : Solids Volume Fraction versus Corrected Solids Compressive Pressure for C-P Cell Experiments

TABLE 5.5 : Linear Regression Analysis on Porosity Data for C-P Cell Experiments B.1 and B.2 Combined and the Corrected Solids Compressive Pressure

	Linear Region		
	I	J	IJ
B	1.281×10^{-3}	6.26×10^{-3}	2.773×10^{-3}
β	0.424	0.29	0.355
r^2	0.988	0.937	0.978

Linear regression analysis using the porosity versus *corrected* solids compressive pressure data in each of the regions I and J (as shown in Figure 5.6), and over the entire data range IJ, for the

two tests yielded values for B and β in each of these regions (see Equations 3.3). The results of the regression analysis are shown in Table 5.5.

The intersection of the two linear regions was calculated from the regression data and is at $p_s = 138669$ Pa (region I-J).

5.2.3 Common Experimental Problems

C-P cell tests are time consuming to set-up and a single experiment can last in excess of 12 hours, during the course of the experiment the test is prone to various operational failures and as a result experiments often have to be aborted.

Some of the more common experimental problems experienced were as follows:

- the top rubber membrane deteriorates with time and often develops pinhole leaks, allowing air to enter the cake sample,
- if an inadequate seal is formed between the bottom filter paper or the cake sample and the cell wall, or if the cake develops small cracks, the permeate bypasses the cake sample and results in exaggerated permeate flow rates, and
- if the fluid filled chamber is not adequately sealed, it will slowly drain under pressure, the resultant movement of the cell base deforms the cake sample.

5.3 RESULTS OF SETTLING TESTS

The results of the settling tests to determine porosity and permeability correlation data in the low solids compressive pressure range are tabulated in Appendix C.

5.3.1 Determination of Porosity at Low Solids Compressive Pressures

Settling tests (Tests C.1, C.2 and C.3) were performed using different volumes of sludge in measuring cylinders and allowing the sludge to settle over a period of 3 weeks. A plot of the final equilibrium height of the sediment versus the volume dry solids per unit cross-sectional area is shown in Figure 5.7. A linear regression analysis on the data yields values for the parameters a and b in accordance with Equation 3.138 of Section 3.6.2.1.

$$a = 23.90$$

$$b = 0.9808$$

$$r^2 = 0.995$$

From Equation 3.136 and Equation 3.137, the parameters B and β respectively, were determined (see Equations 3.3). The solids compressive pressure range for these experiments was, $19.15 \leq p_s \leq 400.58$ Pa.

$$B = 0.03558$$

$$\beta = 0.01915$$

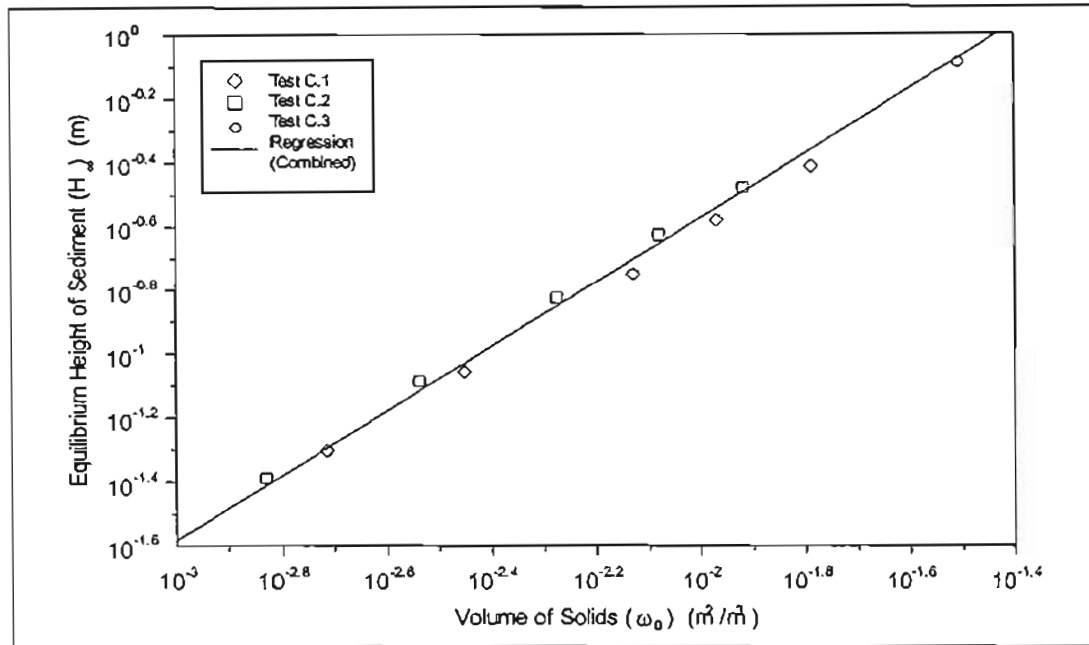


FIGURE 5.7 : Equilibrium Settling Heights of Sediment versus Volume of Solids per Unit Area

5.3.2 Determination of Permeability at Low Solids Compressive Pressures

Settling tests to determine permeability at low solids compressive pressure were performed using different initial concentrations of sludge, the results are tabulated in Appendix C. A plot of the initial settling velocity of the surface of the sediment versus the initial porosity of the suspension is shown in Figure 5.8. From Figure 5.8 the dilute, intermediate and consolidation settling regions were identified.

$$\varepsilon_L = 0.977$$

$$\varepsilon_{ij} = 0.9738$$

For each point in the consolidation settling region, $\varepsilon_{in} < \varepsilon_{ij}$, the permeability was determined from Equation 3.145 and the solids compressive pressure from the initial porosity of the suspension, and the porosity correlation parameters determined in Section 5.3.1 above, in accordance with Equation 3.135. A plot of the permeability versus solids compressive pressure is shown in Figure 5.9. A linear regression analysis on the data yielded values for F and δ (see Equations 3.3). The solids compressive pressure range for these experiments was $4 \times 10^{-7} \leq p_s \leq 40.6$ Pa.

$$F = 1.030 \times 10^{-13}$$

$$\delta = 0.05382$$

$$r^2 = 0.945$$

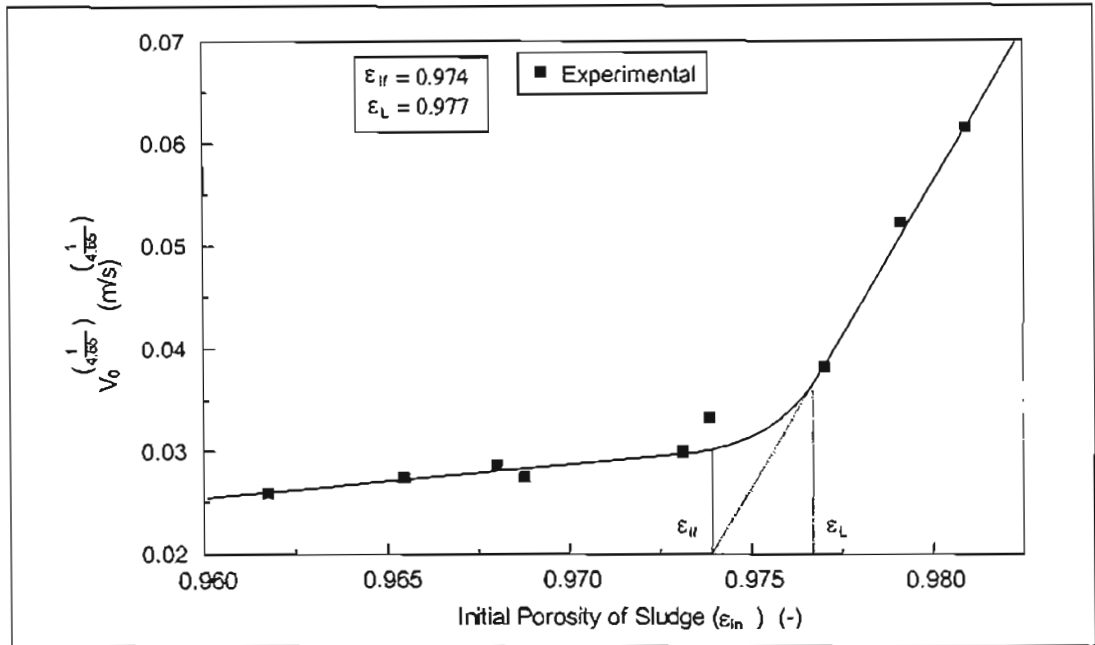


FIGURE 5.8 : Initial Settling Velocity of the Sediment Surface versus Initial Porosity of the Suspension

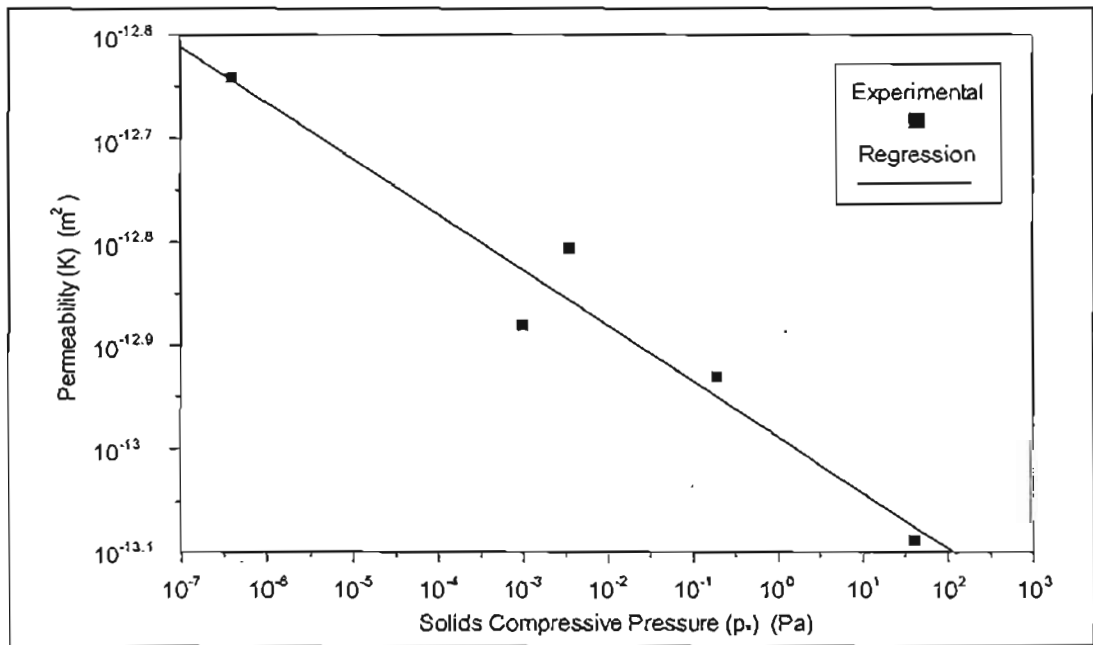


FIGURE 5.9 : Permeability versus Solids Compressive Pressure for Settling Experiments

5.4 RESULTS OF DIRECT SHEAR TESTS

The results of the three direct shear tests (Tests D.1, D.2 and D.3) to determine the angle of shearing resistance and hence the coefficient of earth pressure at rest are tabulated in Appendix D. A plot of horizontal shear force versus horizontal shear displacement for the three tests is shown in Figure 5.10, Figure 5.11 and Figure 5.12.

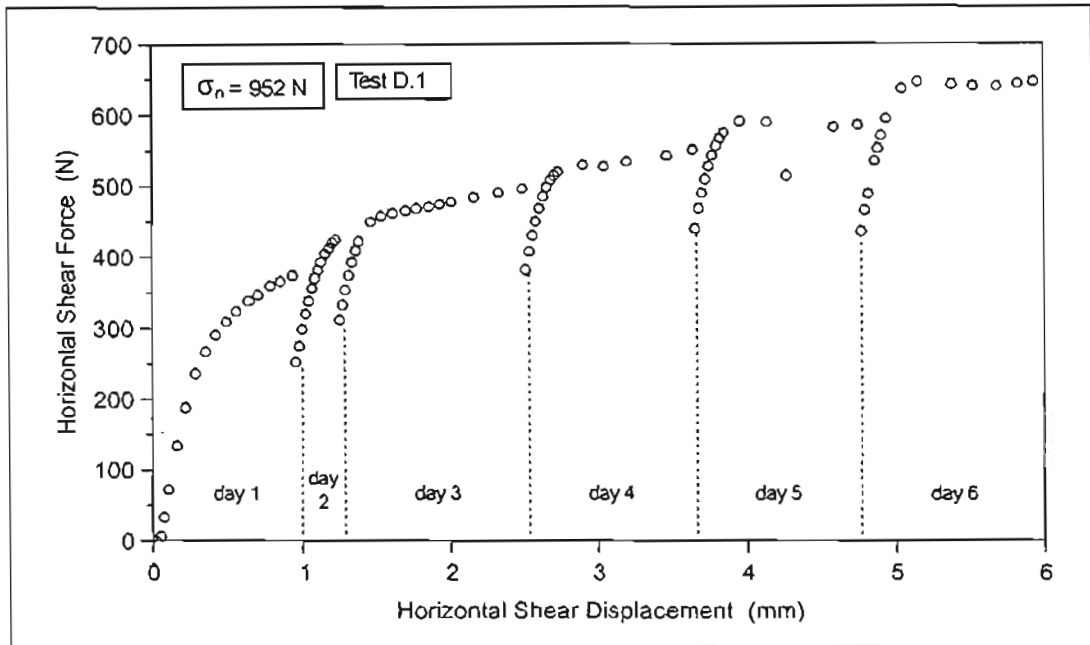


FIGURE 5.10 : Horizontal Shear Force versus Horizontal Shear Displacement for Direct Shear Test D.1

If the shear rate is too large, there is insufficient time for drainage of the pore water in the sample, and the associated increase in pore water pressure results in a reduced maximum shear stress where failure occurs. After completion of the first days shearing, the motor controlling the shear rate was shut down overnight, during this time any pore water pressure that may have built up, had time to dissipate.

On start up the following morning the shear stress rose steeply beyond the value where it appeared to be approaching a constant value the day before (This is clearly evident for Test D.1 and Test D.2). This indicated that the build up of pore pressure was indeed a problem and the initial shear rate for the tests was too great. For this reason the second days testing was terminated and the gears on the motor adjusted so that the sample would be sheared at half the original shearing rate.

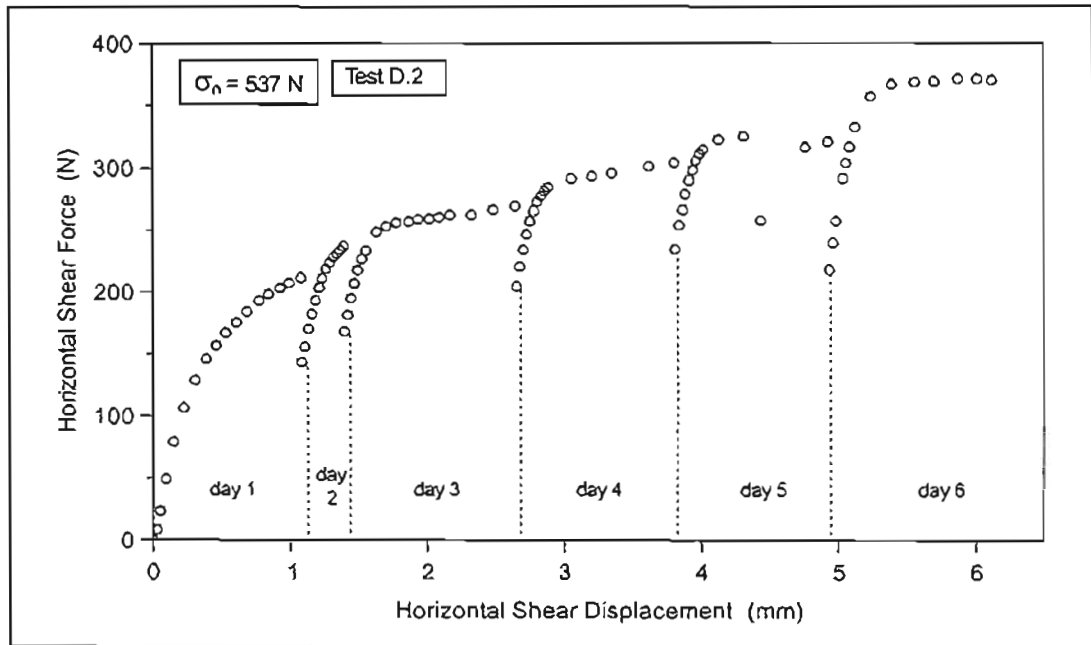


FIGURE 5.11 : Horizontal Shear Force versus Horizontal Shear Displacement for Direct Shear Test D.2

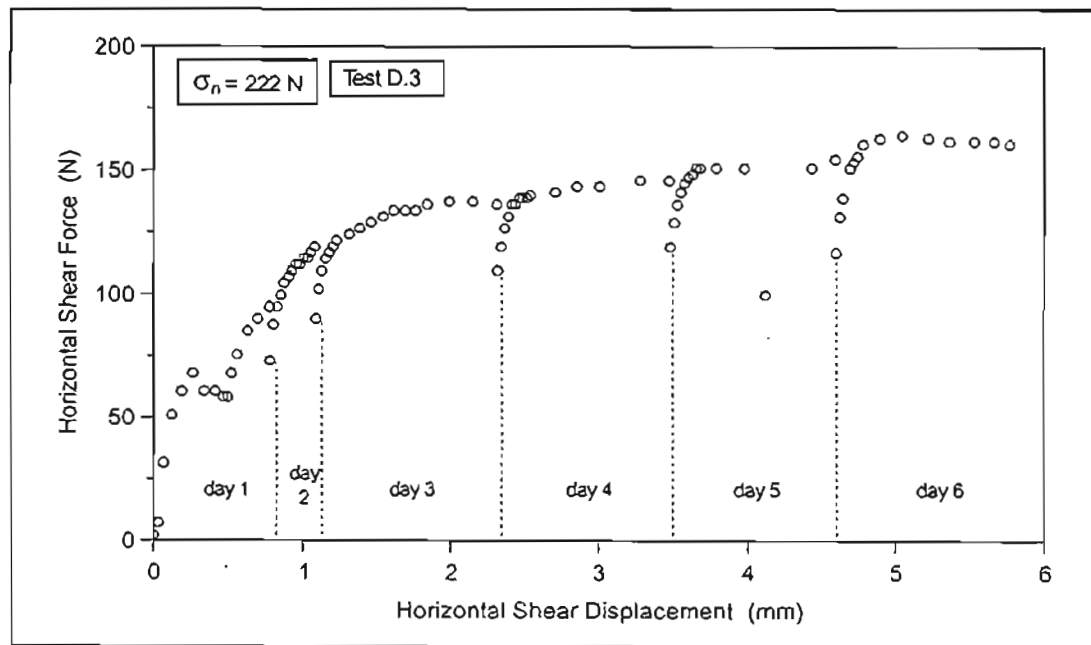


FIGURE 5.12 : Horizontal Shear Force versus Horizontal Shear Displacement for Direct Shear Test D.3

Since the direct shear tests took several days to complete, shut down of the motor overnight also facilitated in reducing the build up of pore pressure. The sudden drop in horizontal shear stress observed for all three tests during day 5 was as a result of the carriage that the shear boxes sit on being disturbed and the fixed arm of the top half of the shear box being displaced slightly away from the force transducer, this had no overall adverse effect on the test result. The shear test was complete when the sample failed and the horizontal shear stress reached a

constant value. The peak value indicated the horizontal shear stress where failure occurred. The horizontal shear stress is given by the horizontal shear force divided by the area of the shear box. The maximum horizontal shear stress where the sample failed is given in Table 5.6 for the three direct shear tests. A plot of the maximum horizontal shear stress versus the normal stress is shown in Figure 5.13.

TABLE 5.6 : Maximum Horizontal Shear Stress and Normal Stress Data for Direct Shear Tests

Test	Normal Stress (Pa)	Maximum Horizontal Shear Stress (Pa)
D.1	264583	179667
D.2	149278	103222
D.3	61667	45639

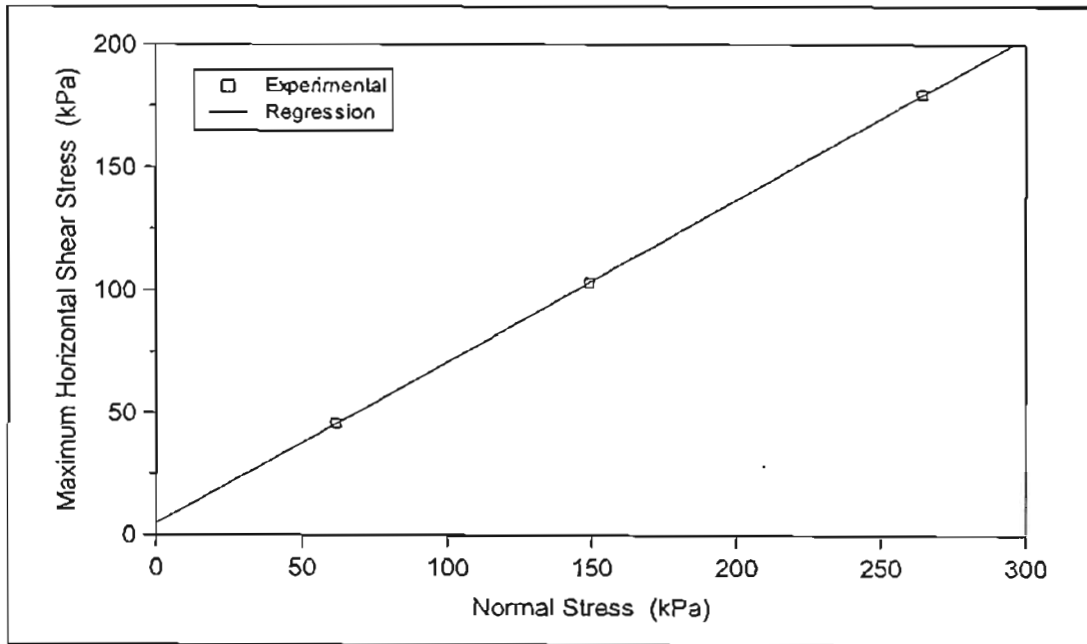


FIGURE 5.13 : Relationship between Maximum Horizontal Shear Stress and Normal Stress for Direct Shear Tests

A linear regression using the maximum horizontal shear stress versus normal stress data yielded the following values (see Equation 3.122):

$$\tan \phi = 0.6606$$

$$c = 4800 \text{ Pa}$$

The correlation coefficient, r^2 , for the regression was 0.999994.

The resultant angle of shearing resistance of 33.4 degrees was substituted into Equation 3.121 and the following value for the coefficient of earth pressure at rest was obtained:

$$k_0 = 0.396$$

5.5 RESULTS OF PLANAR FILTRATION TESTS

The results of the planar constant pressure filtration experiments are tabulated in Appendix E. The experiments were conducted at four different applied filtration pressures: 100 kPa, 200 kPa, 300 kPa and 400 kPa. The filtration time for the experiments at each applied pressure was incremented from 5 minutes to 30 minutes at 5 minute intervals. The feed solids concentration of the sludge was constant at 29.2 kg/m^3 for all the experiments.

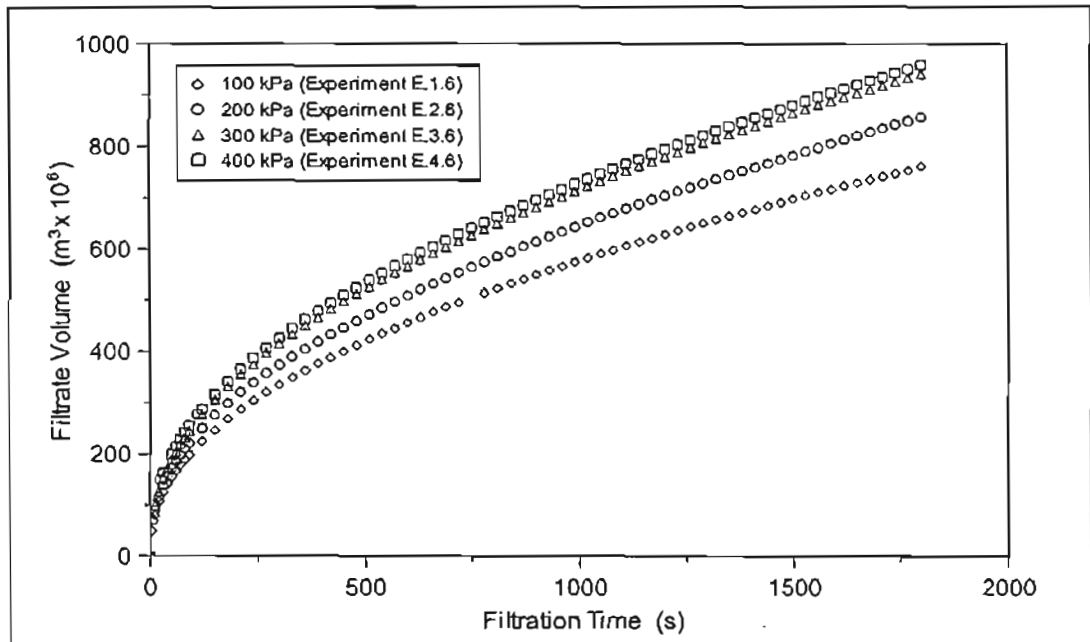


FIGURE 5.14 : Effect of Filtration Pressure on Filtrate Volume for Planar Filtration Experiments E.1.6, E.2.6, E.3.6 and E.4.6

The variation of filtrate volume with respect to time and applied pressure is shown in Figure 5.14. For clarity, only the data for experiments with filtration times of 30 minutes is shown. The filtrate volume increased with filtration pressure. Figure 5.15 to Figure 5.18 show the filtrate volume profiles for each of the experiments at each applied pressure. Although it appears in Figure 5.14 that the filtrate volume profile for the applied pressure of 300 kPa lies very close to that of 400 kPa, it is evident from Figure 5.17 that the filtrate volume profile for the applied pressure of 300 kPa and a filtration time of 30 minutes is higher than the trend set by the other experiments at the same pressure. Figure 5.15 to Figure 5.18 show that the repeatability of filtrate volume with respect to time between tests at the same applied pressure was good, with the filtrate volume profiles for experiments at shorter filtration times lying very close to one another.

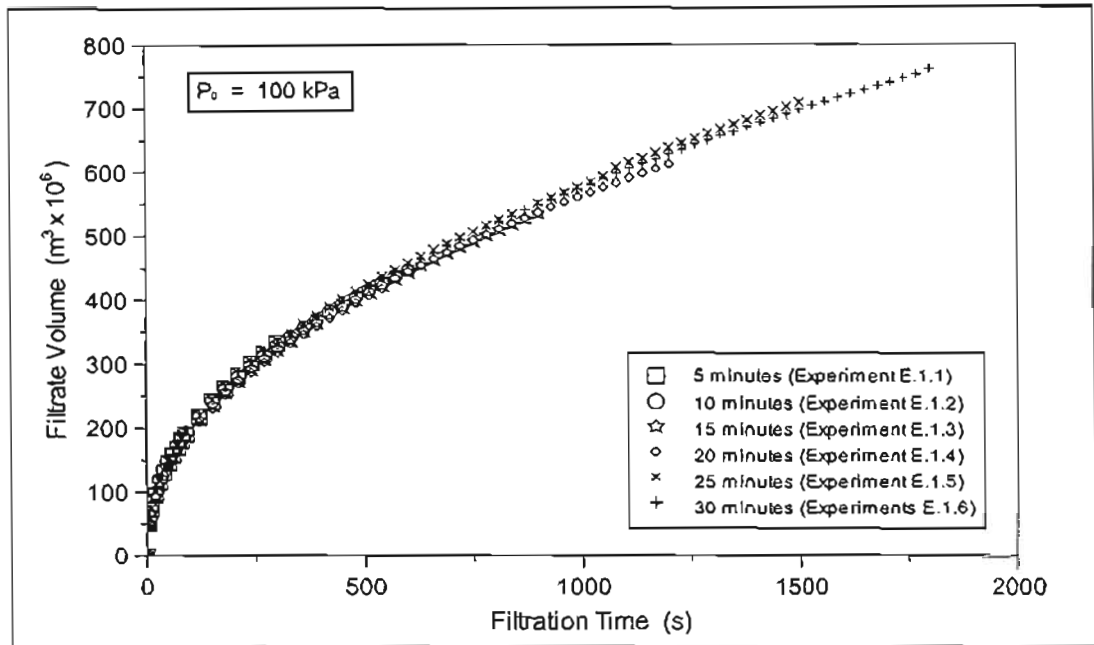


FIGURE 5.15 : Filtrate Volume versus Time for Planar Filtration Experiments at an Applied Pressure of 100 kPa

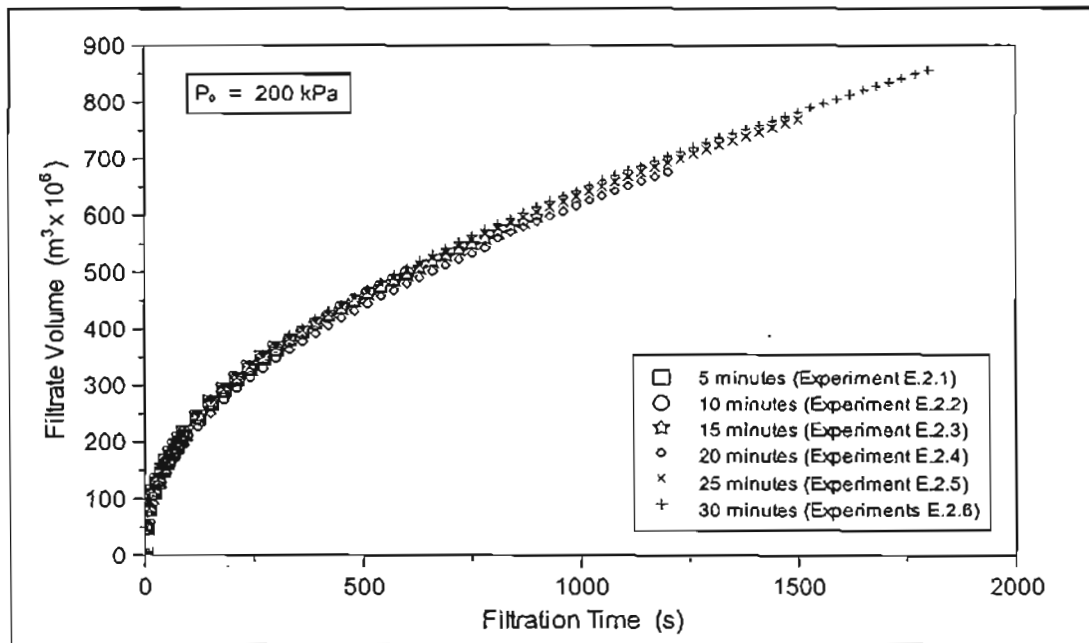


FIGURE 5.16 : Filtrate Volume versus Time for Planar Filtration Experiments at an Applied Pressure of 200 kPa

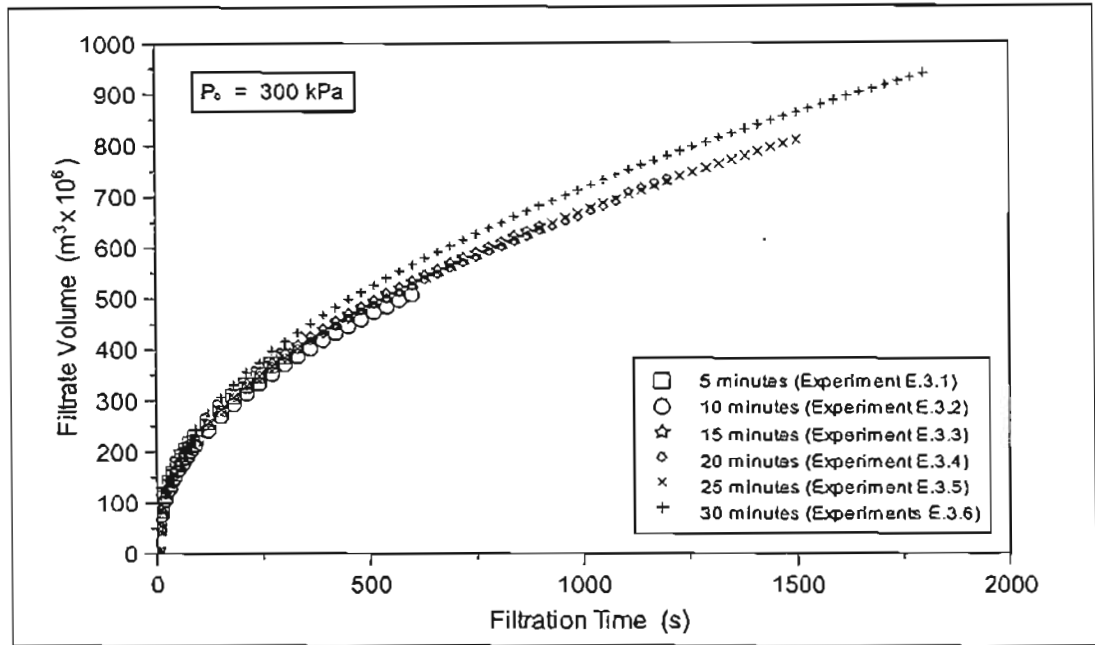


FIGURE 5.17 : Filtrate Volume versus Time for Planar Filtration Experiments at an Applied Pressure of 300 kPa

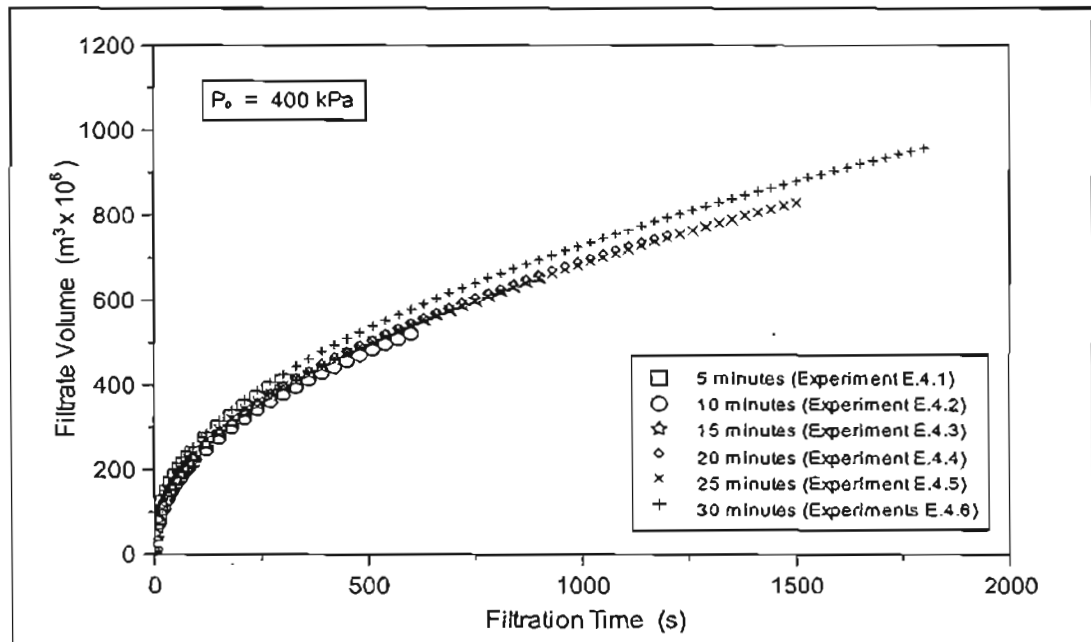


FIGURE 5.18 : Filtrate Volume versus Time for Planar Filtration Experiments at an Applied Pressure of 400 kPa

The variation of average cake dry solids concentration with respect to time and applied pressure is shown in Figure 5.19. Despite the scatter of the experimental data, the average cake dry solids concentration appears to remain constant with respect to filtration time, and to increase with increasing applied filtration pressure. Although the data shows some scatter, particularly for the applied pressure of 200 kPa, this trend can be confirmed by comparing the average values for each of the filtration pressures as shown in Table 5.7.

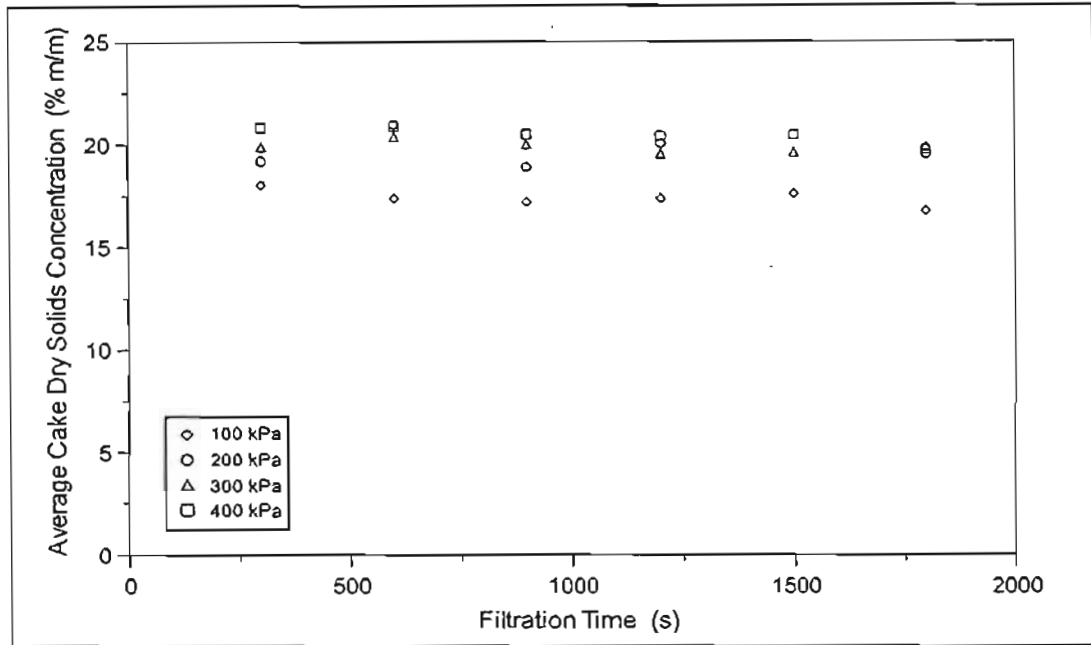


FIGURE 5.19 : Effect of Filtration Pressure on Average Cake Dry Solids Concentration for Planar Filtration Experiments

TABLE 5.7 : Average Values of the Average Cake Dry Solids Concentrations at each Applied Pressure for the Constant Pressure Planar Filtration Experiments

Applied Pressure (kPa)	Average Cake Dry Solids Concentration (% m/m)
100	17.4
200	19.72
300	19.87
400	20.45

The variation of cake thickness with respect to filtration time and applied pressure is shown in Figure 5.20. The cake thicknesses were not measured directly but calculated using the mass of wet cake and the average cake dry solids concentration. As shown in Figure 5.20, the cake thickness increased with filtration time. Since the data is derived from other experimental data, namely the average cake dry solids, which in itself showed some scatter, no significant effect of filtration pressure on cake thickness is detectable.

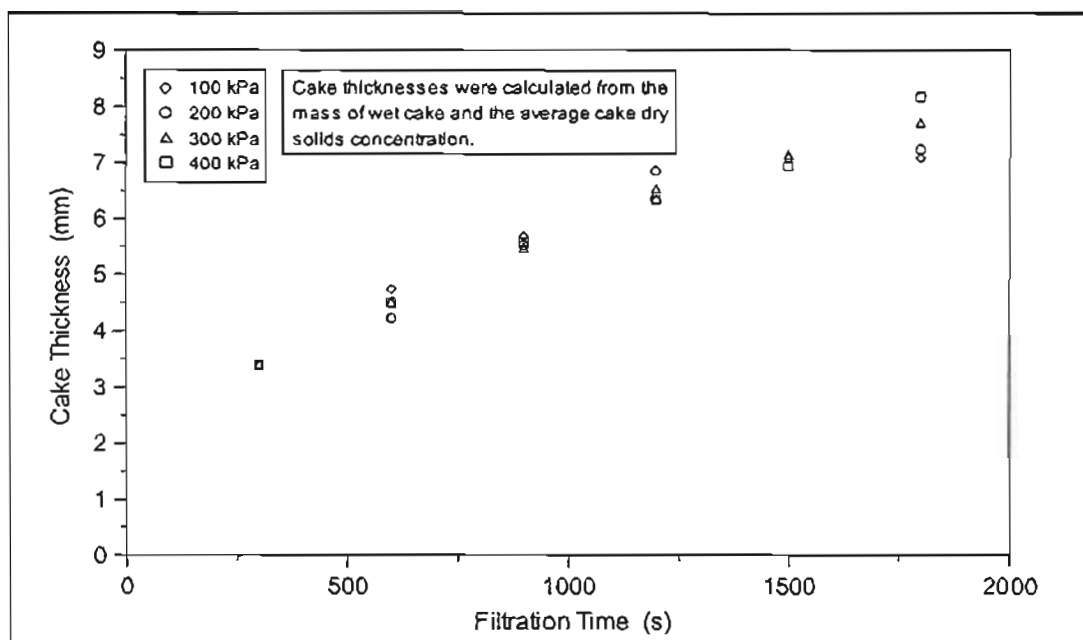


FIGURE 5.20 : Effect of Filtration Pressure on Calculated Cake Thickness for Planar Filtration Experiments

5.5.1 Determination of Medium Resistance

The average flow rate of water from the filter cell at a constant applied pressure of 90 kPa was found to be $5.459 \times 10^{-5} \text{ m}^3/\text{s}$. From Equation 3.54 the medium resistance of the filter cell was calculated to be $2.845 \times 10^{10} \text{ m}^{-1}$.

5.6 RESULT OF FULL-SCALE TUBULAR FILTER PRESS EXPERIMENTS

The results of the full-scale Tubular Filter Press Experiments at Wiggins Water Works are tabulated in Appendix F. Tests were conducted at operating pressures of approximately 200 kPa, 300 kPa and 400 kPa and at two different limiting filtrate flow rates. The timer setting on the control panel was set so that the limiting filtrate flow rate would be 6 s/l and 8.5 s/l respectively, and the average feed solids concentration was 27.1 kg/m^3 for the first set of tests. The feed solids concentration of the sludge was then reduced and the tests repeated. The average feed solids concentration for the second set of tests was 16.5 kg/m^3 . In order to reduce excessively long filtration times at the reduced feed solids concentration, the timer setting for the limiting filtrate flow rate was set to 4.25 s/l and 6 s/l respectively. The feed solids concentration of the filtrate for all the tests can be considered to be zero, the filtrate was clear and no suspended solids could be observed. A total of twelve tests were conducted, however it was subsequently discovered that due to an incomplete cleaning cycle immediately prior to the first test, and the inclusion of a significant volume of mains water in the piping prior to the first test conducted after the medium resistance tests, that the results of these two tests were no longer applicable, and as a result, had to be discarded.

Repeatability of the experimental results was difficult to quantify, due to the slight variations in final operating pressure, pressurisation time, feed solids concentration and medium resistance that were unavoidable due to the very nature of the TFP process. It was for this reason that a rigorous statistical analysis was not undertaken, and it seemed sufficient for the repeatability to be inferred from the graphs of filtrate volume versus time, which clearly show that the experiments performed under similar operating conditions agree very well with each other, especially in light of the differences observed between experiments at different operating conditions. .

Figure 5.21, Figure 5.22 and Figure 5.23 show typical gauge pressure, feed volume and feed flow rate profiles with respect to time.

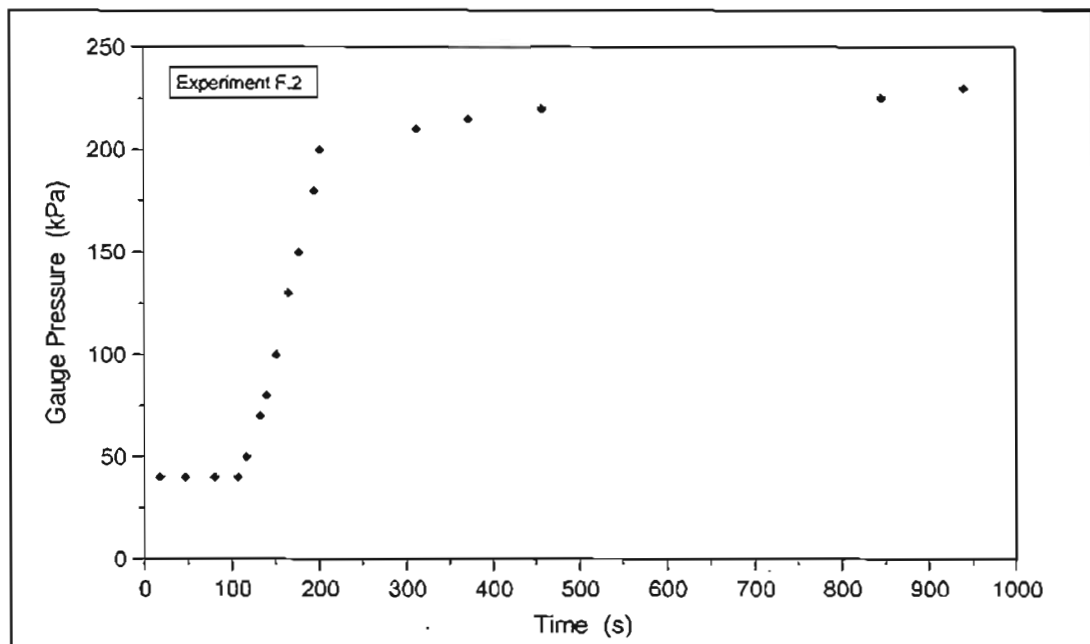


FIGURE 5.21 : Gauge Pressure Readings for Experiment F.2

After the cake removal cycle was completed and the discharge valve closed, the tubes and the reject manifold should be empty. When the filtration cycle was initiated, the feed sludge was pumped into the tubes from above, as a result, the pressure gauge on the feed line indicated a constant pressure until and the tubes had filled, thereafter, the applied pressure began to increase to its preset value (see Figure 5.21). The increase in applied pressure was therefore a good indicator that the tubes had been filled and that filtration had begun.

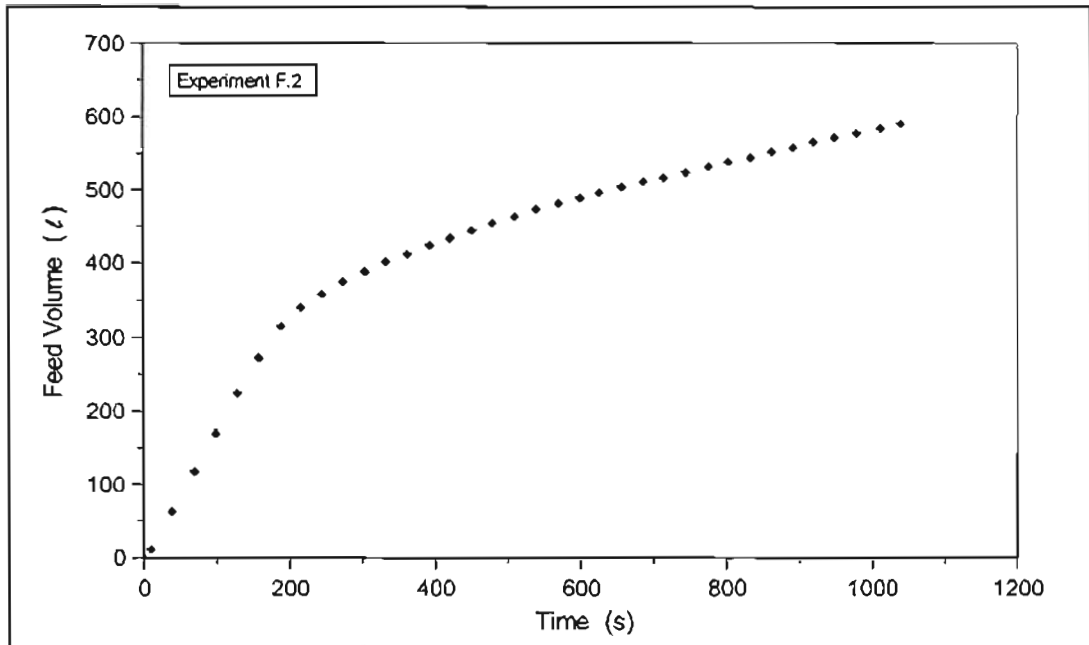


FIGURE 5.22 : Feed Volume Readings for Experiment F.2

The electromagnetic flow meter was situated on the feed line and therefore measured the feed sludge volume required to fill the tubes, reject manifold, inlet manifold and the section of piping from the feed valve to the inlet manifold. Only once the tubes and reject manifold were filled, was the volume of feed sludge pumped, equal to the volume of filtrate produced. This is evident in Figure 5.22 and Figure 5.23. Figure 5.22 shows a linear increase in volume while the tubes and manifolds were filling, and only once the tubes were full, was the typical parabolically shaped volume profile associated with filtration observed. This is mirrored in Figure 5.23 which clearly shows the constant feed flow rate as the manifolds and tubes were filling, followed only then by the characteristic decline in flow rate, as a result of filtration.

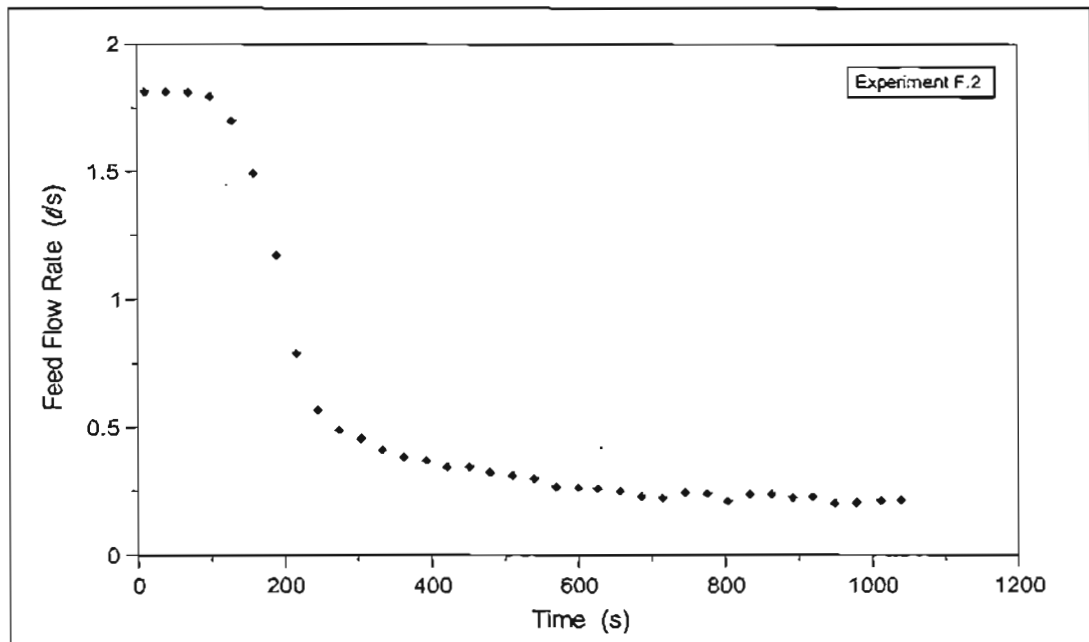


FIGURE 5.23 : Feed Flow Rate Profile for Experiment F.2

Ideally, at the time when the applied pressure begins to increase, indicating the tubes have been filled, the volume reading on the electromagnetic flow meter should equal the combined volume of the tubes, reject manifold, inlet manifold. In practice however, this is seldom the case. While the tubes are filling, the increase in hydrostatic pressure at the bottom of the tubes will cause filtrate to begin to permeate out of the tubes before the tubes are full. In addition there may be a residual amount of feed sludge in the reject manifold and tubes after the cake removal cycle has been completed. For the volume versus time data collected from the plant to be useful, it must be normalised to exclude the time and volume of feed sludge required to fill the tubes, reject and inlet manifolds, and so reflect the actual filtrate volume with respect to time. The reject manifold has a specialised funnel type structure to facilitate ease of removal of the cake from the manifold: its volume was calculated to be 0.0438 m³. The volume required to fill the double tube curtain was calculated to be 0.1895 m³. The volume of the inlet manifold and section of pipe from the feed valve to the inlet manifold was not known but could be considered negligible compared to the combined volume of the tubes and reject manifold.

For the purposes of this investigation, the zero time of the filtration was taken from when the tubes and manifolds were filled and the applied pressure began to increase. It was assumed that any filtrate formed whilst the tubes were being filled, which began as a result of the increasing hydrostatic pressure, was negligible. Where possible, the time taken for the tubes to fill was observed by visually examining the tubes; this reading was subjective since it relied on noting the degree of inflation of the tubes, and since the tubes were not transparent, the exact level of the feed sludge in the tubes could not be accurately determined. The tube filling time could also be estimated by observing the time for the volume of feed sludge pumped to equal the combined volume of the tubes and reject and inlet manifolds. These two estimates served only as confirmation of the zero time of filtration which was determined from the gauge pressure versus time readings.

Once the zero time for the filtration had been located, the corresponding zero volume for the filtration could be determined from the volume versus time readings. The time and volume of feed required to fill the tubes and manifolds, as determined from examining the pressurisation profile, was tabulated for each test in Table 5.8. The average initial feed flow rate, delivered by the feed pump during the period of constant gauge pressure whilst the tubes were filling, is also included in Table 5.8. The good agreement between the filling volume and time data and the average initial flow rate of the feed pump, indicates that the increase in gauge pressure did accurately indicate completion of tube filling and the start of filtration, since the volume time relationship did not reflect the marked decrease in flow rate that would have been observed if filtration had already commenced.

TABLE : 5.8 Feed Concentration, Tube Filling Time, Tube Filling Volume and Average Initial Feed Flow Rate for Tubular Filter Press Experiments

Test	Feed Concentration (kg/m ³)	Filling Time (s)	Filling Volume (ℓ)	Ratio of Filling Volume to Time (ℓ/s)	Average Initial Feed Flow Rate (ℓ/s)
F.1	28.6	88	193	2.19	2.07
F.2	26.3	117	204	1.74	1.73
F.3	27.3	112	207	1.85	1.80
F.4	25.6	124	218	1.76	1.74
F.5	26.9	95	196	2.06	2.04
F.6	17.8	116	194	1.67	1.67
F.7	15.3	115	200	1.74	1.72
F.8	17.1	110	199	1.81	1.76
F.9	16.1	111	197	1.77	1.76
F.10	15.4	94	179	1.90	1.89

The MONO feed pump and the pressure gauge were situated at the base of the Tubular Filter Press. The initial reading on the pressure gauge whilst the tubes were filling was therefore the discharge pressure required to pump the feed sludge to the top of the Tubular Filter Press (see Figure 5.21). Any pressure in the tubes during this time was only be due to the hydrostatic pressure as the feed sludge began to fill the tubes. Once the tubes were full, the pressure in the tubes was determined by the influence of the pump and the hydrostatic component. Since the tubes were in a vertical orientation, the difference in hydrostatic pressure between the top and the bottom of the tube was significant, and given by:

$$\Delta P_H = \rho_{av} g l \quad (5.1)$$

where ΔP_H = hydrostatic pressure difference between top and bottom of vertical tube, (Pa)

ρ_{av} = average density of sludge, (kg/m³)

For the purposes of this investigation, it was assumed that the filtration behaviour of the Tubular Filter Press could be represented by an equivalent plant where the pressure distribution through the tubes was constant and equal to the average pressure along the tubes. Since the pump and the pressure gauge were below the level of the tube curtain (see Figure 5.24), there was an additional hydrostatic pressure correction to the pressure data obtained from the plant. The corrected applied filtration pressure was therefore given by the following expression:

$$P_0 = PI - \rho_{av} g (H_2 + H_1) / 2 \quad (5.2)$$

The feed volume, time and gauge pressure data obtained from the Tubular Filter Press were processed as described above to reflect the actual filtrate volume versus time and applied pressure versus time behaviour of the Tubular Filter Press.

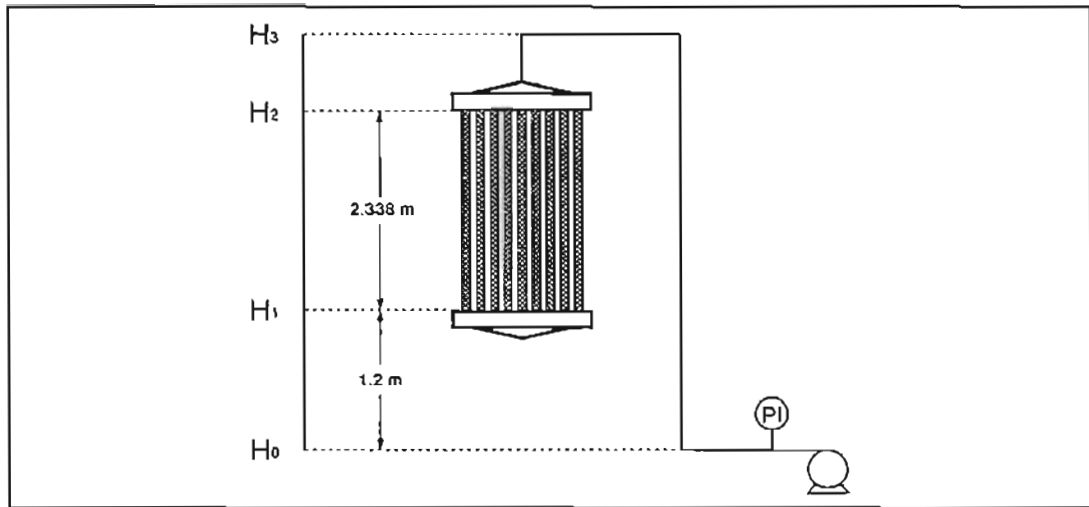


FIGURE 5.24 : Position of Vertical Tube Curtain with respect to the Feed Pump

Figure 5.25 to Figure 5.27 show the applied filtration pressure response of the Tubular Filter Press. For clarity during the initial pressurisation period, some of the latter applied pressure versus time data have been excluded from Figure 5.25 to Figure 5.27. The applied filtration pressure increased sharply with respect to time and then reached a plateau where the applied filtration pressure remained relatively constant. In some cases a slight variation in final applied pressure was observed in the plateau phase, in these cases the final applied filtration pressure was taken as the average pressure in this region.

Generally, the results of these experiments were, to some extent, subject to the influence of variations in operational parameters which could not be controlled exactly, such as initial medium resistance (dependent on the previous cleaning cycle) or initial feed flow, which led to some individual cases showing apparent anomalies from the trends.

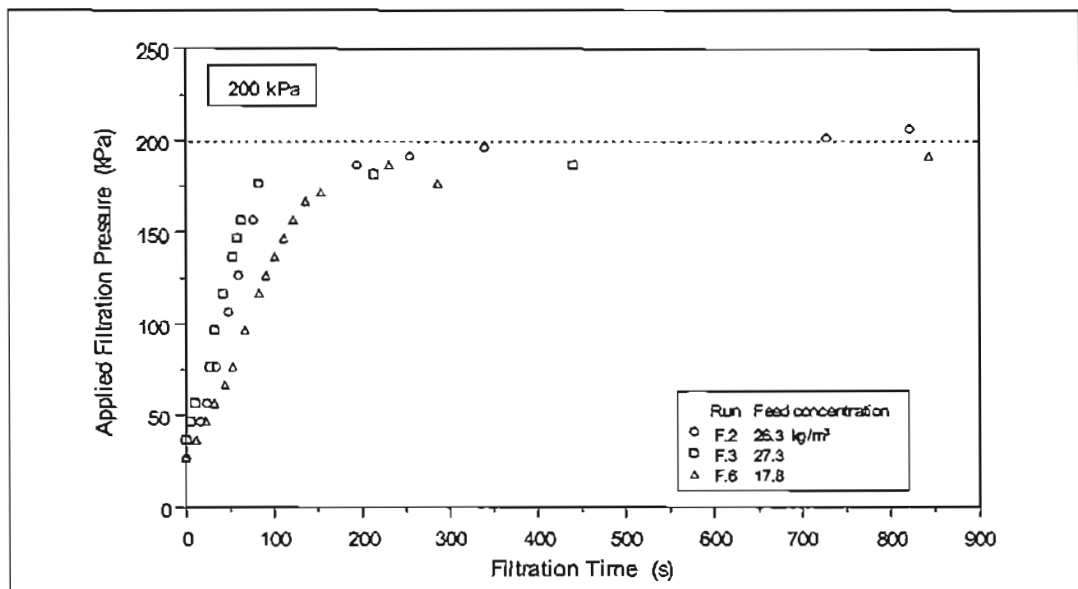


FIGURE 5.25 : Pressurisation Profiles for Experiments Conducted at Operating Pressures of Approximately 200 kPa

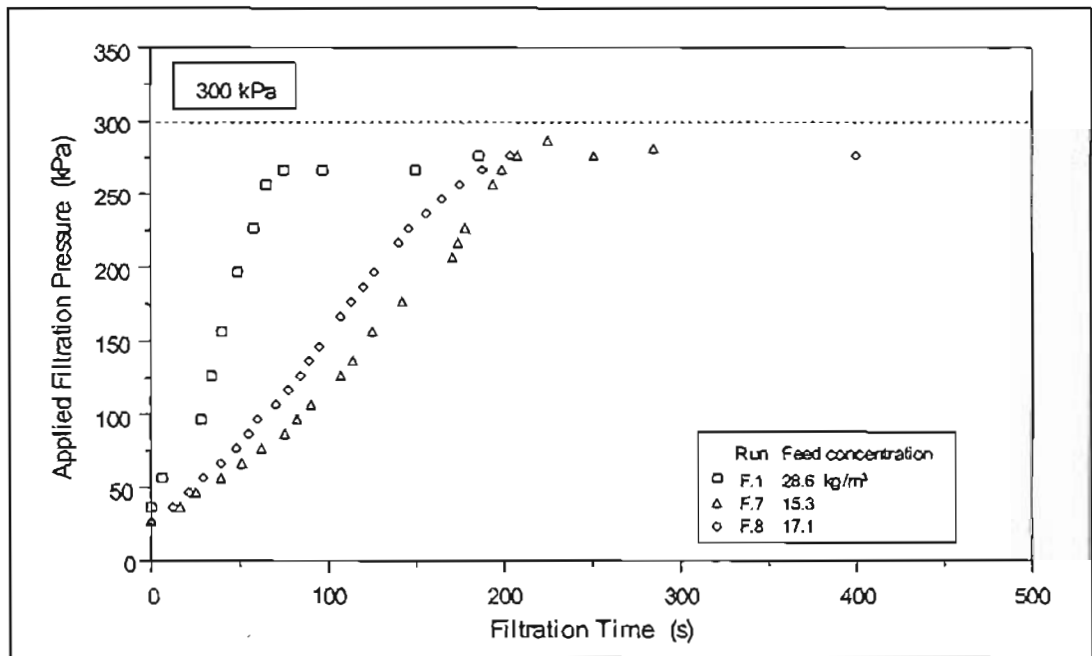


FIGURE 5.26 : Pressurisation Profiles for Experiments Conducted at Operating Pressures of Approximately 300 kPa

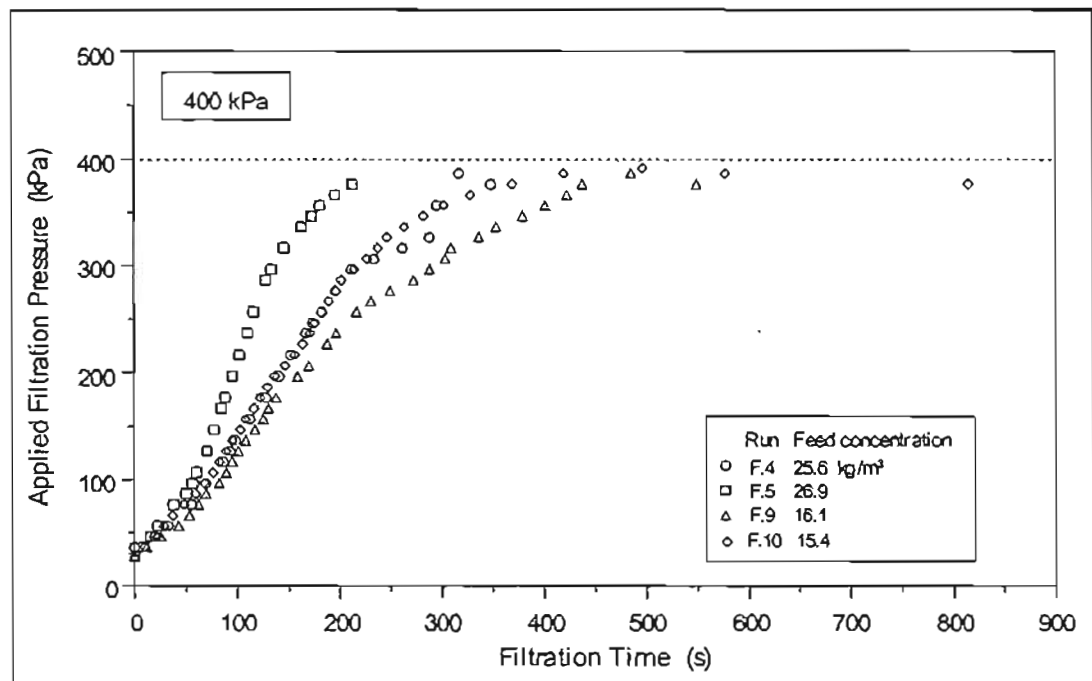


FIGURE 5.27 : Pressurisation Profiles for Experiments Conducted at Operating Pressures of Approximately 400 kPa

The pressurisation response of the Tubular Filter Press was found to be dependent on the degree of *back pressure* or resistance to flow. Figure 5.25 to Figure 5.27 show that tests with a greater feed solids concentration generally show a more rapid pressurisation of the tubes to the final operating pressure. This is because the greater the feed solids concentration, the greater the rate of cake deposition, and hence the greater the increase in resistance to flow,

which resulted in a more rapid pressurisation response. The pressurisation response was therefore also influenced by other factors that affected the initial rate of cake deposition, such as the initial medium resistance and the initial flow rate of the feed pump.

Figure 5.28 to Figure 5.30 show the relationship of filtrate volume with respect to time.

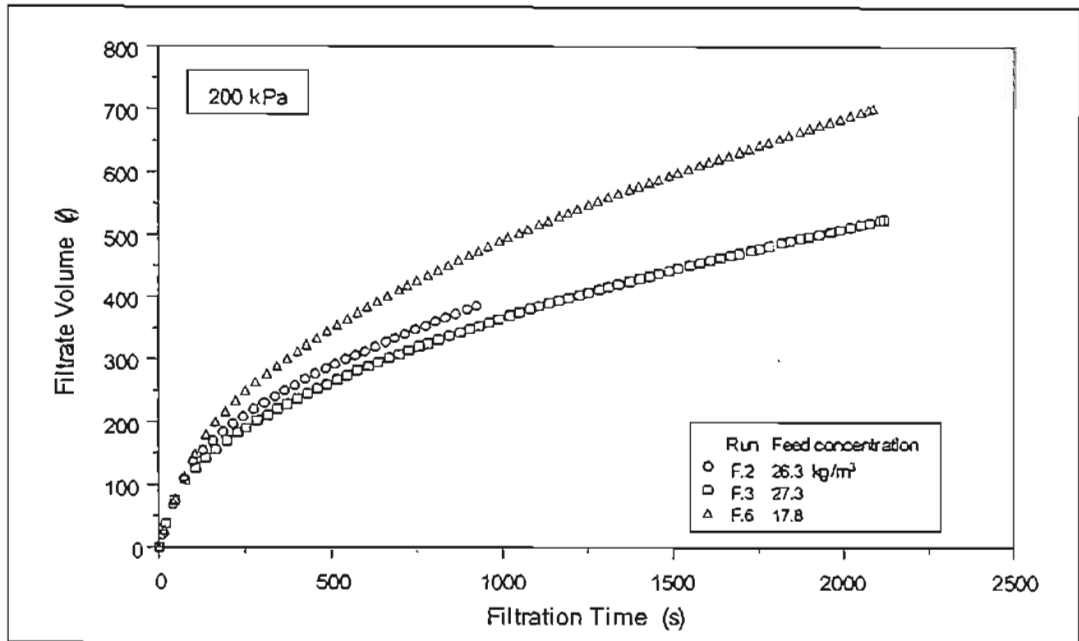


FIGURE 5.28 : Filtrate Volume Profiles for Experiments Conducted at Operating Pressures of Approximately 200 kPa

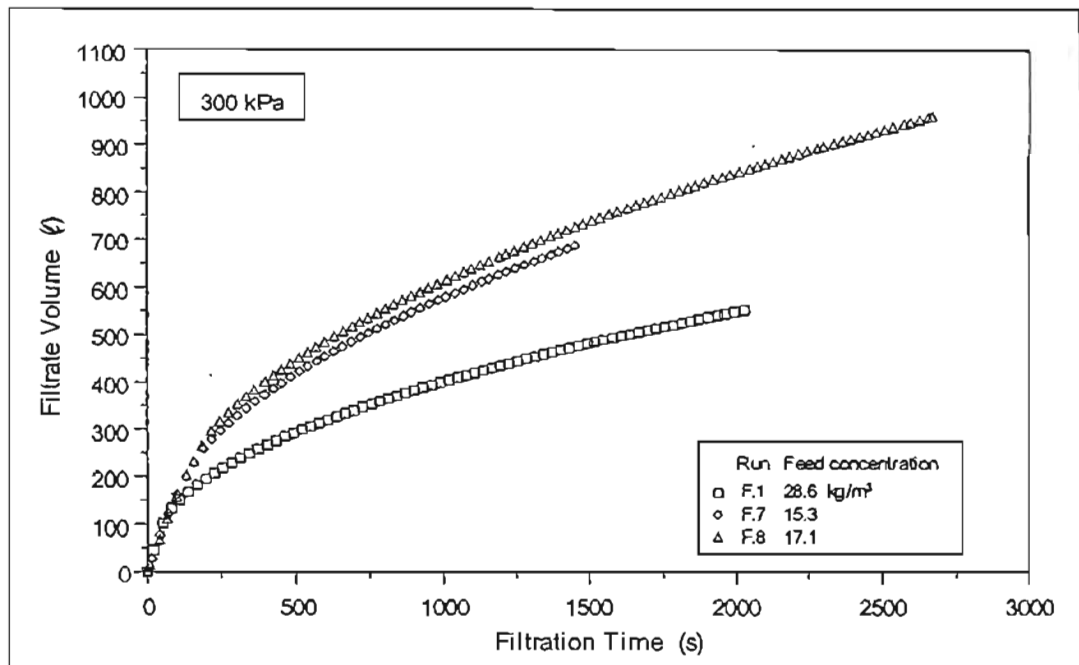


FIGURE 5.29 : Filtrate Volume Profiles for Experiments Conducted at Operating Pressures of Approximately 300 kPa

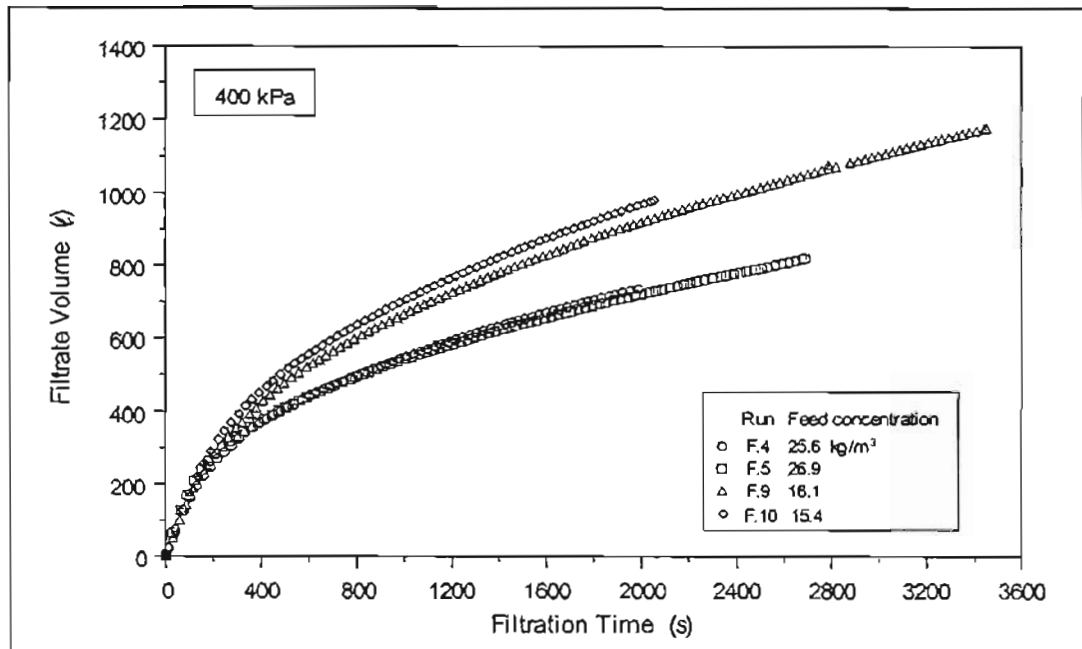


FIGURE 5.30 : Filtrate Volume Profiles for Experiments Conducted at Operating Pressures of Approximately 400 kPa

Although there were slight differences in the applied pressure and feed solids concentration, the differences were considered sufficiently small so that tests conducted at similar applied pressures and feed solids concentrations could be grouped together for comparative purposes. At similar feed solids concentrations, the filtrate volume with respect to time increased with time and applied pressure. At similar applied pressures, the filtrate volume with respect to time decreased with increasing feed solids concentration. At the same applied pressure and feed solids concentration, the volume versus time behaviour of separate filtration tests should be equivalent. Given the slight variation in feed solids concentration and applied pressure between tests, this similarity in filtrate volume versus time was observed.

Figure 5.31 to Figure 5.33 show the relationship of the average cake dry solids concentration of the cake sampled from collection bin 2, with respect to time at each of the approximate applied pressures. The individual points on these graphs represent the end-point concentrations of each experiment. Two samples of cake were taken from cake collection bin 2. The first unscreened sample was a representative sample of the cake as it was collected in the cake collection bin, including any flush fluid that may have been entrained along with cake flakes due to inadequate drainage on the cake conveyor. The second sample was placed on a screen to facilitate and complete any further drainage that may have occurred, and therefore represented the cake concentration of the cake if drainage on the conveyor had been ideal. There appeared to be no specific trend with regard to filtration time and pressure for the unscreened cake samples taken from cake collection bin 2. This was due to the variable nature of the cake removal mechanism and hence the variable degree of entrained flush fluid that discharged to

cake collection bin 2. It was observed that if a large amount of cake was discharged onto the conveyor belt, drainage was poor.

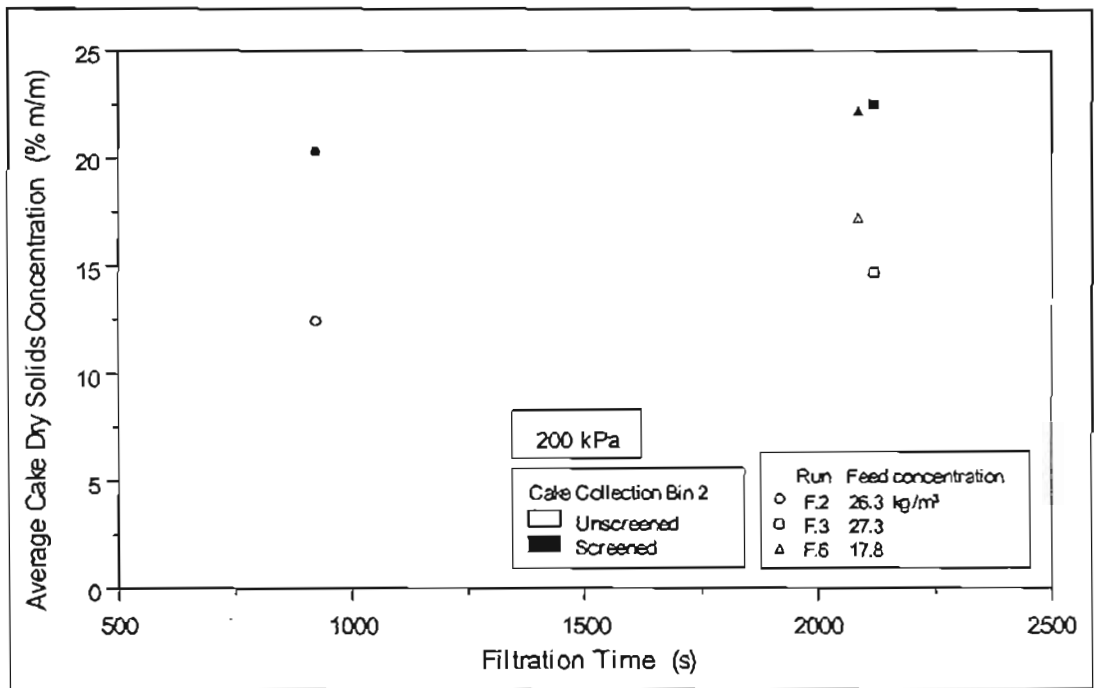


FIGURE 5.31 : Average Cake Dry Solids Concentration Profiles for Experiments Conducted at Operating Pressures of Approximately 200 kPa

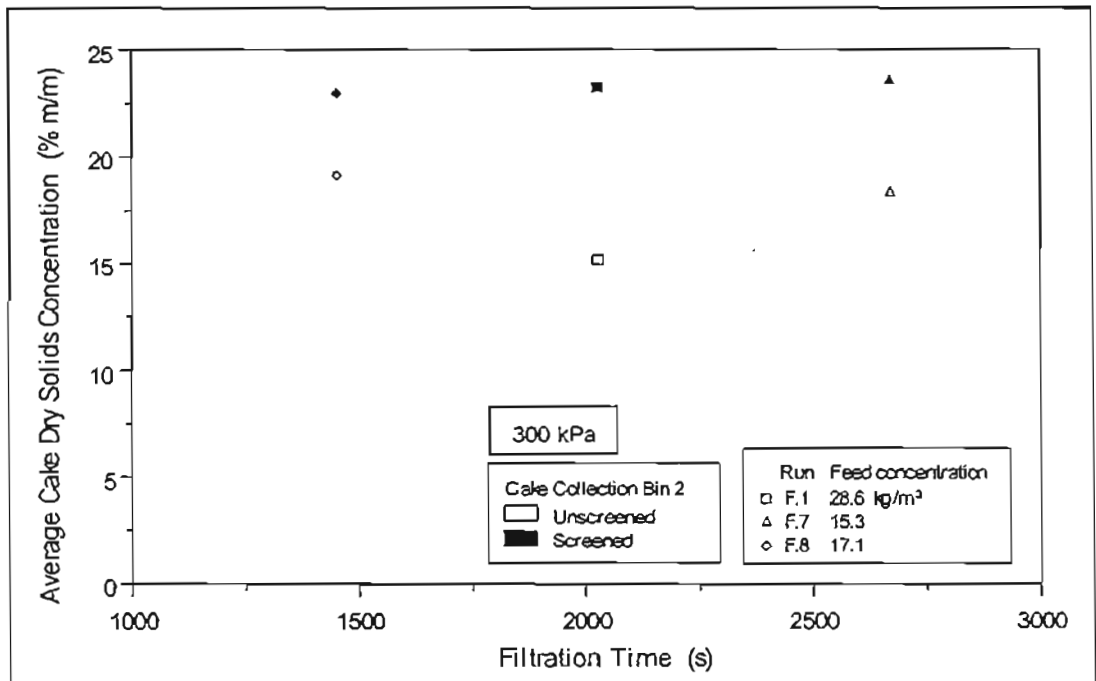


FIGURE 5.32 : Average Cake Dry Solids Concentration Profiles for Experiments Conducted at Operating Pressures of Approximately 300 kPa

Figure 5.34 shows that the average cake concentration for the screened cake samples, increases with respect to time and filtration pressure.

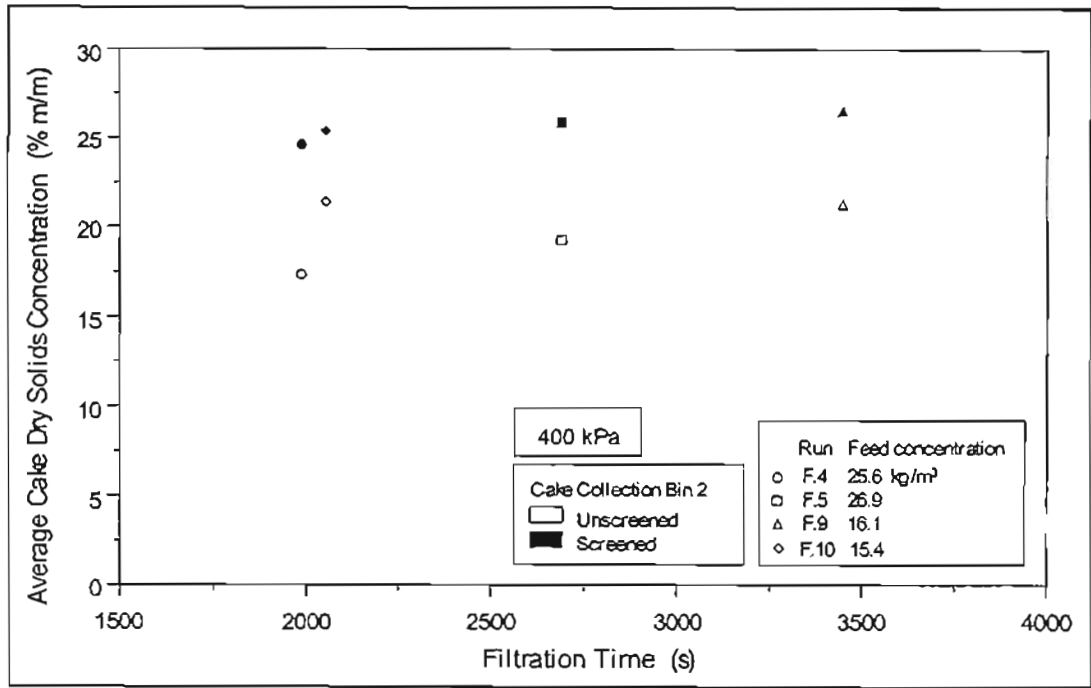


FIGURE 5.33 : Average Cake Dry Solids Concentration Profiles for Experiments Conducted at Operating Pressures of Approximately 400 kPa

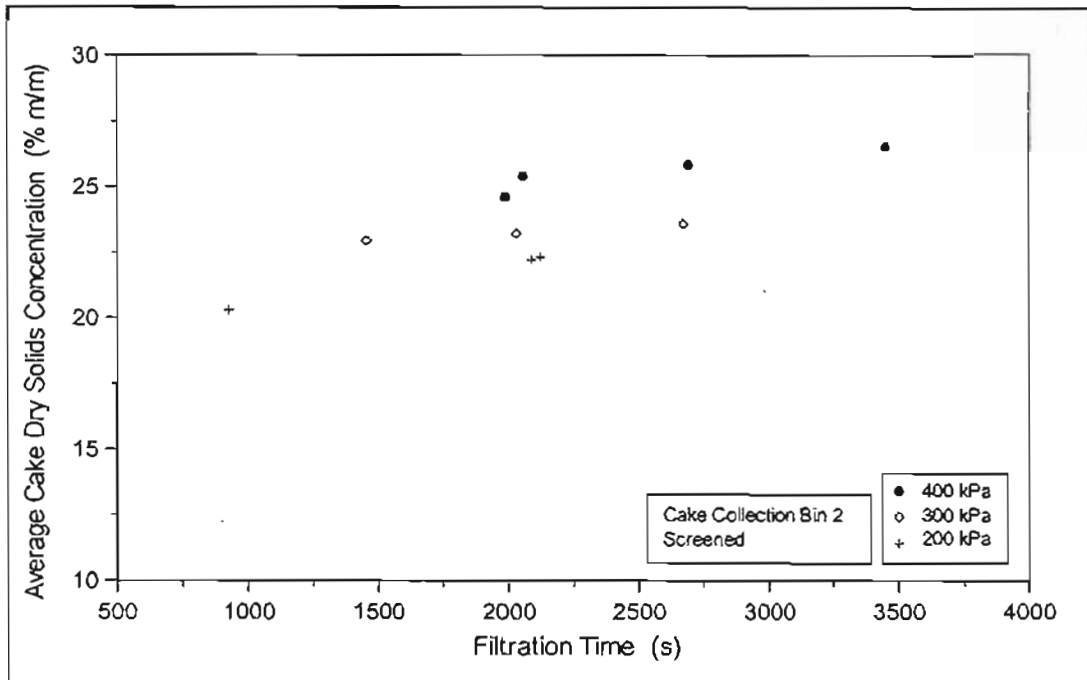


FIGURE 5.34 : Average Cake Dry Solids Concentration of Screened Cake Samples

The system was also not completely closed, since a small amount of mains water was introduced to the system when the cake conveyor belt was being cleaned, it was assumed to be negligible.

5.6.1 Cake Recovery

The cake recovery is the fraction of the total cake dry solids, deposited in the tubes during the filtration cycle, that is actually recovered during the cake removal cycle. Due to the nature of operation of the Tubular Filter Press, an accurate mass balance over the system could not be performed, the exact amount of dry cake solids deposited in the tubes could therefore not be calculated, as a result the exact cake recovery could not be determined. The approximate amount of dry solids deposited and hence the approximate cake recovery could however, be determined from the volume of filtrate and the volume of cake recovered (see sample calculation in Appendix F). The approximate cake recovery is sufficiently accurate to identify any trends in the cake recovery with regard to the operational variables.

Figure 5.35 shows the variation of recovery with respect to the feed solids concentration. Although there is significant scatter in the data, a linear regression analysis shows that the overall trend is for recovery to increase with feed solids concentration. Identifying and joining tests conducted at similar operating pressures and similar final filtration times confirms this trend.

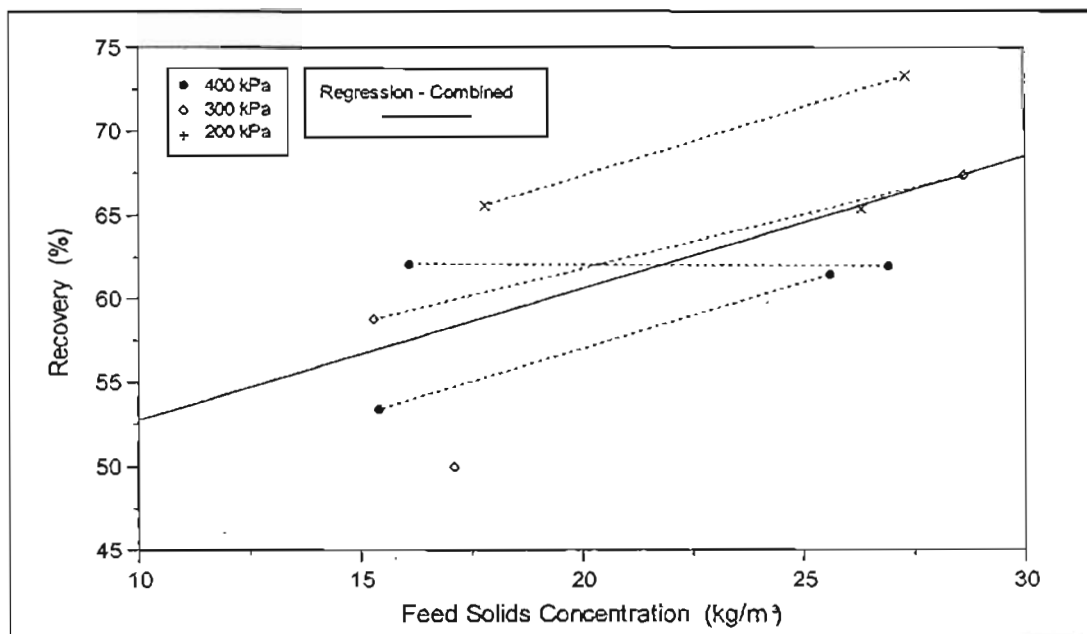


FIGURE 5.35 : Effect of Feed Solids Concentration on Cake Recovery

Figure 5.36 shows the variation of recovery with respect to the final filtration time. Although there is significant scatter in the data, a linear regression analysis shows that the overall trend is for recovery to increase slightly with final filtration time. Identifying and joining tests conducted at similar operating pressure and similar feed solids concentrations confirms this trend. As the filtration time increases, so does the cake thickness, for internal cylindrical filtration, as the cake thickness increases, the proportion of the loosely consolidated outer cake

layers decreases and hence the cake recovery increases. As discussed in Section 3.7.2.1, this trend was also observed by Rencken (1992).

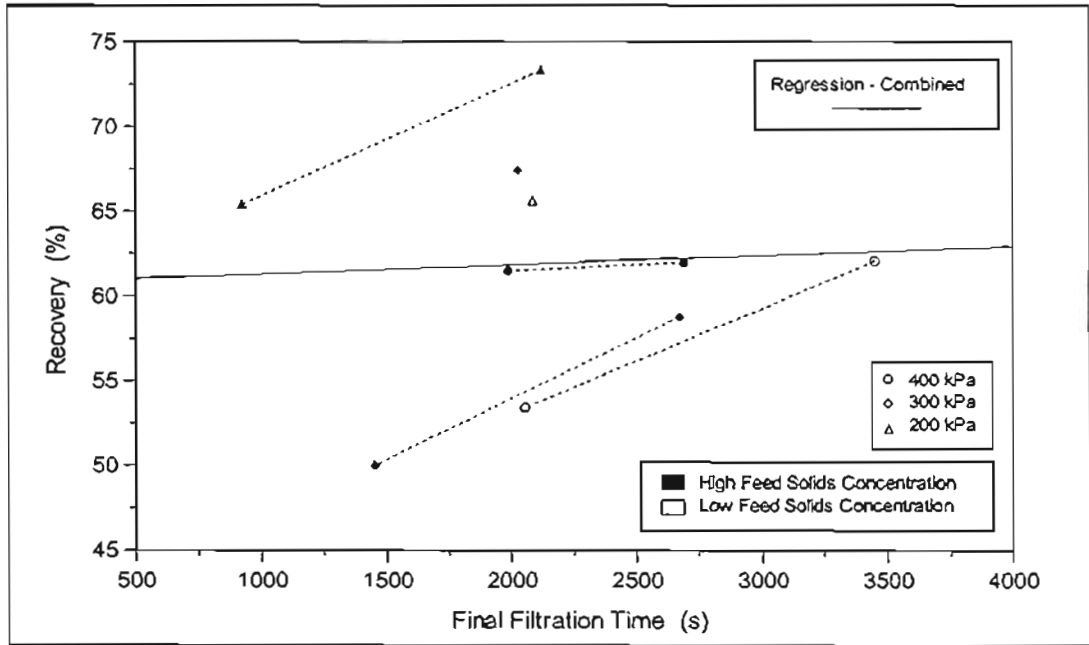


FIGURE 5.36 : Effect of Final Filtration Time on Cake Recovery

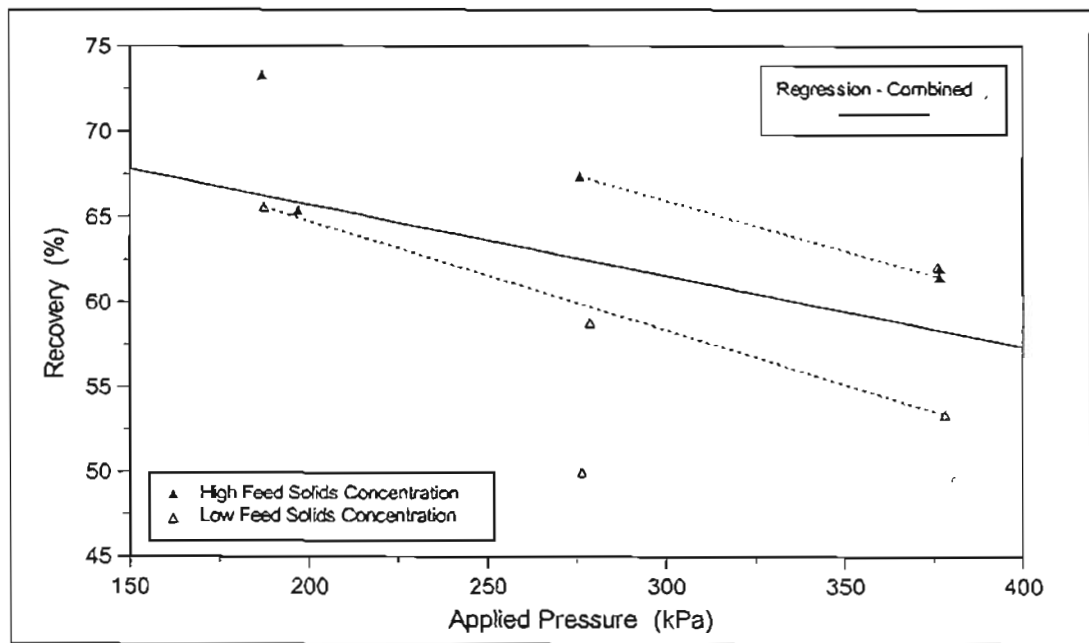


FIGURE 5.37 : Effect of Filtration Pressure on Cake Recovery

Figure 5.37 shows the variation of recovery with respect to the applied filtration pressure. Although there is significant scatter in the data, a linear regression analysis shows that the overall trend is for recovery to decrease with applied filtration pressure. Identifying and joining tests conducted at similar feed solids concentrations and with similar final filtration times

confirms this trend. Rencken (1992), observed the opposite trend with respect to filtration pressure, he observed recovery to increase significantly with increasing filtration pressure.

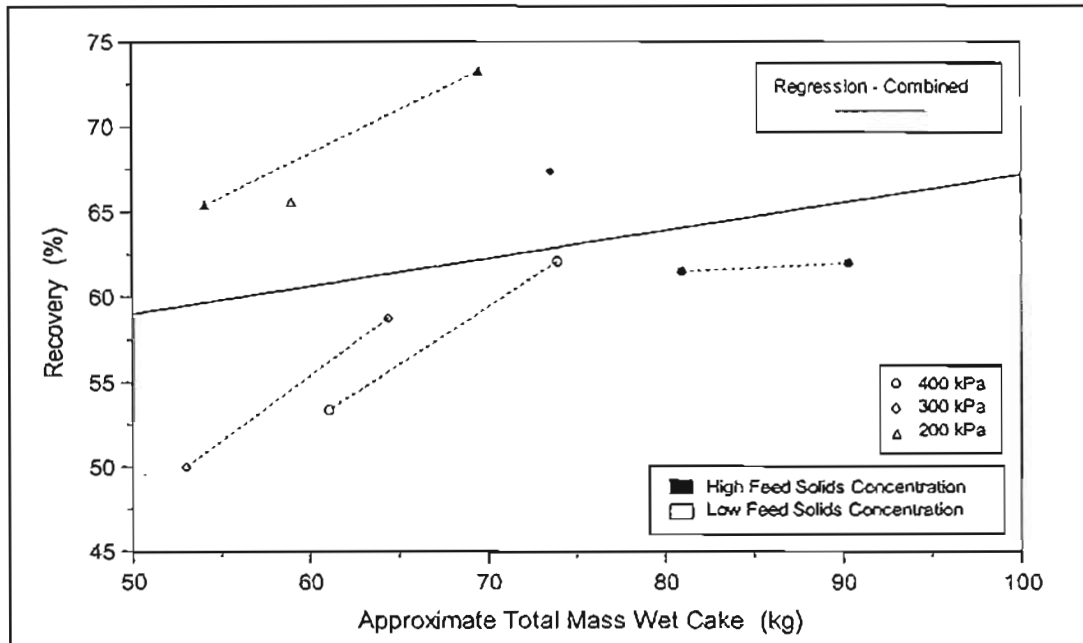


FIGURE 5.38 : Effect of Approximate Total Mass Wet Cake on Cake Recovery

Figure 5.38 shows the variation of recovery with respect to the approximate total mass wet cake in the tubes. The approximate total mass wet cake was calculated from the actual recovered mass of dry cake and the screened average cake dry solids concentration (see sample calculation in Appendix F). Although there is significant scatter in the data, a linear regression analysis shows that the overall trend is for recovery to increase with approximate total mass wet cake. Identifying and joining tests conducted at similar operating pressures and with similar feed solids concentrations verifies this trend.

As discussed in Section 3.7.2.1, this trend was also observed by Rencken (1992). For the horizontal internal cylindrical apparatus studied by Rencken (1992), the relationship between recovery and mass wet cake could be directly related to the relationship of mass wet cake to filtration time. For the vertical Tubular Filter Press however, the mass of wet cake in the tubes is believed to have a direct and independent influence on the cake recovery. Due to the vertical orientation of the tubes, the greater the weight of the cake in the tubes, the greater the ease at which it can be stripped away from the tubes walls by the flush fluid. The less time the cake is exposed to the high shear imposed by the flush fluid in the tubes before being removed, the greater the cake recovery.

From the significant scatter observed in Figure 5.35 to Figure 5.38, it is clear that the recovery is a complex function and not strongly dependent on any one operational variable. Generally all the trends observed by Rencken (1992), are confirmed, except for the relationship between

recovery and filtration pressure. This highlights the complex nature of the cake recovery and illustrates that recovery is also strongly dependent on plant specific factors such as the nature of the recovery mechanism and the plants physical design, and not operational parameters alone. Rencken (1992), also observed that recovery was dependent on the tube length and the flow rate of the flush fluid through the tubes.

It is important both in terms of optimising plant production and finding stable operating regimes, that the recovery of the plant be predicted with reasonable accuracy. Provided the recovery mechanism is not changed, for example by changing the number of flushes or the flow rate of the flush fluid, and the characteristics of the sludge remain constant, it may be possible to derive an accurate recovery correlation to predict the plant recovery, based on the general trends observed above with regard to the key operational variables. The mass of wet cake is in turn a function of the operating pressure, feed solids concentration and final filtration time, so the recovery correlation may be derived in terms of these three operational variables. Table 5.9 summarises the recovery data for the tests.

TABLE 5.9 : Relationship between Recovery and Key Operational Variables

Test	m_w (kg)	s_f (kg/m ³)	t_f (s)	P_0 (kPa)	R (%)
F.1	73.6	28.6	2027	275.9	67.4
F.2	54.1	26.3	923	196.9	65.4
F.3	69.5	27.3	2119	186.8	73.3
F.4	81.0	25.6	1988	376.5	61.5
F.5	90.3	26.9	2689	376.5	62
F.6	59.0	17.8	2085	187.4	65.6
F.7	64.4	15.3	2671	279	58.8
F.8	53.0	17.1	1452	276.6	50
F.9	73.9	16.1	3449	375.9	62.1
F.10	61.1	15.4	2054	378	53.4

5.6.2 Determination of Medium Resistance

The results of the tests to determine the resistance of the tube fabric are tabulated in Appendix F (Test F.11 and Test F.12). During the course of each test, the MONO pump delivered a constant flow rate, even after the tubes had been filled, thus the flow rate was observed to be independent of the gauge pressure. The flow rate was 1.93 l/s for Test F.11 and 1.89 l/s for Test F.12. The resistance of the medium was significantly less than that of the filter cake, as a result the pressure response of the system remained low. Once the tubes had been filled, the gauge pressure rose immediately to 50 kPa for both tests. Thereafter the pressure increased slightly with time. The increase in pressure could be attributed directly to a gradual increase in the

medium resistance. Although the feed tank was cleaned and contained mains water, the associated pumps, valves, manifolds and piping were still contaminated with sludge. Although minimal, these solids began to *blind* the medium, increasing the resistance and causing the associated increase in pressure with respect to time. The increase in pressure was more significant for Test F.12 since more solids were introduced to the system from the flush pump and associated piping after the first cleaning sequence. The initial resistance of the medium after the cleaning cycle had been initiated was found to result in an initial gauge pressure of 50 kPa for both tests. During the cleaning cycle of each test, no cake was observed to be removed from the tubes. After the gauge pressure had been corrected to account for the hydrostatic pressure component, and the medium resistance calculated using Equation 3.55. The average medium resistance of the Tubular Filter Press was found to be $1.986 \times 10^{11} \text{ m}^{-1}$.

5.7 PERMEABILITY AND POROSITY CORRELATIONS : STANDARD LABORATORY SLUDGE CHARACTERISATION

The results of the C-P cell tests and settling tests, were fitted to the permeability and porosity correlations for multiple parameter sets, Equations 3.3, to obtain the standard laboratory characterisation for the sludge under investigation.

Equations 3.3 require that a solids compressive pressure, p_{si} , be identified where the porosity and permeability are assumed constant for solids compressive pressures below this value. The minimum value for p_{si} is the solids compressive pressure corresponding to the porosity of the feed sludge (see Equation 3.98 of Section 3.4.4.3). From the porosity data at low solids compressive pressure, obtained from settling tests, the minimum value for p_{si} would be given by the following expression:

$$p_{si} \geq p_{sf} = \left(\frac{1 - \epsilon_f}{B} \right)^{\frac{1}{b}} = \left(\frac{1 - \epsilon_f}{0.03558} \right)^{\frac{1}{0.01913}} \quad (5.5)$$

The value of p_{si} , determined empirically or by some other means, must be greater than or equal to this minimum value.

The complete sludge characterisation determined from standard laboratory C-P cell and settling tests is given below. The cake compressibility, as indicated by the magnitude of the exponents varies, with solids compressive pressure. Except for very low solids compressive pressures where the cake is mildly compressible, the cake is extremely compressible with the compressibility of the cake decreasing slightly with solids compressive pressure in the higher solids compressive pressure range. The data corrected for the effects of wall friction show a slightly decreased compressibility. The effects of correcting the data for wall friction will only be able to be fully assessed once the correlation data has been incorporated into the predictive filtration model and the results compared to filtration data.

5.7.1 Wall Friction in C-P Cell Tests Neglected

$$K = 1.030 \times 10^{-13} p_{sf}^{-0.05382} \quad 0 \leq p_s \leq p_{sf} \quad (5.6.a)$$

$$K = 1.030 \times 10^{-13} p_s^{-0.05382} \quad p_{sf} \leq p_s \leq 2212 \text{ Pa} \quad (5.6.b)$$

$$K = 1.911 \times 10^{-8} p_s^{-1.629} \quad 2212 \leq p_s \leq 133226 \text{ Pa} \quad (5.6.c)$$

$$K = 1.963 \times 10^{-10} p_s^{-1.241} \quad 133226 \leq p_s \leq 331011 \text{ Pa} \quad (5.6.d)$$

$$K = 4.289 \times 10^{-13} p_s^{-0.759} \quad p_s \geq 331011 \text{ Pa} \quad (5.6.e)$$

$$(1 - \varepsilon) = 0.03558 p_{sf}^{0.01915} \quad 0 \leq p_s \leq p_{sf} \quad (5.6.f)$$

$$(1 - \varepsilon) = 0.03558 p_s^{0.01915} \quad p_{sf} \leq p_s \leq 5684 \text{ Pa} \quad (5.6.g)$$

$$(1 - \varepsilon) = 7.344 \times 10^{-4} p_s^{0.468} \quad 5684 \leq p_s \leq 145558 \text{ Pa} \quad (5.6.h)$$

$$(1 - \varepsilon) = 5.039 \times 10^{-3} p_s^{0.306} \quad p_s \geq 145558 \text{ Pa} \quad (5.6.i)$$

5.7.2 Wall Friction in C-P Cell Tests Accounted

$$K = 1.030 \times 10^{-13} p_{sf}^{-0.05382} \quad 0 \leq p_s \leq p_{sf} \quad (5.7.a)$$

$$K = 1.030 \times 10^{-13} p_s^{-0.05382} \quad p_{sf} \leq p_s \leq 1316 \text{ Pa} \quad (5.7.b)$$

$$K = 2.771 \times 10^{-9} p_s^{-1.474} \quad 1316 \leq p_s \leq 128368 \text{ Pa} \quad (5.7.c)$$

$$K = 9.145 \times 10^{-11} p_s^{-1.184} \quad 128368 \leq p_s \leq 318222 \text{ Pa} \quad (5.7.d)$$

$$K = 3.133 \times 10^{-13} p_s^{-0.736} \quad p_s \geq 318222 \text{ Pa} \quad (5.7.e)$$

$$(1 - \varepsilon) = 0.03558 p_{sf}^{0.01915} \quad 0 \leq p_s \leq p_{sf} \quad (5.7.f)$$

$$(1 - \varepsilon) = 0.03558 p_s^{0.01915} \quad p_{sf} \leq p_s \leq 3680 \text{ Pa} \quad (5.7.g)$$

$$(1 - \varepsilon) = 1.281 \times 10^{-3} p_s^{0.424} \quad 3680 \leq p_s \leq 138669 \text{ Pa} \quad (5.7.h)$$

$$(1 - \varepsilon) = 6.260 \times 10^{-3} p_s^{0.29} \quad p_s \geq 138669 \text{ Pa} \quad (5.7.i)$$

5.8 COMPARISON BETWEEN FILTRATION MODEL AND FILTRATION EXPERIMENTS : STANDARD LABORATORY CHARACTERISATION

The constant pressure compressible cake filtration model, and the predictive solution procedures described in Section 3.3, have been incorporated into the computer programme, COMPRESS, written in the C++ programming language. The point contact model was used for all model predictions in this section, the new area contact model will be evaluated and discussed later (see Section 5.11).

5.8.1 Planar Filtration Experiments

Figure 5.39 to Figure 5.50 show the comparison between the results of the planar filtration experiments and the predictions of the constant pressure compressible cake filtration model,

using the laboratory sludge characterisation obtained from the C-P cell and settling tests (see Section 5.7).

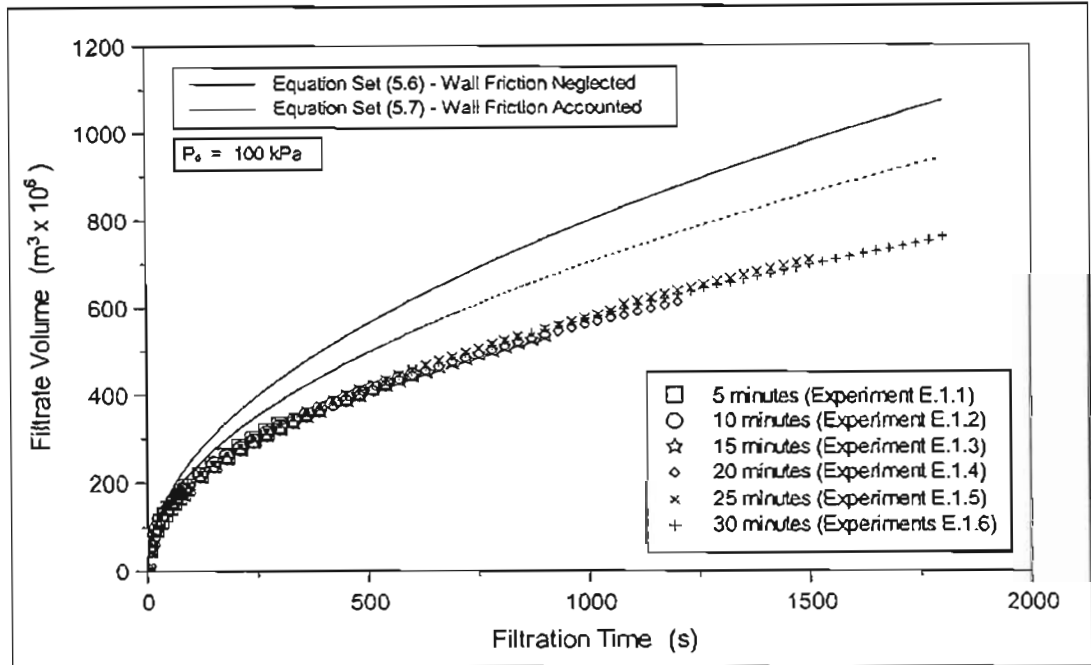


FIGURE 5.39 : Comparison between Experimental and Predicted Filtrate Volumes for Planar Filtration at 100 kPa using the Laboratory Sludge Characterisation

In the same manner as the objective function is used to evaluate the extent by which the model output resulting from an assumed set of model parameters agrees with the experimental data, during the direct search strategy of the regressive solution procedure, Equation 3.87 can be used to provide a quantitative assessment of the extent by which the model predictions using the sludge characterisations of Section 5.7, agree with the results of the planar filtration experiments.

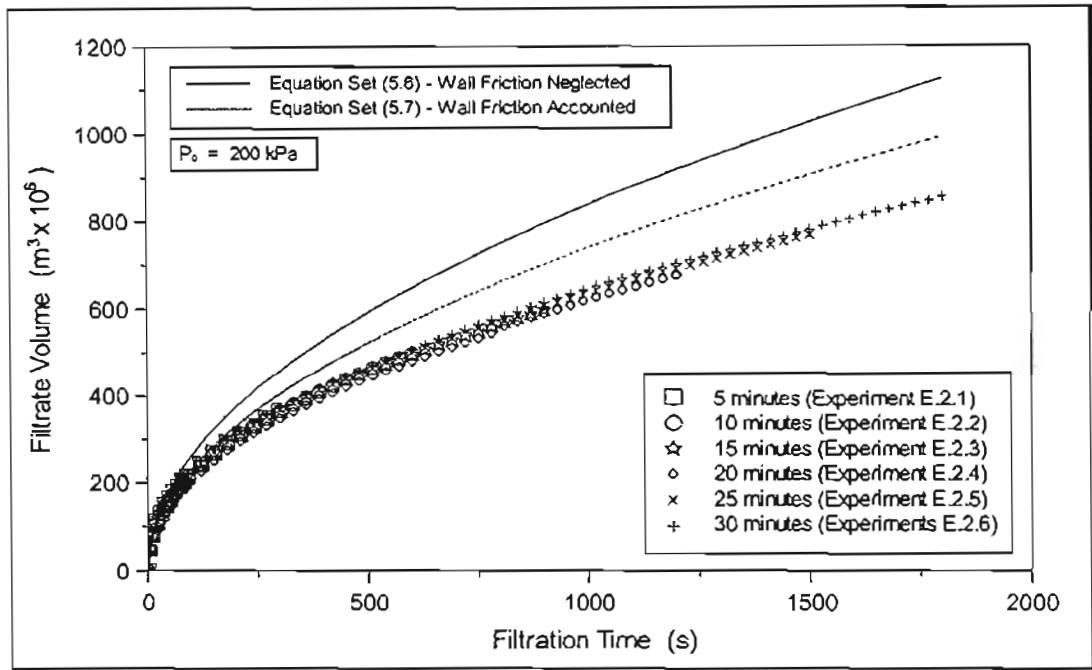


FIGURE 5.40 : Comparison between Experimental and Predicted Filtrate Volumes for Planar Filtration at 200 kPa using the Laboratory Sludge Characterisation

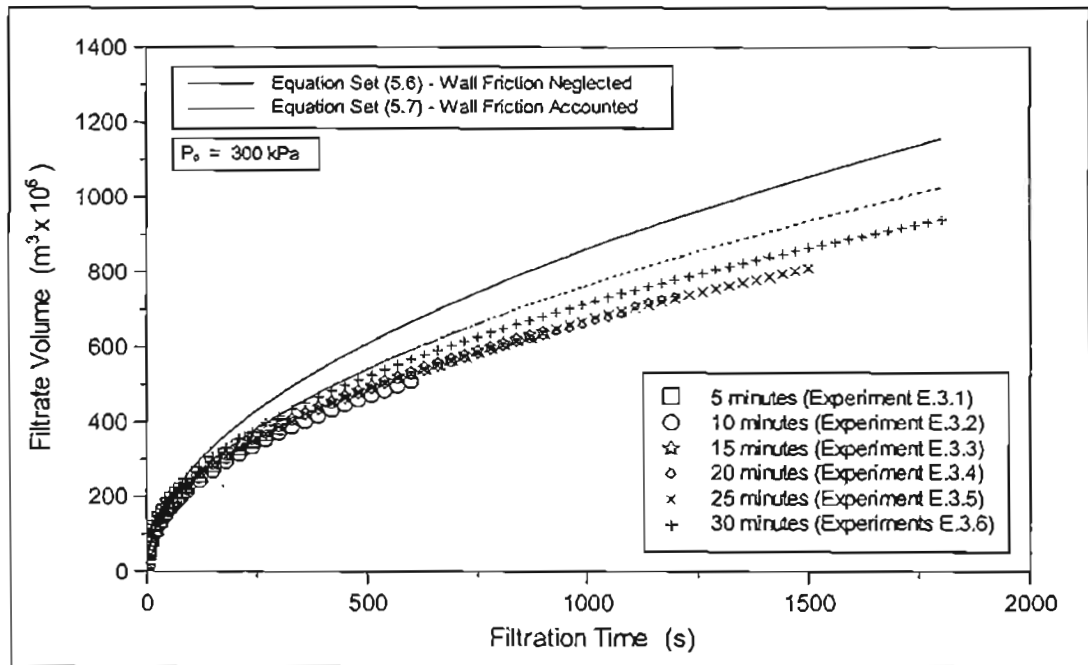


FIGURE 5.41 : Comparison between Experimental and Predicted Filtrate Volumes for Planar Filtration at 300 kPa using the Laboratory Sludge Characterisation

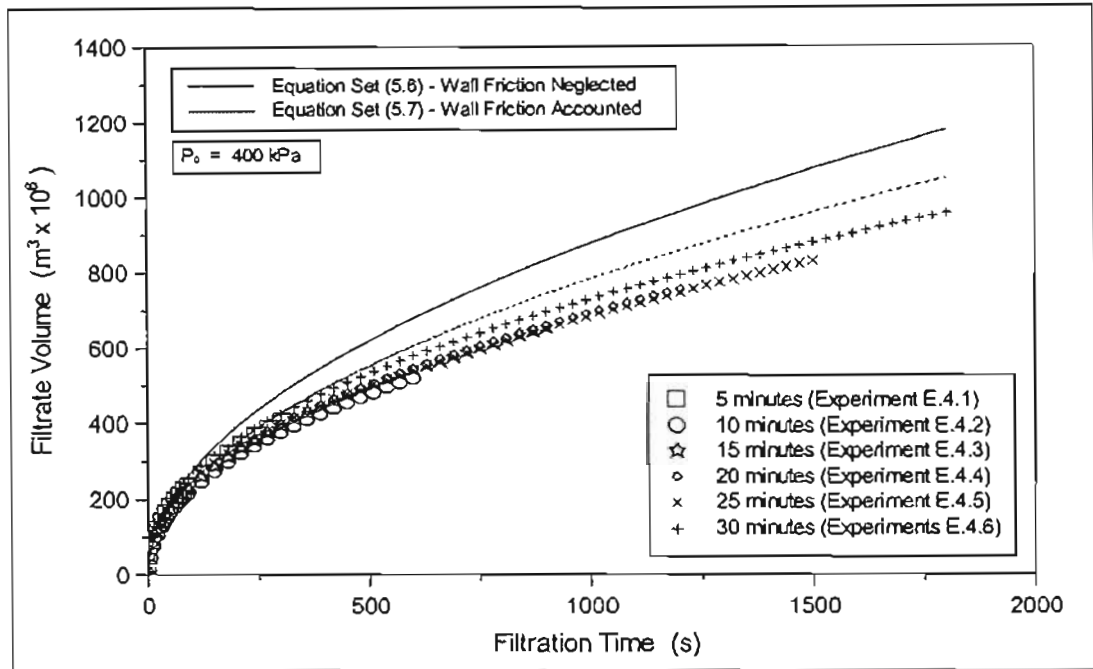


FIGURE 5.42 : Comparison between Experimental and Predicted Filtrate Volumes for Planar Filtration at 400 kPa using the Laboratory Sludge Characterisation

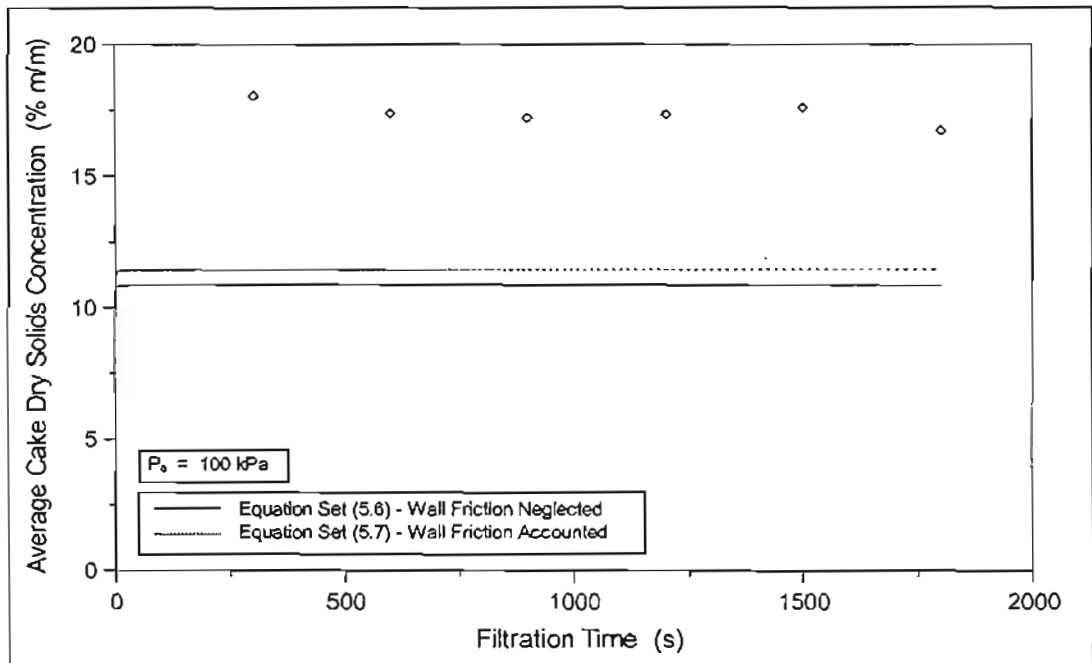


FIGURE 5.43 : Comparison between Experimental and Predicted Average Cake Dry Solids Concentrations for Planar Filtration at 100 kPa using the Laboratory Sludge Characterisation

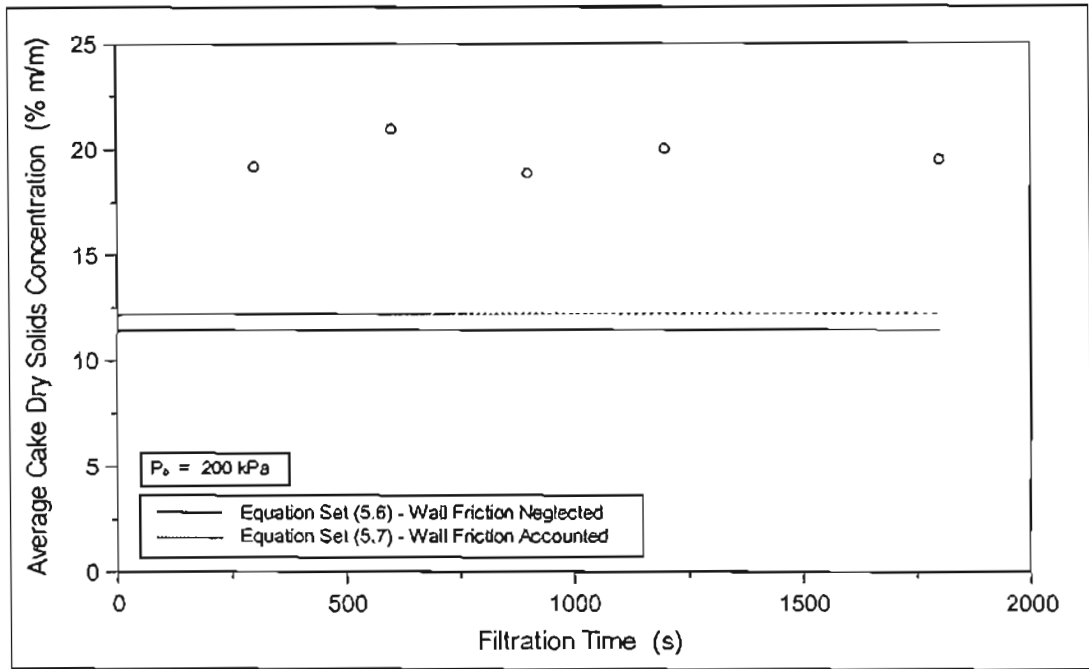


FIGURE 5.44 : Comparison between Experimental and Predicted Average Cake Dry Solids Concentrations for Planar Filtration at 200 kPa using the Laboratory Sludge Characterisation

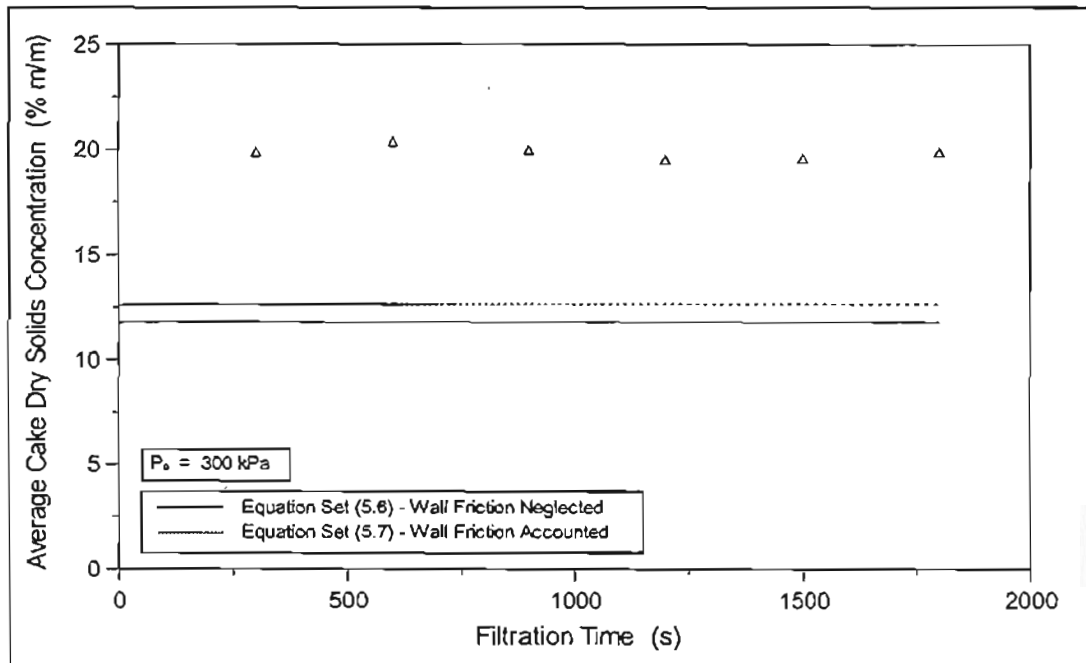


FIGURE 5.45 : Comparison between Experimental and Predicted Average Cake Dry Solids Concentrations for Planar Filtration at 300 kPa using the Laboratory Sludge Characterisation

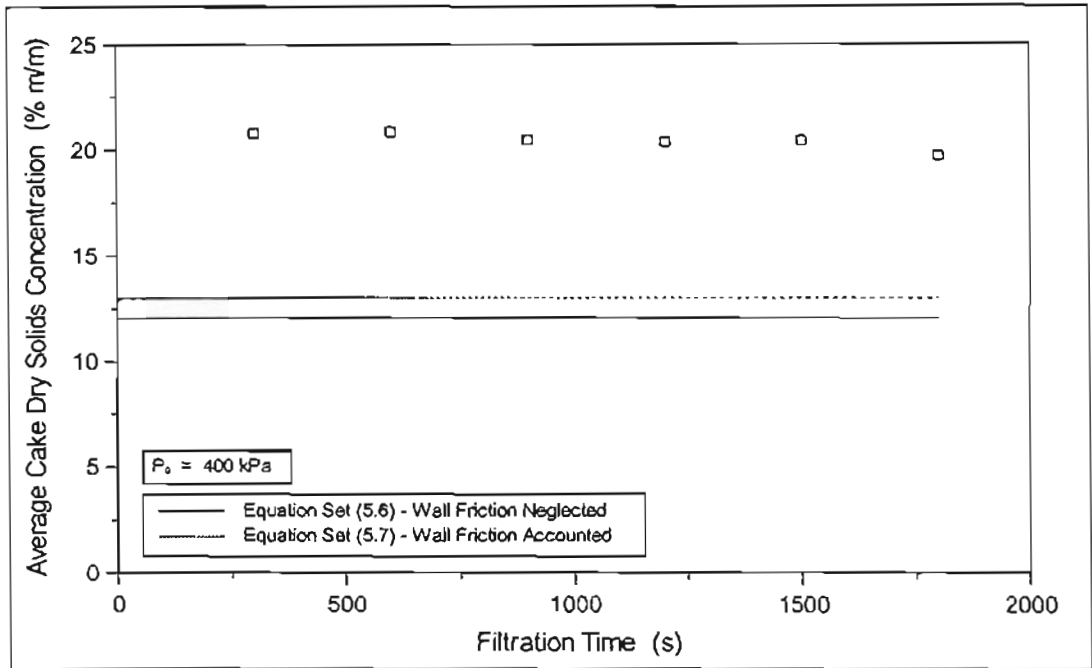


FIGURE 5.46 : Comparison between Experimental and Predicted Average Cake Dry Solids Concentrations for Planar Filtration at 400 kPa using the Laboratory Sludge Characterisation

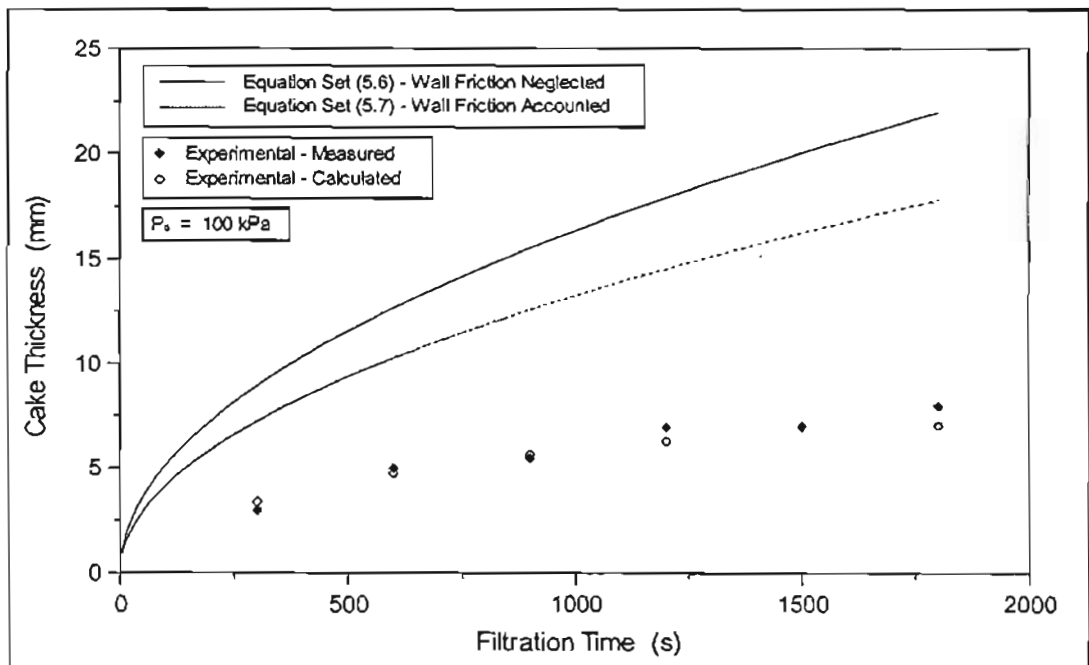


FIGURE 5.47 : Comparison between Experimental and Predicted Cake Thickness for Planar Filtration at 100 kPa using the Laboratory Sludge Characterisation

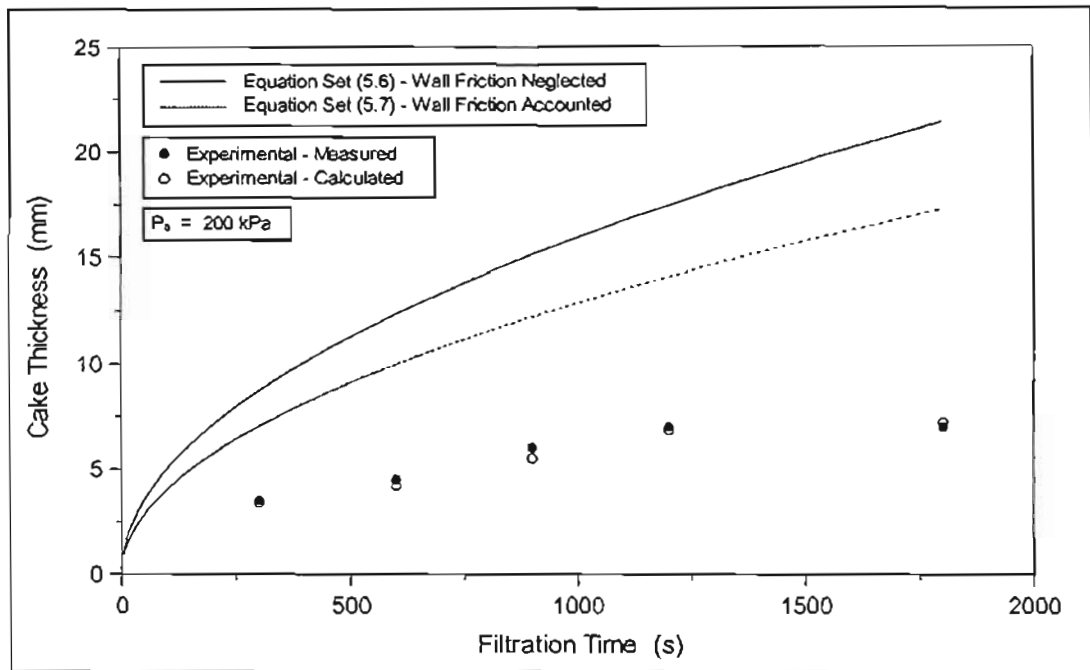


FIGURE 5.48 : Comparison between Experimental and Predicted Cake Thickness for Planar Filtration at 200 kPa using the Laboratory Sludge Characterisation

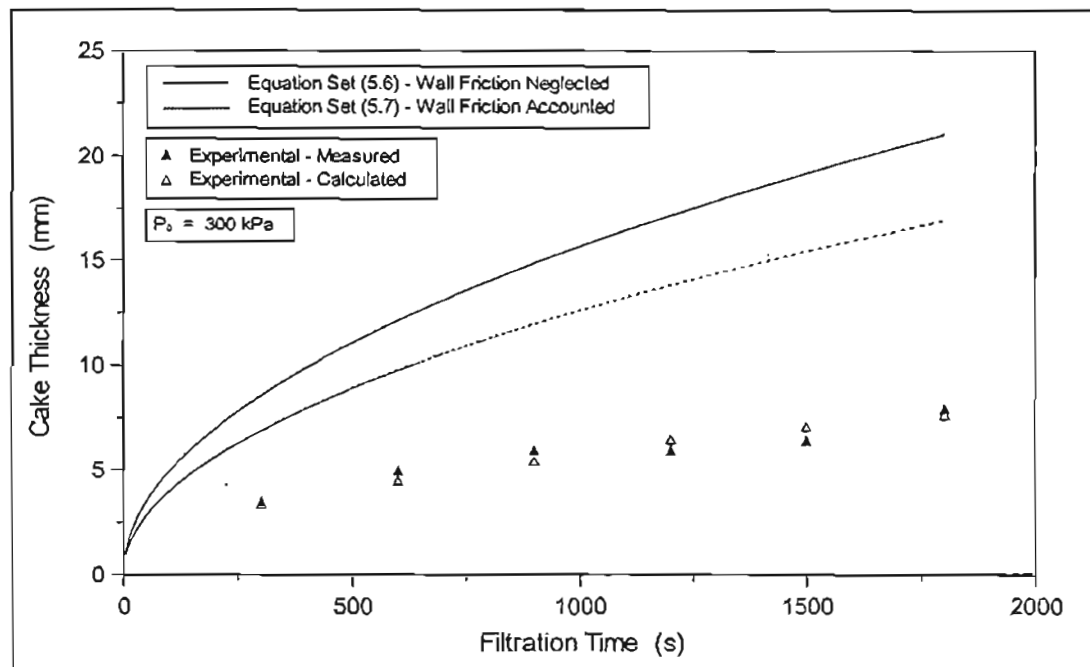


FIGURE 5.49 : Comparison between Experimental and Predicted Cake Thickness for Planar Filtration at 300 kPa using the Laboratory Sludge Characterisation

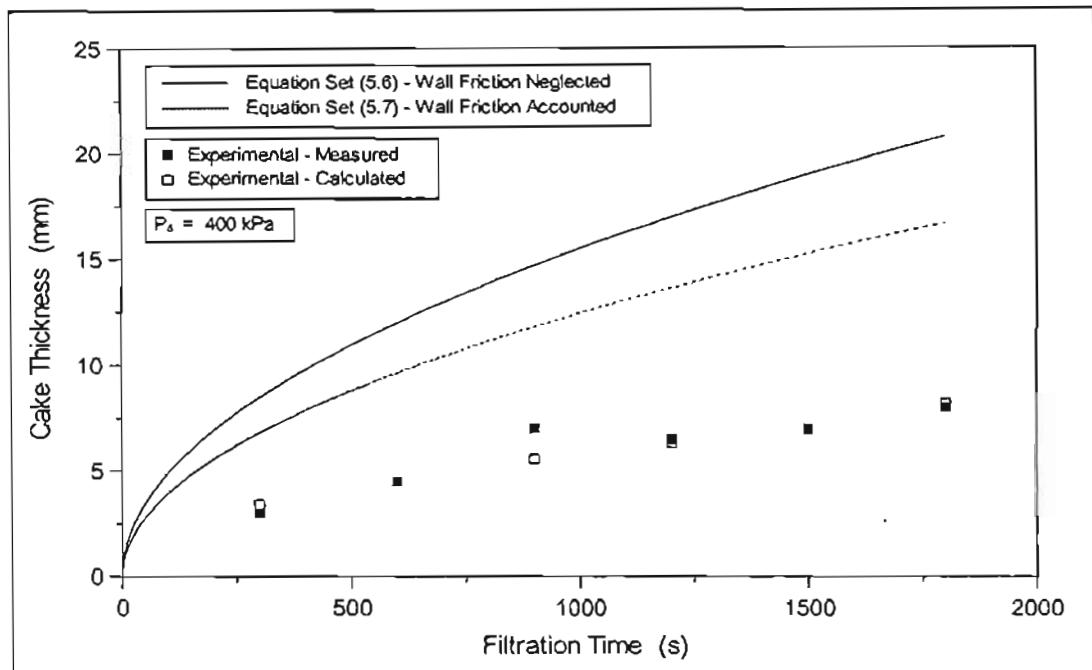


FIGURE 5.50 : Comparison between Experimental and Predicted Cake Thickness for Planar Filtration at 400 kPa using the Laboratory Sludge Characterisation

Table 5.10 and Table 5.11 show the values of the objective function for Equations 5.6 and Equations 5.7 respectively. The results in Table 5.10 and Table 5.11 were obtained from the computer program, REGRESS, which is discussed in Section 5.9. The cake pressure drop and average porosity components of the Equation 3.87 arise from a time independent analysis (see Section 3.4.2.1), and are therefore not a direct comparison of the model predictions to the experimental data. The components of Equation 3.87 that are of real consequence in this discussion are the filtrate volume and cake thickness components arising from the time dependent analysis (Section 3.4.2.2). Experiment E.2.5 was not included in the analysis since the average cake dry solids concentration was not determined.

TABLE 5.10 : Quantitative Assessment of the Agreement between the Planar Filtration Experiments and the Model Output using Equations 5.6

Test	$a(\Delta P_c)$	$a(\varepsilon_{av})$	$a(V_f)$	$a(\theta)$	a
E.1.1 - E.1.6 (100 kPa)	7483.57	61.25	32.10	162.51	1934.86
E.2.1 - E.2.6 (200 kPa)	14339.50	67.08	25.07	172.09	3650.95
E.3.1 - E.3.6 (300 kPa)	21082.50	67.42	21.31	153.91	5331.29
E.4.1 - E.4.6 (400 kPa)	27385.90	68.57	20.08	154.15	6907.17
E.1.1 - E.4.6 (All)	19259.00	66.10	24.52	160.57	4877.54

TABLE 5.11 : Quantitative Assessment of the Agreement between the Planar Filtration Experiments and the Model Output using Equations 5.7

Test	$\alpha(\Delta P_c)$	$\alpha(\varepsilon_{av})$	$\alpha(V_f)$	$\alpha(\theta)$	α
E.1.1 - E.1.6 (100 kPa)	7394.31	60.90	16.23	112.92	1896.09
E.2.1 - E.2.6 (200 kPa)	14286.80	67.08	12.08	119.87	3621.45
E.3.1 - E.3.6 (300 kPa)	20818.90	67.41	9.48	105.12	5250.23
E.4.1 - E.4.6 (400 kPa)	26915.20	68.57	9.50	104.19	6774.35
E.1.1 - E.4.6 (All)	18991.70	66.02	11.81	110.29	4794.95

Figure 5.39 to Figure 5.50, and Table 5.10 to Table 5.11 show that the agreement between the planar filtration results and the model predictions with regard to filtrate volume, average cake dry solids concentration and cake thickness, is improved, when Equations 5.7, which account for the effects of wall friction in C-P cell tests, are incorporated into the model.

Although Equations 5.7 provide a reasonable prediction of filtrate volume with respect to time, an average error of approximately 12 % over the range of filtration pressures and times, the error between experimental and predicted cake thickness is large, approximately 110 %. The increased error observed for the cake thickness may be due to cake losses.

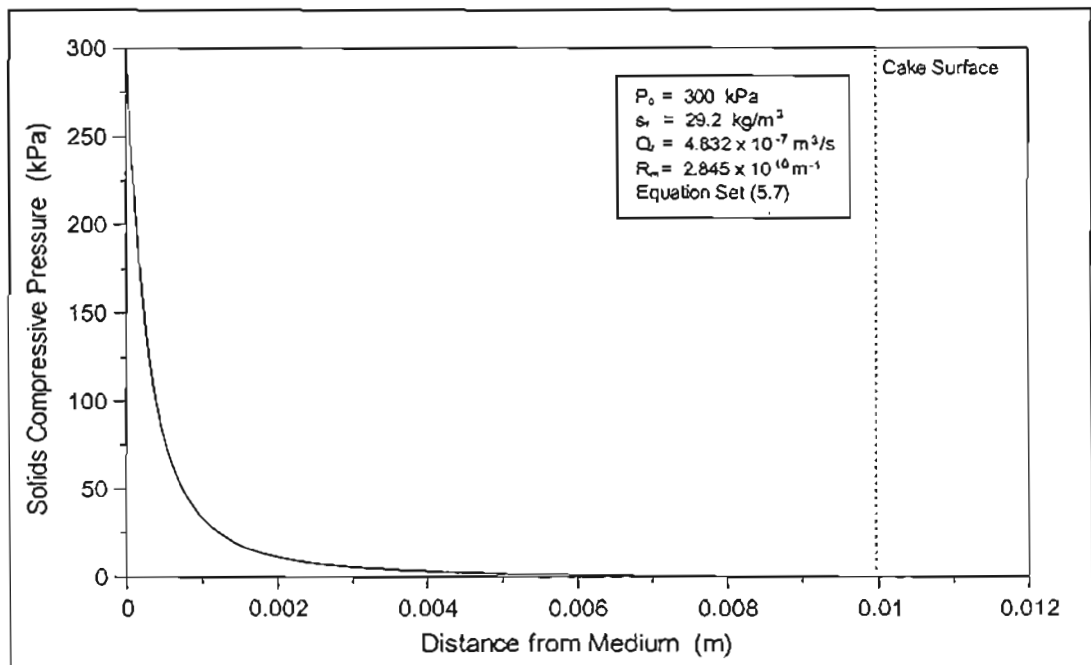


FIGURE 5.51 : Calculated Solids Compressive Pressure Profile through Planar Filtration Cake Characterised by Equations 5.7

Consider the calculated solids compressive pressure profile through a planar compressible cake 10 mm thick, at a pressure of 300 kPa, a feed solids concentration of 29.2 kg/m³, a medium resistance of 2.845 × 10¹⁰ m⁻¹, and using Equations 5.7 (see Figure 5.43). Assume that the cake is completely characterised by Equations 5.7, and as such, the calculated solids

compressive pressure profile is an accurate representation of the actual solids compressive pressure profile through the cake.

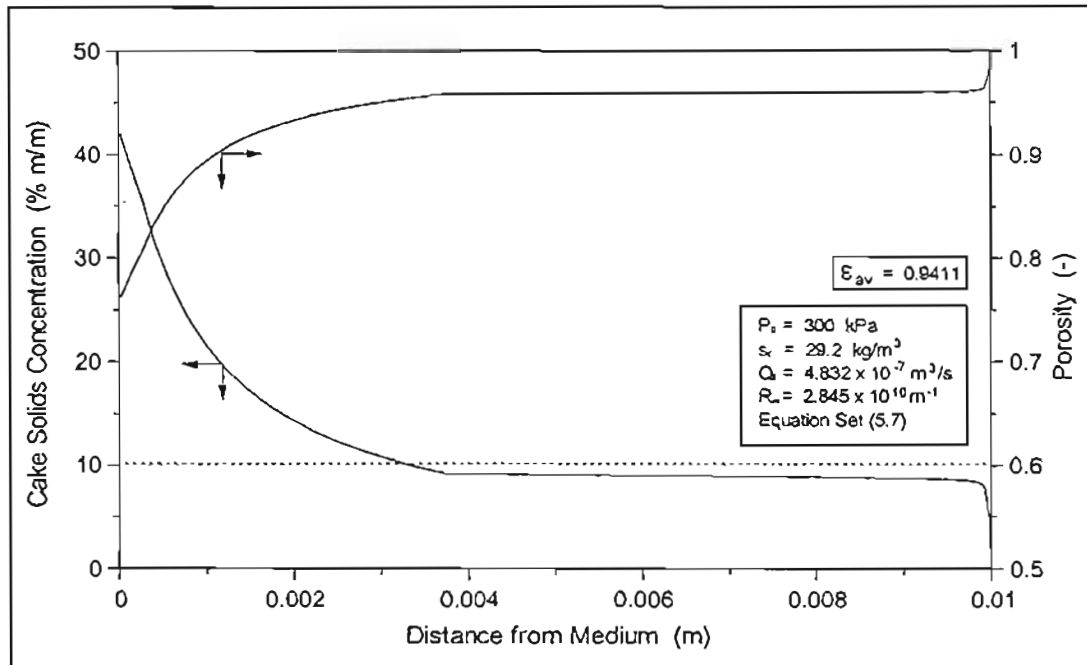


FIGURE 5.52: Calculated Cake Solids Concentration and Porosity Profile through Planar Filtration Cake Characterised by Equations 5.7

It is evident that the outer cake layers experience very low solids compressive pressures. These outer cake layers will be very loose and unconsolidated and as a result will not bind strongly onto the cake structure. As a result, these outer cake layers may be easily removed by any external shear forces that may exist during or after the filtration. Figure 5.52 shows typical cake solids concentration and porosity profiles through a the cake as determined by the solids compressive pressure profile in Figure 5.51. It is clear from Figure 5.52 that the outer cake layers remain unconsolidated at a relatively constant cake solids concentration which is approximately three times that of the feed sludge. This unconsolidated outer cake layer represents approximately 60 % by thickness, of the total cake structure.

After the completion of the filtration and during recovery of the filter cake, the cake may be partly removed by external shear forces imposed on the cake due to the nature of the cake recovery method. As a result, the experimentally observed cake thickness may have been lower than the actual cake thickness, and the experimentally observed average cake dry solids concentration may have been higher than the actual average cake dry solids concentrations. To determine the extent of any possible cake loss by external shear forces after the completion of the filtration, the rheology of the sludge needs to be known as a function of cake solids concentration so that the rheological property profile through the cake can be determined. The degree and nature of the external shear forces exerted on the cake during the cake removal must also known.

During the constant pressure planar filtration experiments, in order to remove the excess sludge after the completion of the filtration, prior to dismantling the cell and recovering the cake, the filter cell was tipped and the sludge poured out of the filter cell (see Section 5.2). During this time the cake would have been exposed to external shear forces due to the movement of the excess sludge out of the cell and also due to gravitational forces acting tangentially to the cake surface. In this discussion an attempt is made to determine to what degree the cake may have been degraded during this phase of the experimental procedure.

The sludge studied by Rencken (1992), was found to be very similar to the sludge used in this study, the sludges originated from similar processes, and showed very similar physical properties and filtration characteristics. To illustrate the possible effects of cake loss, it will be assumed, for the purposes of this discussion, that the rheological behaviour of the sludge studied by Rencken (1992), was an adequate approximation of the rheological properties of the sludge used in this study. Rencken (1992), found that the sludge exhibited Bingham plastic behaviour over a solids concentration range of 3.58 % m/m to 16.71 % m/m and obtained the following relationships:

$$\tau_0 = \frac{7.3268 \times 10^{-4} e^{0.1270c_s}}{1.4292c_s^{3.5805}} \quad c_s \in [3.58, 16.71] \quad (5.8)$$

where c_s = solids concentration of sludge, (% m/m)
 τ_0 = yield stress of bingham plastic, (Pa)

$$\eta = 8.1422 \times 10^{-4} c_s - 2.1914 \times 10^{-4} \quad c_s \in [3.58, 11.1] \quad (5.9)$$

where η = coefficient of rigidity, (Pa.s)

The coefficient of rigidity was found to increase sharply for solids concentrations greater than 11.1 % m/m, and no longer obeyed the linear relationship as given by Equation 5.9. The yield stress of the sludge as described by Equation 5.8 was also found to increase sharply for sludge concentrations greater than 10 % m/m.

The rheological properties of Rencken (1992), were obtained at a temperature of 20.5 °C, the planar filtration experiments were conducted at a temperature of 22 °C, although the temperature dependence of the rheological properties are unknown, the difference in temperature is assumed not to be significant within the context of this discussion.

In Figure 5.53, Equation 5.8 and Equation 5.9 are plotted against the cake solids concentration to give an indication of the expected rheological property profile through the outer cake layers. Except for a thin surface layer of cake where the rheological properties of the

cake rise steeply from that of the feed sludge, the rheology of the outer cake layer remains relatively constant and is represented by a Bingham plastic with a yield stress and coefficient of rigidity that increases slightly from approximately 3.5 Pa to 4.5 Pa and 0.0068 Pa.s to 0.0073 Pa.s respectively. If Equation 5.8 and Equation 5.9 are used to extrapolate slightly to estimate the rheological properties of the feed sludge at 2.88 % m/m (29.2 kg/m³), the feed sludge is found to behave almost like a newtonian fluid, with a very low yield stress of approximately 0.03 Pa and a coefficient of rigidity of approximately 0.0021 Pa.s. The feed sludge at a solids concentration of 2.88 % m/m was found to flow freely from the cell.

Due to the complex and variable nature of cake loss, it will be difficult to obtain an accurate mathematical model to account for the extent of cake loss based on the sludge rheology. The cake loss was mainly due to two mechanisms, shear forces exerted on the cake surface due to the movement of the excess feed sludge as it flowed out of the cell, and flow of the unconsolidated outer cake layer itself, due to gravitational forces acting tangentially to the cake surface, as the cell was tipped to its side. The extent of the shear forces, due to the flow of the excess feed sludge out of the cell, depended on the amount of excess feed sludge in the cell, the rate at which the cell was tipped to allow the feed sludge to pour out of the cell and if any swirling of the feed sludge occurred. The flow of the outer unconsolidated layer due to tangential gravitational forces depended on the extent of the gravitational force and the period of time which the cake was exposed to this force. Since the cell was tipped in excess of 90 degrees to facilitate removal of the excess feed sludge, the tangential gravitational force will be at its maximum.

If the combined action of the flow of the excess feed sludge out of the cell and tangential gravitational force was sufficient to shear the cake surface, it is likely, due to the relatively constant rheological nature of the outer cake layer, that the entire outer cake layer was removed to a limiting point in the cake where the yield stress and coefficient of rigidity began to increase sharply. However, due to the complex and variable nature of the cake loss mechanism combined with the fact that the rheological properties increase slightly, the extent to which the cake loss approaches the limiting value could vary. From the rheological behaviour given by Equation 5.8 and Equation 5.9 and the cake solids concentration profile through the cake (Figure 5.53), this limiting cake solids concentration can be identified at a cake solids concentration of approximately 10 % m/m. This corresponds to a cake thickness of approximately 3.35 mm and hence a possible associated decrease in cake thickness of up to 66.5 %. The calculated average cake concentration at a cake thickness of 3.35 mm is 19.16 % m/m, compared to the original 12.67 % m/m, represents a possible increase in cake dry solids concentration of up to 51.2 %.

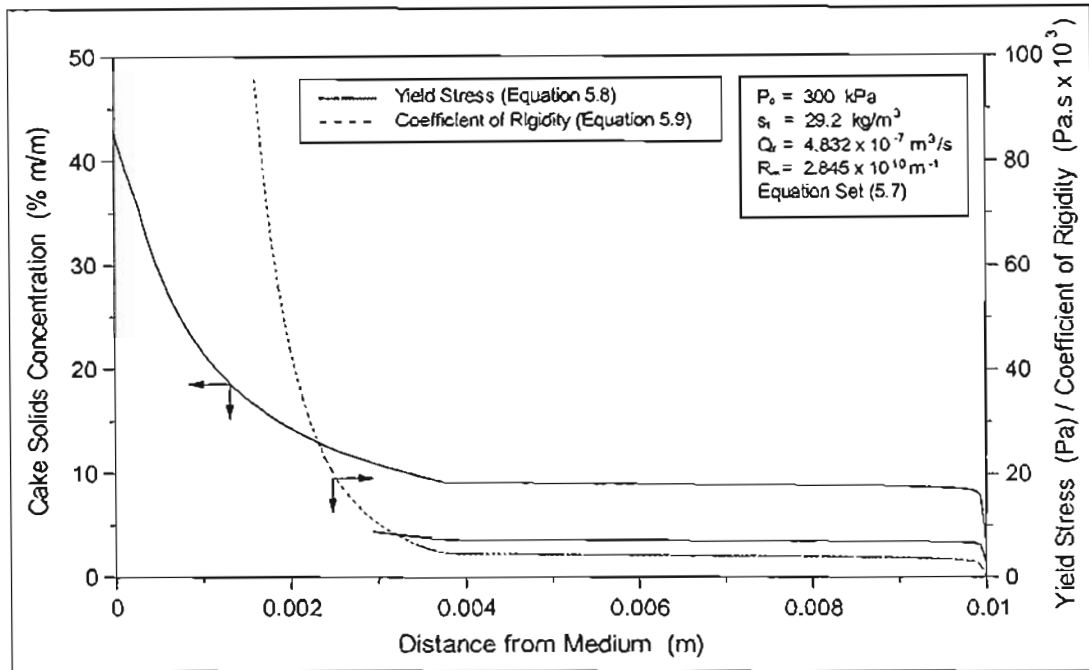


FIGURE 5.53 : Rheological Property Profiles through Planar Filtration Cake Characterised by Equations 5.7

The solids compressive pressure profiles, with respect to the dimensionless distance through the cake for planar filtration, remain relatively constant with respect to time (after the initial stage of the filtration when the cake pressure drop has stabilised and the effect medium resistance is no longer significant). As a result, dimensionless porosity profiles through the cake and hence average cake dry solids concentrations remain relatively constant. The limiting value of cake loss should therefore be independent of filtration time and cake thickness, at the same applied pressure.

If the effect of cake loss is significant, it will have an adverse effect on the predictions of the constant pressure compressible filtration model. If the sludge has been accurately characterised using settling and C-P cell tests, then despite the fact that the experimentally observed and predicted filtrate volumes will be in good agreement, experimentally observed cake thicknesses may be less than those predicted by the model, and experimentally observed average cake dry solids concentrations may be higher than those predicted by the model.

Figure 5.54 and Figure 5.55 show to what extent the results of the model output to predict planar filtration performance at an applied pressure of 300 kPa using Equations 5.7 may be affected by cake loss.

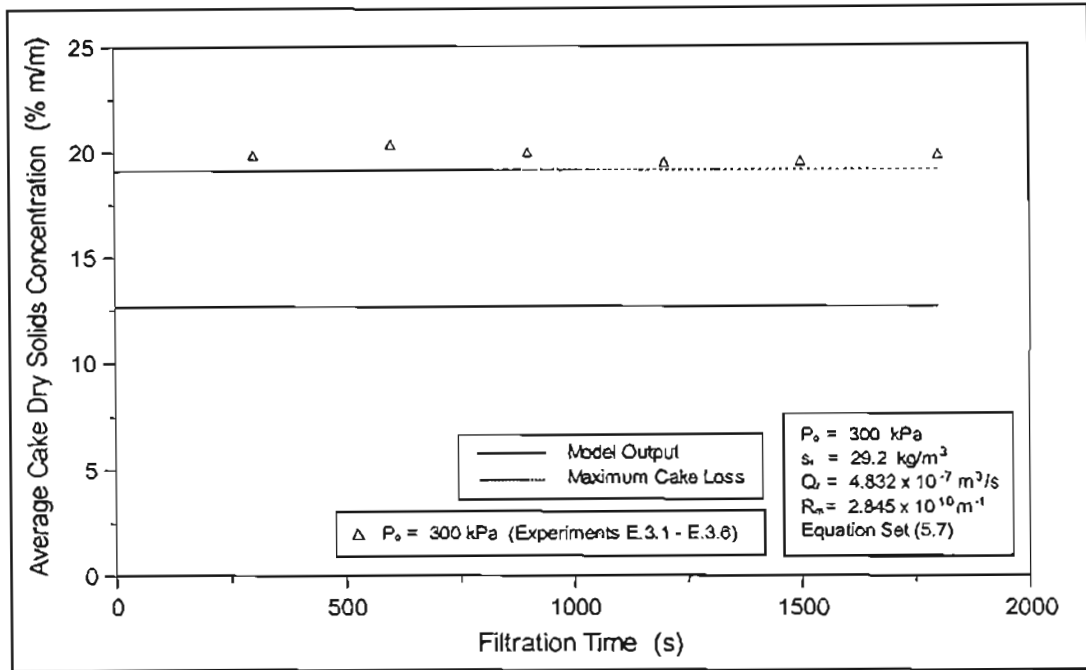


FIGURE 5.54 Effect of Cake Loss on Predicted Average Cake Dry Solids Concentration for Planar Filtration Cake Characterised by Equations 5.7

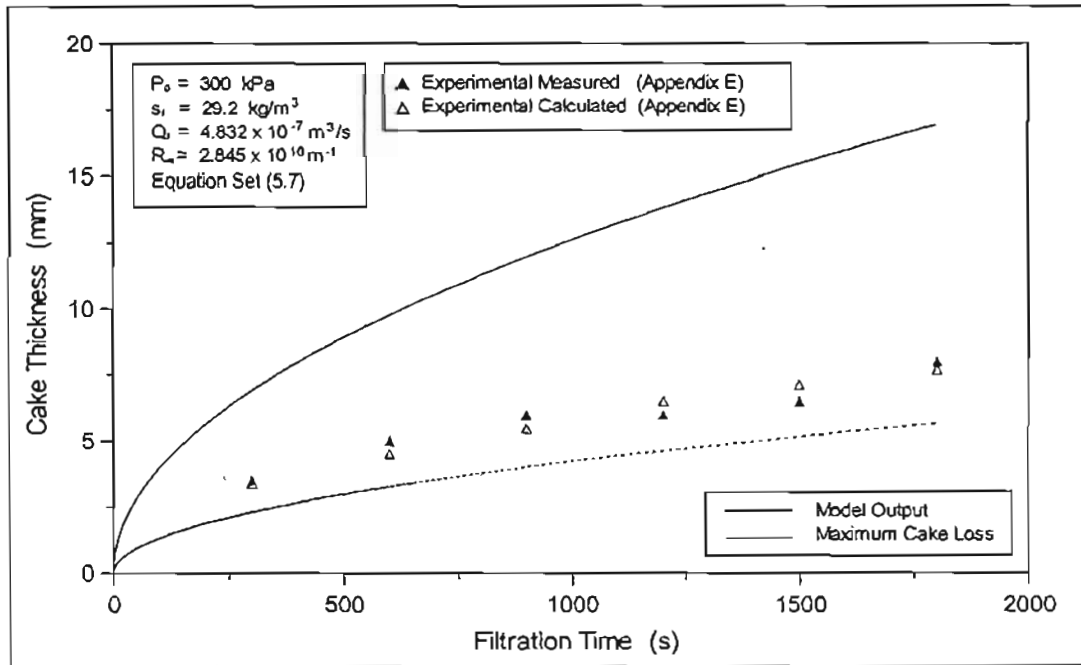


FIGURE 5.55 Effect of Cake Loss on Predicted Cake Thickness for Planar Filtration Cake Characterised by Equations 5.7

Although Equations 5.7 are not a very accurate characterisation of the sludges filtration behaviour, as is evident from the agreement between the experimental and predicted filtrate volume versus time profiles, a much larger discrepancy was observed between the predicted and experimental average cake solids concentration and cake thickness with respect to filtration

time. Once the results of the filtration model had been adjusted to include the effects of cake loss, the agreement between the experimental and predicted average cake solids concentration and cake thickness with respect to filtration time, is brought to within a similar accuracy as observed between the experimental and predicted filtrate volume versus time profiles. This would indicate that cake loss does indeed appear to be affecting the results obtained from the planar filtration experiments. Due the variable nature of cake loss, it could also have accounted for the scatter in the experimentally observed average cake dry solids and cake thickness data (see Section 5.5).

Table 5.12 shows to what extent the cake thickness is expected to decrease, and the average cake dry solids concentration is expected to increase, at different filtration pressures, of a cake with filtration properties characterised by Equations 5.7 and rheological properties given by Equation 5.8 and Equation 5.9, using the assumption that the cake below the limiting cake concentration of 10 % (m/m) is lost.

TABLE 5.12 : Maximum Limiting Cake Loss with respect to Filtration Pressure

Pressure (kPa)	Decrease in Cake thickness (%)	Increase in Average Cake Dry Solids Concentration (%)
100	69.3	45.5
200	68.0	50.4
300	66.5	51.2
400	66.0	52.1

5.8.2 Tubular Filter Press Experiments

Figure 5.56 to Figure 5.65 show the comparison between the filtrate volume profiles for Tubular Filter Press experiments and the predictions of the compressible cake filtration model, using the sludge characterisation obtained from the C-P cell and settling tests (see Section 5.7).

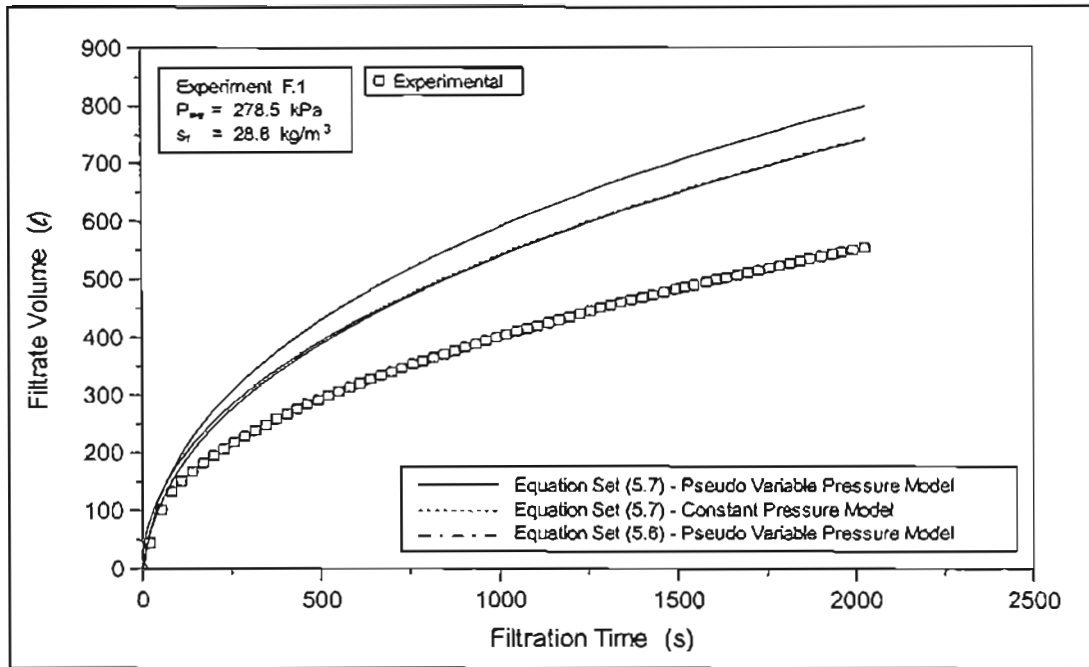


FIGURE 5.56 : Comparison between Experimental and Predicted Filtrate Volume Profiles for the Tubular Filter Press Experiment F.1 using the Laboratory Sludge Characterisation

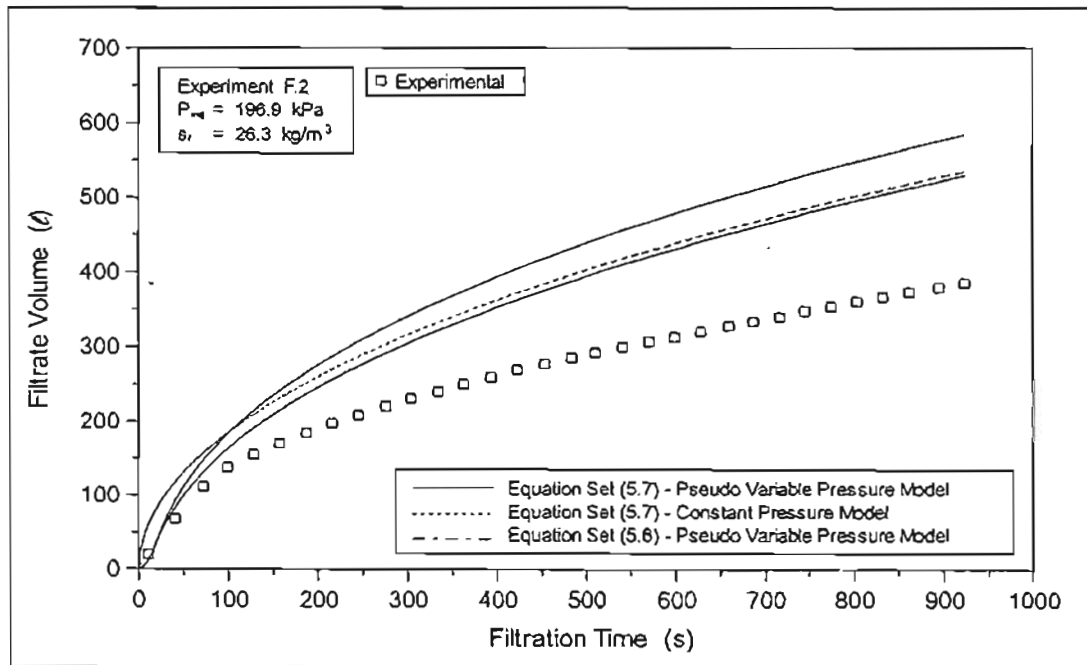


FIGURE 5.57 : Comparison between Experimental and Predicted Filtrate Volume Profiles for the Tubular Filter Press Experiment F.2 using the Laboratory Sludge Characterisation

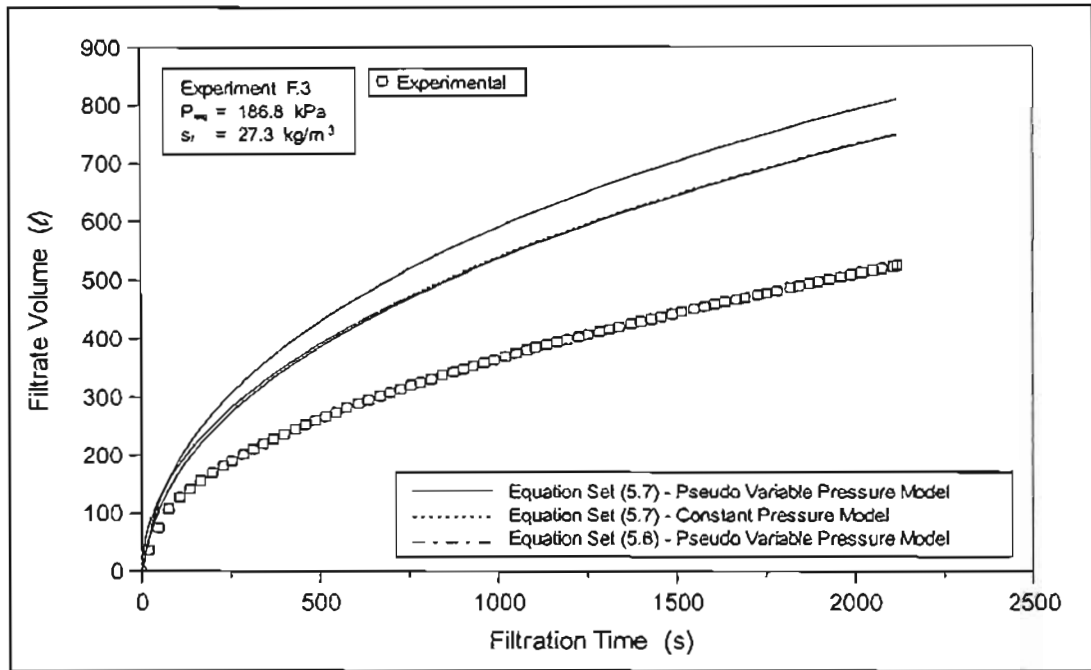


FIGURE 5.58 : Comparison between Experimental and Predicted Filtrate Volume Profiles for the Tubular Filter Press Experiment F.3 using the Laboratory Sludge Characterisation

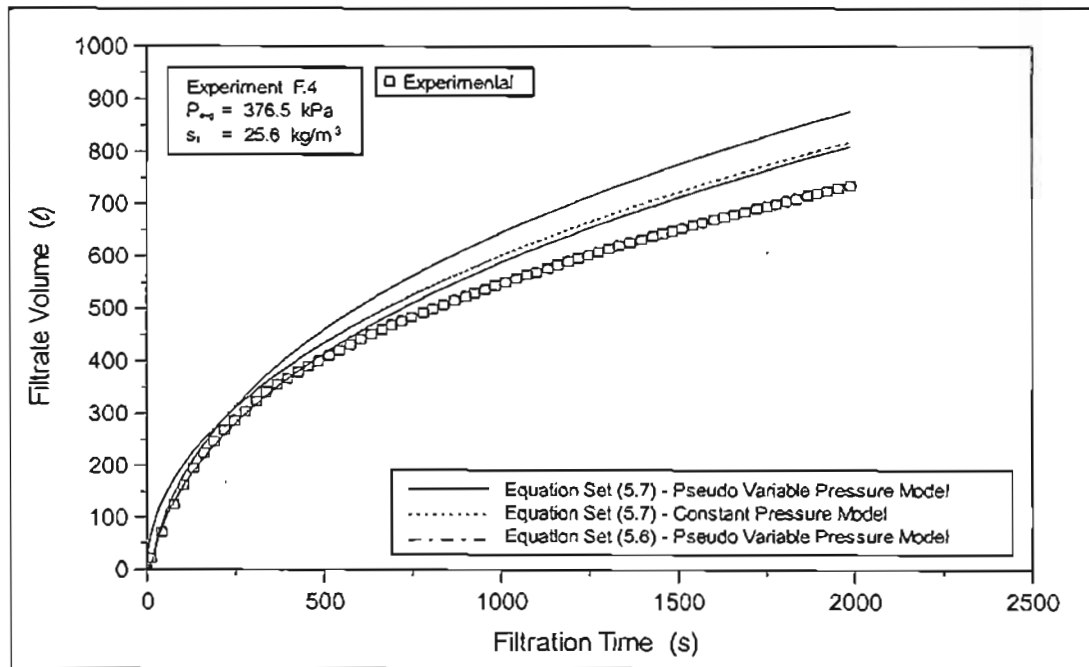


FIGURE 5.59 : Comparison between Experimental and Predicted Filtrate Volume Profiles for the Tubular Filter Press Experiment F.4 using the Laboratory Sludge Characterisation

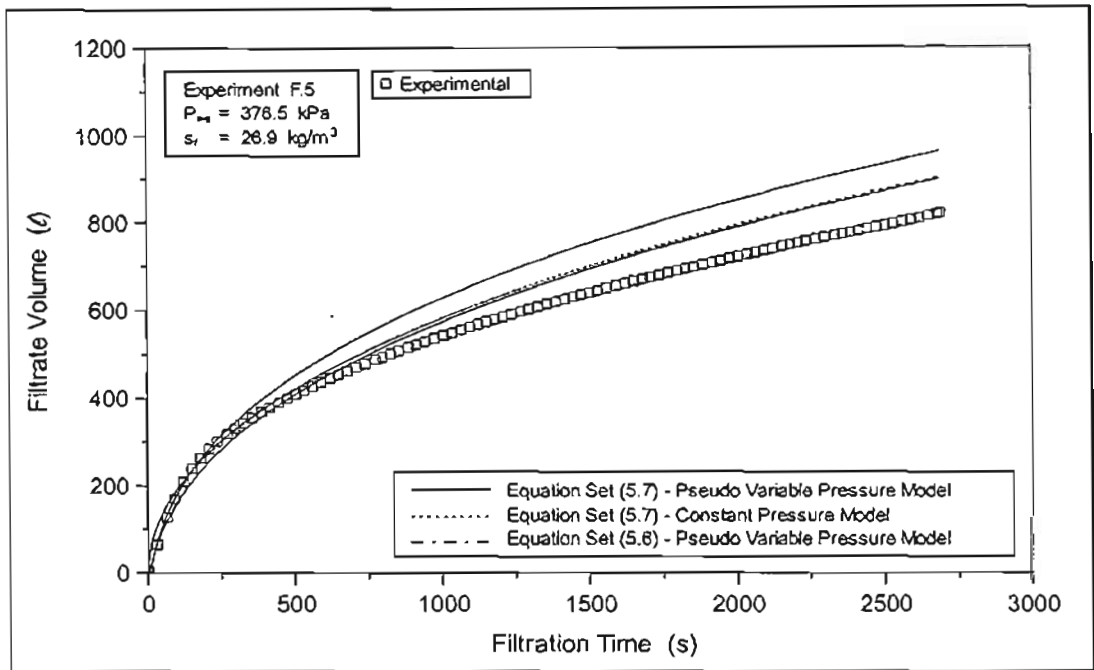


FIGURE 5.60 : Comparison between Experimental and Predicted Filtrate Volume Profiles for the Tubular Filter Press Experiment F.5 using the Laboratory Sludge Characterisation.

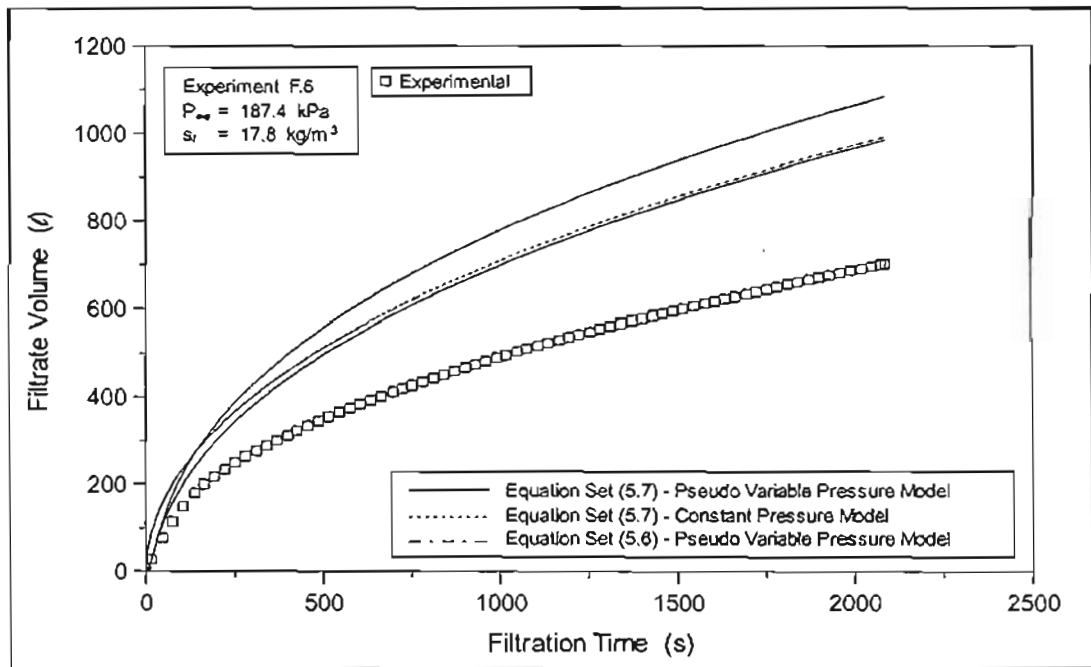


FIGURE 5.61 : Comparison between Experimental and Predicted Filtrate Volume Profiles for the Tubular Filter Press Experiment F.6 using the Laboratory Sludge Characterisation

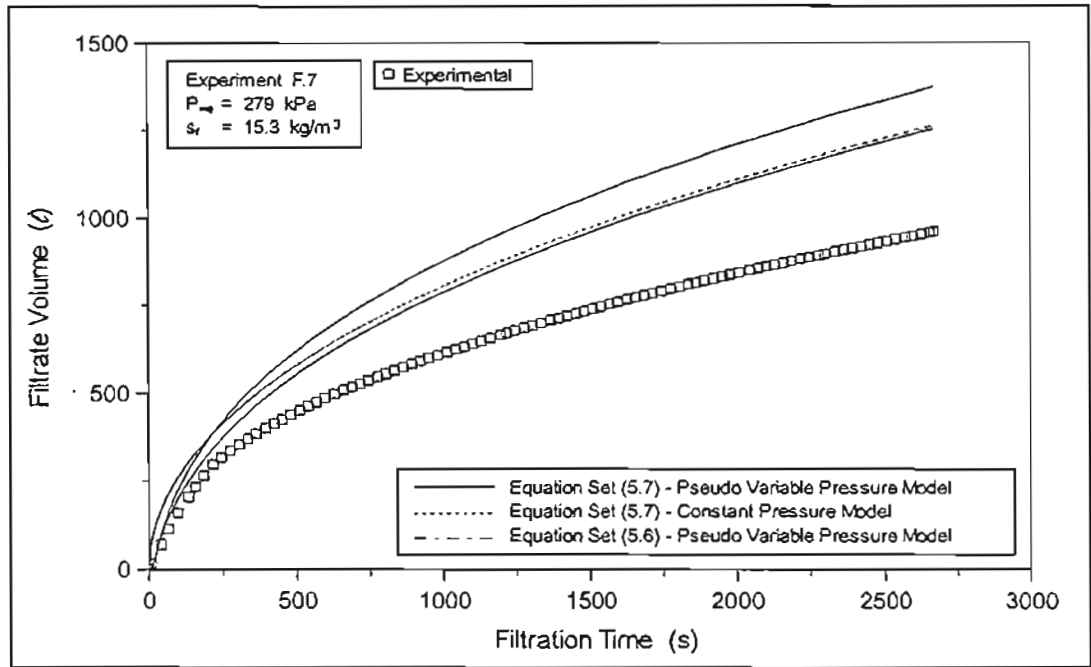


FIGURE 5.62 : Comparison between Experimental and Predicted Filtrate Volume Profiles for the Tubular Filter Press Experiment F.7 using the Laboratory Sludge Characterisation

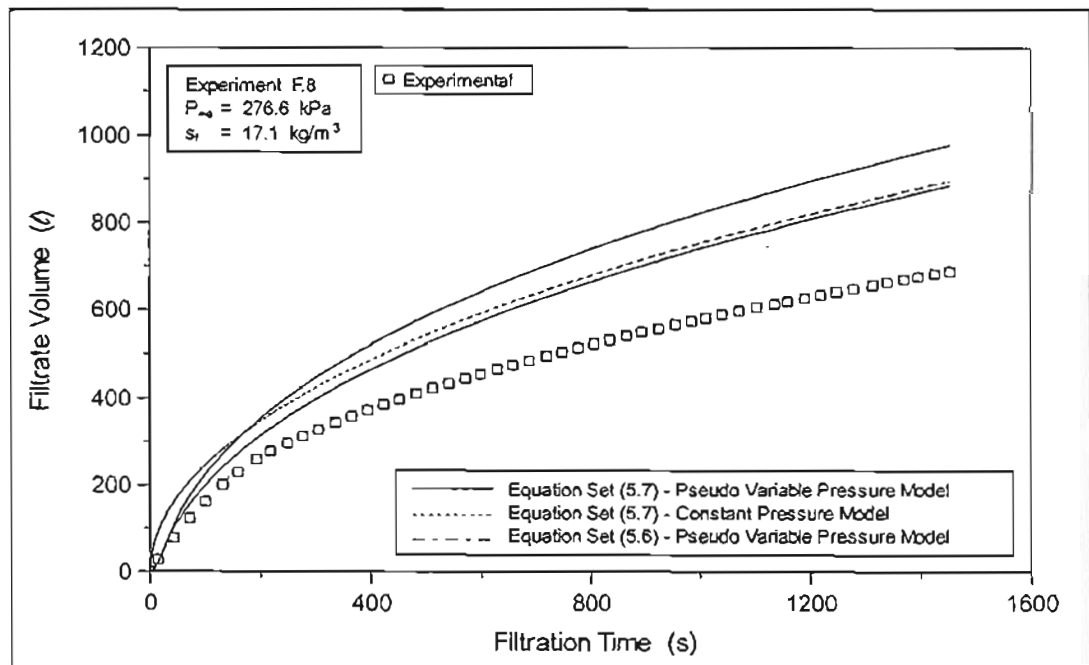


FIGURE 5.63 : Comparison between Experimental and Predicted Filtrate Volume Profiles for the Tubular Filter Press Experiment F.8 using the Laboratory Sludge Characterisation

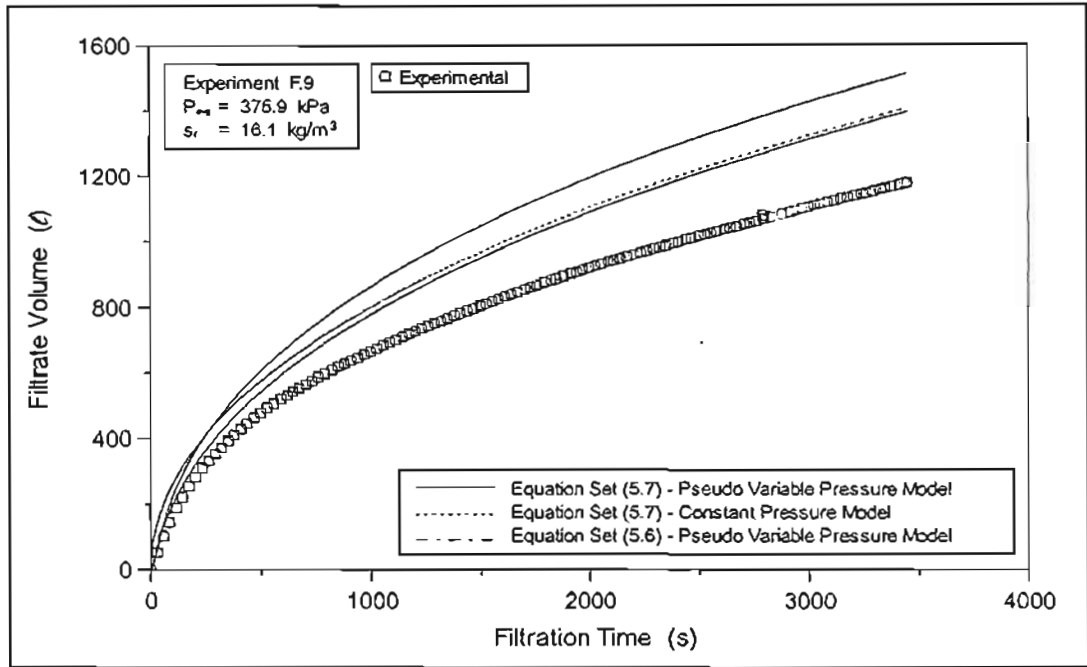


FIGURE 5.64 : Comparison between Experimental and Predicted Filtrate Volume Profiles for the Tubular Filter Press Experiment F.9 using the Laboratory Sludge Characterisation

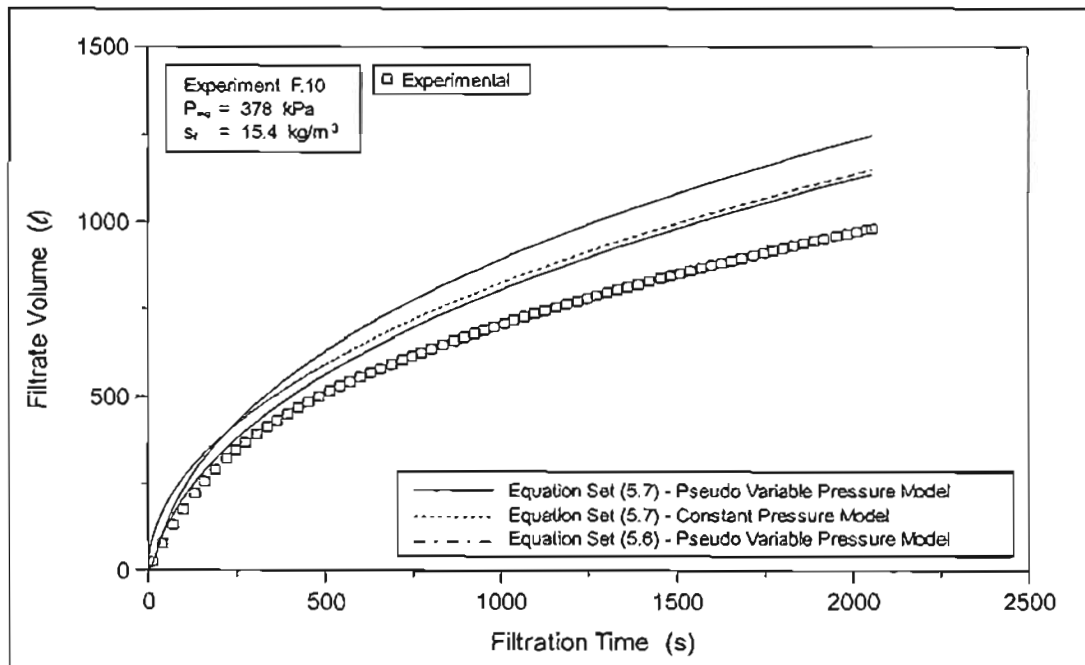


FIGURE 5.65 : Comparison between Experimental and Predicted Filtrate Volume Profiles for the Tubular Filter Press Experiment F.10 using the Laboratory Sludge Characterisation

Due to variations in the feed solids concentration, final applied pressure and pressurisation time, for each of the Tubular Filter Press experiments, the comparisons between the filtrate volume versus time behaviour of the Tubular Filter Press experiments and the predictions of

the filtration model are presented separately for each experiment. In Figure 5.56 to Figure 5.65, the output of the pseudo variable pressure solution procedure is presented utilising Equations 5.6 and Equations 5.7 in the model. For comparative purposes, the output of the constant pressure solution procedure using Equations 5.7 is also presented.

From Figure 5.56 to Figure 5.65, it is evident that the pseudo variable pressure model accounts very well for the initial, almost linear, filtrate volume versus time response of the Tubular Filter Press, during the initial pressurisation period. During conventional constant pressure filtration, the initial high constant applied pressure results in a very high initial filtrate flow rate, limited only by the resistance of the medium. The flow rate then decreases as the filter cake builds up and the combined resistance of the medium and the cake increases, resulting in the conventional parabolically shaped filtrate volume versus time profile. This behaviour is clearly shown by the output of the constant pressure solution procedure in Figure 5.56 to Figure 5.65. During the variable pressure filtration, the initial applied pressure is low, resulting in a low initial filtrate flow rate, as the filter cake grows and the combined cake and medium resistance increases, so too does the applied pressure. The net effect during the initial pressurisation period is an almost constant initial filtrate flow rate, resulting in an initial linear filtrate volume profile during the pressurisation period, followed thereafter by the conventional parabolic filtrate volume profile once the constant applied pressure has been reached.

From Figure 5.56 to Figure 5.65, it is evident that, after the initial pressurisation period, the difference between the predicted filtrate volumes, using the constant pressure and pseudo variable pressure solution procedures, decreases with time. Due to the more rapid initial cake growth, the filter cake formed under constant pressure conditions will be thicker than the cake formed under the variable pressure conditions, at the end of the pressurisation period. As a result, the cake formed under variable pressure conditions will have a lower overall resistance, and hence, at the same applied pressure, a higher filtrate flow rate. The filtrate volume will therefore increase more rapidly, at the same point in time, for the cake formed under variable pressure conditions, than the cake formed under constant pressure conditions, decreasing the difference between the total filtrate volumes. However, the more rapid increase in filtrate volume will result in a more rapid cake growth, and hence, a more rapid increase in overall resistance. The net affect will be that the filtrate volume and cake thickness of the variable pressure filtration will approach the filtrate volume and cake thickness of the constant pressure filtration with time, but the rate of approach will decrease with time (see Figure 5.66).

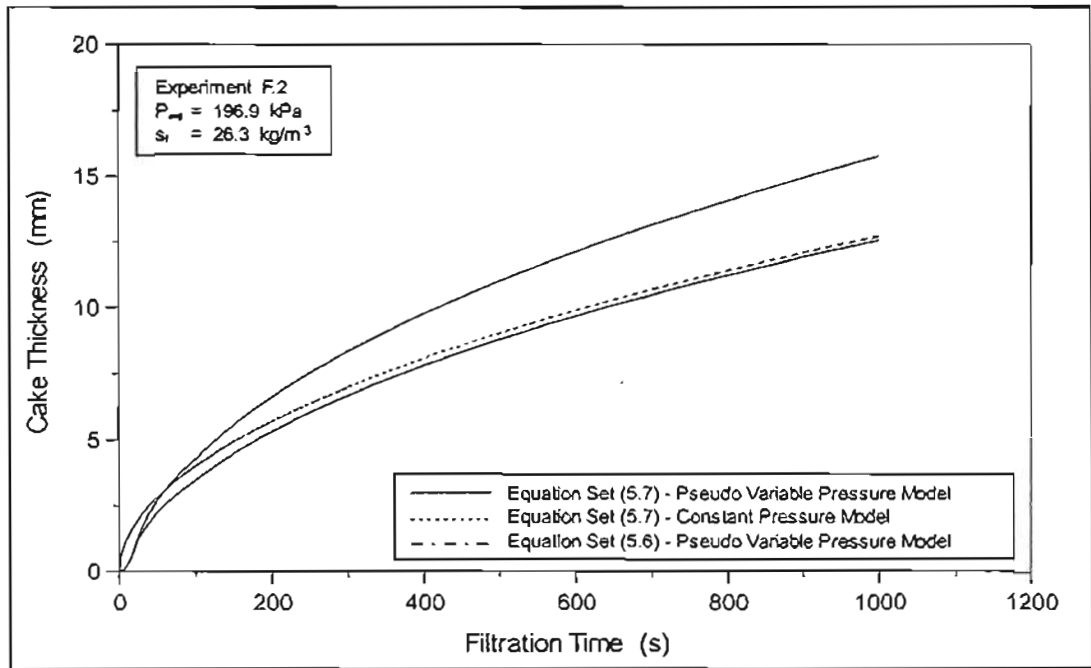


FIGURE 5.66 : Predicted Cake Thickness Profiles for Experiment F.2

TABLE 5.13 : Quantitative Assessment of the Agreement between the Tubular Filter Press Experiments and the Model Output using Equations 5.6

Test	$a(\Delta P_c)$	$a(\varepsilon_{av})$	$a(V_f)$	$a(\theta)$	a
F.1	36532.50	73.57	46.78	269.66	9231.04
F.2	19838.50	67.60	54.57	242.57	5054.54
F.3	26992.90	71.85	61.11	303.90	6858.13
F.4	37374.60	74.40	19.92	207.97	9424.06
F.5	32457.20	76.24	17.47	218.82	8202.10
F.6	19213.40	64.23	60.42	234.45	4895.62
F.7	30549.10	70.19	45.27	258.29	7736.48
F.8	28200.80	69.60	44.80	244.43	7144.73
F.9	38676.60	74.23	31.66	255.76	9761.83
F.10	34556.50	72.68	29.25	233.33	8728.92
Combined	29350.40	73.07	38.44	240.37	7430.08

The computer programme REGRESS (see Section 5.9), does not incorporate the pseudo variable pressure solution procedure, as a result the values for the objective function in Table 5.13 and Table 5.14, are determined using the constant pressure solution procedure. From Figure 5.56 to Figure 5.65, it is evident that the difference between the output of the constant pressure and pseudo variable pressure solution procedures after the initial pressurisation period, is not significant. Therefore Equation 3.87 still provides a very good quantitative assessment of the accuracy of the model output, provided experimental data obtained during the variable pressure period, is omitted.

TABLE 5.14 : Quantitative Assessment of the Agreement between the Tubular Filter Press Experiments and the Model Output using Equations 5.7

Test	$a(\Delta P_c)$	$a(\varepsilon_{av})$	$a(V_f)$	$a(\rho)$	a
F.1	36532.50	73.57	34.05	197.38	9209.73
F.2	19838.50	67.60	39.07	172.74	5032.98
F.3	26992.90	71.85	46.56	224.43	6834.47
F.4	37374.60	74.40	9.86	146.70	9406.40
F.5	32457.20	76.24	8.56	158.64	8184.85
F.6	19213.40	64.23	44.20	166.57	4874.39
F.7	30549.10	70.19	31.22	185.87	7714.71
F.8	28200.80	69.60	30.16	174.82	7123.50
F.9	38676.60	74.23	20.02	185.15	9741.19
F.10	34556.50	72.68	16.97	165.98	8709.00
Combined	29350.40	73.07	25.53	172.66	7409.89

From Figure 5.56 to Figure 5.65, and the values of the filtrate volume component of Equation 3.87 given in Table 5.13 to Table 5.14, it is clear that the accuracy of the model output to predict the filtrate volume profiles, is increased when the sludge characterisation, which accounts for the effects of wall friction, Equation 5.7, is included in the model. The filtration behaviour is consistent between tests, but a general increase in accuracy is observed with increasing applied pressure.

The same general trends were observed with respect to filtrate volume, for both the results of the planar filtration experiments and the results of the Tubular Filter Press experiments when compared to the predictions of the filtration model, indicating a consistent filtration behaviour. Generally the model accuracy was better for the planar filtration experiments, however, the difficulty in assessing the exact start of filtration for the Tubular Filter Press experiments may have contributed to the variability and increased inaccuracy between the experimental results and the model predictions. For the Tubular Filter Press, the larger the final applied pressure, the less significant the applied pressure distribution along the length of the tube due to the hydrostatic pressure component. Although the planar filtration tests also show an increase in accuracy with applied pressure, the relative difference in applied pressure between the top and bottom of the tubes, could account for the larger difference in accuracy observed between tests over the range of final applied pressures for the Tubular Filter Press.

Figure 5.67 to Figure 5.72 show the comparison between the average cake dry solids concentrations for the Tubular Filter Press experiments and the predictions of the compressible cake filtration model using the sludge characterisation obtained from the C-P cell and settling tests (see Section 5.7). Where applicable, experiments at similar operating pressures and feed

solids concentrations have been grouped together, due to the insensitivity of the average cake dry solids concentration to these experimental parameters. For these cases, the outputs of the filtration model have been determined using the average pressure, average feed solids concentration and where applicable, average pressurisation time, for the two experiments. The predicted average cake concentrations at each experiments final filtration times have been determined using the experiments own unique operating conditions in the model. In addition to the screened and unscreened experimental cake dry solids concentrations, an indication is given of the expected average cake dry solids concentration with respect to time, of a cake characterised by Equations 5.7, that has experienced cake losses up to a internal dry solids concentration of 10 % m/m.

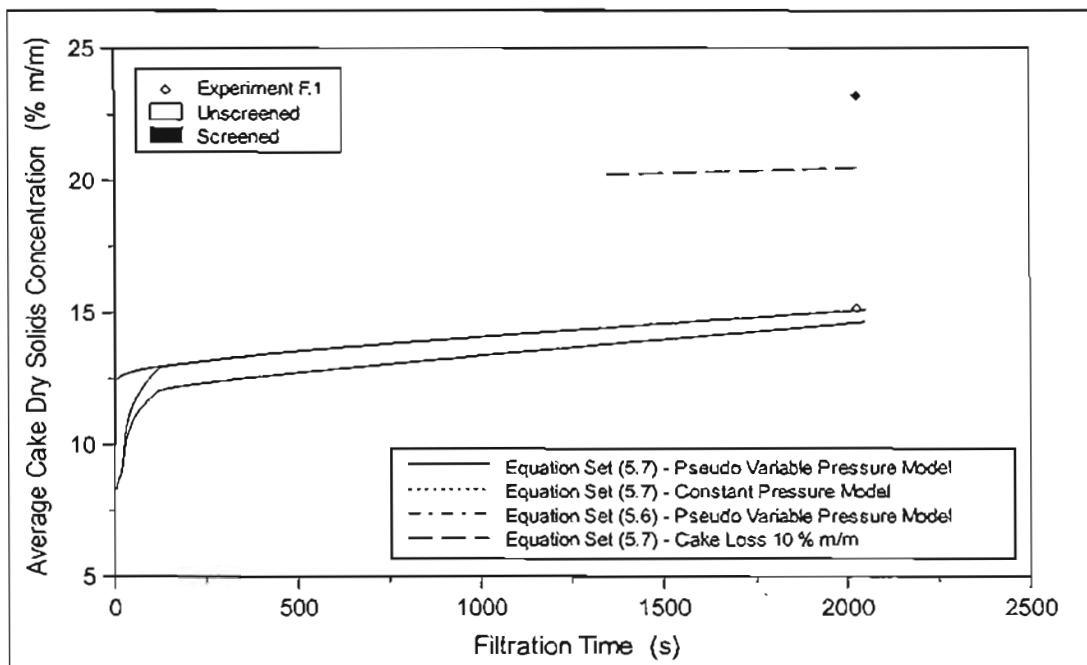


FIGURE 5.67 : Comparison between Experimental and Predicted Average Cake Dry Solids Concentration for the Tubular Filter Press Experiment F.1 using the Laboratory Sludge Characterisation

Figure 5.67 to Figure 5.72 show clearly the increase in average cake dry solids concentration during the initial pressurisation stage of the variable pressure calculation, as the applied pressure increased with time. After the initial pressurisation period, the difference between the predicted average cake dry solids concentrations using the constant pressure and variable pressure solution procedures was insignificant.

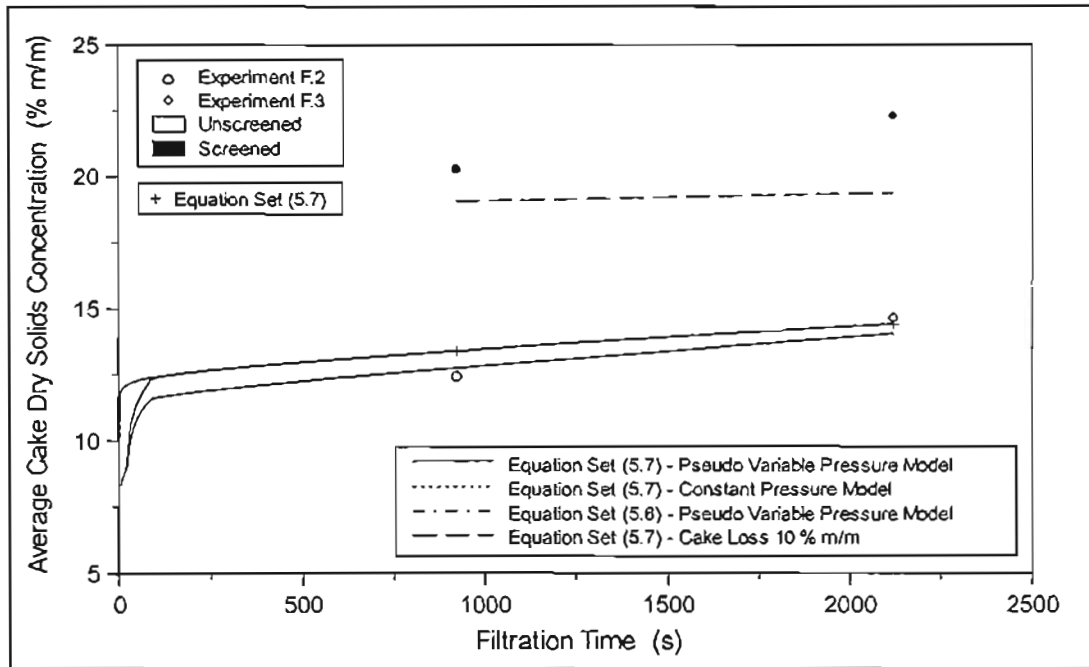


FIGURE 5.68 : Comparison between Experimental and Predicted Average Cake Dry Solids Concentration for the Tubular Filter Press Experiment F.2 and Experiment F.3 using the Laboratory Sludge Characterisation

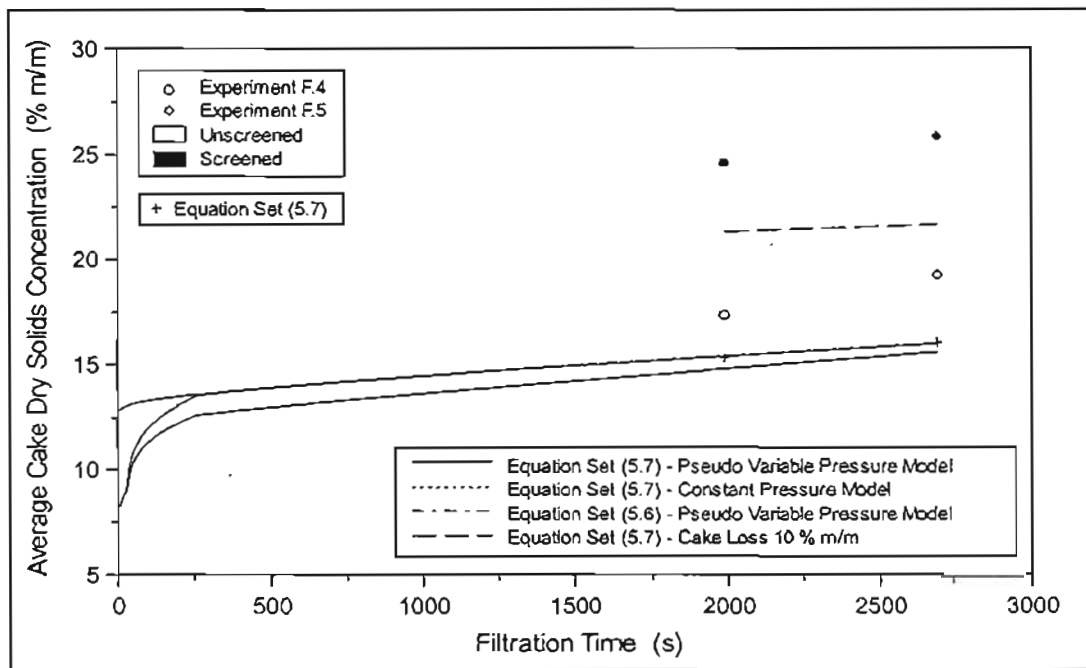


FIGURE 5.69 : Comparison between Experimental and Predicted Average Cake Dry Solids Concentration for the Tubular Filter Press Experiment F.4 and Experiment F.5 using the Laboratory Sludge Characterisation

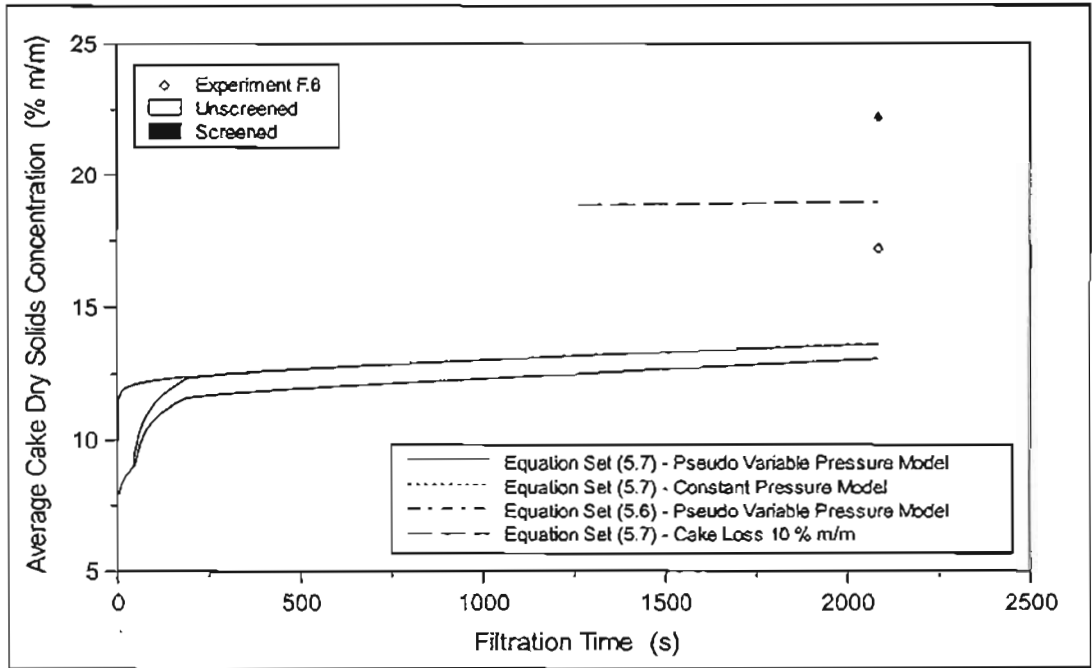


FIGURE 5.70 : Comparison between Experimental and Predicted Average Cake Dry Solids Concentration for the Tubular Filter Press Experiment F.6 using the Laboratory Sludge Characterisation

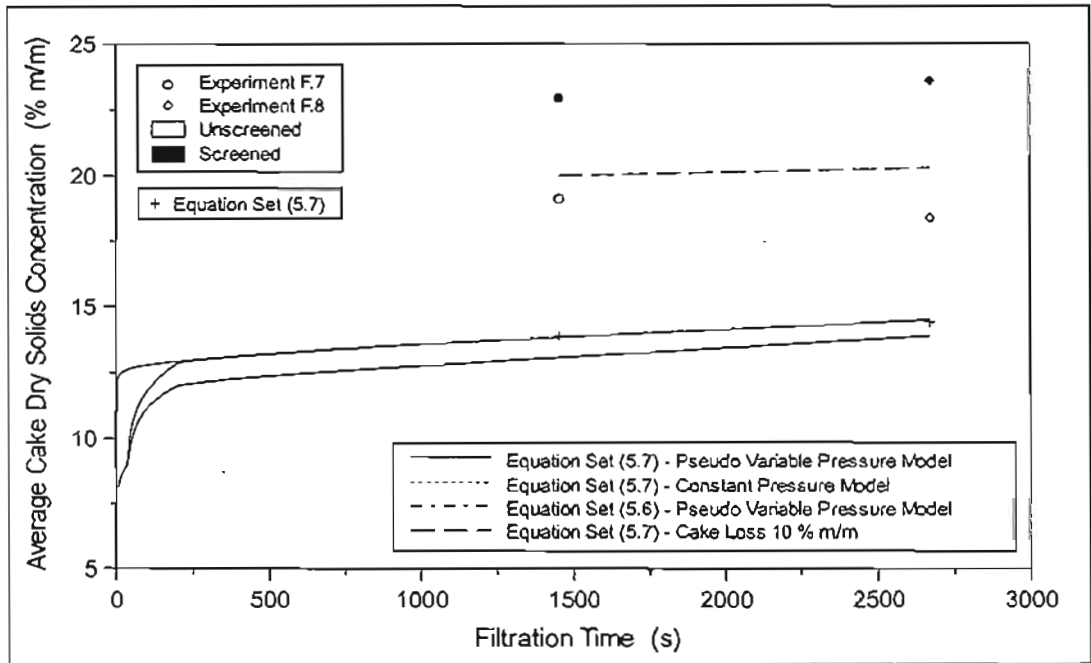


FIGURE 5.71 : Comparison between Experimental and Predicted Average Cake Dry Solids Concentration for the Tubular Filter Press Experiment F.7 and Experiment F.8 using the Laboratory Sludge Characterisation

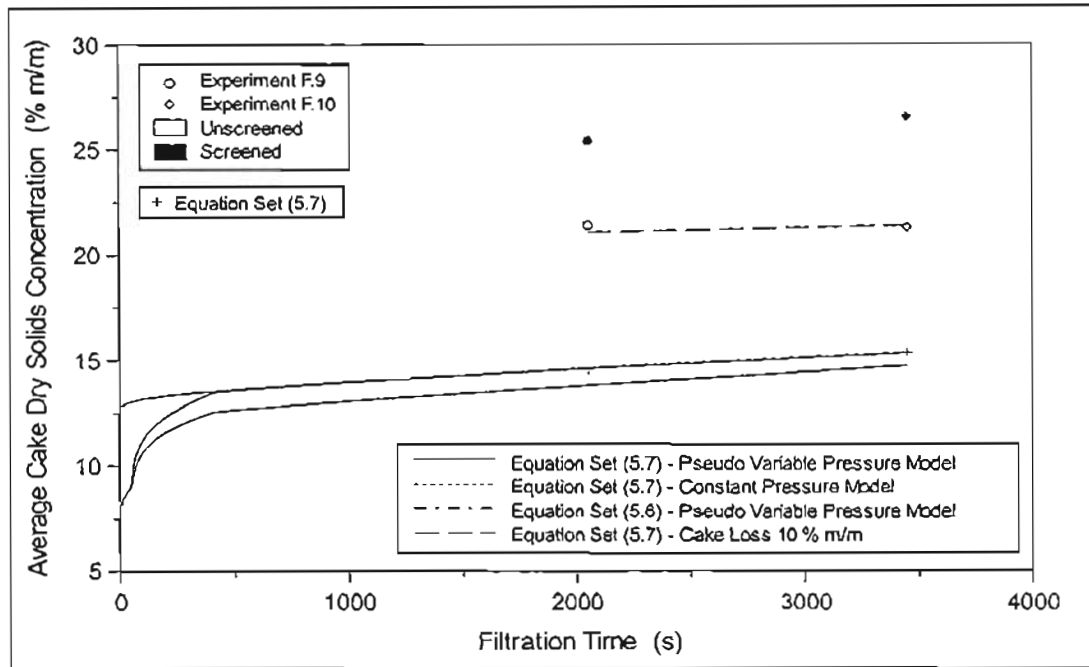


FIGURE 5.72 : Comparison between Experimental and Predicted Average Cake Dry Solids Concentration for the Tubular Filter Press Experiment F.9 and Experiment F.10 using the Laboratory Sludge Characterisation

Figure 5.67 to Figure 5.72, and the value of the cake thickness component of the objective function given in Table 5.13 to Table 5.14, show that the accuracy of the model output to predict the average cake dry solids concentration and hence the cake thickness as well, is increased when the sludge characterisation, which accounts for the effects of wall friction, Equation 5.7, is included in the model. The screened average cake solids concentrations were used to determine the experimental cake thickness in Equation 3.87.

Figure 5.67 to Figure 5.72 show a gradual increase in the predicted average cake dry solids concentration with time. For constant pressure filtration, there is an initial extremely sharp increase in average cake dry solids concentration, due the rapid initial increase in cake pressure drop as the cake grows, and the effect of the medium resistance becomes insignificant. For variable pressure filtration, this effect is dominated by the gradual increase in cake pressure drop as a result of the increasing applied pressure. After the initial increase in average cake dry solids concentration, the average cake solids concentration for internal cylindrical filtration, continues to increase with time, unlike planar filtration, where the average cake dry solids concentration at a constant applied pressure, remains relatively constant. This increase in average cake dry solids concentration with time, for internal cylindrical filtration occurs for two reasons. For internal cylindrical filtration, as cake thickness increases, in addition to the decrease in solids compressive pressure at the medium (see Section 3.2.3.2), the solids compressive pressure profile through the cake becomes less *hyperbolically* shaped (see Figure 5.73). As a result, a larger proportion of the cake is subjected to a higher solids compressive pressure, the cake is therefore more consolidated and has a higher average cake dry solids

concentration. In addition, and perhaps more significant, as the cake thickness increases, the cylindrical nature of the cake becomes more apparent, the proportion of the cake volume composed of the unconsolidated layers decreases and the overall cake dry solids concentration increases. It is for these same reasons that the cake recovery is observed to increase with time, and hence cake thickness (see Section 5.6.1).

The slight difference in predicted average cake dry solids concentration between a cake formed under constant pressure conditions, compared to a cake formed under variable pressure conditions, after the initial pressurisation period, is due to the slightly reduced cake thickness of the cake formed under variable pressure conditions and the effect of cake thickness on average cake dry solids concentration for internal cylindrical filter cakes. For planar filtration, no difference in the predicted cake concentration would be observed after the initial pressurisation period (note: the filtration model assumes that equilibrium cake concentrations are attained instantaneously).

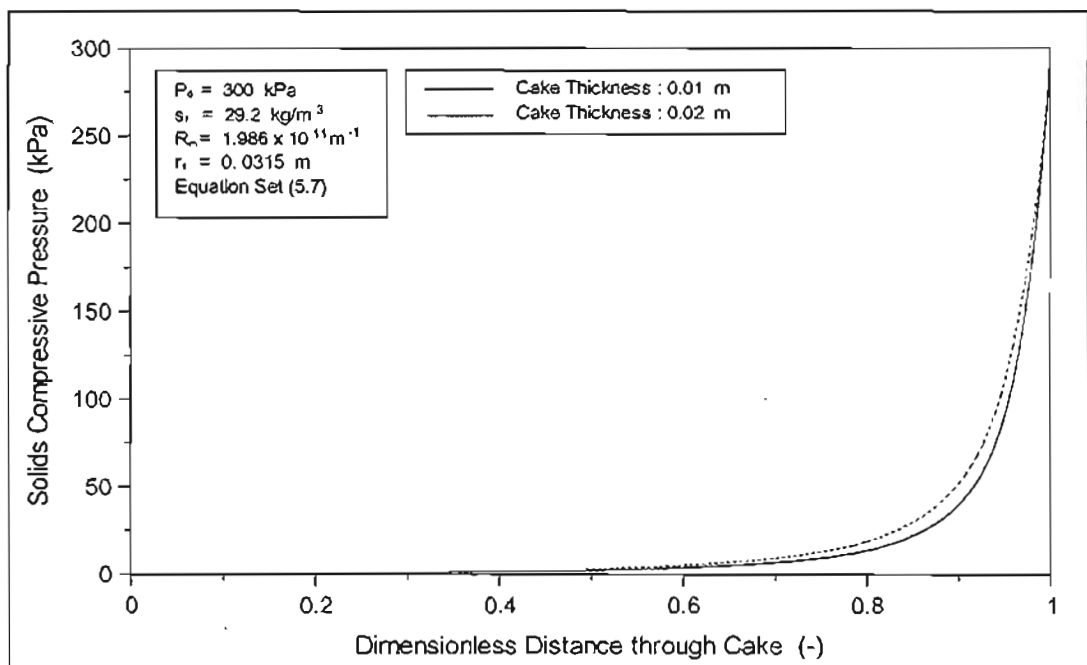


Figure 5.73 : Solids Compressive Pressure Profile through Dimensionless Internal Cylindrical Cake Thickness

The average cake dry solids concentrations of the screened cake samples obtained from the Tubular Filter Press, increased from approximately 20 % m/m to 26 % m/m over the range of filtration times and pressures, compared to the average cake dry solids concentrations obtained from the planar filtration tests, which remained at approximately 20 % m/m over a similar range of pressures, but did not show any trend with respect to time. Although the greater average cake concentrations for the Tubular Filter Press experiments is due in part to the effect of increased average cake dry solids concentration with cake thickness, as is evident from the trend observed with respect to filtration time, the increase can more probably be ascribed to the

more violent cake removal mechanism of the Tubular Filter Press and hence a greater degree of cake loss.

Equations 5.7, although better than Equations 5.6, are not an accurate characterisation of the filtration behaviour, particularly at the lower applied pressures, as is evident from the comparison of the experimental filtrate volume data which is not influenced by the effects of cake loss.

5.9 REGRESSION ANALYSIS

Regression on actual filtration data provides an alternative means for determining the empirical porosity and permeability correlation parameters normally obtained from the standard laboratory-scale test procedures, as described in Section 3.6, and in addition, the parameters specific to the new area contact model developed in Section 3.2. The problem associated with the laboratory tests used to determine the correlation parameters is that there is doubt as to whether the porosity and permeability data obtained from settling tests, C-P cell tests and centrifuge tests, is representative of the porosities and permeabilities that occur in actual filtration. The doubts expressed with regard to the accuracy of C-P cell tests are discussed in Section 3.6.1. Murase et al. (1989), expressed reservations about the accuracy of settling tests, due to network formation between particles and aggregates of particles. They claimed that network formation lead to significant friction between the particles and the inner wall of the cylinder. Rencken (1992), found that when data from centrifuge tests was incorporated into the filtration model, the accuracy of the model output decreased. As a result there is doubt as to the wide-scale applicability of characterisations obtained from the standard laboratory-scale tests. To an extent, these doubts have been confirmed, by the results of Section 5.8, where the results of the planar and Tubular Filter Press experiments were compared to the output of the filtration model using a characterisation obtained from settling tests and C-P cell tests. Over and above the effects of cake loss, the characterisation did not accurately predict the filtration behaviour, despite the fact that the C-P cell data had been corrected to account for the effects of wall friction, without which the characterisation would have been significantly in error.

The regressive solution procedure described in Section 3.4, has been incorporated into the computer programme, REGRESS, written in the C++ programming language.

5.9.1 Evaluation of the Regressive Solution Procedure

The weighting factors on each component of the objective function, Equation 3.87, allow the objective function to be customised or fine tuned to suit a particular regression analysis. The direct search strategy developed for the regressive solution procedure is evaluated in this section, in conjunction with the various analysis techniques using pseudo experimental data created by the filtration model (see Appendix H).

5.9.1.1 Time Independent Analysis

The advantage of the time independent analysis is that it has a very rapid computational time. Filtration properties are calculated at a single fixed point in time, as opposed to the time dependent analysis where the filtration properties are calculated over the entire filtration time.

When the time independent analysis was evaluated using the pseudo experimental data produced by the filtration model (see Appendix H), the method was found to be generally very efficient and accurate in determining the optimum set of model parameters. Occasionally the method converged on local and not the global minimum, however this was to be expected due to the relatively small number of experimental data points used in the analysis.

5.9.1.2 Time Dependent Analysis

When the time dependent analysis was evaluated using the pseudo experimental data produced by the filtration model (see Appendix H), the method was found to be able to locate the global minimum. The method was prone to straddling concave regions of the objective function, although this again is probably due to the relatively small number of experimental data points used in the analysis. In time, the search technique was found to be able to free itself from these concave regions.

Cake loss will affect the experimentally determined cake thickness but will not affect experimental filtrate volume data. As a result, cake loss will affect the results of a time dependent analysis. In light of this, several regressions with the pseudo filtration data were performed, using the filtrate volume component of the objective function alone. It was found that filtrate volume data alone was not sufficient to obtain a unique physical characterisation of the sludge. The results indicated that there appeared to be a locus of porosity and permeability correlation parameters, that could minimise the filtrate volume component of the objective function and that the cake thickness data, or some other equivalent experimental data, was needed to form a determinate system.

5.9.1.3 Combined Analysis

The combined analysis utilises all four components of the objective function. When the combined analysis was evaluated using the pseudo experimental data produced by the filtration model (see Appendix H), the method was found to be the most successful, with the searches consistently converging directly to the global minimum.

5.9.2 Experimental Data

Variance in the experimental data is expected and unavoidable, provided a sufficiently large number of experimental data points are included in the regression analysis, any variation

induced trends in the experimental data should be eliminated, and more general trends will emerge. A large number of experimental data will serve to smooth out the objective function, eliminating any local minima that may exist, covering over any concave regions, and making the global minimum more apparent. The disadvantage in increasing the number of experimental data in the regression analysis, is an increased computational time per iteration of the direct search strategy.

The primary goal of the regression analysis is to obtain the optimum set of porosity and permeability correlation parameters, such that the calculated filtration properties, from the filtration model, match the experimental data as closely as possible. The porosity and permeability correlations are a functional description of the behaviour of the local porosity and permeability with regard to the solids compressive pressure. In order to obtain a meaningful characterisation of the sludge from the experimental data, it is therefore necessary for data to be included in the model that covers a representative range of applied filtration pressures.

If the filtration plant operation is such that the experimental data obtained, is of questionable accuracy, due to cake loss or other factors, then the data in the regression analysis may have to be supplemented or replaced by more controlled laboratory-scale filtration data. In order for the characterisation obtained from laboratory-scale data to be representative of the filtration behaviour of the sludge in a full-scale filtration application, the conditions under which the laboratory-scale filtration data is obtained for the regression analysis, must be representative of the operating conditions of the full-scale plant for which the characterisation is intended.

As discussed in Section 5.12, the filtration model assumes that equilibrium cake porosities are attained instantaneously. The degree of cake equilibrium is dependent on a number of operational parameters, but more significantly, the feed solids concentration, and the final filtration time. If laboratory-scale filtration data is used to characterise a sludge, and this characterisation is used for the design or control of a full-scale plant, if cake equilibrium effects are significant, this could lead to significant errors if the operating conditions of the full-scale plant are not similar to the conditions under which the data for the characterisation was obtained. If cake equilibrium effects are significant under a certain operating regime, and the resulting experimental data is incorporated into a regression analysis, during the course of the regression, the effects of cake equilibrium will be absorbed into the model parameters. The resulting characterisation may therefore not be accurate for another operating regime where the equilibrium effects are no longer significant. In order to account for any equilibrium effects that may exist, laboratory-scale data should therefore be obtained at a similar operating regime as the full-scale plant.

The filtration behaviour of the sludge may also be influenced by how the sludge is conditioned immediately prior to filtration. For instance, when the sludge is pumped from a holding tank,

the action of the centrifugal pump, may break up any particle aggregates that may be present, and the filtration characteristics of the sludge may be significantly changed. It is therefore important that the sludge be conditioned in the same manner before any laboratory-scale filtration tests.

5.9.3 The Effect of Inaccuracies in Experimental Data

The accuracy of the result obtained from a regression analysis is directly dependent on the accuracy of the experimental data used in the analysis. Inaccuracies in the experimental data may be imposed directly onto the data due to limitations in the accuracy of the instrument used to measure the experimental property, or due to limitations of the measurement technique. In addition, unsuitable experimental methodologies may inadvertently change an experimental property prior to its measurement.

In this section, an attempt is made to identify some significant sources of experimental error and to determine to what extent these will affect the various components of the objective function and hence influence the results obtained from the regression analysis. For the purposes of this discussion it is assumed that the sludge is characterised by Equations 5.7, and the discussion is illustrated in context of a cake 10 mm thick formed under planar filtration conditions, at an applied pressure of 300 kPa and a feed solids concentration of 29.2 kg/m³. The point contact filtration model is used.

5.9.3.1 Cake Loss

As discussed in Section 5.8.1, and observed in the results of both the planar and Tubular Filter Press experiments, the effects of cake loss can be significant for sludges of the type investigated in this study.

Cake loss can therefore be expected to have a significant impact on the results obtained from the regression analysis. For the purposes of this discussion, assume that the experimental data used in the regression analysis includes only the single experimental point described above, which has experienced cake loss up to an internal cake dry solids concentration of 10 % m/m, that the experimental filtrate flow rate has been measured correctly, and that during the course of the direct search technique (see Section 3.4.1), a reflected point in the complex correctly characterised the sludge, i.e. the model parameters in the reflected point were equivalent to those given by Equations 5.7.

5.9.3.1.1 Time Independent Analysis

As discussed in Section 5.8.1, the experimentally observed cake thickness of 3.35 mm would be calculated from a mass balance. Using the experimentally observed filtrate flow rate of 4.832×10^{-7} m³/s and the model parameters equivalent to Equations 5.7, the solids compressive pressure and liquid pressure profiles through the cake would be calculated.

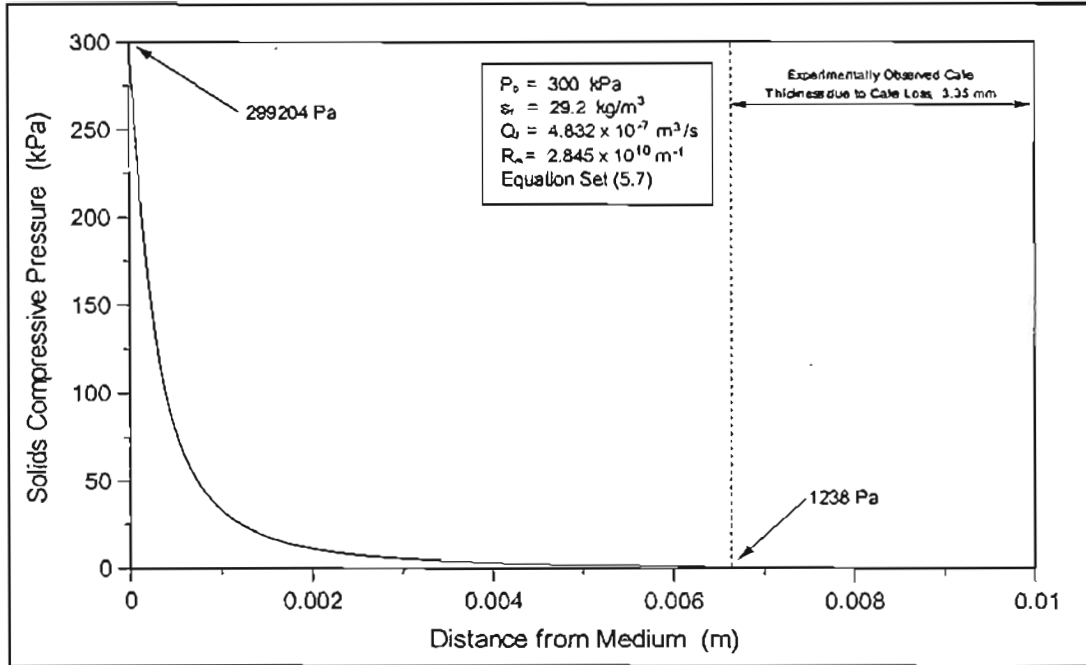


FIGURE 5.74 : Calculated Solids Compressive Pressure Profile through Cake Thickness resulting from Cake Loss

As shown in Figure 5.74, the cake pressure drop at a cake thickness of 3.35 mm would be calculated to be 1238 Pa. The calculated cake pressure drop would then be compared to the experimentally observed cake pressure drop of 299204 as determined from Equation 3.54, Equation 3.57, and the correctly measured experimental filtrate flow rate. The cake pressure drop component of the objective function (see Section 3.4.2) would be evaluated to be 24068. If there had been no cake loss, it would be zero.

From the calculated solids compressive pressure profile, the porosity profile through the cake is calculated, see Figure 5.75. At the cake thickness of 3.35 mm resulting from cake loss (region BC in Figure 5.75), the average porosity of the cake would be calculated to be 0.9603. The experimentally observed average cake porosity of the degraded cake is 0.9073 (19.16 % m/m), see Section 5.8.1. The porosity of the feed sludge at 29.2 kg/m³ is 0.9874. The average porosity component of the objective function (see Section 3.4.2) would be evaluated to be 66.2. If there had been no cake loss, it would be zero.

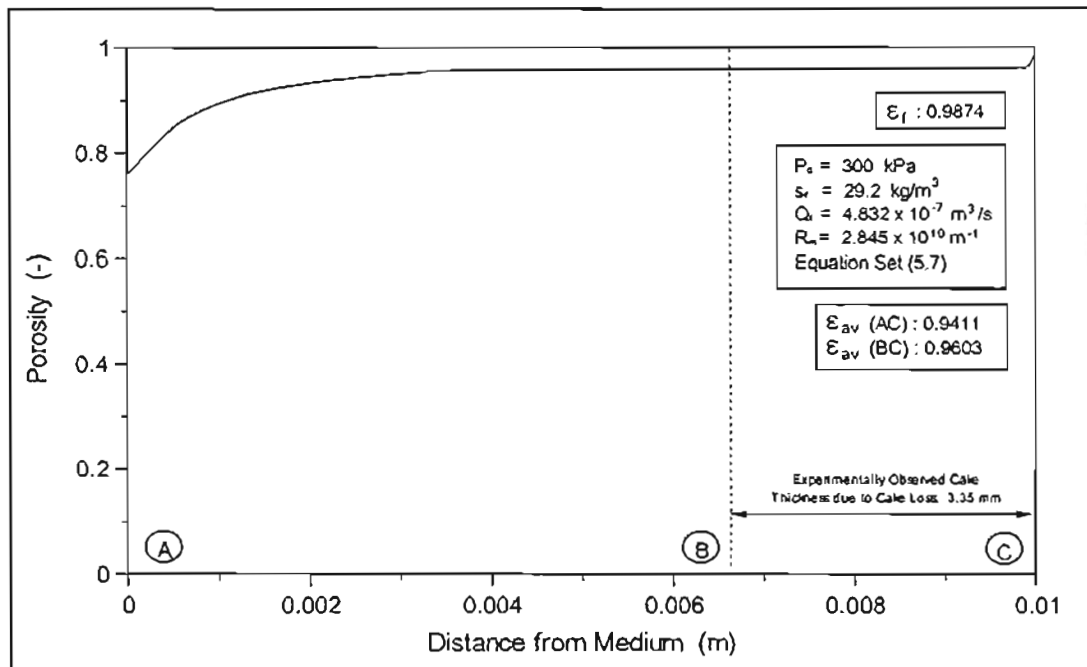


FIGURE 5.75 : Calculated Porosity Profile Through Cake Thickness resulting from Cake Loss

The above discussion illustrates how cake loss can influence the objective function during a time independent analysis in the context of if the true sludge characterisation had been located during the search, but how will cake loss influence the final result obtained from the regression analysis. If the mechanism of cake loss is a consistent and an inherent property of the design and operation of the filtration plant, then it is possible that the effects of cake loss may be compensated for by the model parameters. The regression analysis may produce model parameters that result in an accurate fit between the predicted and experimental data, despite the fact that the experimental data has been influenced by the effects of cake loss. These model parameters will be accurate in terms of predicting the plant performance, but will not however, be a true physical reflection of the sludge characterisation, and can be regarded as a plant specific characterisation. The cake loss mechanism will be a complex function of sludge rheology, plant design and plant operation, as a result the plant specific characterisation may no longer be applicable if the operation of the plant, particularly operational parameters specific to cake removal, are changed.

A comparison of the results of the planar filtration tests to the output of the filtration model using the laboratory characterisation given by Equations 5.7 in Section 5.8, indicated that the planar filtration tests had been affected by cake loss. A time independent regression analysis was performed on the planar filtration data to determine the effect cake loss will have on the result of the time independent regression analysis. Test E.3.6 and Test E.4.6 were omitted from the regression analysis data because the filtrate volume profiles indicated a slightly different filtration behaviour from the other tests. Test E.2.5 was also excluded since the experimental

data was incomplete. The result of the regression analysis, which included the correlation data from the settling tests given by Equation 5.7.b and Equation 5.7.g, is shown in Table 5.15.

TABLE : 5.15 Results of Time Independent Regression Analysis on Planar Filtration Experimental Data

Seed : 1	$W_1 = 1, W_2 = 1, W_3 = 0, W_4 = 0$		$a = 79.629$
F	1.03×10^{-13}	$a(\Delta P_c)$	148.132
δ	0.4751	$a(\varepsilon_{av})$	11.1253
B	0.03555	$a(V_f)$	-
β	0.09349	$a(\theta)$	-

Although Equations 5.7 were determined not to be an accurate characterisation of the filtration behaviour, they are considered sufficiently accurate for comparative purposes to determine the effect of cake loss on the time independent analysis. The regression analysis includes the settling data and will therefore find an additional correlation parameter set in the higher solids compressive pressure range. The alternative characterisation to Equations 5.7, for a single correlation parameter set in the higher solids compressive pressure range, from Section 5.2, is as follows:

$$K = 1.030 \times 10^{-13} p_{sf}^{-0.05382} \quad 0 \leq p_s \leq p_{sf} \quad (5.10.a)$$

$$K = 1.030 \times 10^{-13} p_s^{-0.05382} \quad p_{sf} \leq p_s \leq 694 \text{ Pa} \quad (5.10.b)$$

$$K = 3.139 \times 10^{-10} p_s^{-1.28} \quad p_s \geq 694 \text{ Pa} \quad (5.10.c)$$

$$(1 - \varepsilon) = 0.03558 p_{sf}^{0.01915} \quad 0 \leq p_s \leq p_{sf} \quad (5.10.d)$$

$$(1 - \varepsilon) = 0.03558 p_s^{0.01915} \quad p_{sf} \leq p_s \leq 1995 \text{ Pa} \quad (5.10.e)$$

$$(1 - \varepsilon) = 2.773 \times 10^{-3} p_s^{0.355} \quad p_s \geq 1995 \text{ Pa} \quad (5.10.f)$$

A comparison of Equation 5.10.c and Equation 5.10.f with the results of the regression analysis show that the correlation parameters differ considerably. With regard to the permeability correlation parameters, cake loss reduces the cake thickness, however the filtrate flow rate data, like the filtrate volume data is not affected, therefore at the reduced cake thickness, the cake would appear to be less permeable. As a result, the parameter F from the regression analysis is considerably lower than in Equation 5.10.c. The average cake porosity is also greatly reduced by the effects of cake loss, as a result the parameter B is much greater than in Equation 5.10.f. With the outer cake layers removed by the effects of the cake loss, in an attempt to reconcile the cake permeability and average porosity, the compressible nature of the sludge, as indicated by the magnitude of the exponents δ and β is hidden from the time independent analysis. The effect is greatest with regard to the cake porosity correlation, since the average porosity is affected directly by cake loss. The reduced compressibility, although in evidence in the permeability correlation, is less affected since cake loss reduces the cake

thickness and not the filtrate flow rate, both of which indicate the total permeability of the cake. The similarity of the coefficients F and B from the regression analysis and the settling test correlation data, is an anomaly of the programme REGRESS, which limits the intersection of the correlation data with the settling test correlation data at 1 Pa.

The time independent analysis appears to be very sensitive to inaccuracies in the experimental data, due to the sensitivity of the cake pressure component of the objective function, particularly for very compressible sludge like the sludge used in this investigation. The time independent analysis is therefore not suitable if the experimental data has been influenced by the effects of cake loss. In such cases the time independent analysis will produce a result that is not a true physical characterisation of the sludge.

5.9.3.1.2 Time Dependent Analysis

Returning to the discussion on how cake loss will influence the objective function, in context of the true physical sludge characterisation being identified during the regression analysis.

The filtrate volume versus time profile is not affected by cake loss and hence the calculated and experimentally observed filtrate volume profiles should be equal. The filtrate volume profile component of the objective function (see Section 3.4.2), will therefore be zero.

The cake thickness at the end of the filtration is affected by cake loss. The calculated cake thickness at the final filtration time (626 seconds), will be 10 mm, the experimentally observed cake thickness is 3.35 mm. The cake thickness component of the objective function (see Section 3.4.2) would therefore be evaluated to be 198. If there had been no loss of the cake, it would be zero.

How will cake loss affect the final result of a time dependent characterisation? The time dependent analysis includes the filtrate volume data which is not affected by cake loss. The filtrate data alone is not, however, sufficient to obtain a unique characterisation, and the cake thickness data is required for a determinate system. Although the cake thickness is reduced by cake loss, it is possible that the time dependent regression analysis may be able to obtain a plant specific characterisation that will reconcile both the filtrate volume and cake thickness profiles. The plant specific characterisation will produce the same filtrate volume profile as the true physical characterisation, however the plant specific characterisation will produce a lower cake thickness profile which corresponds to the effects of the cake loss. In order to obtain a lower cake thickness at the same filtrate volume, the plant specific characterisation will have to produce a decreased average cake porosity profile. The experimental average cake porosity is decreased by the effects of cake loss, therefore, provided the cake loss is not extreme or variable, it may be possible to obtain a plant specific characterisation from the time dependent analysis that can accurately predict filtrate volume, cake thickness and average cake porosity.

5.9.3.2 Filtrate Flow Rate

Solids compressive pressure profiles through very compressible filter cakes behave like highly exponential functions, and are strong functions of the filtrate flow rate, as shown Figure 5.56. Errors in the measured filtrate flow rate will only affect the time independent components of the objective function. The measured filtrate flow rate is used to calculate the solids compressive pressure profile through the cake to determine both the calculated cake pressure drop and calculated average porosity.

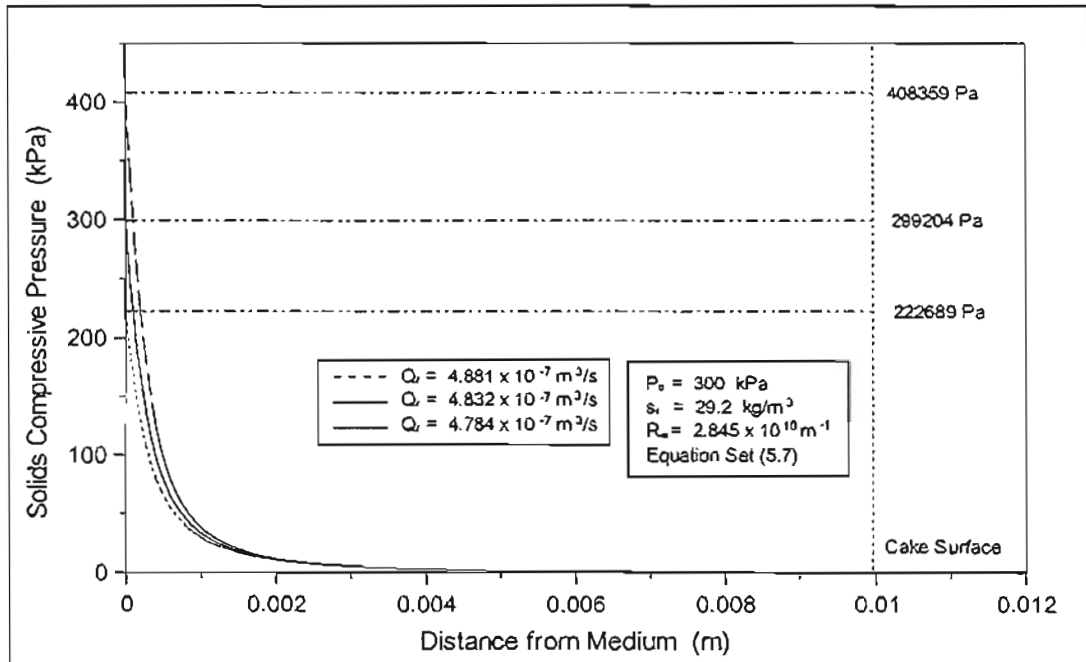


FIGURE 5.76 : Effect of Filtrate Flow Rate on Calculated Cake Pressure Drop

The correct filtrate flow rate for a planar filtration cake 10 mm thick, formed at an applied pressure of 300 kPa, and assumed to be correctly characterised by Equations 5.7 is $4.832 \times 10^{-7} \text{ m}^3/\text{s}$. Figure 5.76 and Figure 5.77 and Table 5.16 show to what extent the calculated cake pressure drop and calculated average porosity are affected if the measured filtrate flow rate is in error of only 1 %, and to what extent this affects the time independent components of the objective function. This discussion assumes that no cake loss has occurred.

The calculated cake pressure drop is directly dependent on the calculated solids compressive pressure profile, for a 1 % increase in the measured filtrate flow rate, the error in the calculated cake pressure drop was 36.5 %, for a 1 % decrease in the filtrate flow rate, the error in the calculated cake pressure drop was 25.6 %. The measured filtrate flow rate is also used to determine the experimentally observed cake pressure drop by Equation 3.54 and Equation 3.57. These errors are reflected directly in the cake pressure drop component of the objective function as shown in Table 5.16.

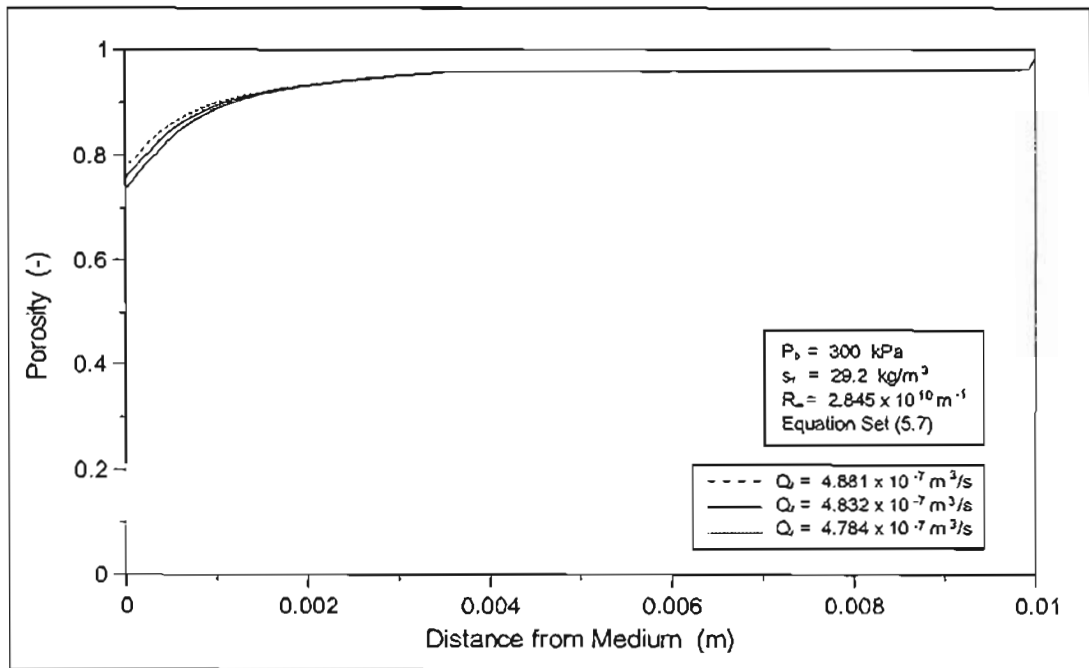


FIGURE 5.77 : Effect of Filtrate Flow Rate on Calculated Porosity Profile

The local porosity is not a very strong function of the solids compressive pressure (see Figure 5.77), in addition the average porosity is an integrated value and therefore less influenced by changes in the measure filtrate flow rate. The calculated average porosity experiences an error of only 0.2 % for both a 1 % increase and decrease in the measured filtrate flow rate. Table 5.16 shows to what extent the 1 % error in measured filtrate flow rate, affects the average porosity component of the objective function.

Provided inaccuracies in the measured filtrate flow rate are not biased, and there is sufficient experimental data in the regression analysis, the final result of the regression analysis should not be adversely influenced. The cake pressure drop component of the objective function is however, a strong function of the filtrate flow rate for very compressible sludges. If the accuracy of the flow rate data is questionable, it may be advisable to weight the other components of the objective function so that the relatively high valued cake pressure component of the objective function does not predominate the regression analysis.

TABLE 5.16 : Variation of Calculated Cake Pressure Drop the Average Porosity and the Time Independent Components of the Objective Function with Filtrate Flow Rate

Q_f (m ³ /s)	ΔP_c (Pa)	$a(\Delta P_c)$ (-)	ϵ_{av} (-)	$a(\epsilon_{av})$ (-)
4.881×10^{-7}	408359	36.5	0.9392	3.94
4.832×10^{-7}	299204	0	0.9411	0
4.784×10^{-7}	222689	25.6	0.9429	4.05

5.9.3.3 Cake Compressibility

The degree of cake compressibility does not directly influence the results of the regression analysis, but serves to exaggerate the errors between the calculated and experimental properties, as reflected in the objective function, due to the effects of cake loss and filtrate flow rate described above. The degree of cake loss and the influence of incorrectly measure filtrate flow rates are dependent on the shape of the solids compressive pressure profile, which is dependent on the degree of cake compressibility.

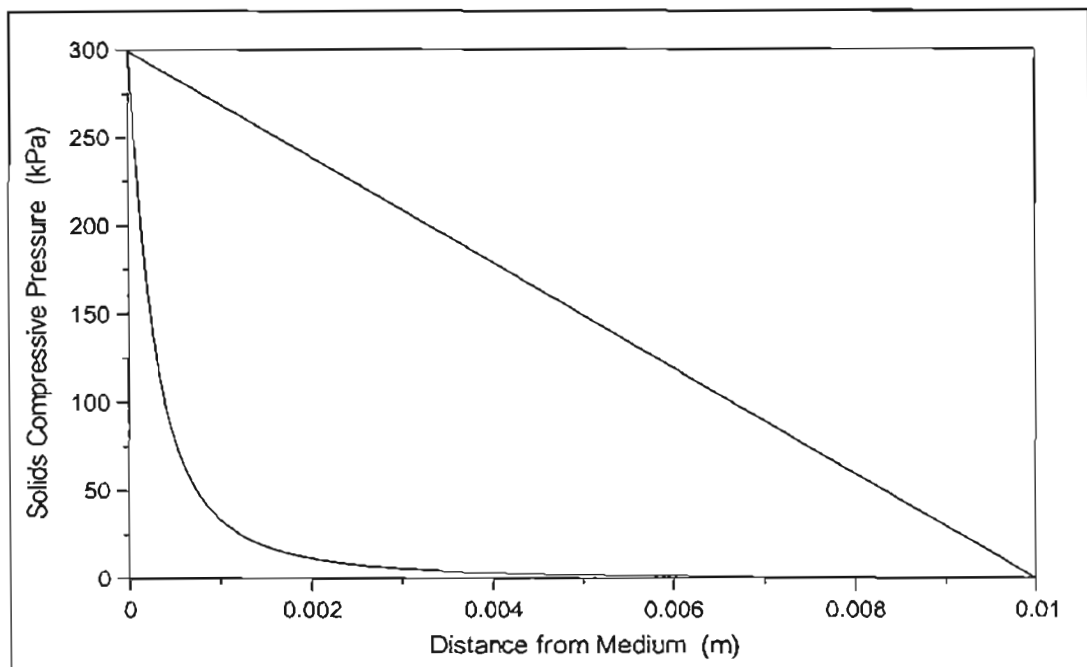


FIGURE 5.78 : Comparison between Incompressible and Highly Compressible Solids Compressive Pressure Profiles

The sludge used for this study is highly compressible and forms an *exponentially* shaped solids compressive pressure profile. As a result, this presents an extreme case for the effects of factors such as cake loss and errors in measured filtrate flow rates discussed above. For comparative purposes, consider the other extreme, an incompressible cake. An incompressible cake has a constant structural profile, and the porosity and permeability profiles through the cake are no longer functions of the solids compressive pressure. The solids compressive pressure profile for an incompressible cake is linear (see Figure 5.78). The rheology of the cake may therefore also be uniform since the cake is evenly consolidated. Cake loss may therefore not be significant, and cannot affect the average porosity of the cake. The calculated cake pressure drop for an incompressible cake has a linear relationship with filtrate flow rate, and as a result errors in calculated cake pressure drops are directly proportional to errors in the measured filtrate flow rate, and not proportional to a high power as for highly compressible cakes. Since porosity profiles through the cake are constant, the calculated average porosities are constant and independent of the filtrate flow rate.

Errors in experimental methodology and measurement are therefore less likely to affect the results of a regression analysis, as the compressibility of the cake decreases.

5.9.3.4 Miscellaneous Factors

Other factors, specific to the operation a filtration plant may alter the value of experimental filtration property prior to measurement. For example, during the operation of the Tubular Filter Press, flush fluid may be entrained with the cake removed from the tubes and dumped onto the roller during the cake removal cycle. If drainage along the cake conveyor is inadequate, this will result in entrained flush fluid reporting to the cake collection bins. This will result in decreased average cake dry solids concentrations and hence increased calculated experimental cake thickness. This will have adverse affects on both the time independent components and cake thickness component of the objective function.

5.9.4 Results of Regression Analysis

The time independent analysis is very sensitive to inaccuracies in experimental data, particularly for very compressible sludges, and as shown in Section 5.9.3.1.1 and Section 5.9.3.2, and can produce highly erroneous results. Whilst evaluating the regressive solution procedure utilising pseudo experimental data (Appendix H), it was found that the most reliable regression technique was the combined analysis, however, the sensitivity of the time independent components of the objective function, are likely to negatively influence the accuracy of the final result. The most reliable regression technique is therefore the time dependent analysis.

As discussed in Section 5.8, the results of both the planar filtration experiments and the full-scale Tubular Filter Press experiments have been influenced by the effects of cake loss. Cake loss can have a significant effect on the results obtained from the regression analysis. As a result, a true physical sludge characterisation cannot be obtained from this data. However, as discussed in Section 5.9.3.1.2, it may still however be possible to obtain a plant specific characterisation from a time dependent analysis of the data.

Plant specific characterisations may in some respects be more useful than the true sludge characterisation, as they provide a direct and accurate means of predicting the filtration properties of the plant. Alternatively the filtration properties that are affected by cake loss would have to be determined from the true sludge characterisation after cake losses have been predicted from a rheological basis. An accurate plant specific characterisation is only possible if the cake loss mechanism is a consistent property of the plant operation. This should be the case, provided the method of cake removal, and the operational parameters that govern cake

removal remain constant. If the cake recovery mechanism is changed, the plant specific characterisation may no longer be valid.

5.9.4.1 Planar Filtration Experiments

The cake loss that occurred during the planar filtration experiments was a direct result of the experimental procedure, and the susceptibility of the sludge used in this investigation, to cake shear. Now that the significance of cake loss has been identified, the experimental procedure can be modified accordingly, to significantly reduce, and possibly eliminate, cake loss. Cake thickness and filtrate volume data alone are sufficient to obtain an accurate characterisation of the sludge via a time dependent regression analysis. The experimental procedure may therefore also be extended to include more sophisticated experimental techniques to measure cake thicknesses in situ, before the cake is sheared.

From a time dependent regression analysis on the planar filtration experimental data (Appendix I), the following plant specific characterisation for the sludge and the planar filtration apparatus was obtained.

$$K = 1.030 \times 10^{-13} p_{sf}^{-0.05382} \quad 0 \leq p_s \leq p_{sf} \quad (5.11.a)$$

$$K = 1.030 \times 10^{-13} p_s^{-0.05382} \quad p_{sf} \leq p_s \leq 403 \text{ Pa} \quad (5.11.b)$$

$$K = 1.841 \times 10^{-10} p_s^{-1.302} \quad p_s \geq 403 \text{ Pa} \quad (5.11.c)$$

$$(1 - \varepsilon) = 0.03558 p_{sf}^{0.01915} \quad 0 \leq p_s \leq p_{sf} \quad (5.11.d)$$

$$(1 - \varepsilon) = 0.03558 p_s^{0.01915} \quad p_{sf} \leq p_s \leq 267 \text{ Pa} \quad (5.11.e)$$

$$(1 - \varepsilon) = 5.631 \times 10^{-3} p_s^{0.349} \quad p_s \geq 267 \text{ Pa} \quad (5.11.f)$$

Figure 5.79 to Figure 5.90 show the comparison between the results of the planar filtration experiments and the predictions of the constant pressure compressible cake filtration model, using the plant specific characterisation, given by Equation 5.11, obtained from the time dependent regression analysis (see Appendix I). The predictions of the constant pressure compressible cake filtration model, using the characterisation given by Equations 5.7, is included for comparative purposes.

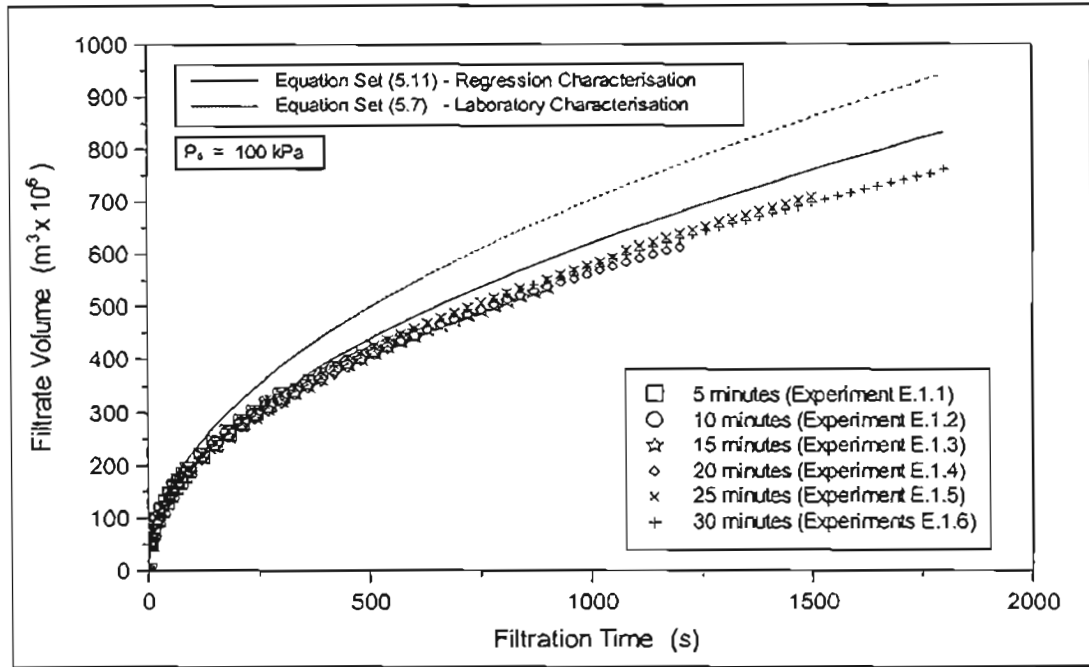


FIGURE 5.79 : Comparison between Experimental and Predicted Filtrate Volumes for Planar Filtration at 100 kPa using the Regression Sludge Characterisation

Figure 5.79 to Figure 5.90 show that the plant specific characterisation given by Equations 5.11, shows a significant improvement to the characterisation given by Equations 5.7, and accurately predicts the filtrate volume, average cake dry solids concentration and cake thickness with respect to filtration time.

A comparison of the laboratory characterisation given by Equations 5.10, where the C-P cell data is treated singularly, to the plant specific characterisation given by Equations 5.11, shows that they are similar. The correlation data obtained from the settling tests, was utilised in the regression analysis to obtain the plant specific characterisation, and therefore the permeability and porosity correlation data obtained from the regression analysis given by Equation 5.11.c and Equation 5.11.f respectively, can be considered to be the equivalent to the permeability and porosity correlation information that would normally be obtained from C-P cell tests, given by Equation 5.10.c and Equation 5.10.f respectively.

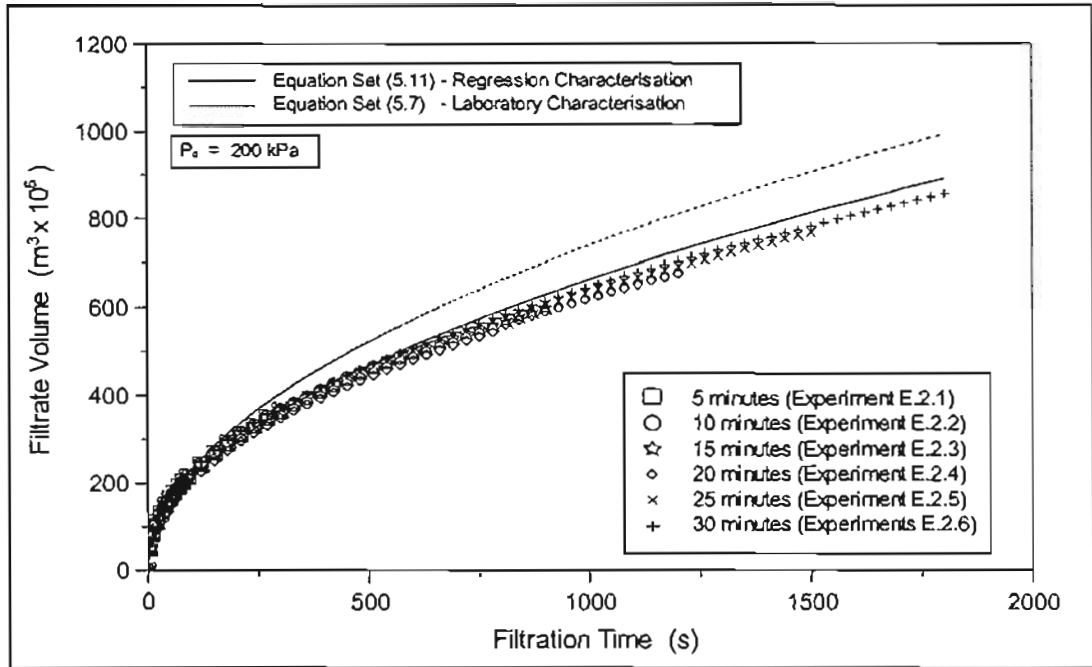


FIGURE 5.80 : Comparison between Experimental and Predicted Filtrate Volumes for Planar Filtration at 200 kPa using the Regression Sludge Characterisation

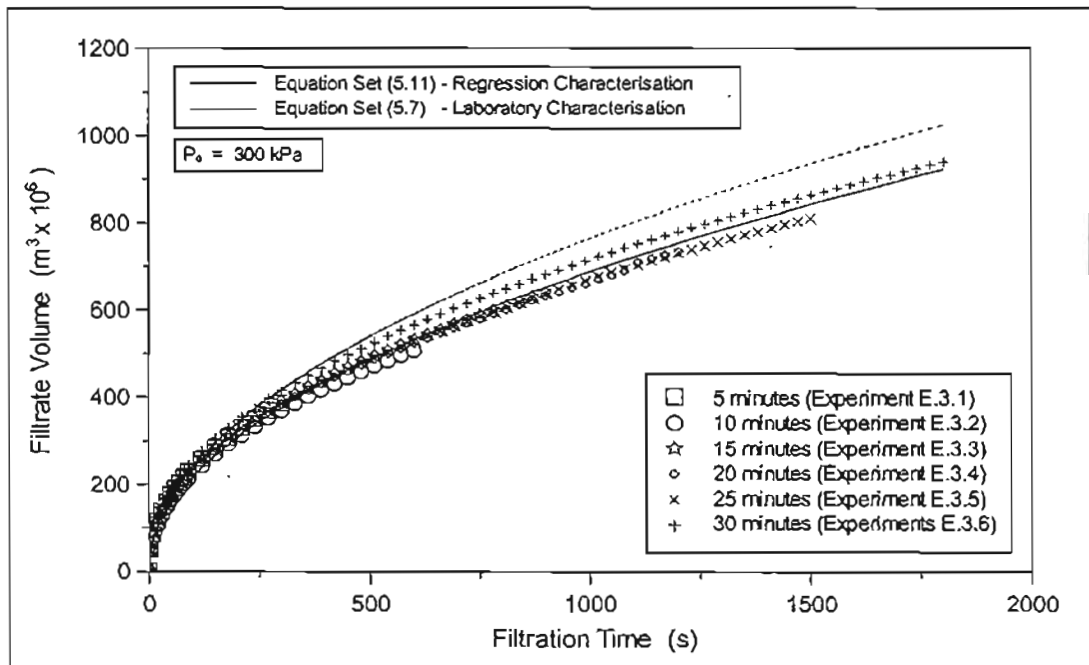


FIGURE 5.81 : Comparison between Experimental and Predicted Filtrate Volumes for Planar Filtration at 300 kPa using the Regression Sludge Characterisation

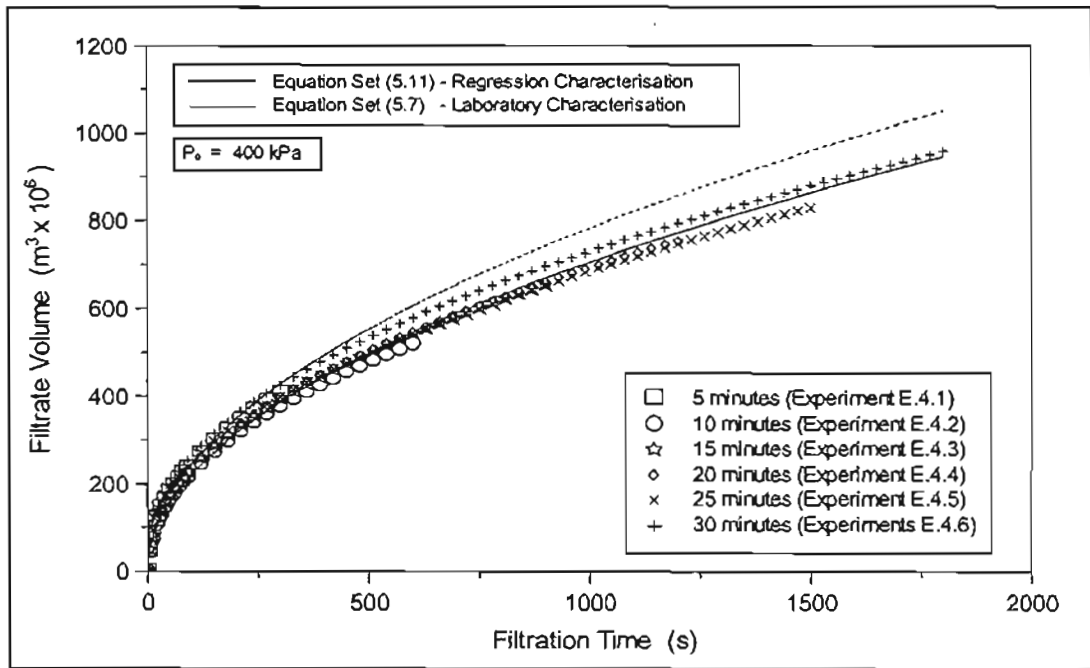


FIGURE 5.82 : Comparison between Experimental and Predicted Filtrate Volumes for Planar Filtration at 400 kPa using the Regression Sludge Characterisation

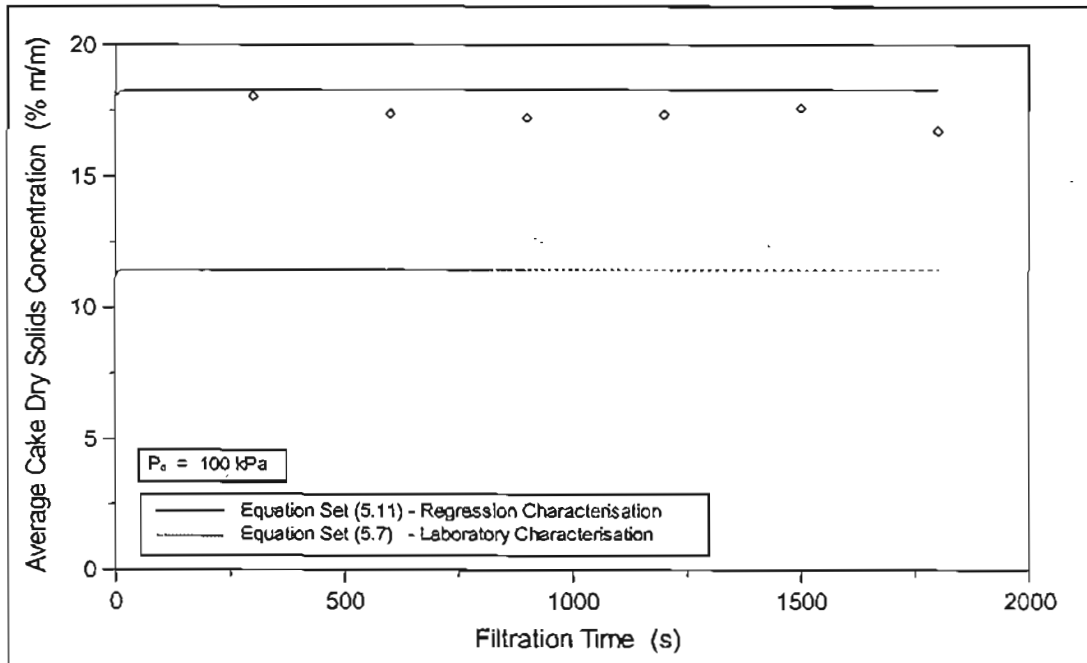


FIGURE 5.83 : Comparison between Experimental and Predicted Average Cake Dry Solids Concentrations for Planar Filtration at 100 kPa using the Regression Sludge Characterisation

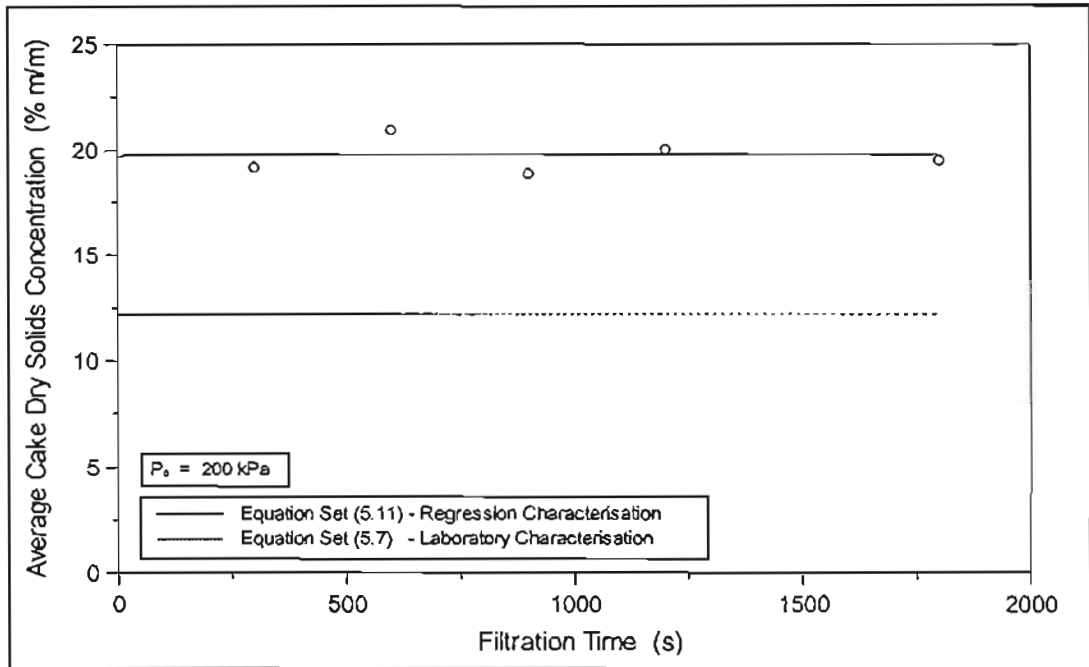


FIGURE 5.84 : Comparison between Experimental and Predicted Average Cake Dry Solids Concentrations for Planar Filtration at 200 kPa using the Regression Sludge Characterisation

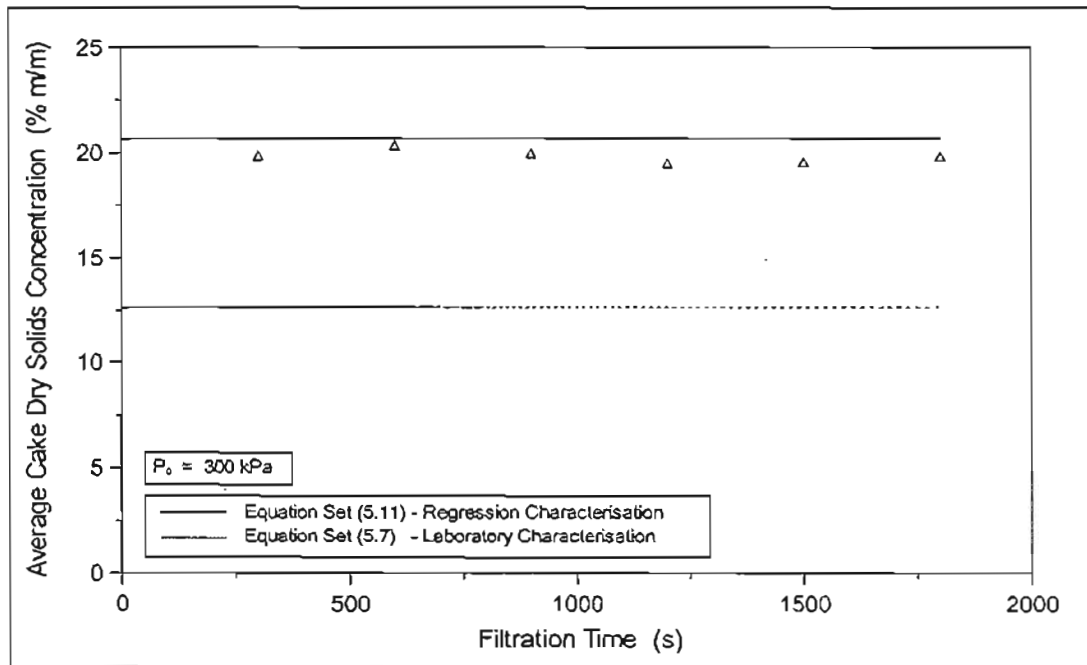


FIGURE 5.85 : Comparison between Experimental and Predicted Average Cake Dry Solids Concentrations for Planar Filtration at 300 kPa using the Regression Sludge Characterisation

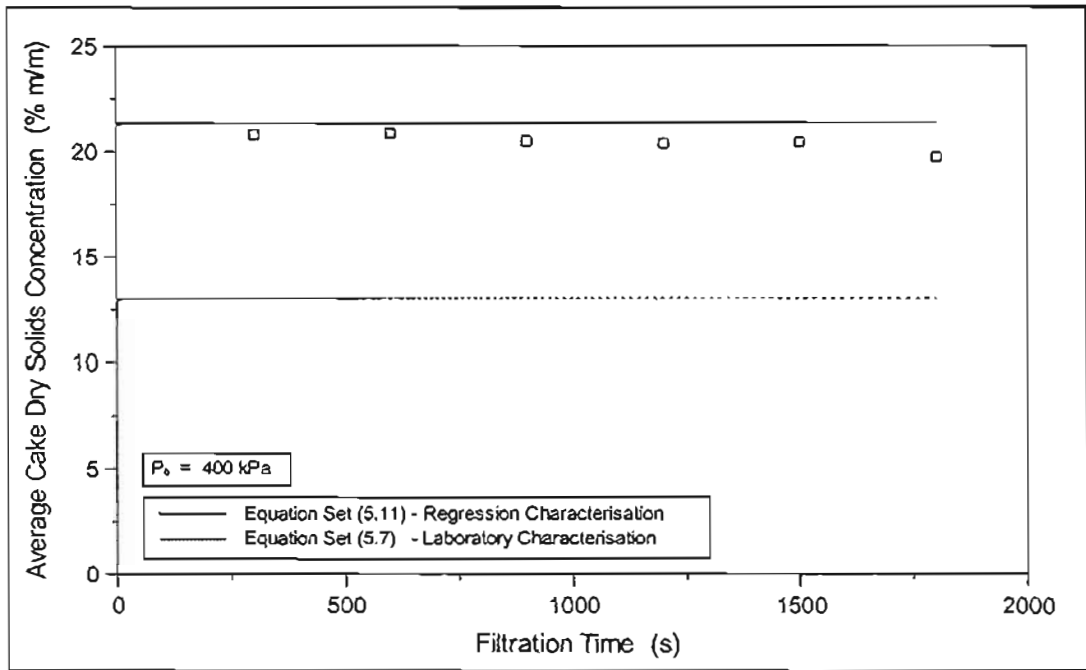


FIGURE 5.86 : Comparison between Experimental and Predicted Average Cake Dry Solids Concentrations for Planar Filtration at 400 kPa using the Regression Sludge Characterisation

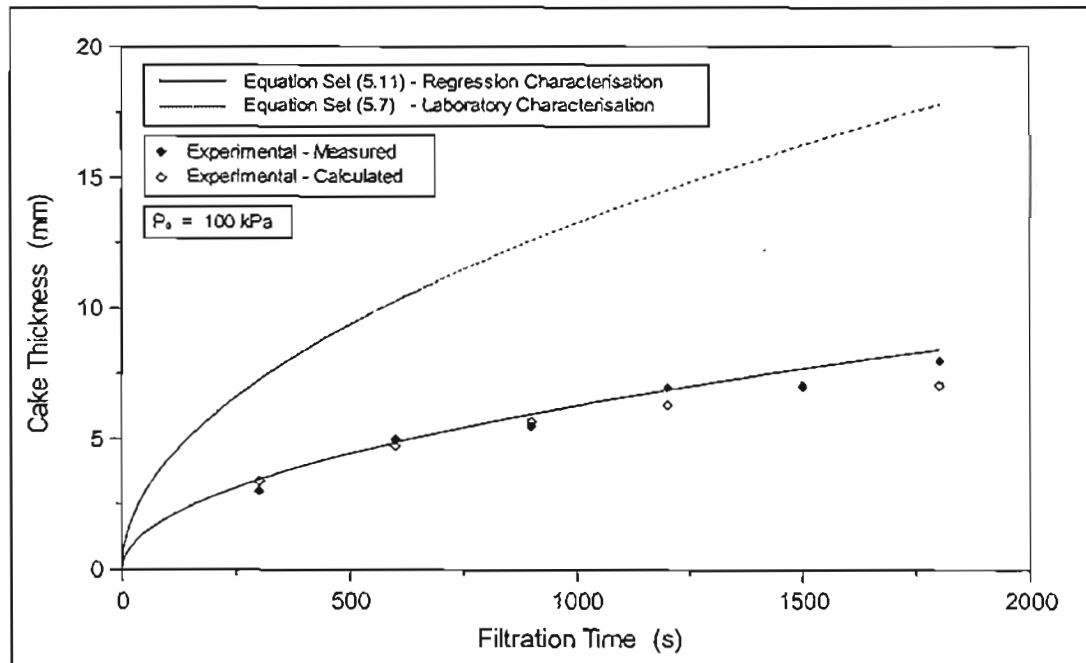


FIGURE 5.87 : Comparison between Experimental and Predicted Cake Thickness for Planar Filtration at 100 kPa using the Regression Characterisation

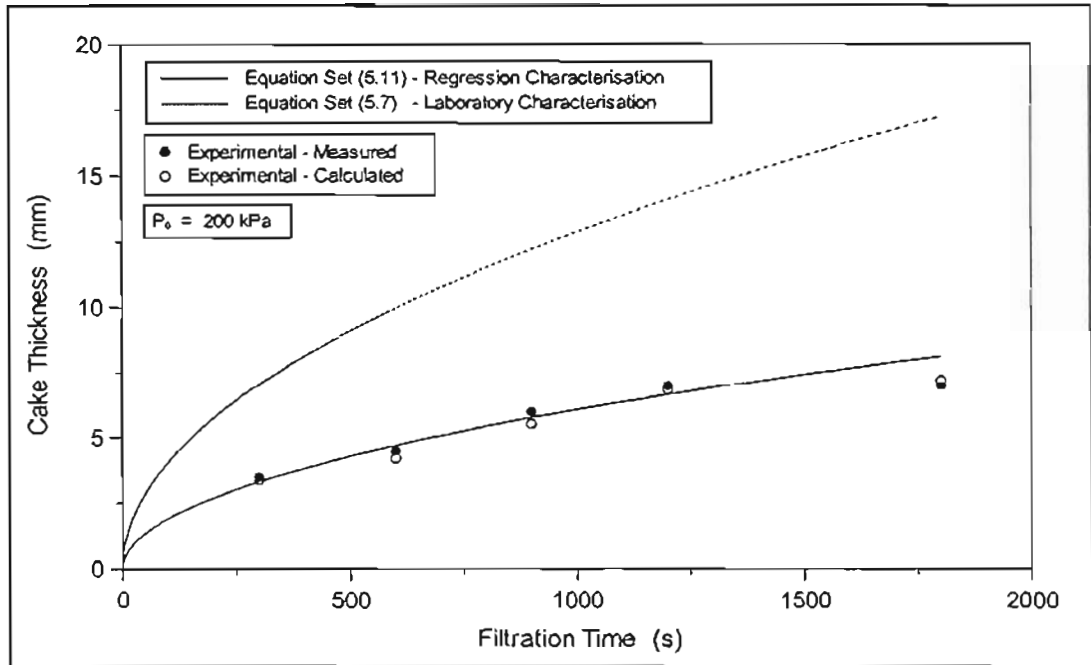


FIGURE 5.88 : Comparison between Experimental and Predicted Cake Thickness for Planar Filtration at 200 kPa using the Regression Characterisation

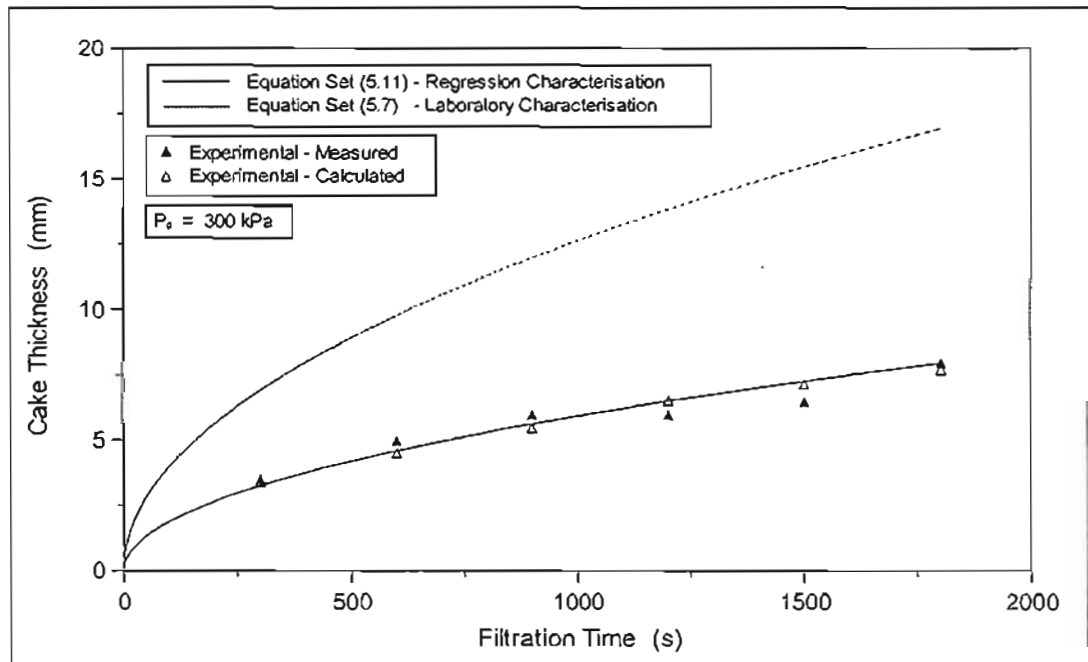


FIGURE 5.89 : Comparison between Experimental and Predicted Cake Thickness for Planar Filtration at 300 kPa using the Regression Characterisation

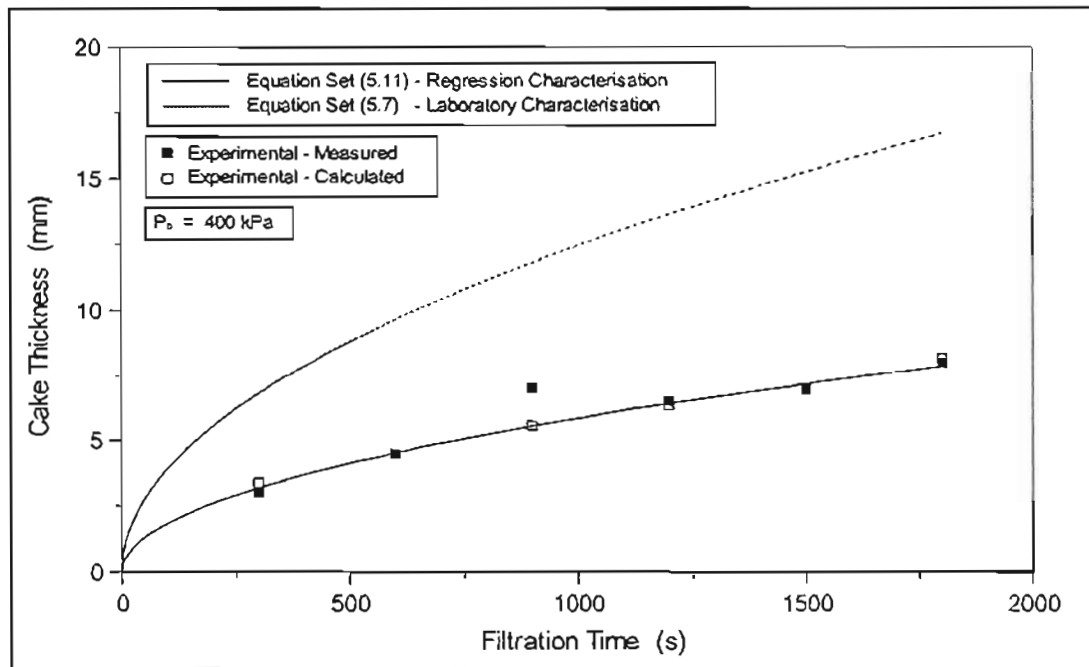


FIGURE 5.90 : Comparison between Experimental and Predicted Cake Thickness for Planar Filtration at 400 kPa using the Regression Characterisation

The difference in the cake compressibility between the laboratory and plant specific characterisation, as indicated by the magnitude of the exponents, is less than 2 %, for both the porosity and permeability correlations. The poor agreement observed between the results of the planar filtration experiments and the output of the filtration model using the laboratory characterisation given by Equations 5.7, with regard to the cake thickness and average cake dry solids concentration, have been explained in Section 5.8.1, to be due to the effects of cake loss. However, it appears that the effect of cake loss was not sufficient to mask the compressible nature of the sludge, when the experimental data was used in the regression analysis. The compressible nature of the sludge may have been represented despite the effects of cake loss, however, the possibility cannot be overlooked that the effects of cake loss for the planar filtration experiments may have been negligible, despite the rheological considerations given in Section 5.8.1.

As determined in Section 5.8.1, the characterisation given by Equations 5.7, is not an accurate characterisation filtration behaviour of the sludge, despite the effects of cake loss. If the effects of cake loss are not as significant as previously supposed, the characterisation given by Equations 5.11, may therefore be a more accurate physical characterisation of the sludge, than that given by Equations 5.7. The filtrate volume component of the objective function, evaluated with the filtration data obtained from the Tubular Filter Press and using the plant specific characterisation given by Equations 5.11, resulted in a value of 19.45. This shows an improvement over the value obtained utilising the laboratory characterisation given by Equations 5.7, of 28.08 (see Table 5.14).

The poor agreement observed between the results of the planar filtration experiments and the output of the filtration model using the laboratory characterisation given by Equations 5.7, may have been due to:

- an inaccurate laboratory characterisation due to the results of the C-P cell tests not being representative of the behaviour of the porosity and permeability with solids compressive pressure during filtration,
- significant errors in the determination of other experimental parameters used in the filtration model or in the analysis of experimental data obtained from C-P cell tests , such as the solids density or liquid viscosity,
- inadequacies in the filtration model,
- cake loss,
- or a combination of these factors.

In light of the possible sources of error mentioned above, the characterisation obtained from a regression analysis has a number of advantages over a laboratory characterisation. The correlation parameters are obtained from actual filtration data and therefore, in context of the filtration model, there can be no doubt as to their representivity of the behaviour of the porosity and permeability with solids compressive pressure during filtration, compared to other non-filtration laboratory methods. The parameters are obtained directly from the filtration data and the filtration model, and therefore there is no possibility of the parameters being distorted indirectly, through the processing of the raw experimental data, such as what may occur during the analysis of C-P cell, or other laboratory characterisation data.

A likely source of error in the determination of the physical properties needed for the filtration model (and the analysis of C-P cell data), is the correct determination of the liquid viscosity. As shown in Appendix A, the viscosity of water is a function of temperature, therefore large errors can be introduced, if the temperature of the sludge is not accurately determined. In the event that some of the experimentally determined physical properties used in the model have been incorrectly determined, or the filtration data has been affected by cake loss, the regression analysis will absorb these effects as much as possible, within the flexibility of the filtration model, into the correlation parameters. The characterisation obtained in this case would however be a plant specific characterisation and not a true physical characterisation of the sludges filtration behaviour.

5.9.4.2 Tubular Filter Press

As a result of cake loss, a true sludge characterisation cannot be obtained from experimental data obtained from the Tubular Filter Press. Cake loss is an inherent part of the operation of the Tubular Filter Press due to the cake removal mechanism. A true characterisation for the Tubular Filter Press can however, be obtained from laboratory-scale planar or internal

cylindrical filtration experiments, provided the operating parameters such as feed solids concentration, filtration pressure and final filtration times, and the nature of sludge conditioning directly prior to filtration, are similar.

From a time dependent regression analysis on the Tubular Filter Press experimental data (Appendix I), the following plant specific characterisation for the sludge and the Tubular Filter Press was obtained.

$$K = 1.030 \times 10^{-13} p_{sf}^{-0.05382} \quad 0 \leq p_s \leq p_{sf} \quad (5.12.a)$$

$$K = 1.030 \times 10^{-13} p_s^{-0.05382} \quad p_{sf} \leq p_s \leq 1 \text{ Pa} \quad (5.12.b)$$

$$K = 1.1226 \times 10^{-13} p_s^{-0.5455} \quad p_s \geq 1 \text{ Pa} \quad (5.12.c)$$

$$(1 - \varepsilon) = 0.03558 p_{sf}^{0.01915} \quad 0 \leq p_s \leq p_{sf} \quad (5.12.d)$$

$$(1 - \varepsilon) = 0.03558 p_s^{0.01915} \quad p_{sf} \leq p_s \leq 2456 \text{ Pa} \quad (5.12.e)$$

$$(1 - \varepsilon) = 3.18 \times 10^{-3} p_s^{0.3285} \quad p_s \geq 2456 \text{ Pa} \quad (5.12.f)$$

A comparison of the laboratory characterisation given by Equations 5.10, where the C-P cell data is treated singularly, to the plant specific characterisation obtained from the Tubular Filter Press data, given by Equations 5.12, show that although the porosity correlation data, is similar, the permeability correlation data differs considerably in both the degree of compressibility and the order of magnitude of the coefficient. This is due to the severity of cake loss on the Tubular Filter Press filtration data.

Figure 5.91 to Figure 5.100 show the comparison between the filtrate volume profiles for Tubular Filter Press experiments and the predictions of the constant compressible cake filtration model, using the plant specific characterisation given by Equations 5.12. The output of the pseudo variable pressure solution procedure using the characterisation given by Equations 5.12, is included for comparative purposes. It is important to remember that the programme REGRESS, utilises the constant pressure solution procedure. Equations 5.12, are therefore the optimum characterisation for the constant pressure solution procedure, and the validity of the variable pressure solution procedure cannot be evaluated using Equations 5.12. The predictions of the pseudo variable pressure compressible cake filtration model, using the characterisation given by Equations 5.7, is also included for comparative purposes.

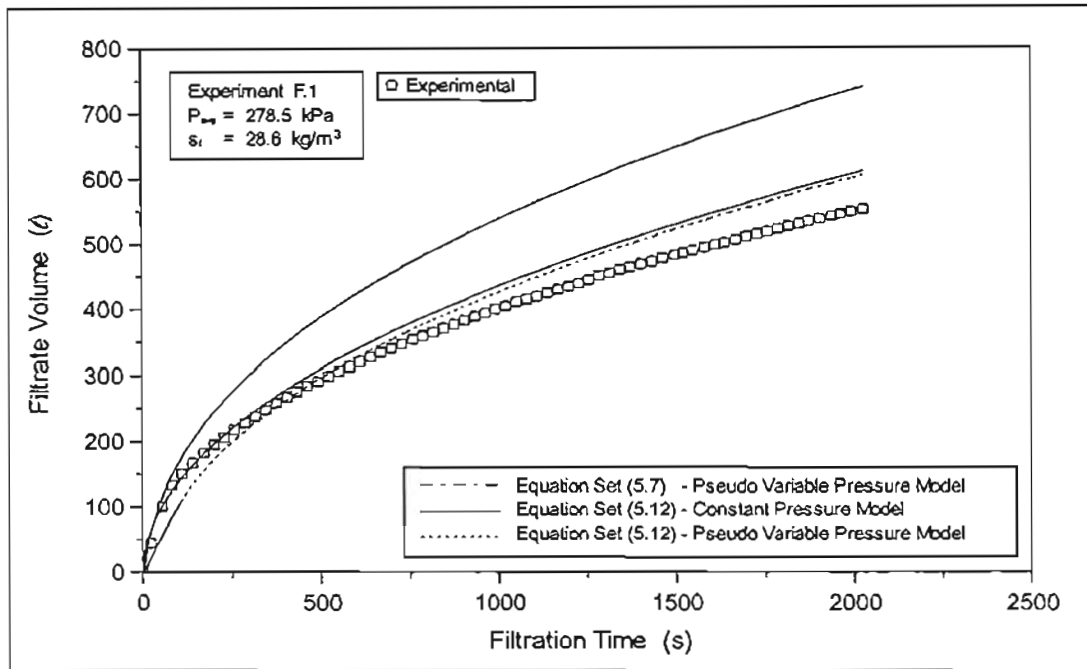


FIGURE 5.91 : Comparison between Experimental and Predicted Filtrate Volume Profiles for the Tubular Filter Press for Experiment F.1 using the Plant Specific Characterisation

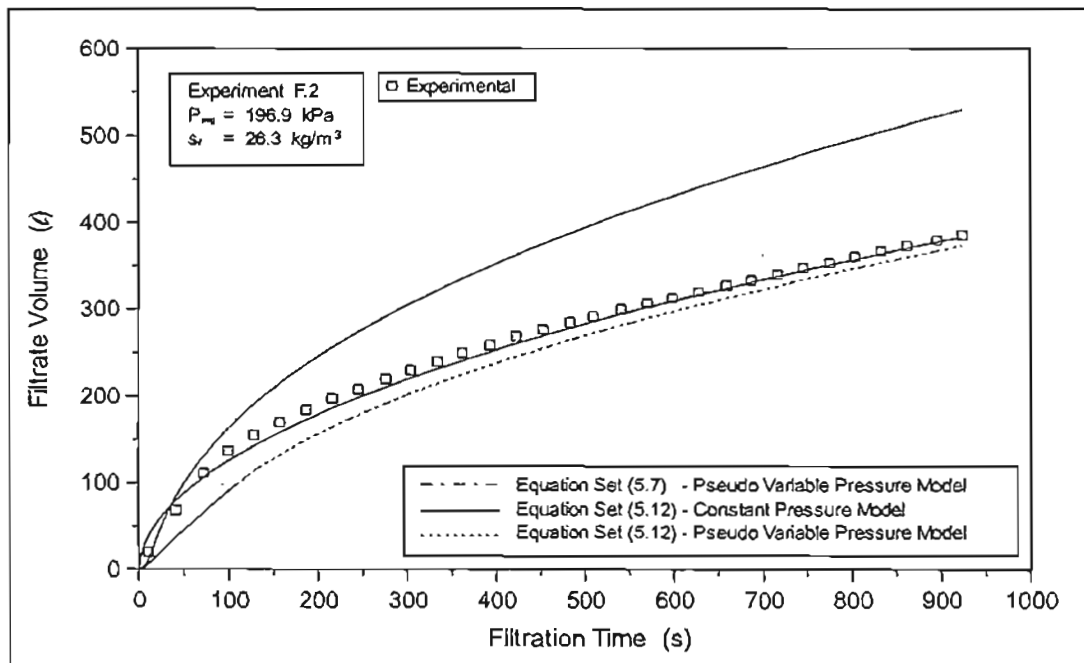


FIGURE 5.92 : Comparison between Experimental and Predicted Filtrate Volume Profiles for the Tubular Filter Press for Experiment F.2 using the Plant Specific Characterisation

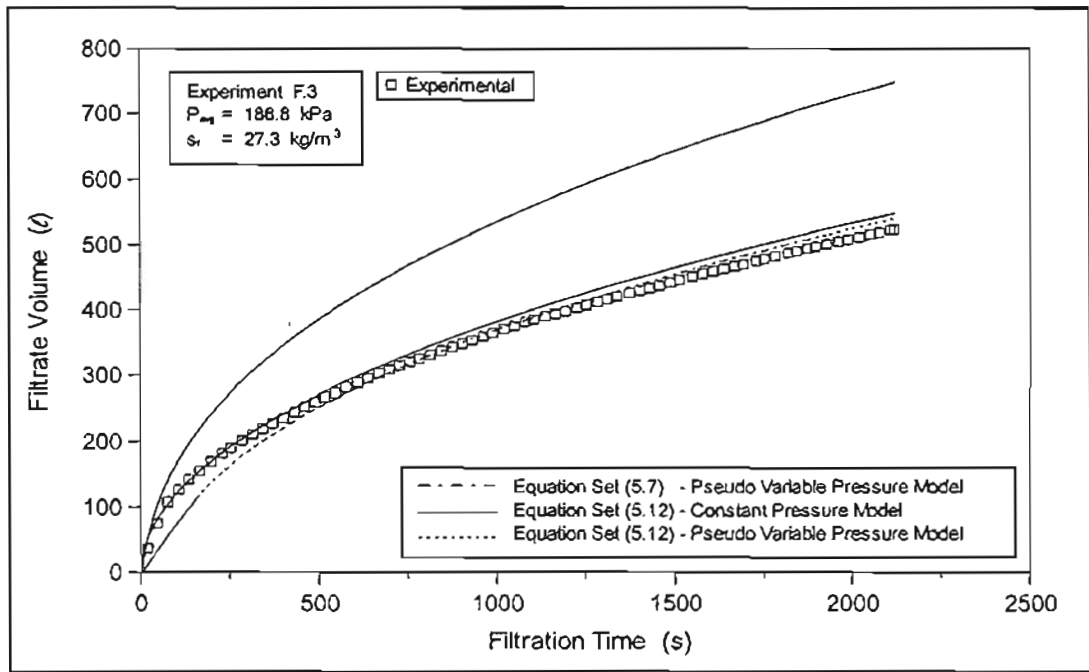


FIGURE 5.93 : Comparison between Experimental and Predicted Filtrate Volume Profiles for the Tubular Filter Press for Experiment F.3 using the Plant Specific Characterisation

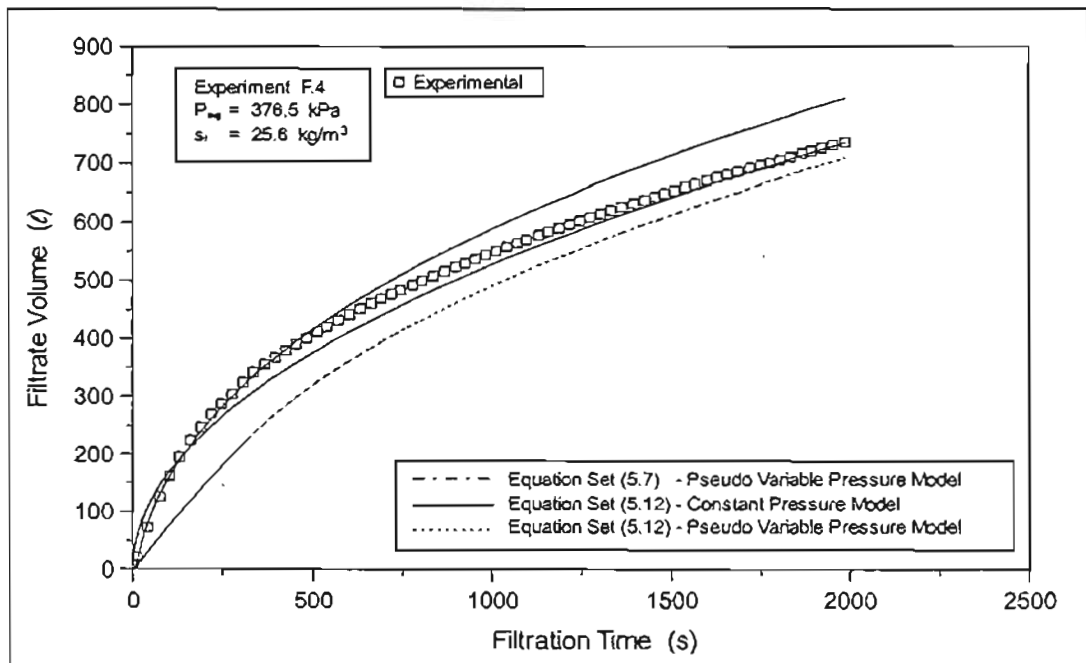


FIGURE 5.94 : Comparison between Experimental and Predicted Filtrate Volume Profiles for the Tubular Filter Press for Experiment F.4 using the Plant Specific Characterisation

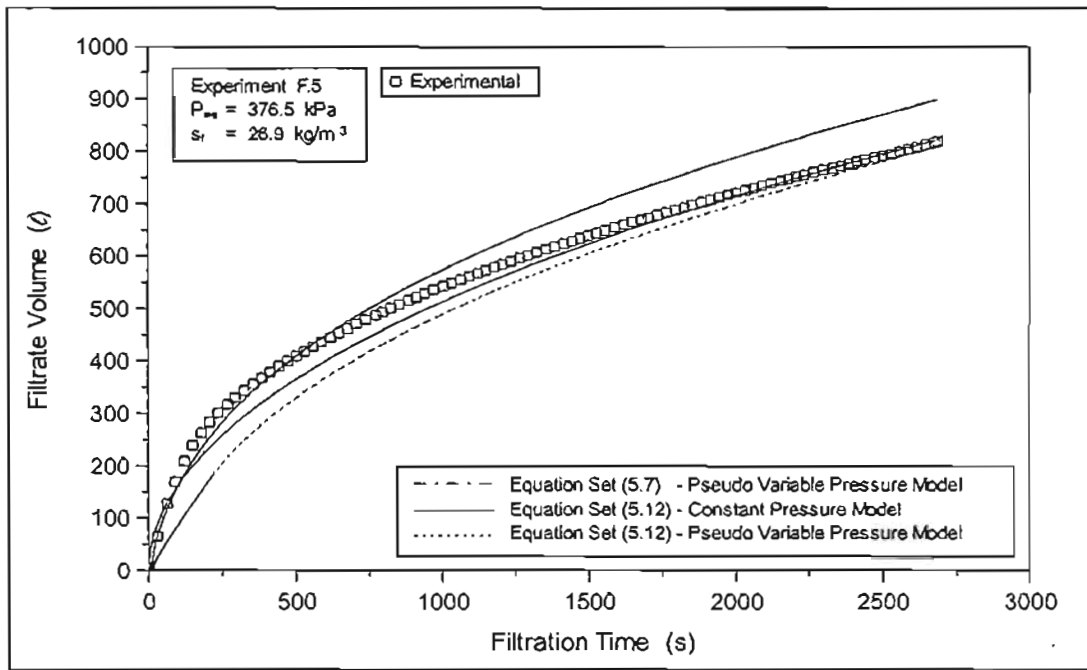


FIGURE 5.95 : Comparison between Experimental and Predicted Filtrate Volume Profiles for the Tubular Filter Press for Experiment F.5 using the Plant Specific Characterisation

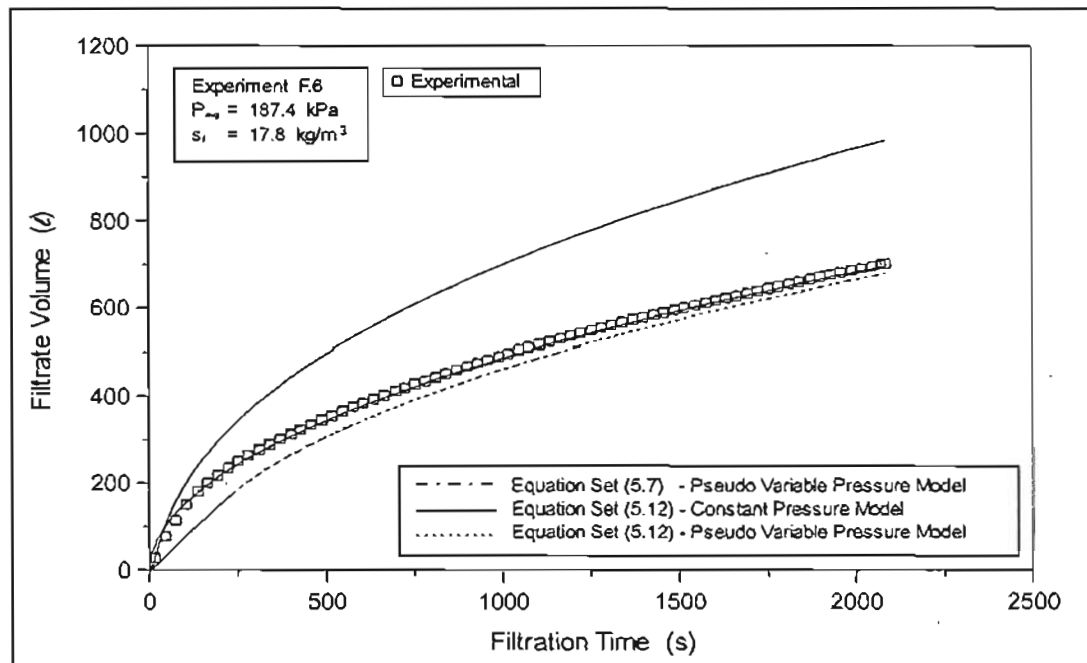


FIGURE 5.96 : Comparison between Experimental and Predicted Filtrate Volume Profiles for the Tubular Filter Press for Experiment F.6 using the Plant Specific Characterisation

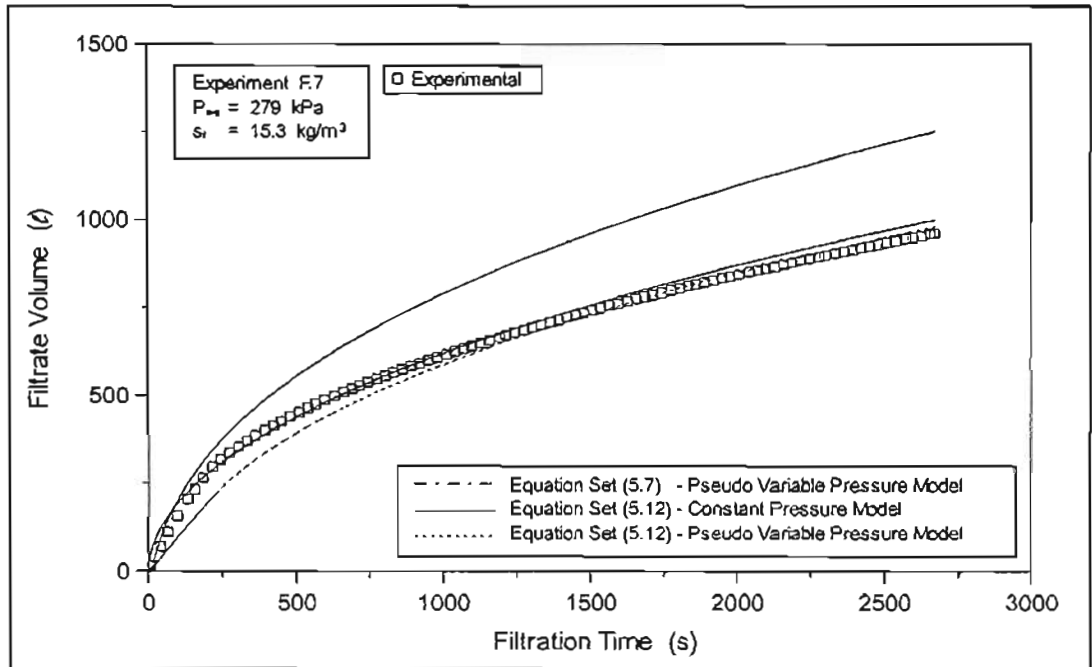


FIGURE 5.97 : Comparison between Experimental and Predicted Filtrate Volume Profiles for the Tubular Filter Press for Experiment F.7 using the Plant Specific Characterisation

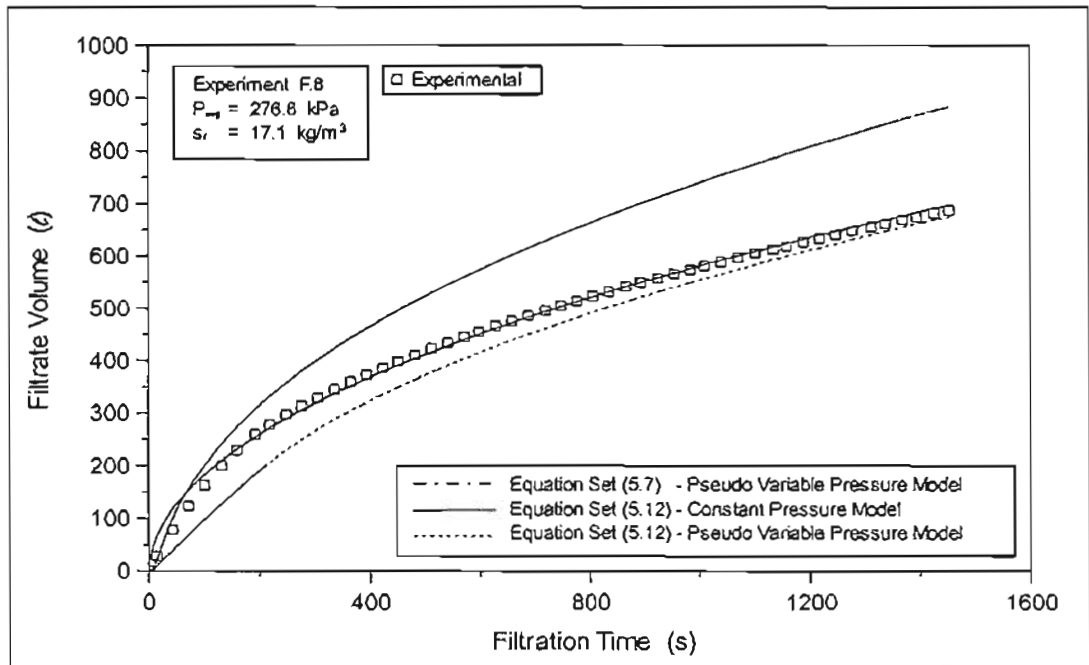


FIGURE 5.98 : Comparison between Experimental and Predicted Filtrate Volume Profiles for the Tubular Filter Press for Experiment F.8 using the Plant Specific Characterisation

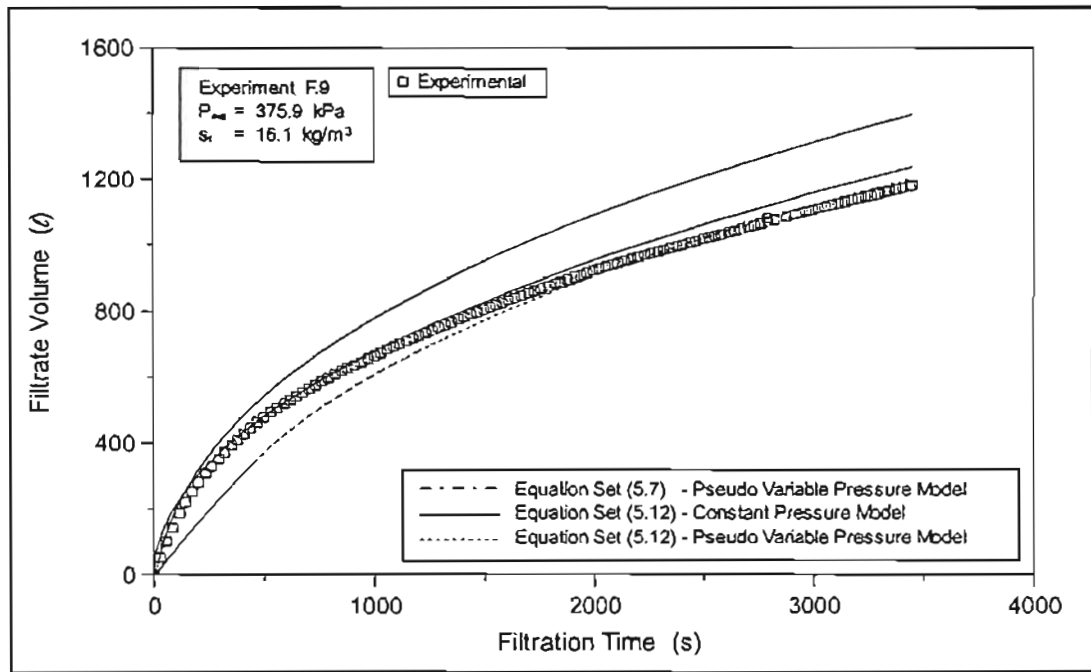


FIGURE 5.99 : Comparison between Experimental and Predicted Filtrate Volume Profiles for the Tubular Filter Press for Experiment F.9 using the Plant Specific Characterisation

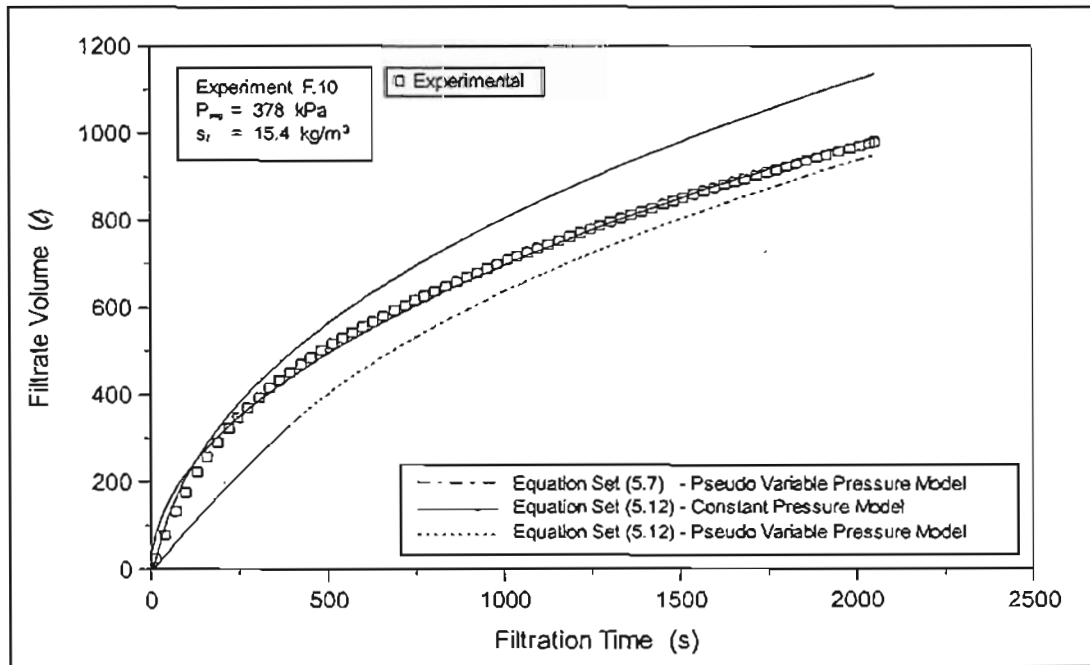


FIGURE 5.100 : Comparison between Experimental and Predicted Filtrate Volume Profiles for the Tubular Filter Press for Experiment F.10 using the Plant Specific Characterisation

The plant specific characterisation for the Tubular Filter Press, Equations 5.12, shows a significant improvement over the laboratory characterisation, Equations 5.7, and accurately

predicts the filtrate volume versus time over the range of experimental operating pressures and feed solids concentrations.

Figure 5.101 to Figure 5.106 show the comparison between the average cake dry solids concentrations for the Tubular Filter Press experiments and the predictions of the constant compressible cake filtration model, using the plant specific characterisation given by Equations 5.12. Where applicable, experiments at similar operating pressures and feed solids concentrations have been grouped together, due to the insensitivity of the average cake dry solids concentration to these experimental parameters. For these cases, the outputs of the filtration model have been determined using the average pressure, average feed solids concentration and where applicable, average pressurisation time, for the two experiments. The predicted average cake concentrations at each experiments final filtration times have been determined using the experiments own unique operating conditions in the model. The predicted average cake concentration for the pseudo variable pressure and constant pressure solution procedures, using the characterisation given by Equations 5.7, is included for comparative purposes, as well as an indication of the expected average cake dry solids concentration with respect to time, of a cake characterised by Equations 5.7, that has experienced cake loss up to a internal dry solids concentration of 10 % m/m.

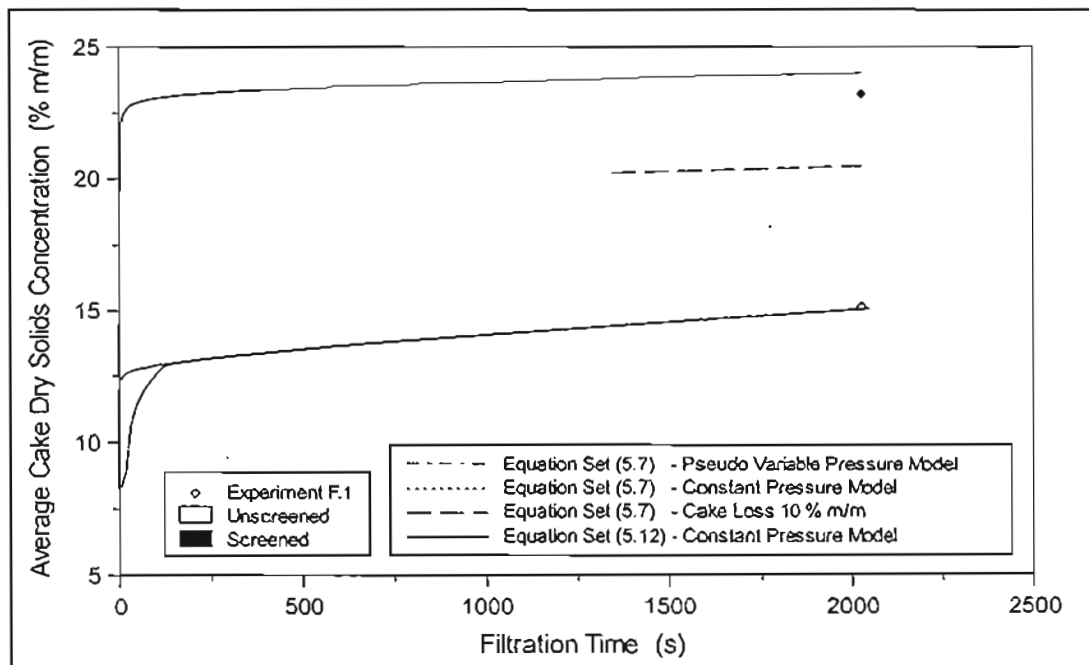


FIGURE 5.101 : Comparison between Experimental and Predicted Average Cake Dry Solids Concentration for the Tubular Filter Press Experiment F.1 using the Plant Specific Characterisation

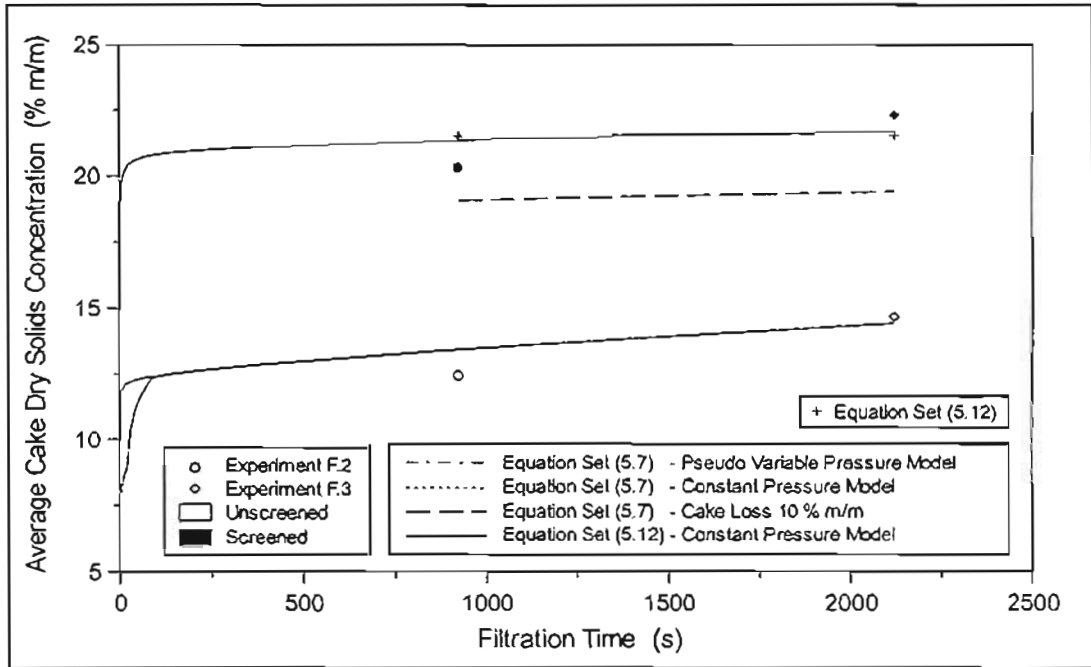


FIGURE 5.102 : Comparison between Experimental and Predicted Average Cake Dry Solids Concentration for the Tubular Filter Press Experiment F.2 and Experiment F.3 using the Plant Specific Characterisation

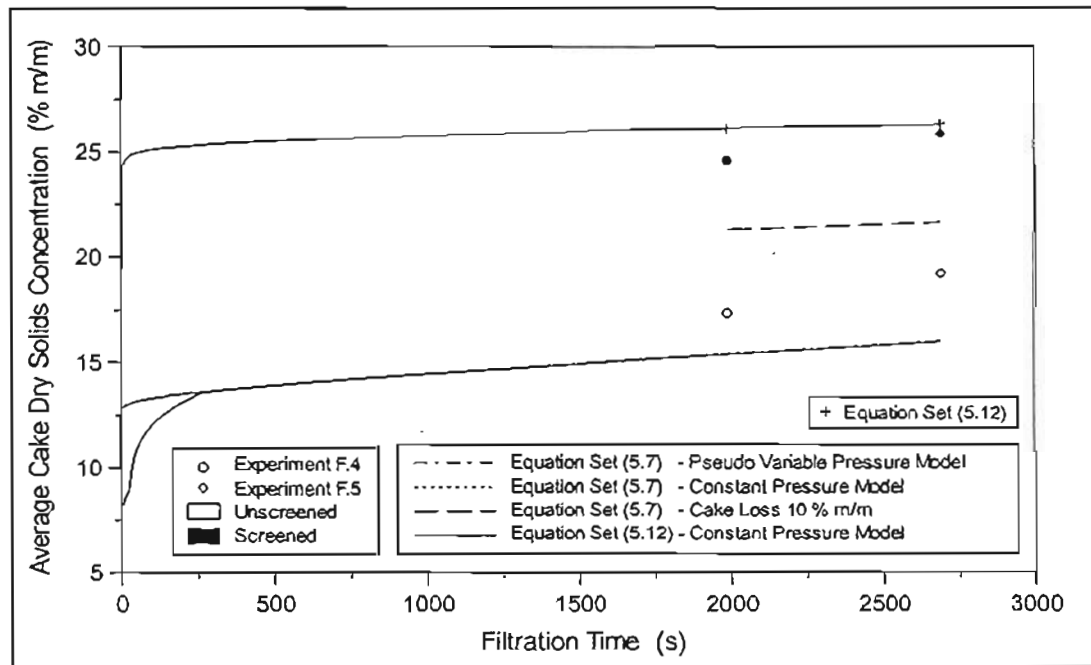


FIGURE 5.103 : Comparison between Experimental and Predicted Average Cake Dry Solids Concentration for the Tubular Filter Press Experiment F.4 and Experiment F.5 using the Plant Specific Characterisation

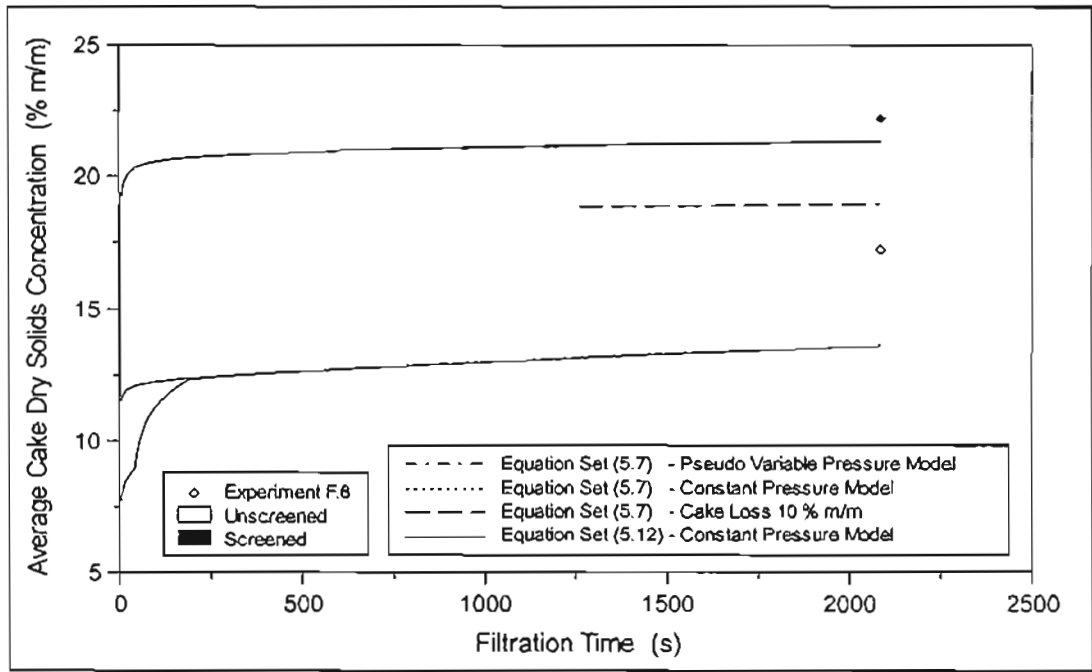


FIGURE 5.104 : Comparison between Experimental and Predicted Average Cake Dry Solids Concentration for the Tubular Filter Press Experiment F.6 using the Plant Specific Characterisation

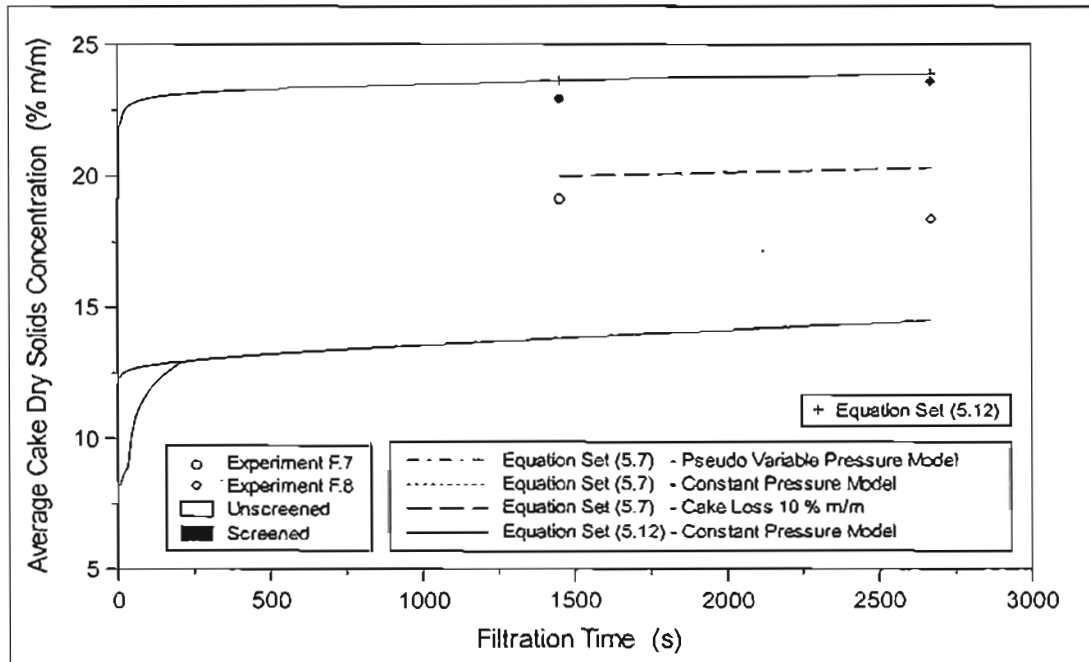


FIGURE 5.105 : Comparison between Experimental and Predicted Average Cake Dry Solids Concentration for the Tubular Filter Press Experiment F.7 and Experiment F.8 using the Plant Specific Characterisation

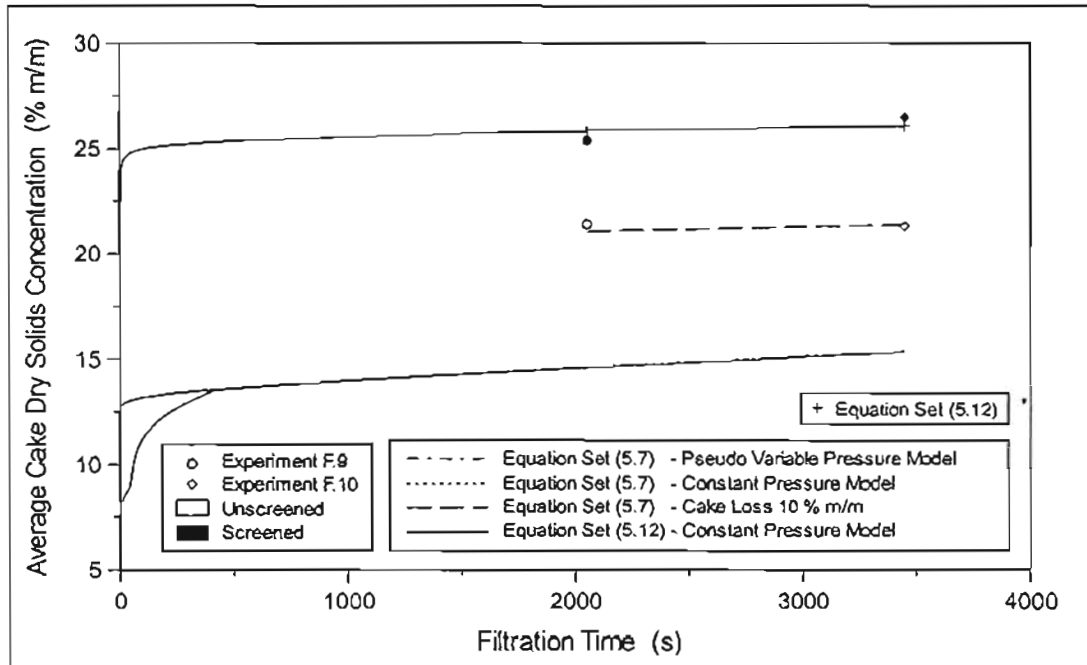


FIGURE 5.106 : Comparison between Experimental and Predicted Average Cake Dry Solids Concentration for the Tubular Filter Press Experiment F.9 and Experiment F.10 using the Plant Specific Characterisation

The filtration model using the constant pressure solution procedure, and the plant specific characterisation, Equation 5.12, accurately predicts the average cake dry solids concentration of the screened cake samples. The plant specific characterisation shows a significant improvement over the laboratory characterisation, Equations 5.7, even after an attempt is made to account for cake loss from a rheological basis. From Figure 5.101 to Figure 5.106, it is evident that due to the variability of the extent which flush fluid is entrained with the recovered cake, as a result of inadequate drainage on the cake conveyor belt, it would not be possible to obtain an accurate plant specific characterisation for the unscreened cake samples.

If an accurate true sludge characterisation has been obtained from either laboratory tests, or from a regression analysis on filtration data that has not experienced cake loss, and an accurate plant specific characterisation has been obtained from full-scale plant data, then it is possible that the two characterisations can be used in conjunction with one another to accurately predict cake losses.

5.10 OPTIMISATION AND CONTROL OF THE TUBULAR FILTER PRESS

In the process flow diagram of the Tubular Filter Press given in Section 4.6 (Figure 4.5), the system was closed for experimental purposes, in order to ensure the properties of the sludge remained constant. For the experimental study, the Tubular Filter Press was also operated on a batch basis. The process flow diagram for the normal continuous operation of the Tubular

Filter Press, at Wiggins Water Works is given in Figure 5.107. The exact process flow diagram for the Tubular Filter Press will depend on the particular application, however Figure 5.107 can be considered typical.

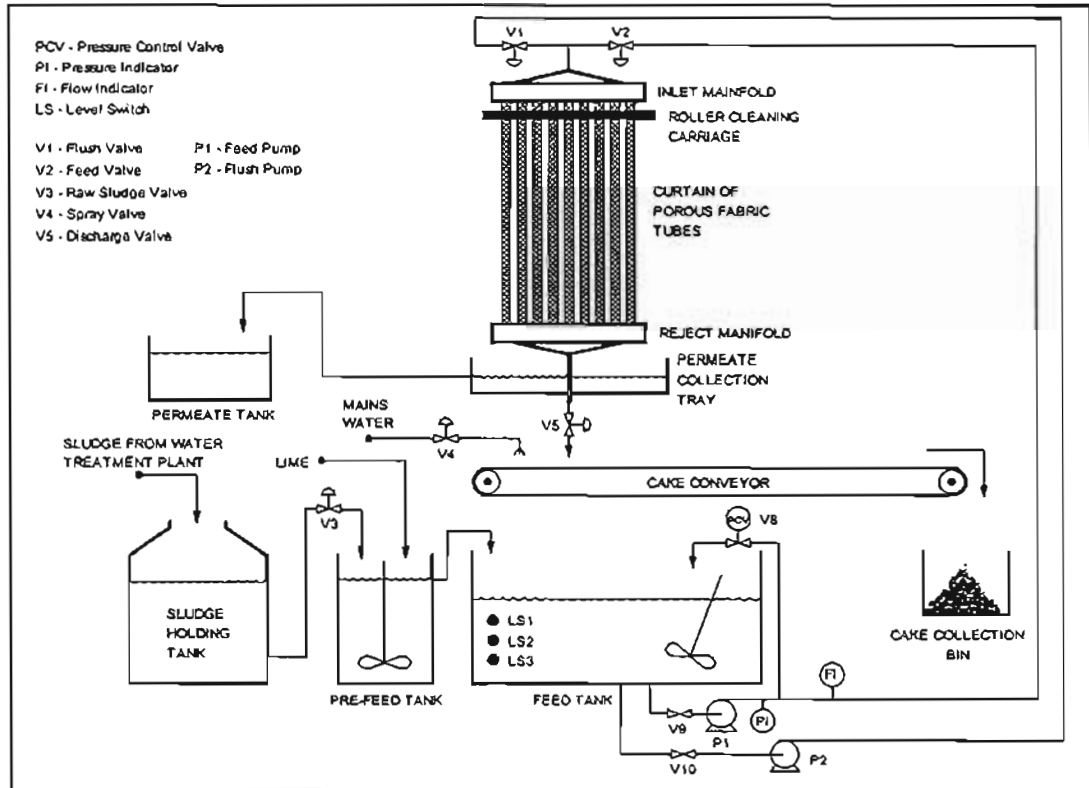


FIGURE 5.107 : Schematic Diagram of the Continuous Tubular Filter Press Process at Wiggins Water Works

The continuous operation of the Tubular Filter Press has previously been controlled by setting a predetermined limiting flux (Pryor and Mullan, 1998). In view of efficient plant operation, the use of final filtrate flux to control the operation of the plant is undesirable. The final filtrate flux is dependent on the feed solids concentration, the operating pressure and the final filtration time, and the plant recovery is in turn a complex function of these three operational parameters. Plant recovery plays an integral role in the performance of the plant, and therefore the use of final filtrate flux as a control parameter may lead to unpredictable and unstable plant behaviour. In Appendix G a control and optimisation strategy is proposed for the continuous operation of the Tubular Filter Press, and it is shown that the principle control parameters available to the operator to control and optimise the Tubular Filter Press are the final filtration time and the operating pressure.

5.11 EVALUATION OF NEW AREA CONTACT MODEL

Figure 5.108 shows the comparison between the main cumulative filtration properties, namely filtrate volume, average cake dry solids concentration and cake thickness, with respect to

filtration time, predicted using the point contact model and the new area contact model. For the purposes of the comparison, planar filtration geometry was used, the filtration pressure was 300 kPa, and the sludge was assumed to be characterised by Equations 5.7. Although in the context of the point contact model, Equations 5.7 were not an accurate characterisation of the filtration behaviour of the sludge investigated for this study, the characterisation is considered to be a sufficiently accurate, and typical characterisation of the type of sludge used in this study in order to investigate the applicability of the new area contact model. To highlight the differences between the output of the point contact model and the output of the area contact model, using the sludge characterisation given by Equations 5.7, the extreme case of the area contact model was used. The coefficient of area contact in the area contact function (Equation 3.10), was set to its maximum value, $A_0 = 1$. The point-area compressive pressure was set to the minimum feasible value for the Equations 5.7 (see Section 3.2.4.3), which results in the maximum feasible region of area contact. The minimum point-area compressive pressure for Equations 5.7, at an applied filtration pressure of 300 kPa was evaluated to be, $p_{sa} = 89326$ Pa.

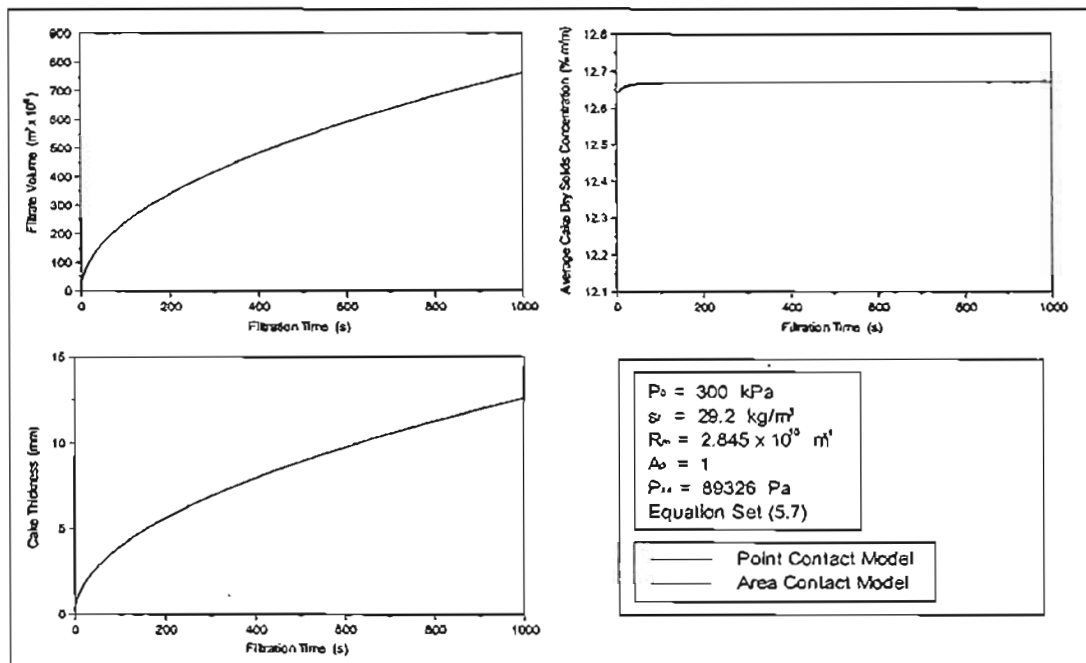


FIGURE 5.108 : Comparison between output of Point Contact and Area Contact Filtration Models using Sludge Characterisation given by Equations 5.7

Figure 5.108 shows that the difference between the predicted cumulative filtration properties for the point contact and area contact models using the sludge characterisation given by Equations 5.7 was negligible. The lines in Figure 5.108 representing the output of the models are essentially superimposed on one another. The area contact model could therefore not account for the differences between the experimental results and the output of the point contact model in Section 5.8.

Figure 5.109 shows the difference between the calculated solids compressive pressure profiles through a cake 10 mm thick, using the point contact and area contact models. The solids compressive pressure profiles are typical for a super compressible cake as characterised by Equations 5.7. Figure 5.109 shows that the point in the cake structure where the solids compressive pressure rises above the point-area compressive pressure, which represents the point where the interparticle contact changes from point contact to area contact, occurs in the last 4.47 % of the overall cake thickness. The influence of the area contact model is therefore restricted to only 4.47 % of the overall cake structure, and as a result there is little difference observed between the calculated solids compressive pressure profiles. Although not clear in Figure 5.109, the calculated solids compressive pressure at the medium for the area contact model is 295845 Pa, compared to 299204 Pa for the point contact model. The very slight difference in the solids compressive pressure profiles in the area contact region, has little effect on the overall cake porosity and permeability which is reflected in the output of the models shown in Figure 5.108.

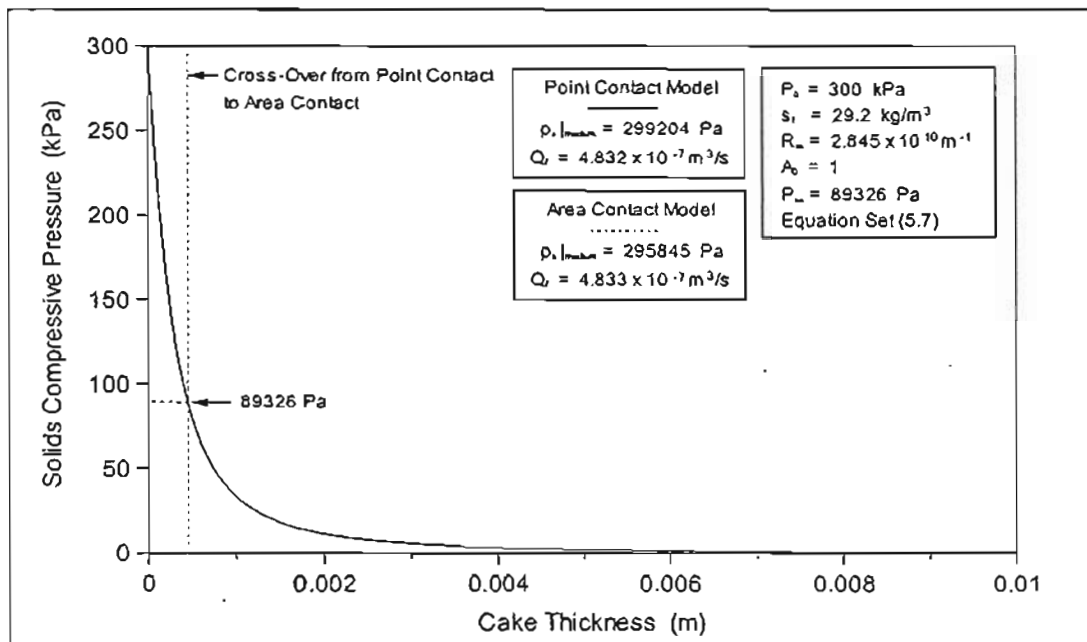


FIGURE 5.109 : Comparison between Calculated Solids Compressive Pressure Profiles using the Point Contact and Area Contact Filtration Models and the Sludge Characterisation given by Equations 5.7

Figure 5.110 shows the difference between the calculated porosity profiles through the cake, resulting from the solids compressive pressure profiles, for the area contact and point contact models, as expected, there is no noticeable difference.

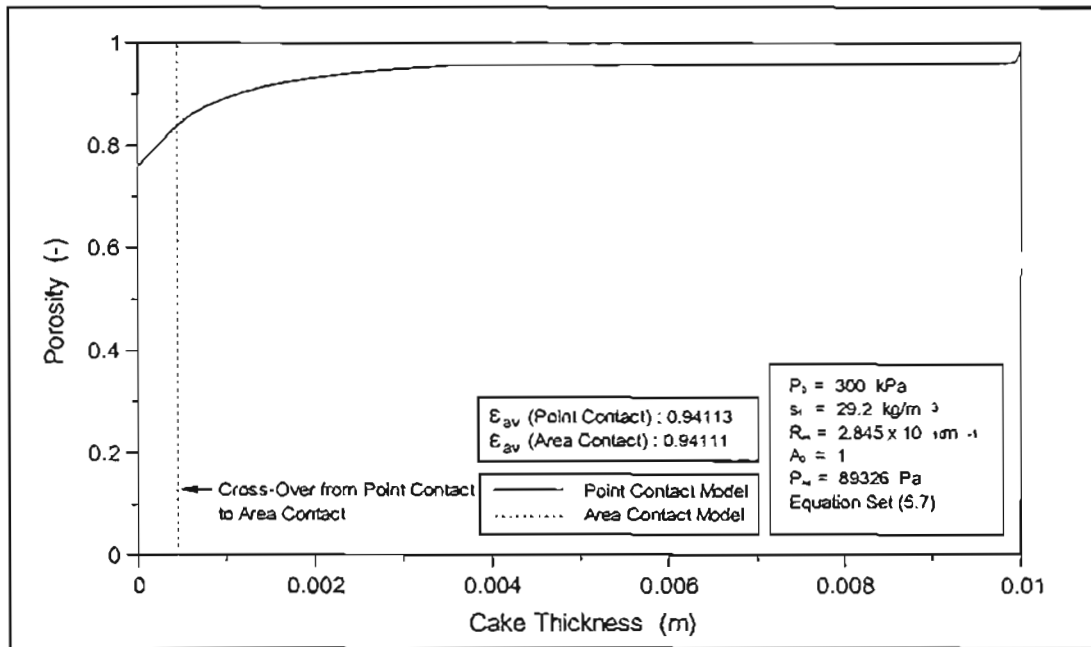


FIGURE 5.110 : Comparison between Calculated Porosity Profiles using the Point Contact and Area Contact Filtration Models and the Sludge Characterisation given by Equations 5.7

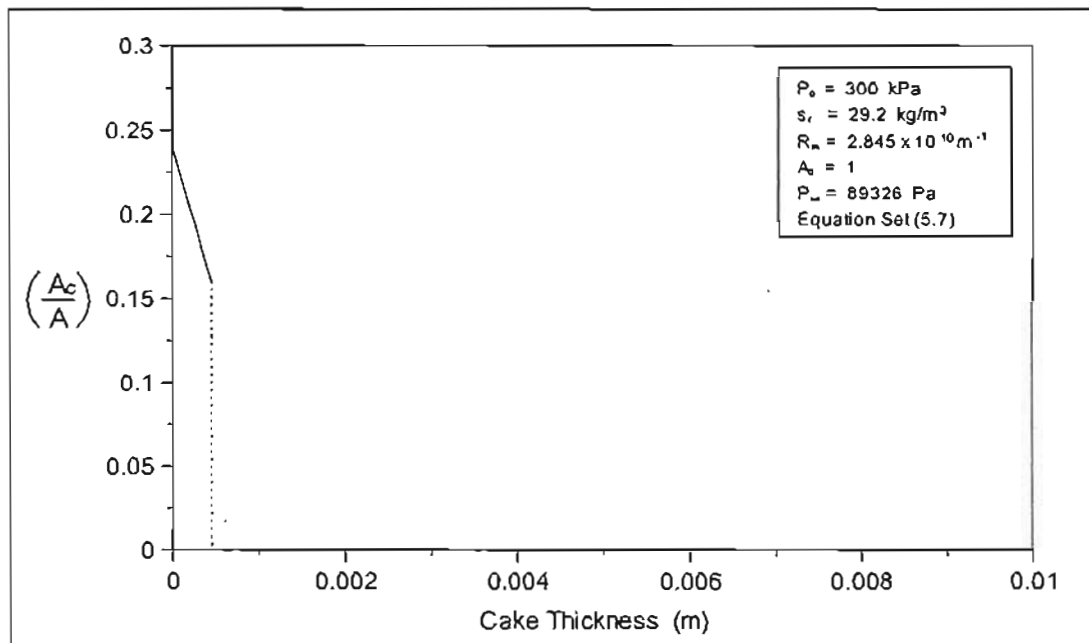


FIGURE 5.111 : Area Contact through Cake Characterised by Equations 5.7

Figure 5.111 shows the ratio of area contact to total area with respect to distance through the cake. In the point contact region, which represents the bulk of the cake structure, the area contact is zero. Once the applied pressure exceeds the point-area compressive pressure, there is a step increase in area contact. In the area contact region, the ratio of area contact to total area is given by the product of the local solidosity and the coefficient of area contact (see Equation 3.10). The degree of area contact rises steeply due to the sharp decrease in local cake porosity

in this region as shown in Figure 5.110. With the maximum possible coefficient of area contact, the degree of area contact approaches a maximum of 25 % at the medium.

Due to the insensitivity of the model output to the degree of area contact for this particular slurry type, no meaningful result would be obtained by attempting to regress for the parameters in the area contact model from the experimental data.

The use of the point contact models to model the filtration behaviour of sludges such as the water works sludge in this investigation is therefore justified. The validity and applicability of the area contact model will have to be investigated with slurry types that exhibit a greater intrinsic degree of area contact, i.e. slurry types that consist of solid particles that have a more flake like structure, that result in cakes that are less compressible and have a less porous overall cake structure.

5.12 EFFECTS OF INSTANTANEOUS CAKE EQUILIBRIUM ASSUMPTION

A primary assumption in the development of the filtration theory is that equilibrium porosities are attained instantaneously with changing solids compressive pressure, i.e. the cake is always in equilibrium. However, in actual filtration this is not the case, during the initial stages of filtration, the cake growth is rapid, and subsequently the cake structure is not in equilibrium. Only as the filtrate flow rate and hence the cake growth rate decreases, will the cake structure begin to obtain equilibrium as it has time to consolidate under the solids compressive pressure. If cake equilibrium effects are significant, it can have a number of effects with regard to evaluating the performance of a filtration plant. For instance, in terms of the filtration theory, the feed solids concentration should have no effect on the cake equilibrium, however in reality, as feed solids concentration increases so does the initial cake growth rate, and as such the resultant initial cake structure will be further from the equilibrium cake structure. Cakes formed from dilute feed solids concentrations are therefore more likely to be in equilibrium because the cake structure is exposed to greater periods of solids compressive stress per unit mass solids deposited as the increased amount of filtrate (per unit solids deposited) flows through the cake structure.

Filtration can therefore be regarded as being divided into two conceptual phases. The *cake growth phase*, whilst the filtrate flow rates are still relatively high. The filtrate flow rate decreases rapidly and then levels off, cake growth becomes relatively insignificant and the filtration can now be regarded to be in a *cake consolidation phase* as the filtrate flows through the cake structure with little cake growth.

Cake equilibrium effects can be observed in the planar filtration tests conducted by Rencken (1992). After the initial period of the filtration, the effect of the medium resistance becomes insignificant and the theoretical dimensionless solids compressive pressure profile through a planar filtration cake, remains relatively constant. As a result the dimensionless porosity profile and calculated average cake porosity should be constant with respect to time. The planar filtration tests conducted by Rencken (1992), show that the experimental cake solids concentrations are initially below the relatively constant value predicted by the filtration model, and increase slowly with time becoming relatively constant in the region of the predicted value.

A cake structure that is not in equilibrium will be more porous and therefore be more permeable than an equal mass of cake at equilibrium. Non-equilibrium cake structures will therefore deposit a greater mass of solids before a predetermined limiting flux is attained than equilibrium cake structures. As a result, if the operation of a plant is to terminate at a certain final flux, the higher the feed solids concentration, the larger the amount of solids that will be deposited before the filtration cycle terminates.

If the filtration is not allowed to operate in the consolidation phase for a sufficiently long period of time, the average cake solids concentration could be lower than expected. The unconsolidated cake structure may also be structurally weaker than an equilibrium cake structure, this could have adverse effects on the cake recovery for plants such as the Tubular Filter Press where the cake is hydraulically removed by the feed sludge. Obtaining an optimum dry solids production rate is then a trade off between operating in the cake consolidation phase for long enough to ensure a good recovery without adversely extending the filtration cycle time, and hence lowering production rates.

Chapter 6

Conclusion

The sludge at Wiggins Water Works was found to be extremely compressible. The compressibility of the sludge was found to be dependent on the solids compressive pressure and therefore did not obey the simple forms of the porosity and permeability correlations as given by Equations 3.1 and Equation 3.2. Equations 3.3, which are an extension of Equations 3.1, were able to accurately account for the changes in the compressible nature of the sludge over the range of solids compressive pressures.

The principle laboratory-scale test to determine the empirical parameters in the porosity and permeability correlations, is the C-P cell test. Various weaknesses in C-P cell testing were identified in the literature, which could lead to errors in the characterisation obtained from C-P cell tests. Due care must be taken in all design and optimisation calculations that utilise this data, since there can be no guarantee that the characterisation is representative of the porosity and permeability in actual filtration. The main source of error in C-P cell tests was identified as being the effect of friction between the cake sample and the wall of the C-P cell, particularly for low solids compressive pressures. A new C-P cell was designed and constructed that could measure the transmitted pressure through the cake sample in the C-P cell, in addition to the applied pressure. The data obtained from the C-P cell was corrected for the effects of wall friction using a model proposed by Shirato et al. (1968). The model was found to accurately predict the transmitted pressure for applied pressures less than 250 kPa. The characterisation which has been corrected for the effects of wall friction showed a significant improvement in predicting the filtration behaviour of the sludge, over the characterisation which had not been corrected. However, despite accounting for the effects of wall friction, the characterisation was still found not to be an accurate characterisation of the filtration behaviour of the sludge. The result serves to highlight that characterisations obtained from the standard non-filtration laboratory methods, cannot be guaranteed to be a true reflection of the filtration characteristics of the sludge.

The coefficient of earth pressure at rest is a model parameter unique to the internal cylindrical geometry, and other non-planar filtration geometries of the constant pressure compressible cake filtration model. The effect of the coefficient of earth pressure at rest is negligible during the normal operation of the Tubular Filter Press. An experimental procedure for determining the coefficient of earth pressure at rest had not been documented, and previously the value of the coefficient of earth pressure at rest had been assumed (Rencken, 1992). The direct shear test was identified as a feasible experimental procedure to determine the coefficient of earth pressure at rest. The procedure was documented and the coefficient of earth pressure at rest was determined for the Wiggins Water Works sludge.

In order to validate the filtration model and the associated solution procedures that have been developed, and incorporated into the computer programmes COMPRESS and REGRESS, laboratory-scale planar filtration tests were performed, in addition to the full-scale Tubular Filter Press filtration tests performed on the pilot-plant at the Wiggins Water Works.

Unlike laboratory filtration experiments, where the experimental parameters can be tightly controlled, during the full-scale application of constant pressure filtration such as the Tubular Filter Press, the nature of the process can introduce additional operational variables, that depending on their significance, may require the revision of the filtration model and the associated solution procedures. During the operation of the Tubular Filter Press, it was observed that once the tubes had been filled, it took approximately 100 to 400 seconds for the tubes to become fully pressurised. It was found that the pressurisation profile was relatively linear and that the final pressurisation time was dependent on the feed solids concentration and the final applied pressure. If the pressurisation time becomes a significant part of the overall filtration time, the constant pressure filtration model may not be able to adequately account for the filtration behaviour of the plant. A new pseudo variable pressure solution procedure was developed to account for the initial variable pressure stage of the filtration. The pseudo variable pressure solution procedure treated the filtration as a series of constant pressure filtrations, allowing the cake to grow, and evaluating the filtration properties at the end of a fixed time step. The applied pressure for each filtration calculation over the fixed time interval was the average of the applied variable pressure profile over the interval. Since the cake was compressible, before the cake was allowed to grow over the next time interval, the cake was compressed at the increased average pressure of the next time interval, to determine the initial cake structure for the subsequent growth stage. The filtrate volume and filtrate flow rate at the end of the subsequent growth stage were adjusted to include the effects of the compression. The principle assumption of the pseudo variable pressure solution procedure is that compression of the previously deposited cake is completed during the growth of the cake over the next time interval. Provided the time step is small, the calculation should approximate simultaneous cake growth and compression, where the cake structure is always in equilibrium. The pseudo variable pressure solution procedure was able to account accurately for the initial linear filtrate volume versus time behaviour, observed during the pressurisation period of the Tubular Filter Press. It was found that provided the filtration time was significantly longer than the pressurisation time, the difference between the output of the constant pressure solution procedure and the pseudo variable pressure solution procedure became negligible. The validity of the pseudo variable pressure solution could not be properly ascertained since an accurate true sludge characterisation was not obtained. It is recommended that applicability of the pseudo variable pressure solution procedure be investigated further.

The cake recovery during the cleaning cycle of the Tubular Filter Press was investigated as it is essential, for the control and optimisation of the Tubular Filter Press, that the cake recovery be predicted with a reasonable degree of accuracy. Rencken (1992), investigated the cake recovery mechanism for the horizontal Tubular Filter Press, although he was able to predict cake losses due to the shearing of the

cake by the flush fluid, in situ, prior to the action of the rollers, he concluded it was impossible to obtain a general model that could account for the cake losses due to the action of the roller cleaning carriage and the hydraulic conveyance of the dislodge cake. The recovery mechanism of the vertical Tubular Filter Press differs considerably to that studied by Rencken (1992). The cake recovery of the Tubular Filter Press over a range of operating conditions, was found to vary between 50 to 73 %. Some general trends in cake recovery were observed with regard to the main operational parameters. Recovery was observed to increase with increasing feed solids concentration, final filtration time and the total mass of wet cake deposited in the tubes. The recovery was however, observed to decrease with increasing filtration pressure, this is in contrast to the observations of Rencken (1992), who observed the recovery to increase significantly with increasing filtration pressure. This illustrates that the nature of cake recovery is extremely complex and dependent on the filtration plant and the associated recovery mechanism, as well as the properties of the sludge. The cake recovery was found to be a complex function, not strongly dependent on any one particular operational parameter. It is recommended that further work be conducted on the nature of cake recovery, so that the mechanisms involved can be better understood, to assist in the development of recovery correlation.

Drainage of the excess flush fluid from the recovered cake on the conveyor belt was found to be inadequate and variable. Inadequate and variable drainage reduces the efficiency of the process and makes effective control and optimisation of the process difficult. It is recommended that the method of cake drainage and conveyance be optimised.

The standard laboratory characterisation methods to characterise the filtration behaviour of the sludge, require specialised testing equipment, are difficult to perform, lengthy and often prone to failure, in addition, there is doubt as to the accuracy and applicability of characterisations obtained from the non-filtration standard laboratory techniques. An immediate, reliable and accurate method of determining the filtration characteristics of the sludge is therefore necessary for the efficient control and optimisation of the Tubular Filter Press. This is particularly important if the quality, and hence the filtration behaviour, of the feed sludge to the Tubular Filter Press is variable. In addition, the area contact model is novel, and a method for determining the parameters specific to the area contact model, is necessary. A regressive solution procedure was developed that enables the filtration characteristics of the sludge, and the parameters specific to the area contact model, to be determined by regressing on actual filtration data. In order for the regressive solution procedure to be of general and practical use, it was developed to utilise filtration data that is immediately available and does not require specialised and sophisticated experimental equipment or techniques. Due to the numerical complexity of the filtration model, the regressive solution procedure utilises a direct search technique. A direct search technique was developed that is an extension of the COMPLEX method of Box (1965). The objective function of the direct search technique incorporated terms originating from a time independent and a time dependent analysis of the filtration data. The regressive solution procedure was evaluated using pseudo experimental data produced by the filtration model, both the time independent and time dependent analyses were able to converge

onto the solution, but the combined analysis was found to be most effective. The effects of inaccuracies in the experimental data on the results of the regression analysis was investigated. Cake loss and the incorrect determination of the filtrate flow rate were found to significantly influence the results of the regression analysis. The effects of inaccuracies in the experimental data was found to increase with increasing cake compressibility. The time independent analysis was found to be most sensitive to the effects of inaccuracies in the experimental data. A true physical characterisation cannot be obtained if the experimental data has been affected by cake loss, however it was found that a plant specific characterisation could be obtained from a time dependent regression analysis. Provided the cake loss mechanism is consistent, the plant specific characterisation can absorb the effects of cake loss into the model parameters. The identification of an accurate plant specific characterisation has important consequences for the Tubular Filter Press where cake loss is an inherent part of the process, as it negates the need to model the filtration cycle and filtration cycle separately and the performance of the filter can be obtained directly from the initial operating parameters. Plant specific characterisations obtained for the planar filtration experiments and the Tubular Filter Press were found to accurately predict the filtration performance, and showed a significant improvement over the characterisations obtained from the standard laboratory techniques. The computer programme REGRESS that incorporates the regressive solution procedure, utilises the constant pressure solution procedure, the plant specific characterisation obtained is therefore not applicable to the pseudo variable pressure solution procedure. It is recommended that the pseudo variable pressure solution procedure be incorporated into the programme REGRESS so that plant specific characterisations can be obtained in context of the pseudo variable pressure solution procedure, so that the validity of the solution procedure can be investigated. The regressive solution procedure was found to be an effective means of determining both the true physical or plant specific characterisation of the sludge. The sludge at Wiggins Water Works exhibited negligible area contact behaviour and as a result the ability of the regressive solution procedure to determine the parameters specific to the area contact model could not be evaluated.

Due to the super compressible nature of the sludge at Wiggins Water Works, the filter cake was found to be highly susceptible to the effects of cake loss, as the bulk of the cake structure remained loose and unconsolidated. Cake loss was found to have an unexpected, yet significant effect on the results obtained from the laboratory-scale, planar filtration experiments. Cake loss is an inherent part of the cake removal mechanism of the Tubular Filter Press, as a result a true physical sludge characterisation cannot be obtained from Tubular Filter Press data. However, a true physical characterisation can be obtained from laboratory-scale filtration experiments, provided the experimental data is not affected by cake loss. A true physical characterisation is essential for the control and optimisation of the Tubular Filter Press process. A true physical characterisation obtained from regressing on filtration data is preferential to a characterisations obtained form the standard non-filtration laboratory methods, as the latter characterisation cannot be guaranteed to be representative of the filtration behaviour of the sludge. It is therefore recommended that the planar filtration experimental technique be amended to eliminate the effects of cake loss, or new measurement techniques utilised, that will enable filtration properties such as

cake thickness to be measured, in situ, during the filtration or prior to dismantling the filter cell to recover the cake. This will enable accurate true physical characterisations to be obtained from the planar filtration experiments. It is also recommended that the rheology of the sludge with respect to solids concentration be investigated in order to provide a better understanding of the nature of cake loss. This will assist in predicting the extent of cake loss, or assist in the formulation of a recovery correlation for the Tubular Filter Press.

A control and optimisation strategy has been proposed for the continuous operation of the Tubular Filter Press. In order for the continuous operation of the Tubular Filter Press to be effectively controlled and optimised, the final filtration time should be fixed explicitly and not determined by the final filtrate flux, as was done previously. The principle control variables available to the operator are the final filtration time and the operating pressure. In addition to the true physical characterisation of the sludges filtration behaviour, the recovery characterisation of the sludge must be known. The recovery characterisation can be made available in the form of an empirical recovery correlation or as an accurate plant specific characterisation. The recovery characterisation is dependent on both the rheological and filtration properties of the sludge, in addition to the physical configuration and recovery mechanism of the filtration plant, and is therefore specific to a particular plant, recovery cycle and sludge type. It is recommended that the control strategy be implemented to determine its validity.

A literature survey was conducted to determine if the constant pressure compressible cake filtration model developed by Rencken (1992), could be extended or improved. Various assumptions in the development of the filtration model were identified that could limit wide-scale applicability of the filtration model, and hence the wide-scale marketability of the Tubular Filter Press technology. A principle and common assumption made in the development of the filtration model is that the particles within filter cake are in point contact with one another. This assumption is highly idealistic. Based on a heuristically developed area contact function, a new generalised area contact model was developed that can account for any area contact that may exist between the particles in a filter cake. The area contact model was found to have a negligible effect on the output of the filtration model, compared to the output of the filtration model when the point contact assumption was used. This was due to the nature of the sludge at the Wiggins Water Works, which was found to produce a filter cake that exhibited a very low degree of area contact. The sludge produced a cake that was super compressible, the bulk of the cake was loosely consolidated, and as a result, area contact was restricted to a very small region of cake next to the medium. The area contact model is novel and therefore its validity still has to be ascertained. The area contact model may be beneficial for the wide-scale applicability of the Tubular Filter Press, particularly for sludge types that can be expected to exhibit a large degree of area contact. These sludges would consist of fibrous or flake-like solid particles, and produce consolidated cakes with a low to moderate degree of compressibility. It is recommended that the validity of the area contact model be investigated.

The constant pressure compressible cake filtration model and the associated predictive solution procedures, and the regressive solution procedure, have been incorporated into two user-friendly Windows 95 computer programmes titled COMPRESS and REGRESS respectively. The programmes COMPRESS and REGRESS should greatly assist in the design, control and optimisation of the Tubular Filter Press process, and hence greatly assist in the exploitation and commercialisation of the Tubular Filter Press technology.

References

- Aragaki, T., Hiraoka, S., Yamada, I., Murase, T., Iritani, E., and Shirato, M. (1989). **Generalised Relation Between Liquid Pressure and Solid Compressive Pressure in Non-unidimensional Filter Cakes**, *Journal of Chemical Engineering of Japan*, 22(4), 358-362.
- Atkins, P.W. (1991). *Physical Chemistry*, 4th Edition, Oxford University Press, Bungay.
- Bierck, B.R., Wells, S.A., and Dick, R.I. (1988). **Compressible Cake Formation: Monitoring Cake Formation and Shrinkage using Synchrotron X-rays**, *Journal WPCF*, 60(5), 645-650.
- Box, M.J. (1965). **A New Method of Constrained Optimisation and a Comparison with Other Methods**, *Computer Journal*, 8, 42-52.
- Chase, G.G., Arconti, J., and Kanel, J. (1994). **The Effect of Filter Cakes on Filter Medium Resistance**, *Separation Science and Technology*, 29(16), 2179-2196.
- Chase, G.G., and Willis, M.S. (1992). **Compressive Cake Filtration**, *Chemical Engineering Science*, 47(6), 1373-1381.
- D'Arcy, H.P.G. (1856). *Les Fontaines publiques de la Ville de Dijon*, Dalmont, Paris.
- Grace, H.P. (1953). **Resistance and Compressibility of Filter Cakes**, *Chemical Engineering Progress*, 49(6), 303-318.
- Henry, J.D., Lui, A.P., and Kuo, C.H. (1976). **A Dual Functional Solid Liquid Separation Process Based on Filtration and Settling**, *Journal of the American Institute of Chemical Engineers*, 22(3), 433-441.
- Iritani, E., Sumi, H., and Murase, T. (1991). **Analysis of Filtration Rate in Clarification Filtration of Power-Law Non-Newtonian Fluids-Solids Mixtures under Constant Pressure by Stochastic Model**, *Journal of Chemical Engineering of Japan*, 24(5), 581-586.
- Leu, W.F. (1981). **Cake Filtration**, PhD, Department of Chemical Engineering, University of Houston, Houston.
- Lu, W., Tiller, F.M., Cheng, F., and Chien, C. (1970). **A New Method to Determine Local Porosity and Filtration Resistance of Filter Cakes**, *Journal of Chinese Institute of Chemical Engineers*, 1, 45-53.
- Michaels, A.S., and Bolger, J.C. (1962). **Settling Rates and Sediment Volumes of Flocculated Kaolin Suspensions**, *Industrial and Engineering Chemistry. Fundamentals*, 1(1), 24-33.

- Muir-Wood, D. (1990). *Soil Behaviour and Critical State Soil Mechanics*, Cambridge University Press, New York.
- Murase, T., Iwata, M., Adachi, T., Gmachowski, L., and Shirato, M. (1989). An Evaluation of Compression-Permeability Characteristics in the Intermediate Concentration Range by use of Centrifugal and Constant-Rate Compression Techniques, *Journal of Chemical Engineering of Japan*, 22(4), 378-384.
- Perry, R.H., and Green, D.W. (1984). *Perry's Chemical Engineers' Handbook*, 6th Edition, McGraw-Hill, Tokyo.
- Pillay, V.L. (1991). **Modelling of Turbulent Cross-Flow Microfiltration of Particulate Suspensions**, PhD, Department of Chemical Engineering, University of Natal, Durban.
- Pryor, M.P., and Mullan, D.J. (1998). **The Development of an Exxpress Unit for the Dewatering of Water Works Sludges and the Production of Potable Water**, 568/1/98, Water Research Commission.
- Rencken, G.E. (1992). **Performance Studies of the Tubular Filter Press**, PhD, Department of Chemical Engineering, University of Natal, Durban.
- Richardson, J.F., and Zaki, W.N. (1954). **Sedimentation and Fluidisation: Part 1**, *Transactions. Institution of Chemical Engineers*, 32, 35-53.
- Rowe, P.W., and Borden, L. (1966). A New Consolidation Cell, *Geotechnique*, 16(2), 162-170.
- Ruth, B.F. (1935). **Studies in Filtration III - Derivation of General Filtration Equations**, *Industrial and Engineering Chemistry*, 27(6), 708-723.
- Shen, C., Russel, W.B., and Auzerai, F.M. (1994). **Colloidal Gel Filtration: Experiment and Theory**, *Journal of the American Institute of Chemical Engineers*, 40(11), 1876-1891.
- Shirato, M., and Aragaki, T. (1969). **The Relations Between Hydraulic and Compressive Pressure in Non-unidimensional Filter Cakes**, *Kagaku Kogaku*, 33(2), 205-207.
- Shirato, M., and Aragaki, T. (1972). **Verification of Internal Flow Mechanism of Cake Filtration**, *Filtration and Separation* (May/June), 290-297.
- Shirato, M., Aragaki, T., Mori, R., and Sawamoto, K. (1968). **Predictions of Constant Pressure and Constant Rate Filtrations based upon an Approximate Correction for Side Wall Friction in Compression Permeability Cell Data**, *Journal of Chemical Engineering of Japan*, 1(1), 86-90.

Shirato, M., Murase, T., Iritani, E., and Hayashi, N. (1983). **Cake Filtration - A Technique for Evaluating Compression-Permeability Data at Low Compressive Pressure**, *Filtration and Separation*, (September/October), 404-406.

Shirato, M., Sambuichi, M., Kato, H., and Aragaki, T. (1969). **Internal Flow Mechanism in Filter Cakes**, *Journal of the American Institute of Chemical Engineers*, 15(3), 405-409.

Sorensen, P., Christensen, J., and Bruus, J. (1995). **Effect of Small Scale Solids Migration in Filter Cakes During Filtration of Wastewater Solids Suspensions**, *Water Environment Research*, 67(1), 25-32.

× Tiller, F. M. (1966). **Filtration Theory Today**, *Chemical Engineering*, (June 20), 151-162.

Tiller, F.M., and Cooper, H. (1962). **The Role of Porosity in Filtration V: Porosity Variation in Filter Cakes**, *Journal of the American Institute of Chemical Engineers*, 8(4), 445-449.

Tiller, F.M., and Cooper, H.R. (1960). **The Role of Porosity in Filtration IV: Constant Pressure Filtration**, *Journal of the American Institute of Chemical Engineers*, 6(4), 595-601.

Tiller, F.M., Haynes, S.H., and Lu, W. (1972). **The Role of Porosity in Filtration VII: Effect of Side-Wall Friction in Compression-Permeability Cells**, *Journal of the American Institute of Chemical Engineers*, 18(1), 13-20.

Tiller, F.M., and Huang, C.J. (1961). **Filtration Equipment : Theory**, *Industrial and Engineering Chemistry*, 53(7), 529-537.

× Tiller, F.M., and Leu, W.F. (1980). **Basic Data Fitting in Filtration**, *Journal of The Chinese Institute of Chemical Engineers*, 11, 61-70.

Tiller, F.M., and Lu, W. (1972). **The Role of Porosity in Filtration VIII: Cake Nonuniformity in Compression-Permeability Cells**, *Journal of the American Institute of Chemical Engineers*, 18(3), 569-572.

Tiller, F.M., and Shirato, M. (1964). **The Role of Porosity in Filtration VI: New Definition of Filtration Resistance**, *Journal of the American Institute of Chemical Engineers*, 10(1), 61-67.

Tiller, F.M., and Yeh, C.S. (1985). **The Role of Porosity in Filtration Part X: Deposition of Compressible Cakes on External Radial Surfaces**, *Journal of the American Institute of Chemical Engineers*, 31(8), 1241-1248.

Tiller, F.M., Yeh, C.S., and Leu, W.F. (1987). **Compressibility of Particulate Structures in Relation to Thickening, Filtration and Expression - A Review**, *Separation Science and Technology*, 22(2-3), 1037-1063.

Tosun, I., and Sahioglu, S. (1987). **On the Constancy of Average Porosity in Filtration**, *The Chemical Engineering Journal*, 34, 99-106.

Tosun, I., and Willis, M. S. (1982). **On the Validity of the "Power Law" Approximation in Filtration Theory**, *Chemical Engineering Science*, 37(9), 1421-1422.

Tosun, I., and Willis, M.S. (1983). **Drag Stress - Pressure Drop Relationship in Filtration**, *Chemical Engineering Science*, 38(3), 485-487.

Tosun, I., and Willis, M.S. (1985). **Energy Efficiency in Cake Filtration**, *Filtration and Separation*, (March/April), 126-127.

Tosun, I., and Willis, M.S. (1989). **Making the Case for Multiphase Filtration Theory**, *Filtration and Separation*, (July/August), 295-299.

Tosun, I., Yetis, U., Willis, M.S., and Chase, G.G. (1993). **Specific Cake Resistance: Myth or Reality**, *Water Science and Technology*, 28(1), 91-101.

Ullman's Encyclopaedia of Industrial Chemistry, (1996), 5th Edition, VCH, Weinheim.

Wakeman, R.J. (1981). **The Formation and Properties of Apparently Incompressible Filter Cakes under Vacuum on Downward Facing Surfaces**, *Transactions. Institution of Chemical Engineers*, 59, 260-270.

Willis, M.S. (1983). **A Multiphase Theory of Filtration**, *Progress in Filtration and Separation 3*, R.J. Wakeman, ed., Elsevier, Amsterdam.

Willis, M.S., Collins, R.M., and Bridges, W.G. (1983). **Complete Analysis of Non-Parabolic Filtration Behaviour**, *Chem Eng Res Des*, 61(March), 96-109.

Willis, M.S., Shen, M., and Gray, K.J. (1974). **Investigation of the Fundamental Assumptions Relating Compression-Permeability Data with Filtrations**, *The Canadian Journal of Chemical Engineering*, 52, 331-337.

× Willis, M.S., and Tosun, I. (1980). **A Rigorous Cake Filtration Theory**, *Chemical Engineering Science*, 35, 2427-2438.

Willis, M.S., Tosun, I., Choo, W., Chase, G.G., and Desai, F. (1989). **Dispersed Multiphase Theory and its Application to Filtration**, *Advances in Porous Media*, M.Y. Copracioglu, ed., Elsevier, Amsterdam, 179-293.

- ♣ Willis, M.S., Tosun, I., and Collins, R.M. (1985). **Filtration Mechanisms**, *Chem Eng Res Des*, 63(May), 175-182.
- Wu, Y. (1994). **An Analysis of Constant-Pressure Filtration**, *Chemical Engineering Science*, 49(6), 831-836.
- Yeh, S.H. (1985). **Cake Deliquoring and Radial Filtration**, PhD, Department of Chemical Engineering, University of Houston, Houston.

Appendix A

Physical Properties of Solid-Liquid System

The laboratory-scale experiments were conducted in a controlled environment where the ambient temperature remained at 22 °C. The ambient temperature for the full-scale filtration experiments was 27 °C. Where applicable, the physical properties of the filtrate are assumed to be adequately approximated by that of pure water, since the exact dissolved content of the filtrate was unknown but found to be negligible.

A.1 SOLIDS DENSITY

Density of water at 25 °C : 997.045 kg/m³ (Perry's, 1984)

TABLE A.1 : Results of Experiments to determine the Solids Density

	Bottle 1	Bottle 2	Bottle 3	Bottle 4	Bottle 5
Calibrated Bottle Volume (m ³)	4.99562E-05	4.99321E-05	4.99523E-05	4.99479E-05	4.99542E-05
Bottle Mass (g)	36.4127	36.8759	36.2207	37.4066	34.5426
Bottle + Solids Mass (g)	41.7573	45.2392	42.9016	44.2149	41.5177
Bottle + Solids + Water Mass (g)	89.2399	91.4331	89.8535	91.0334	88.377
Solids Mass (g)	5.3446	8.3633	6.6809	6.8083	6.9751
Water Mass (g)	47.4826	46.1939	46.9519	46.8185	46.8593
Water Volume (m ³)	4.76233E-05	4.63308E-05	4.70911E-05	4.69573E-05	4.69982E-05
Solids Volume (m ³)	2.33287E-06	3.62129E-06	2.86125E-06	2.99064E-06	2.95602E-06
Solids Density (kg/m ³)	2291.0	2309.5	2335.0	2276.5	2359.6

Average Solids Density : 2314.3 kg/m³

A.2 LIQUID DENSITY

Density of water at 22 °C : 997.770 kg/m³ (Perry's, 1984)

Density of water at 27 °C : 996.513 kg/m³ (Perry's, 1984)

A.3 LIQUID VISCOSITY

Atkins (1991), gives the following expression for the viscosity of water over its liquid range as a function of temperature:

$$\mu = \mu_{20} 10^{-[(1.37023(\varphi-20)+0.000836(\varphi-20)^2)/(\varphi+109)]} \quad (\text{A.1})$$

where φ = temperature, (°C)

μ_{20} = viscosity of water at 20 °C, (Pa.s)

Equation A.1 is accurate to less than 1 percent over the entire liquid range.

Ullman's Encyclopaedia of Industrial Chemistry (1996), gives the viscosity of water at 20 °C as:

$$\mu_{20} = 1.002 \times 10^{-3} \text{ Pa.s}$$

From Equation A.1 the following viscosities are obtained:

$$\mu_{22} = 9.548 \times 10^{-4} \text{ Pa.s}$$

$$\mu_{27} = 8.512 \times 10^{-4} \text{ Pa.s}$$

Appendix B

Results of Compression-Permeability Cell Tests

B.1 RESULT OF C-P CELL TEST B.1

Date : 4/2/97

Head of filtrate : 3.308 m

Diameter of C-P cell : 155 mm

Mass wet cake : 121.47 g

Mass dry cake : 55.67 g

Calculated final cake thickness : 4.77 mm

Calculated final porosity : 0.7327

The C-P cell was assembled and compression of the cake at 50 kPa begun at 22:00 on the 3/2/97.

TABLE B.1 : Results of C-P Cell Test B.1

Time of Reading	Applied Pressure (kPa)	Transmitted Pressure (kPa)	Top Dial Gauge (mm)	Bottom Dial Gauge (mm)	Permeate Volume (ml)	Time (s)	Cake Thickness (mm)	Porosity (-)	Permeability (m ²)
8:11	50	35	15.050	8.540	4	162	11.150	0.8857	4.294E-16
9:36	100	78	11.705	8.420	3	277	7.925	0.8391	1.339E-16
11:11	150	131	10.435	8.300	2	288	6.775	0.8118	7.338E-17
12:26	200	180	9.775	8.205	1	182	6.210	0.7947	5.322E-17
13:32	250	233	9.210	8.095	1	221	5.755	0.7785	4.062E-17
14:52	300	285	8.750	7.960	1	265	5.430	0.7652	3.196E-17
16:26	360	347	8.268	7.788	2	615	5.120	0.7510	2.597E-17
17:32	405	397	7.945	7.648	3	327	4.937	0.7418	2.355E-17
18:25	460	450	7.633	7.503	1	345	4.770	0.7327	2.157E-17

Results of the wall friction analysis for Test B.1 given by the computer programme: CPCELL

$$k_{of} = 0.38042$$

$$c = 39447 \text{ Pa}$$

$$\sigma = 3.794$$

TABLE B.2 : Results of Wall Friction Analysis for C-P Cell Test B.1

p_A (Pa)	p_T (Pa)	p_T/p_A (-)	L/D (-)	$(p_T)_{calc}$ (Pa)	$(p_s)_{calc}$ (Pa)	$(p_s)_{final}$ (Pa)
50000	35000	0.7000	0.07193	34073	41891	41891
100000	78000	0.7800	0.05113	84674	92283	92283
150000	131000	0.8733	0.04371	133689	141754	141754
200000	180000	0.9000	0.04006	182055	190937	190937
250000	233000	0.9320	0.03713	230591	240204	240204
300000	285000	0.9500	0.03503	279067	289440	292500
360000	347000	0.9639	0.03303	337295	348552	353500
405000	397000	0.9802	0.03185	380961	392884	401000
460000	450000	0.9783	0.03077	434243	447021	455000

B.2 RESULT OF C-P CELL TEST B.2

Date : 6/2/97

Head of filtrate : 3.308 m

Diameter of C-P cell : 155 mm

Mass wet cake : 122.2 g

Mass dry cake : 55.29 g

Calculated final cake thickness : 4.82 mm

Calculated final porosity : 0.7373

The C-P cell was assembled and compression of the cake at 50 kPa begun at 24:00 on the 5/2/97.

TABLE B.3 : Result of C-P Cell Test B.2

Time of Reading	Applied Pressure (kPa)	Transmitted Pressure (kPa)	Top Dial Gauge (mm)	Bottom Dial Gauge (mm)	Permeate Volume (ml)	Time (s)	Cake Thickness (mm)	Porosity (-)	Permeability (m^2)
10:52	50	35	15.935	5.180	4	157	10.823	0.8830	4.302E-16
12:08	100	78	12.625	5.130	3	266	7.565	0.8326	1.331E-16
13:49	150	126	11.410	5.050	2	281	6.430	0.8031	7.139E-17
14:48	200	174	10.750	4.950	1	174	5.870	0.7843	5.262E-17
16:09	250	228	10.180	4.840	1	218	5.410	0.7660	3.871E-17
17:33	300	280	9.765	4.725	1	273	5.110	0.7522	2.920E-17
20:25	350	337	9.320	4.570	1	284	4.820	0.7373	2.647E-17

Results of the wall friction analysis for Test B.2 given by the computer programme: CPCELL

$$k_{of} = 0.68734$$

$$c = 27231 \text{ Pa}$$

$$\sigma = 3.641$$

TABLE B.4 : Result of Wall Friction Analysis for C-P Cell Test B.2

p_A (Pa)	p_T (Pa)	p_T/p_A (-)	L/D (-)	$(p_T)_{calc}$ (Pa)	$(p_s)_{calc}$ (Pa)	$(p_s)_{final}$ (Pa)
50000	35000	0.7000	0.06984	34351	41926	41926
100000	78000	0.7800	0.04881	82481	91045	91045
150000	126000	0.8400	0.04148	129579	139596	139596
200000	174000	0.8700	0.03787	176328	187959	187959
250000	228000	0.9120	0.03490	223528	236553	236553
300000	280000	0.9333	0.03297	270604	285080	290000
350000	337000	0.9629	0.03110	318112	333829	343500

Appendix C

Results of Settling Tests

C.1 RESULTS OF SETTLING TESTS TO DETERMINE POROSITY AT LOW SOLIDS COMPRESSIVE PRESSURE

C.1.1 Result of Settling Test C.1

Date of start of test : 14/11/96

Date of end of test : 9/12/96

Initial solids concentration of sludge : 85.99 kg/m³

TABLE C.1 : Result of Porosity Settling Test C.1

Cylinder Material	Cylinder Internal Diameter (mm)	Initial Height (m)	Final Equilibrium Height (m)	Dry Solids Volume per unit Area (m ³ /m ²)	Solids Compressive Pressure (Pa)
glass	63	0.4375	0.389	0.016256	209.87
plastic	62	0.2885	0.264	0.010719	138.40
plastic	89.5	0.2	0.179	0.007431	95.94
plastic	60	0.095	0.088	0.003530	45.57
glass	37	0.052	0.05	0.001932	24.94

C.1.2 Result of Settling Test C.2

Date of start of test : 15/11/96

Date of end of test : 9/12/96

Initial solids concentration of sludge : 61.29 kg/m³

TABLE C.2 : Result of Porosity Settling Test C.2

Cylinder Material	Cylinder Internal Diameter (mm)	Initial Height (m)	Final Equilibrium Height (m)	Dry Solids Volume per unit Area (m ³ /m ²)	Solids Compressive Pressure (Pa)
plastic	80	0.454	0.333	0.012023	155.23
glass	60	0.314	0.237	0.008316	107.36
plastic	89	0.2	0.15	0.005297	68.38
plastic	61.5	0.1095	0.082	0.002900	37.44
glass	73	0.056	0.041	0.001483	19.15

C.1.3 Result of Settling Test C.3

Date of start of test : 20/11/96

Date of end of test : 9/12/96

Initial solids concentration of sludge : 80.5 kg/m³

TABLE C.3 : Result of Porosity Settling Test C.3

Cylinder Material	Cylinder Internal Diameter (mm)	Initial Height (m)	Final Equilibrium Height (m)	Dry Solids Volume per unit Area (m ³ /m ²)	Solids Compressive Pressure (Pa)
perspex	54	0.892	0.82	0.031027	400.58

**C.2 RESULTS OF SETTLING TESTS TO DETERMINE PERMEABILITY
AT LOW SOLIDS COMPRESSIVE PRESSURE**

C.2.1 Result of Settling Test C.4

Date : 10/1/97

Solids concentration of sludge : 79.78 kg/m³

TABLE C.4 : Result of Permeability Settling Test C.4

Time (min)	Interface Displacement (mm)		
	Cylinder 1	Cylinder 2	Cylinder 3
0	0	0	0
296	0.9	1	1.5
408	1.5	1.3	1.75
495	1.8	1.5	2
847	2.5	2.5	3
962	3	3	3.2
Initial Height (mm)	160	234	294
V_0 (m/s)	5.270E-08	5.113E-08	6.043E-08
r^2	0.977	0.996	0.942

C.2.2 Result of Settling Test C.5

Date : 23/1/97

Solids concentration of sludge : 72.14 kg/m³

TABLE C.5 : Result of Permeability Settling Test C.5

Time (min)	Interface Displacement (mm)		
	Cylinder 1	Cylinder 2	Cylinder 3
0	0	0	0
237	1.5	1.25	1
315	1.5	1.25	1.25
610	2.5	2.2	2
1329	4.5	4.2	4.5
1489	5	4.75	5
1646	5.5	5	5.5
Initial Height (mm)	159	209	221
V_0 (m/s)	5.732E-08	5.290E-08	5.616E-08
r^2	0.968	0.982	0.997

C.2.3 Result of Settling Test C.6

Date : 26/1/97

Solids concentration of sludge : 62.1 kg/m³

TABLE C.6 : Result of Permeability Settling Test C.6

Time (min)	Interface Displacement (mm)		
	Cylinder 1	Cylinder 2	Cylinder 3
0	0	0	0
857	4	4.25	4.25
975	4.5	5	5
1157	5.75	6	5.75
Initial Height (mm)	153	205	248
V_0 (m/s)	7.975E-08	8.521E-08	8.362E-08
r^2	0.996	0.999	0.999

C.2.4 Result of Settling Test C.7

Date : 27/1/97

Solids concentration of sludge : 53.1 kg/m³

TABLE C.7 : Result of Permeability Settling Test C.7

Time (min)	Interface Displacement (mm)		
	Cylinder 1	Cylinder 2	Cylinder 3
0	0	0	0
682	13	10	11
782	14	11	12
881	15.5	12	13
995	17	13	14.5
Initial Height (mm)	161	193	293
V_0 (m/s)	2.954E-07	2.282E-07	2.507E-07
r^2	0.993	0.992	0.993

C.2.5 Result of Settling Test C.8

Date : 29/1/97

Solids concentration of sludge : 48.2 kg/m³

TABLE C.8 : Result of Permeability Settling Test C.8

Time (min)	Interface Displacement (mm)		
	Cylinder 1	Cylinder 2	Cylinder 3
0	0	0	0
81	4	5.5	13
136	6	9	18.5
271	11	13	24
Initial Height (mm)	167	198	277
V_0 (m/s)	6.973E-07	8.786E-07	1.704E-06
r^2	0.991	0.929	0.820

C.2.6 Result of Settling Test C.9

Date : 30/1/97

Solids concentration of sludge : 44.1 kg/m³

TABLE C.9 : Result of Permeability Settling Test C.9

Time (min)	Interface Displacement (mm)		
	Cylinder 1	Cylinder 2	Cylinder 3
0	0	0	0
12	1.5	1.5	6
45	5	5.5	21
190	15	16.5	55
257	17	20	64
Initial Height (mm)	150	194	310
V_0 (m/s)	1.192E-06	1.364E-06	4.460E-06
r^2	0.969	0.983	0.962

C.2.7 Result of Settling Test C.10

Date : 4/2/97

Solids concentration of sludge : 88.4 kg/m³

TABLE C.10 : Result of Permeability Settling Test C.10

Time (min)	Interface Displacement (mm)		
	Cylinder 1	Cylinder 2	Cylinder 3
0	0	0	0
300	1	1.5	0.5
1338	3	4	3
Initial Height (mm)	150	234	277
V_0 (m/s)	3.824E-08	5.143E-08	3.691E-08
r^2	0.978	0.958	0.995

C.2.8 Result of Settling Test C.11

Date : 5/2/97

Solids concentration of sludge : 73.9 kg/m³

TABLE C.11 : Result of Permeability Settling Test C.11

Time (min)	Interface Displacement (mm)		
	Cylinder 1	Cylinder 2	Cylinder 3
0	0	0	0
653	3	2.5	2.5
845	3.5	3.5	3.25
991	4	4	4
Initial Height (mm)	160	230	245
V_0 (m/s)	6.973E-08	6.717E-08	6.551E-08
r^2	0.99	0.997	0.998

C.2.9 Result of Settling Test C.12

Date : 6/2/97

Solids concentration of sludge : 60.4 kg/m³

TABLE C.12 : Result of Permeability Settling Test C.12

Time (min)	Interface Displacement (mm)		
	Cylinder 1	Cylinder 1	Cylinder 1
0	0	0	0
300	2	2	3
1388	10	11	13
Initial Height (mm)	169	223	294
V_0 (m/s)	1.197E-07	1.311E-07	1.566E-07
r^2	0.999	0.998	0.999

C.2.10 Combined Results of Settling Tests

TABLE C.13 : Combined Results of Permeability Settling Tests to determine the Settling Regimes of the Slurry

Initial Solids Concentration (kg/m ³)	$(V_0)_{avg}$ (m/s)	ε_{in} (-)	$(V_0)^{1/4.65}$ (m/s) ^{1/4.65}
44.1	2.339E-06	0.9809	0.06152
48.2	1.093E-06	0.9792	0.05224
53.1	2.581E-07	0.9771	0.03830
60.4	1.358E-07	0.9739	0.03336
62.1	8.287E-08	0.9732	0.03000
72.14	5.547E-08	0.9688	0.02752
73.9	6.747E-08	0.9681	0.02870
79.78	5.475E-08	0.9655	0.02744
88.4	4.220E-08	0.9618	0.02594

For the sludge in the high concentration region, where sedimentation occurs due to consolidation, the solids compressive pressure throughout the height of the cylinder at the start of the test can be assumed constant, and can be determined from the initial porosity of the sludge, and the porosity correlation describing the porosity at low solids compressive pressures:

$$(1 - \varepsilon_{in}) = 0.03558 p_s^{0.01915} \quad (C.1)$$

TABLE C.14 : Relationship between Permeability, Initial Slurry Porosity and Solids Compressive Pressure for Slurry in the Consolidation Settling Regime

ε_{in} (-)	K (m ²)	p_s (Pa)
0.9732	2.284E-13	3.964E-07
0.9688	1.316E-13	9.943E-04
0.9681	1.563E-13	3.502E-03
0.9655	1.175E-13	1.909E-01
0.9618	8.170E-14	4.057E+01

Appendix D

Results of Direct Shear Tests

Solids concentration of cake sample : 32.29 % (m/m)

Area of direct shear box : 6 cm²

Horizontal shear rate (day 1-2) : 0.005 mm/min

Horizontal shear rate (day 3-6) : 0.0026 mm/min

D.1 RESULTS OF DIRECT SHEAR TEST D.1

Normal load : 952.5 N

Normal stress : 264583 Pa

TABLE D.1 : Result of Day 1 of Direct Shear Test D.1

Date : 25/11/96 (day 1)		Start time : 12:17
Horizontal Shear Displacement (mm)	Horizontal Shear Force (N)	Time (min)
0	0	0
0.02	0	14
0.052	6.5	22
0.075	33.2	31
0.105	72.1	43
0.163	134.9	59
0.220	188.6	74
0.288	236.5	90
0.355	267.6	105
0.425	291.2	119
0.495	309.8	133
0.565	324.0	148
0.645	338.5	165
0.705	346.6	178
0.787	359.4	194
0.855	365.8	208
0.938	373.9	225

TABLE D.2 : Result of Day 2 of Direct Shear Test D.1

Date : 26/11/96 (day 2)		Start time : 11:20
Horizontal Shear Displacement (mm)	Horizontal Shear Force (N)	Time (min)
0.958	252.4	0
0.980	275.3	4
1.002	298.3	9
1.025	320.6	14.5
1.045	338.5	19
1.068	356.4	24
1.088	370.6	29
1.110	381.7	35
1.130	392.9	39.5
1.158	405.0	45
1.185	412.4	50
1.207	419.9	55
1.230	424.3	59

TABLE D.3 : Result of Day 3 of Direct Shear Test D.1

Date : 27/11/96 (day 3)		Start time : 7:43
Horizontal Shear Displacement (mm)	Horizontal Shear Force (N)	Time (min)
1.253	311.5	0
1.273	333.1	10
1.293	354.0	19.5
1.317	374.3	29.5
1.340	392.9	39
1.365	409.4	50
1.386	422.2	59.5
1.467	449.9	92
1.535	457.7	120
1.612	461.7	149
1.700	464.8	182.5
1.773	468.5	210
1.858	470.5	242
1.930	474.2	269
2.008	477.3	299
2.160	484.4	356
2.325	491.1	417
2.490	496.2	480

TABLE D.4 : Result of Day 4 of Direct Shear Test D.1

Date : 28/11/96 (day 4)		Start time : 8:16
Horizontal Shear Displacement (mm)	Horizontal Shear Force (N)	Time (min)
2.510	382.0	0
2.535	407.7	9.5
2.558	430.3	19.5
2.580	450.3	29.5
2.605	468.5	39.5
2.630	485.0	50
2.655	498.5	60
2.680	508.3	69.5
2.705	514.8	80
2.731	519.8	89
2.900	530.0	154
3.043	527.9	208
3.200	534.3	267
3.465	542.8	369
3.640	551.2	439

TABLE D.5 : Result of Day 5 of Direct Shear Test D.1

Date : 29/11/96 (day 5)		Start time : 8:10
Horizontal Shear Displacement (mm)	Horizontal Shear Force (N)	Time (min)
3.653	439.5	0
3.680	468.5	10.5
3.700	489.8	20
3.725	509.0	29
3.748	527.9	39.5
3.770	543.1	49.5
3.799	557.0	60
3.823	567.1	70
3.850	574.9	80.5
3.957	591.4	123
4.133	590.4	191
4.265	514.4	233.5
4.590	583.0	364
4.750	586.7	428

TABLE D.6 : Result of Day 6 of Direct Shear Test D.1

Date : 2/12/96 (day 6)		Start time : 7:57
Horizontal Shear Displacement (mm)	Horizontal Shear Force (N)	Time (min)
4.770	435.7	0
4.795	465.8	10
4.818	489.1	19.5
4.863	535.7	40
4.882	553.3	49
4.905	571.2	59.5
4.940	595.5	74.5
5.045	637.7	118.5
5.152	646.8	178
5.380	643.4	244.5
5.520	641.1	298
5.680	640.7	361.5
5.825	644.1	415
5.930	646.8	455.5

D.2 RESULTS OF DIRECT SHEAR TEST D.2

Normal load : 573.4 N

Normal stress : 159278 Pa

TABLE D.7 : Result of Day 1 of Direct Shear Test D.2

Date : 25/11/96 (day 1)		Start time : 12:17
Horizontal Shear Displacement (mm)	Horizontal Shear Force (N)	Time (min)
0	0	0
0.030	8.3	15
0.055	23.6	22
0.095	49.3	32
0.150	79.3	44
0.225	106.6	59
0.305	129.0	74
0.385	146.0	91
0.460	157.0	105
0.530	166.9	120
0.608	175.2	134
0.685	184.1	149
0.775	192.8	166
0.843	198.1	179
0.925	203.2	194
0.992	207.4	208
1.080	211.4	225

TABLE D.8 : Result of Day 2 of Direct Shear Test D.2

Date : 26/11/96 (day 2)		Start time : 11:20
Horizontal Shear Displacement (mm)	Horizontal Shear Force (N)	Time (min)
1.085	143.0	0
1.108	155.9	4.5
1.135	169.7	10
1.160	182.2	15
1.185	193.0	20
1.213	203.4	25
1.235	211.0	29
1.265	218.8	35
1.290	223.6	40
1.320	228.3	45.5
1.345	231.4	50.5
1.368	234.3	55
1.392	237.2	60

TABLE D.9 : Result of Day 3 of Direct Shear Test D.2

Date : 27/11/96 (day 3)		Start time : 7:43
Horizontal Shear Displacement (mm)	Horizontal Shear Force (N)	Time (min)
1.400	167.8	0
1.423	181.6	10
1.445	194.5	20
1.470	207.0	30
1.495	217.5	40
1.525	226.9	50
1.555	233.7	60
1.630	248.7	93
1.702	253.1	120
1.778	256.4	149
1.867	257.3	183
1.937	258.9	210.5
2.018	259.5	242
2.090	260.6	269.5
2.170	262.5	299
2.323	262.7	357
2.483	266.7	417.5
2.647	269.5	481

TABLE D.10 : Result of Day 4 of Direct Shear Test D.2

Date : 28/11/96 (day 4)		Start time : 8:16
Horizontal Shear Displacement (mm)	Horizontal Shear Force (N)	Time (min)
2.655	204.5	0
2.680	220.3	10
2.705	234.5	20
2.730	246.8	30
2.755	257.5	40
2.782	265.8	50
2.808	273.1	60
2.835	277.7	70
2.860	281.7	81
2.885	284.6	90
3.055	291.8	154.5
3.210	293.8	208
3.355	296.0	267.5
3.620	301.4	370
3.805	304.4	439.5

TABLE D.11 : Result of Day 5 of Direct Shear Test D.2

Date : 29/11/96 (day 5)		Start time : 8:10
Horizontal Shear Displacement (mm)	Horizontal Shear Force (N)	Time (min)
3.810	235.0	0
3.840	254.2	11
3.865	266.7	20
3.885	279.3	30
3.913	290.3	40
3.940	298.5	50
3.965	306.2	60
3.990	311.4	70.5
4.015	314.9	80
4.130	322.8	124
4.310	325.7	191
4.430	258.1	216
4.763	316.6	364.5
4.930	321.2	428

TABLE D.12 : Result of Day 6 of Direct Shear Test D.2

Date : 2/12/96 (day 6)		Start time : 7:57
Horizontal Shear Displacement (mm)	Horizontal Shear Force (N)	Time (min)
4.940	218.3	0
4.965	240.2	10.5
4.987	257.6	20
5.038	291.9	40.5
5.060	304.2	50
5.087	317.1	60
5.125	332.8	75
5.239	357.6	119
5.393	367.2	178.5
5.563	368.9	245
5.705	369.3	298.5
5.875	371.6	360.5
6.013	371.3	416
6.120	370.4	454

D.3 RESULTS OF DIRECT SHEAR TEST D.3

Normal load : 222 N

Normal stress : 61667 Pa

TABLE D.13 : Result of Day 1 of Direct Shear Test D.3

Date : 25/11/96 (day 1)		Start time : 12:17
Horizontal Shear Displacement (mm)	Horizontal Shear Force (N)	Time (min)
0	2.4	0
0.032	7.2	60
0.067	31.6	75
0.122	51.1	91
0.187	60.8	106
0.262	68.1	120
0.337	60.8	134
0.412	60.8	150
0.467	58.4	160
0.497	58.4	166
0.522	68.1	176
0.559	75.4	179
0.632	85.2	195
0.700	90.0	209
0.778	94.9	225

TABLE D.14 : Result of Day 2 of Direct Shear Test D.3

Date : 26/11/96 (day 2)		Start time : 11:20
Horizontal Shear Displacement (mm)	Horizontal Shear Force (N)	Time (min)
0.782	73.0	0
0.804	87.6	5
0.830	94.9	10
0.852	99.8	15
0.875	104.6	20
0.907	107.1	25
0.927	109.5	30
0.955	111.9	35.5
0.980	111.9	40
1.007	114.4	46
1.035	114.4	51
1.057	116.8	55.5
1.082	119.2	60

TABLE D.15 : Result of Day 3 of Direct Shear Test D.3

Date : 27/11/96 (day 3)		Start time : 7:43
Horizontal Shear Displacement (mm)	Horizontal Shear Force (N)	Time (min)
1.091	90.0	0
1.110	102.2	11
1.132	109.5	20.5
1.157	114.4	30.5
1.182	116.8	40
1.207	119.2	51
1.232	121.7	60.5
1.317	124.1	93
1.387	126.6	121
1.462	129.0	150
1.544	131.4	183
1.614	133.9	210.5
1.694	133.9	243
1.767	133.9	270
1.844	136.3	300
1.992	137.5	357
2.149	137.5	418
2.312	136.3	481

TABLE D.16 : Result of Day 4 of Direct Shear Test D.3

Date : 28/11/96 (day 4)		Start time : 8:16
Horizontal Shear Displacement (mm)	Horizontal Shear Force (N)	Time (min)
2.317	109.5	0
2.342	119.2	10
2.367	126.6	20
2.392	131.4	30
2.415	136.3	40
2.440	136.3	50.5
2.467	138.7	61
2.490	138.7	70.5
2.517	138.7	81.5
2.539	139.9	90.5
2.707	141.2	155
2.852	143.6	209
3.008	143.6	268
3.282	146.0	370
3.472	146.0	440

TABLE D.17 : Result of Day 5 of Direct Shear Test D.3

Date : 29/11/96 (day 5)		Start time : 8:10
Horizontal Shear Displacement (mm)	Horizontal Shear Force (N)	Time (min)
3.480	119.2	0
3.507	129.0	11
3.527	136.3	20.5
3.550	141.2	30
3.577	144.8	40
3.602	147.2	50
3.632	148.5	60.5
3.657	150.9	71
3.685	150.9	81
3.794	150.9	124
3.979	150.9	191.5
4.117	99.8	214
4.439	150.9	365
4.597	154.6	428.5

TABLE D.18 : Result of Day 6 of Direct Shear Test D.3

Date : 2/12/96 (day 6)		Start time : 7:57
Horizontal Shear Displacement (mm)	Horizontal Shear Force (N)	Time (min)
4.602	116.8	0
4.627	131.4	11
4.649	138.7	20
4.697	150.9	41
4.720	153.3	50
4.744	155.8	60
4.781	160.6	75.5
4.894	163.1	119
5.047	164.3	179
5.225	163.1	245.5
5.362	161.9	299
5.527	161.9	363
5.662	161.9	416.5
5.767	160.6	456.5

Appendix E

Results of Planar Filtration Experiments

The feed solids concentration of the sludge was 29.2 kg/m³ for all the planar filtration experiments.

E.1 RESULTS OF PLANAR FILTRATION EXPERIMENTS AT AN APPLIED PRESSURE OF 100 kPa

E.1.1 Experiment E.1.1

Date : 1/2/97

Filtration pressure : 100 kPa

Filtration time : 5 minutes

TABLE E.1 : Result of Planar Filtration Experiment E.1.1

Time (s)	Mass of Filtrate (g)	Filtrate Volume (m ³)
0	0	0
5	50	5.011E-05
10	73	7.316E-05
20	96	9.621E-05
30	115	1.153E-04
40	131	1.313E-04
50	145	1.453E-04
60	158	1.584E-04
70	169	1.694E-04
80	181	1.814E-04
90	191	1.914E-04
120	218	2.185E-04
150	242	2.425E-04
180	262	2.626E-04
210	282	2.826E-04
240	300	3.007E-04
270	316	3.167E-04
300	332	3.327E-04

Mass wet cake : 62.46 g

Measured cake thickness : 3 mm

Mass dry cake : 11.27 g

Calculated cake thickness : 3.40 mm

Average cake dry solids concentration : 0.1804 m/m

E.1.2 Experiment E.1.2

Date : 1/2/97

Filtration pressure : 100 kPa

Filtration time : 10 minutes

TABLE E.2 : Result of Planar Filtration Experiment E.1.2

Time (s)	Mass of Filtrate (g)	Filtrate Volume (m ³)
0	0	0
4	50	5.011E-05
10	74	7.417E-05
20	99	9.922E-05
30	120	1.203E-04
40	135	1.353E-04
50	149	1.493E-04
60	161	1.614E-04
70	173	1.734E-04
80	183	1.834E-04
90	193	1.934E-04
120	219.5	2.200E-04
150	242	2.425E-04
180	262	2.626E-04
210	280	2.806E-04
240	297	2.977E-04
270	313.5	3.142E-04
300	328.5	3.292E-04
330	342.5	3.433E-04
360	356.5	3.573E-04
390	369	3.698E-04
420	381.5	3.824E-04
450	393	3.939E-04
480	404.5	4.054E-04
510	416	4.169E-04
540	426.5	4.275E-04
570	437	4.380E-04
600	446.5	4.475E-04

Mass wet cake : 86.83 g

Measured cake thickness : 5 mm

Mass dry cake : 15.11 g

Calculated cake thickness : 4.75 mm

Average cake dry solids concentration : 0.1740 m/m

E.1.3 Experiment E.1.3

Date : 30/1/97

Filtration pressure : 100 kPa

Filtration time : 15 minutes

TABLE E.3 : Result of Planar Filtration Experiment E.1.3

Time (s)	Mass of Filtrate (g)	Filtrate Volume (m ³)
0	0	0
6	50	5.011E-05
10	68	6.815E-05
20	94.5	9.471E-05
30	112	1.123E-04
50	142	1.423E-04
60	155	1.553E-04
70	166	1.664E-04
80	177	1.774E-04
90	187	1.874E-04
120	213	2.135E-04
150	235.5	2.360E-04
180	255.5	2.561E-04
210	274.5	2.751E-04
240	291.5	2.922E-04
270	307.5	3.082E-04
300	323	3.237E-04
330	337	3.378E-04
360	351	3.518E-04
390	364	3.648E-04
450	389	3.899E-04
480	400	4.009E-04
510	412	4.129E-04
540	423	4.239E-04
570	433	4.340E-04
600	444	4.450E-04
630	454	4.550E-04
660	463.5	4.645E-04
690	473.5	4.746E-04
720	483	4.841E-04
750	492	4.931E-04
780	501	5.021E-04
810	509.5	5.106E-04

TABLE E.3 : Result of Planar Filtration Experiment E.1.3 (continued)

Time (s)	Mass of Filtrate (g)	Filtrate Volume (m ³)
840	518.5	5.197E-04
870	527	5.282E-04
900	535	5.362E-04

Mass wet cake : 103.8 g

Measured cake thickness : 5.5 mm

Mass dry cake : 17.87 g

Calculated cake thickness : 5.68 mm

Average cake dry solids concentration : 0.1722 m/m

E.1.4 Experiment E.1.4

Date : 30/1/97

Filtration pressure : 100 kPa

Filtration time : 20 minutes

TABLE E.4 : Result of Planar Filtration Experiment E.1.4

Time (s)	Mass of Filtrate (g)	Filtrate Volume (m ³)
0	0	0
5	50	5.011E-05
10	69	6.915E-05
20	92	9.221E-05
30	110	1.102E-04
40	126	1.263E-04
50	140	1.403E-04
60	152	1.523E-04
70	163	1.634E-04
80	174	1.744E-04
90	183	1.834E-04
120	209	2.095E-04
150	231	2.315E-04
180	252	2.526E-04
210	270	2.706E-04
240	287	2.876E-04
270	303	3.037E-04
300	318	3.187E-04
330	333	3.337E-04
360	346	3.468E-04
390	359	3.598E-04
420	372	3.728E-04
450	383	3.839E-04
480	395	3.959E-04
510	406.5	4.074E-04
540	417.5	4.184E-04
570	435.5	4.365E-04
600	445.5	4.465E-04
630	455	4.560E-04
660	465	4.660E-04
690	475	4.761E-04
720	484.5	4.856E-04
750	493.5	4.946E-04

TABLE E.4 : Result of Planar Filtration Experiment E.1.4 (continued)

Time (s)	Mass of Filtrate (g)	Filtrate Volume (m ³)
780	502.5	5.036E-04
810	511.5	5.126E-04
840	520	5.212E-04
870	528.5	5.297E-04
900	537	5.382E-04
930	545	5.462E-04
960	552.5	5.537E-04
990	560.5	5.618E-04
1020	568	5.693E-04
1050	575.5	5.768E-04
1080	583	5.843E-04
1110	590.5	5.918E-04
1140	597.5	5.988E-04
1170	605	6.064E-04
1200	612	6.134E-04

Mass wet cake : 115.7 g

Measured cake thickness : 7 mm

Mass dry cake : 20.09 g

Calculated cake thickness : 6.33 mm

Average cake dry solids concentration : 0.1736 m/m

E.1.5 Experiment E.1.5

Date : 29/1/97

Filtration pressure : 100 kPa

Filtration time : 25 minutes

TABLE E.5 : Result of Planar Filtration Experiment E.1.5

Time (s)	Mass of Filtrate (g)	Filtrate Volume (m ³)
0	0	0
5	50	5.011E-05
10	74	7.417E-05
20	100	1.002E-04
30	120	1.203E-04
40	135	1.353E-04
50	149.3	1.496E-04
70	173	1.734E-04
80	183	1.834E-04
90	194	1.944E-04
120	221	2.215E-04
150	245	2.455E-04
180	266	2.666E-04
210	285	2.856E-04
240	303	3.037E-04
270	319	3.197E-04
300	335	3.357E-04
330	349	3.498E-04
360	363	3.638E-04
390	376.5	3.773E-04
420	389	3.899E-04
450	401.5	4.024E-04
480	413.5	4.144E-04
510	425	4.259E-04
540	436	4.370E-04
570	447	4.480E-04
600	457.5	4.585E-04
630	468	4.690E-04
660	478	4.791E-04
690	487.5	4.886E-04
720	497	4.981E-04
750	506.5	5.076E-04
780	516	5.172E-04

TABLE E.5 : Result of Planar Filtration Experiment E.1.5 (continued)

Time (s)	Mass of Filtrate (g)	Filtrate Volume (m ³)
810	525	5.262E-04
840	533.5	5.347E-04
900	551	5.522E-04
930	559.5	5.608E-04
960	567.5	5.688E-04
990	576	5.773E-04
1020	583.5	5.848E-04
1050	592	5.933E-04
1080	607	6.084E-04
1110	615	6.164E-04
1140	622	6.234E-04
1170	630	6.314E-04
1200	638	6.394E-04
1230	645	6.464E-04
1260	652	6.535E-04
1290	660	6.615E-04
1320	666.5	6.680E-04
1350	674	6.755E-04
1380	681	6.825E-04
1410	688	6.895E-04
1440	694.5	6.961E-04
1470	701.5	7.031E-04
1500	708	7.096E-04

Mass wet cake : 129.75 g

Measured cake thickness : 7 mm

Mass dry cake : 22.85 g

Calculated cake thickness : 7.09 mm

Average cake dry solids concentration : 0.1761 m/m

E.1.6 Experiment E.1.6

Date : 29/1/97

Filtration pressure : 100 kPa

Filtration time : 30 minutes

TABLE E.6 : Result of Planar Filtration Experiment E.1.6

Time (s)	Mass of Filtrate (g)	Filtrate Volume (m ³)
0	0	0
3	50	5.011E-05
7	70	7.016E-05
10	80	8.018E-05
20	107	1.072E-04
30	126	1.263E-04
40	142	1.423E-04
50	155	1.553E-04
60	167	1.674E-04
70	179	1.794E-04
80	189	1.894E-04
90	199	1.994E-04
120	225	2.255E-04
150	247	2.476E-04
180	268	2.686E-04
210	287	2.876E-04
240	304	3.047E-04
270	320	3.207E-04
300	334.5	3.352E-04
330	349	3.498E-04
360	362	3.628E-04
390	375	3.758E-04
420	387	3.879E-04
450	399	3.999E-04
480	411	4.119E-04
510	422	4.229E-04
540	434	4.350E-04
570	444	4.450E-04
600	455	4.560E-04
630	465	4.660E-04
660	475	4.761E-04
690	485	4.861E-04
720	494.5	4.956E-04

TABLE E.6 : Result of Planar Filtration Experiment E.1.6 (continued)

Time (s)	Mass of Filtrate (g)	Filtrate Volume (m ³)
780	513.5	5.146E-04
810	522.5	5.237E-04
840	531.5	5.327E-04
870	540	5.412E-04
900	549	5.502E-04
930	557	5.582E-04
960	565.5	5.668E-04
990	574	5.753E-04
1020	581.5	5.828E-04
1050	590	5.913E-04
1080	597	5.983E-04
1110	605	6.064E-04
1140	613	6.144E-04
1170	620	6.214E-04
1200	628	6.294E-04
1230	635	6.364E-04
1260	642.5	6.439E-04
1290	649.5	6.510E-04
1320	656.5	6.580E-04
1350	663	6.645E-04
1380	670	6.715E-04
1410	676.5	6.780E-04
1440	683.5	6.850E-04
1470	690	6.915E-04
1500	696.5	6.981E-04
1530	703	7.046E-04
1560	709	7.106E-04
1590	715.5	7.171E-04
1620	722	7.236E-04
1650	728	7.296E-04
1680	734	7.356E-04
1710	740	7.417E-04
1740	746	7.477E-04
1770	751.5	7.532E-04
1800	760	7.617E-04

Mass wet cake : 129.00 g

Measured cake thickness : 8 mm

Mass dry cake : 21.60 g

Calculated cake thickness : 7.08 mm

Average cake dry solids concentration : 0.1674 m/m

E.2 RESULTS OF PLANAR FILTRATION EXPERIMENTS AT AN APPLIED PRESSURE OF 200 kPa

E.2.1 Experiment E.2.1

Date : 1/2/97

Filtration pressure : 200 kPa

Filtration time : 5 minutes

TABLE E.7 : Result of Planar Filtration Experiment E.2.1

Time (s)	Mass of Filtrate (g)	Filtrate Volume (m ³)
0	0	0
3	50	5.011E-05
10	83	8.319E-05
20	111	1.112E-04
30	131	1.313E-04
40	149	1.493E-04
50	164	1.644E-04
60	178	1.784E-04
70	191	1.914E-04
80	203	2.035E-04
90	214	2.145E-04
120	242	2.425E-04
150	268	2.686E-04
180	291	2.917E-04
210	311	3.117E-04
240	330	3.307E-04
270	348	3.488E-04
300	364.5	3.653E-04

Mass wet cake : 62.75 g

Measured cake thickness : 3.5 mm

Mass dry cake : 12.04 g

Calculated cake thickness : 3.39 mm

Average cake dry solids concentration : 0.1919 m/m

E.2.2 Experiment E.2.2

Date : 1/2/97

Filtration pressure : 200 kPa

Filtration time : 10 minutes

TABLE E.8 : Result of Planar Filtration Experiment E.2.2

Time (s)	Mass of Filtrate (g)	Filtrate Volume (m ³)
0	0	0
4	50	5.011E-05
10	82	8.218E-05
20	111	1.112E-04
30	132	1.323E-04
40	150	1.503E-04
50	164	1.644E-04
60	178	1.784E-04
70	191	1.914E-04
80	203	2.035E-04
90	214	2.145E-04
120	243	2.435E-04
150	268	2.686E-04
180	291	2.917E-04
210	311.5	3.122E-04
240	330	3.307E-04
270	348	3.488E-04
300	363.5	3.643E-04
330	379.5	3.803E-04
360	394	3.949E-04
390	409	4.099E-04
420	423	4.239E-04
450	437	4.380E-04
480	450	4.510E-04
510	463	4.640E-04
540	475	4.761E-04
570	486	4.871E-04
600	498	4.991E-04

Mass wet cake : 79.15 g

Measured cake thickness : 4.5 mm

Mass dry cake : 16.59 g

Calculated cake thickness : 4.23 mm

Average cake dry solids concentration : 0.2096 m/m

E.2.3 Experiment E.2.3

Date : 30/1/97

Filtration pressure : 200 kPa

Filtration time : 15 minutes

TABLE E.9 : Result of Planar Filtration Experiment E.2.3

Time (s)	Mass of Filtrate (g)	Filtrate Volume (m ³)
0	0	0
4	50	5.011E-05
10	82	8.218E-05
20	111	1.112E-04
30	132	1.323E-04
40	150	1.503E-04
50	165	1.654E-04
60	180	1.804E-04
70	192	1.924E-04
80	204	2.045E-04
90	214	2.145E-04
120	243	2.435E-04
150	268	2.686E-04
180	291	2.917E-04
210	311	3.117E-04
240	330	3.307E-04
270	347	3.478E-04
300	364	3.648E-04
330	380	3.808E-04
360	395	3.959E-04
390	409.5	4.104E-04
420	423	4.239E-04
450	436	4.370E-04
480	449	4.500E-04
510	461.5	4.625E-04
540	473.5	4.746E-04
570	485	4.861E-04
600	496	4.971E-04
630	507.5	5.086E-04
660	518.5	5.197E-04
690	529	5.302E-04
720	539.5	5.407E-04

TABLE E.9 : Result of Planar Filtration Experiment E.2.3 (continued)

Time (s)	Mass of Filtrate (g)	Filtrate Volume (m ³)
750	549.5	5.507E-04
780	559.5	5.608E-04
810	569.5	5.708E-04
840	579	5.803E-04
870	588	5.893E-04
900	597.5	5.988E-04

Mass wet cake : 101.87 g

Measured cake thickness : 6 mm

Mass dry cake : 19.25 g

Calculated cake thickness : 5.52 mm

Average cake dry solids concentration : 0.1890 m/m

E.2.4 Experiment E.2.4

Date : 30/1/97

Filtration pressure : 200 kPa

Filtration time : 20 minutes

TABLE E.10 : Result of Planar Filtration Experiment E.2.4

Time (s)	Mass of Filtrate (g)	Filtrate Volume (m ³)
0	0	0
7	50	5.011E-05
20	92	9.221E-05
30	113	1.133E-04
40	130	1.303E-04
50	146	1.463E-04
60	160	1.604E-04
70	173	1.734E-04
80	185	1.854E-04
90	196	1.964E-04
120	225	2.255E-04
150	250	2.506E-04
180	274	2.746E-04
210	294	2.947E-04
240	313	3.137E-04
270	330	3.307E-04
300	347	3.478E-04
330	363	3.638E-04
360	378	3.788E-04
390	392	3.929E-04
420	406	4.069E-04
450	420	4.209E-04
480	432	4.330E-04
510	445	4.460E-04
540	457	4.580E-04
570	468	4.690E-04
600	480	4.811E-04
630	491	4.921E-04
660	502	5.031E-04
690	512.5	5.136E-04
720	523	5.242E-04
750	533	5.342E-04

TABLE E.10 : Result of Planar Filtration Experiment E.2.4 (continued)

Time (s)	Mass of Filtrate (g)	Filtrate Volume (m ³)
780	543	5.442E-04
810	560	5.613E-04
840	570	5.713E-04
870	579.5	5.808E-04
900	589	5.903E-04
930	598	5.993E-04
960	607	6.084E-04
990	616.5	6.179E-04
1020	625.5	6.269E-04
1050	634	6.354E-04
1080	642	6.434E-04
1110	651	6.525E-04
1140	659.5	6.610E-04
1170	667.5	6.690E-04
1200	675.5	6.770E-04

Mass wet cake : 127.40 g

Measured cake thickness : 7 mm

Mass dry cake : 25.54 g

Calculated cake thickness : 6.85 mm

Average cake dry solids concentration : 0.2005 m/m

E.2.5 Experiment E.2.5

Date : 29/1/97

Filtration pressure : 200 kPa

Filtration time : 25 minutes

TABLE E.11 : Result of Planar Filtration Experiment E.2.5

Time (s)	Mass of Filtrate (g)	Filtrate Volume (m ³)
0	0	0
4	50	5.011E-05
10	83	8.319E-05
20	113	1.133E-04
30	134	1.343E-04
40	151	1.513E-04
50	166	1.664E-04
60	180	1.804E-04
70	192	1.924E-04
80	203	2.035E-04
90	214	2.145E-04
120	243	2.435E-04
150	269	2.696E-04
180	292	2.927E-04
210	314	3.147E-04
240	332	3.327E-04
270	350	3.508E-04
300	367	3.678E-04
330	383	3.839E-04
360	398	3.989E-04
390	412.5	4.134E-04
420	426	4.270E-04
450	440	4.410E-04
480	453	4.540E-04
510	465	4.660E-04
540	478	4.791E-04
570	490	4.911E-04
600	501	5.021E-04
630	512	5.131E-04
660	524	5.252E-04
690	534	5.352E-04
720	545	5.462E-04
750	555	5.562E-04

TABLE E.11 : Result of Planar Filtration Experiment E.2.5 (continued)

Time (s)	Mass of Filtrate (g)	Filtrate Volume (m ³)
780	566	5.673E-04
810	576	5.773E-04
840	585	5.863E-04
870	595.5	5.968E-04
900	605	6.064E-04
930	614	6.154E-04
960	623	6.244E-04
990	632	6.334E-04
1020	641	6.424E-04
1050	649.5	6.510E-04
1080	658	6.595E-04
1110	667	6.685E-04
1140	675	6.765E-04
1170	683	6.845E-04
1200	691.5	6.930E-04
1230	699	7.006E-04
1260	707	7.086E-04
1290	715	7.166E-04
1320	723	7.246E-04
1350	730.5	7.321E-04
1380	738	7.396E-04
1410	745	7.467E-04
1440	753	7.547E-04
1470	761	7.627E-04
1500	768	7.697E-04

Mass wet cake : not measured

Measured cake thickness : 6.5 mm

Mass dry cake : 25.03 g

Calculated cake thickness : -

Average cake dry solids concentration : -

E.2.6 Experiment E.2.6

Date : 29/1/97

Filtration pressure : 200 kPa

Filtration time : 30 minutes

TABLE E.12 : Result of Planar Filtration Experiment E.2.6

Time (s)	Mass of Filtrate (g)	Filtrate Volume (m ³)
0	0	0
6	70	7.016E-05
10	90	9.020E-05
20	116	1.163E-04
30	138	1.383E-04
40	156	1.563E-04
50	172	1.724E-04
60	186	1.864E-04
70	198	1.984E-04
80	210	2.105E-04
90	221	2.215E-04
120	250	2.506E-04
150	276	2.766E-04
180	299	2.997E-04
210	320	3.207E-04
240	339	3.398E-04
270	357	3.578E-04
300	373	3.738E-04
330	389	3.899E-04
360	404	4.049E-04
390	418	4.189E-04
420	432	4.330E-04
450	445	4.460E-04
480	458	4.590E-04
510	471	4.721E-04
540	484	4.851E-04
570	496	4.971E-04
600	508	5.091E-04
630	520	5.212E-04
660	531	5.322E-04
690	542	5.432E-04
720	553	5.542E-04
750	564	5.653E-04

TABLE E.12 : Result of Planar Filtration Experiment E.2.6 (continued)

Time (s)	Mass of Filtrate (g)	Filtrate Volume (m ³)
780	574	5.753E-04
810	584	5.853E-04
840	593	5.943E-04
870	604	6.053E-04
900	614	6.154E-04
930	623.5	6.249E-04
960	633	6.344E-04
990	642	6.434E-04
1020	652	6.535E-04
1050	661	6.625E-04
1080	669.5	6.710E-04
1110	678	6.795E-04
1140	686	6.875E-04
1170	695	6.966E-04
1200	703	7.046E-04
1230	711	7.126E-04
1260	719	7.206E-04
1290	727	7.286E-04
1320	735	7.366E-04
1350	743	7.447E-04
1380	750.5	7.522E-04
1410	757.5	7.592E-04
1440	765.5	7.672E-04
1470	773	7.747E-04
1500	780.5	7.822E-04
1530	788.5	7.903E-04
1560	796	7.978E-04
1590	803.5	8.053E-04
1620	811.5	8.133E-04
1650	819	8.208E-04
1680	826.5	8.283E-04
1710	833.5	8.354E-04
1740	840.5	8.424E-04
1770	847.5	8.494E-04
1800	854.2	8.561E-04

Mass wet cake : 134.10 g

Measured cake thickness : 7 mm

Mass dry cake : 26.16 g

Calculated cake thickness : 7.24 mm

Average cake dry solids concentration : 0.1951 m/m

E.3 RESULTS OF PLANAR FILTRATION EXPERIMENTS AT AN APPLIED PRESSURE OF 300 kPa

E.3.1 Experiment E.3.1

Date : 1/2/97

Filtration pressure : 300 kPa

Filtration time : 5 minutes

TABLE E.13 : Result of Planar Filtration Experiment E.3.1

Time (s)	Mass of Filtrate (g)	Filtrate Volume (m ³)
0	0	0
3.5	50	5.011E-05
10	87	8.719E-05
20	116	1.163E-04
30	138	1.383E-04
40	158	1.584E-04
50	175	1.754E-04
60	190	1.904E-04
70	203	2.035E-04
80	216	2.165E-04
90	228	2.285E-04
120	258	2.586E-04
150	285	2.856E-04
180	308	3.087E-04
210	330	3.307E-04
240	350	3.508E-04
270	369	3.698E-04
300	386	3.869E-04

Mass wet cake : 62.82 g

Measured cake thickness : 3.5 mm

Mass dry cake : 12.49 g

Calculated cake thickness : 3.38 mm

Average cake dry solids concentration : 0.1988 m/m

E.3.2 Experiment E.3.2

Date : 1/2/97

Filtration pressure : 300 kPa

Filtration time : 10 minutes

TABLE E.14 : Result of Planar Filtration Experiment E.3.2

Time (s)	Mass of Filtrate (g)	Filtrate Volume (m ³)
0	0	0
4	50	5.011E-05
10	76	7.617E-05
20	106	1.062E-04
30	127	1.273E-04
40	146	1.463E-04
50	163	1.634E-04
60	176	1.764E-04
70	189	1.894E-04
80	201	2.014E-04
90	212	2.125E-04
120	242	2.425E-04
150	268	2.686E-04
180	291.6	2.923E-04
210	312.5	3.132E-04
240	332	3.327E-04
270	351.5	3.523E-04
300	369	3.698E-04
330	385.5	3.864E-04
360	400.5	4.014E-04
390	416	4.169E-04
420	430	4.310E-04
450	444	4.450E-04
480	457.5	4.585E-04
510	470.5	4.716E-04
540	482	4.831E-04
570	495	4.961E-04
600	506	5.071E-04

Mass wet cake : 84.05 g

Measured cake thickness : 5 mm

Mass dry cake : 17.13 g

Calculated cake thickness : 4.51 mm

Average cake dry solids concentration : 0.2038 m/m

E.3.3 Experiment E.3.3

Date : 30/1/97

Filtration pressure : 300 kPa

Filtration time : 15 minutes

TABLE E.15 : Result of Planar Filtration Experiment E.3.3

Time (s)	Mass of Filtrate (g)	Filtrate Volume (m ³)
0	0	0
3	50	5.011E-05
10	89	8.920E-05
20	120	1.203E-04
30	143	1.433E-04
40	162	1.624E-04
50	179	1.794E-04
60	193	1.934E-04
70	206	2.065E-04
80	218	2.185E-04
90	229	2.295E-04
120	260	2.606E-04
150	287	2.876E-04
180	311	3.117E-04
210	333	3.337E-04
240	353	3.538E-04
270	372	3.728E-04
300	391	3.919E-04
330	407	4.079E-04
360	424	4.249E-04
390	439	4.400E-04
420	454	4.550E-04
450	468	4.690E-04
480	482	4.831E-04
510	495	4.961E-04
540	508	5.091E-04
570	520	5.212E-04
600	532	5.332E-04
630	544	5.452E-04
660	555	5.562E-04
690	567	5.683E-04
720	578	5.793E-04
750	589	5.903E-04

TABLE E.15 : Result of Planar Filtration Experiment E.3.3 (continued)

Time (s)	Mass of Filtrate (g)	Filtrate Volume (m ³)
780	599.5	6.008E-04
810	609.5	6.109E-04
840	620	6.214E-04
870	629.5	6.309E-04
900	639.5	6.409E-04

Mass wet cake : 101.76 g

Measured cake thickness : 6 mm

Mass dry cake : 20.35 g

Calculated cake thickness : 5.47 mm

Average cake dry solids concentration : 0.2000 m/m

E.3.4 Experiment E.3.4

Date : 30/1/97

Filtration pressure : 300 kPa

Filtration time : 20 minutes

TABLE E.16 : Result of Planar Filtration Experiment E.3.4

Time (s)	Mass of Filtrate (g)	Filtrate Volume (m ³)
0	0	0
4	50	5.011E-05
10	87	8.719E-05
20	117	1.173E-04
30	140	1.403E-04
40	159	1.594E-04
50	174	1.744E-04
60	189	1.894E-04
70	202	2.025E-04
80	214	2.145E-04
90	226	2.265E-04
120	256	2.566E-04
150	283	2.836E-04
180	306	3.067E-04
210	328	3.287E-04
240	348	3.488E-04
270	367	3.678E-04
300	384	3.849E-04
330	401	4.019E-04
360	416	4.169E-04
390	431	4.320E-04
420	446	4.470E-04
450	460	4.610E-04
480	474	4.751E-04
510	487	4.881E-04
540	500	5.011E-04
570	512	5.131E-04
600	524	5.252E-04
630	536	5.372E-04
660	547.5	5.487E-04
690	559	5.602E-04
720	570	5.713E-04
750	580	5.813E-04

TABLE E.16 : Result of Planar Filtration Experiment E.3.4 (continued)

Time (s)	Mass of Filtrate (g)	Filtrate Volume (m ³)
780	591.5	5.928E-04
810	601.5	6.028E-04
840	612	6.134E-04
870	622	6.234E-04
900	632	6.334E-04
930	641	6.424E-04
960	651	6.525E-04
990	660	6.615E-04
1020	671	6.725E-04
1050	680	6.815E-04
1080	689	6.905E-04
1110	707	7.086E-04
1140	716.3	7.179E-04
1170	725	7.266E-04
1200	733	7.346E-04

Mass wet cake : 121.14 g

Measured cake thickness : 6 mm

Mass dry cake : 23.65 g

Calculated cake thickness : 6.54 mm

Average cake dry solids concentration : 0.1952 m/m

E.3.5 Experiment E.3.5

Date : 29/1/97

Filtration pressure : 300 kPa

Filtration time : 25 minutes

TABLE E.17 : Result of Planar Filtration Experiment E.3.5

Time (s)	Mass of Filtrate (g)	Filtrate Volume (m ³)
0	0	0
4	50	5.011E-05
10	85	8.519E-05
20	116	1.163E-04
30	139	1.393E-04
40	158	1.584E-04
50	174	1.744E-04
60	189	1.894E-04
70	203	2.035E-04
80	214	2.145E-04
90	226	2.265E-04
120	257	2.576E-04
150	283	2.836E-04
180	307	3.077E-04
210	329	3.297E-04
240	348	3.488E-04
270	367	3.678E-04
300	385	3.859E-04
330	401	4.019E-04
360	418	4.189E-04
390	434	4.350E-04
420	449	4.500E-04
450	463	4.640E-04
480	477	4.781E-04
510	490	4.911E-04
540	503	5.041E-04
570	516	5.172E-04
600	528	5.292E-04
630	540	5.412E-04
660	551	5.522E-04
690	563	5.643E-04
720	574	5.753E-04

TABLE E.17 : Result of Planar Filtration Experiment E.3.5 (continued)

Time (s)	Mass of Filtrate (g)	Filtrate Volume (m ³)
750	585	5.863E-04
780	596	5.973E-04
810	606.5	6.079E-04
840	616.5	6.179E-04
870	627	6.284E-04
900	636	6.374E-04
930	646.5	6.479E-04
960	656.5	6.580E-04
990	666	6.675E-04
1020	675.5	6.770E-04
1050	685	6.865E-04
1080	694	6.956E-04
1110	703	7.046E-04
1140	711.5	7.131E-04
1170	720.5	7.221E-04
1200	729.5	7.311E-04
1230	738	7.396E-04
1260	746	7.477E-04
1290	754.5	7.562E-04
1320	762.5	7.642E-04
1350	771	7.727E-04
1380	778	7.797E-04
1410	786.5	7.883E-04
1440	794.5	7.963E-04
1470	802	8.038E-04
1500	809	8.108E-04

Mass wet cake : 132.75 g

Measured cake thickness : 6.5 mm

Mass dry cake : 25.99 g

Calculated cake thickness : 7.16 mm

Average cake dry solids concentration : 0.1958 m/m

E.3.6 Experiment E.3.6

Date : 28/1/97

Filtration pressure : 300 kPa

Filtration time : 30 minutes

TABLE E.18 : Result of Planar Filtration Experiment E.3.6

Time (s)	Mass of Filtrate (g)	Filtrate Volume (m ³)
0	0	0
12	100	1.002E-04
20	127	1.273E-04
30	153	1.533E-04
40	173	1.734E-04
50	190	1.904E-04
60	205	2.055E-04
70	219	2.195E-04
80	232	2.325E-04
90	245	2.455E-04
120	277	2.776E-04
150	306	3.067E-04
180	331	3.317E-04
210	355	3.558E-04
240	373	3.738E-04
270	397	3.979E-04
300	415	4.159E-04
330	433	4.340E-04
360	450	4.510E-04
390	466	4.670E-04
420	482	4.831E-04
450	497	4.981E-04
480	511	5.121E-04
510	525	5.262E-04
540	539.5	5.407E-04
570	553	5.542E-04
600	565.8	5.671E-04
630	578.3	5.796E-04
660	590.5	5.918E-04
690	602.8	6.041E-04
720	614.4	6.158E-04
750	626	6.274E-04

TABLE E.18 : Result of Planar Filtration Experiment E.3.6 (continued)

Time (s)	Mass of Filtrate (g)	Filtrate Volume (m ³)
780	637.5	6.389E-04
810	648	6.494E-04
840	659.4	6.609E-04
870	670	6.715E-04
900	680.5	6.820E-04
930	690.8	6.923E-04
960	701.1	7.027E-04
990	711.3	7.129E-04
1020	721.5	7.231E-04
1050	731	7.326E-04
1080	741.5	7.432E-04
1110	750.5	7.522E-04
1140	760	7.617E-04
1170	768.8	7.705E-04
1200	778.2	7.799E-04
1230	787.2	7.890E-04
1260	796	7.978E-04
1290	805	8.068E-04
1320	813.3	8.151E-04
1350	822	8.238E-04
1380	830.3	8.322E-04
1410	838.5	8.404E-04
1440	846.6	8.485E-04
1470	854.8	8.567E-04
1500	862.6	8.645E-04
1530	870.4	8.723E-04
1560	878.4	8.804E-04
1590	886.2	8.882E-04
1620	893.7	8.957E-04
1650	901.2	9.032E-04
1680	908.5	9.105E-04
1710	916.1	9.181E-04
1740	923.5	9.256E-04
1770	931	9.331E-04
1800	938.7	9.408E-04

Mass wet cake : 143.40 g

Measured cake thickness : 8 mm

Mass dry cake : 28.49 g

Calculated cake thickness : 7.72 mm

Average cake dry solids concentration : 0.1987 m/m

E.4 RESULTS OF PLANAR FILTRATION EXPERIMENTS AT AN APPLIED PRESSURE OF 400 kPa

E.4.1 Experiment E.4.1

Date : 1/2/97

Filtration pressure : 400 kPa

Filtration time : 5 minutes

TABLE E.19 : Result of Planar Filtration Experiment E.4.1

Time (s)	Mass of Filtrate (g)	Filtrate Volume (m ³)
0	0	0
3	50	5.011E-05
10	88	8.820E-05
20	121	1.213E-04
30	145	1.453E-04
40	165	1.654E-04
50	183	1.834E-04
60	197	1.974E-04
70	211	2.115E-04
80	225	2.255E-04
90	237	2.375E-04
120	270	2.706E-04
150	298	2.987E-04
180	323	3.237E-04
210	346	3.468E-04
240	368	3.688E-04
270	388	3.889E-04
300	406	4.069E-04

Mass wet cake : 63.60 g

Measured cake thickness : 3 mm

Mass dry cake : 13.23 g

Calculated cake thickness : 3.40 mm

Average cake dry solids concentration : 0.2080 m/m

E.4.2 Experiment E.4.2

Date : 31/1/97

Filtration pressure : 400 kPa

Filtration time : 10 minutes

TABLE E.20 : Result of Planar Filtration Experiment E.4.2

Time (s)	Mass of Filtrate (g)	Filtrate Volume (m ³)
0	0	0
10	75	1.002E-05
20	108	2.004E-05
30	129	3.007E-05
40	149	4.009E-05
50	166	5.011E-05
60	180	6.013E-05
70	194	7.016E-05
80	206	8.018E-05
90	217	9.020E-05
120	248	1.203E-04
150	276	1.503E-04
180	300.5	1.804E-04
210	322.5	2.105E-04
240	343	2.405E-04
270	362	2.706E-04
300	379.5	3.007E-04
330	396	3.307E-04
360	412.5	3.608E-04
390	428	3.909E-04
420	442.5	4.209E-04
450	457	4.510E-04
480	470.5	4.811E-04
510	483.5	5.111E-04
540	497	5.412E-04
570	509	5.713E-04
600	521	6.013E-04

Mass wet cake : 83.99 g

Measured cake thickness : 4.5 mm

Mass dry cake : 17.52 g

Calculated cake thickness : 4.49 mm

Average cake dry solids concentration : 0.2086 m/m

E.4.3 Experiment E.4.3

Date : 30/1/97

Filtration pressure : 400 kPa

Filtration time : 15 minutes

TABLE E.21 : Result of Planar Filtration Experiment E.4.3

Time (s)	Mass of Filtrate (g)	Filtrate Volume (m ³)
0	0	0
4	50	5.011E-05
10	80	8.018E-05
20	113	1.133E-04
30	138	1.383E-04
40	158	1.584E-04
50	175	1.754E-04
60	191	1.914E-04
70	204	2.045E-04
80	217	2.175E-04
90	229	2.295E-04
120	260	2.606E-04
150	288	2.886E-04
180	312	3.127E-04
210	335	3.357E-04
240	355	3.558E-04
270	375	3.758E-04
300	395	3.959E-04
330	412	4.129E-04
360	428	4.290E-04
390	444	4.450E-04
420	460	4.610E-04
450	475	4.761E-04
480	490	4.911E-04
510	503	5.041E-04
540	516.5	5.177E-04
570	529	5.302E-04
600	542	5.432E-04
630	554	5.552E-04
660	566	5.673E-04
690	577.5	5.788E-04
720	589	5.903E-04
750	600.5	6.018E-04

TABLE E.21 : Result of Planar Filtration Experiment E.4.3 (continued)

Time (s)	Mass of Filtrate (g)	Filtrate Volume (m ³)
780	611.5	6.129E-04
810	622	6.234E-04
840	633	6.344E-04
870	643	6.444E-04
900	653.5	6.550E-04

Mass wet cake : 103.78 g

Measured cake thickness : 7 mm

Mass dry cake : 21.26 g

Calculated cake thickness : 5.56 mm

Average cake dry solids concentration : 0.2049 m/m

E.4.4 Experiment E.4.4

Date : 30/1/97

Filtration pressure : 400 kPa

Filtration time : 20 minutes

TABLE E.22 : Result of Planar Filtration Experiment E.4.4

Time (s)	Mass of Filtrate (g)	Filtrate Volume (m ³)
0	0	0
4	50	5.011E-05
10	83	8.319E-05
20	118	1.183E-04
30	142	1.423E-04
40	162	1.624E-04
50	178	1.784E-04
60	194	1.944E-04
70	207	2.075E-04
80	220	2.205E-04
90	232	2.325E-04
120	264	2.646E-04
150	292	2.927E-04
210	340	3.408E-04
240	360	3.608E-04
270	380	3.808E-04
300	399	3.999E-04
330	417	4.179E-04
360	434	4.350E-04
390	450	4.510E-04
420	465	4.660E-04
450	480	4.811E-04
480	494	4.951E-04
510	507	5.081E-04
540	521	5.222E-04
570	534	5.352E-04
600	546	5.472E-04
630	558	5.592E-04
660	571	5.723E-04
690	582.7	5.840E-04
720	594.5	5.958E-04
750	606	6.074E-04
780	617	6.184E-04

TABLE E.22 : Result of Planar Filtration Experiment E.4.4 (continued)

Time (s)	Mass of Filtrate (g)	Filtrate Volume (m ³)
810	627	6.284E-04
840	638.5	6.399E-04
870	649	6.505E-04
900	659	6.605E-04
930	669	6.705E-04
960	679	6.805E-04
990	688.5	6.900E-04
1020	698	6.996E-04
1050	707.5	7.091E-04
1080	717	7.186E-04
1110	725.5	7.271E-04
1140	735	7.366E-04
1170	744	7.457E-04
1200	752	7.537E-04

Mass wet cake : 118.05 g

Measured cake thickness : 6.5 mm

Mass dry cake : 24.06 g

Calculated cake thickness : 6.33 mm

Average cake dry solids concentration : 0.2038 m/m

E.4.5 Experiment E.4.5

Date : 29/1/97

Filtration pressure : 400 kPa

Filtration time : 25 minutes

TABLE E.23 : Result of Planar Filtration Experiment E.4.5

Time (s)	Mass of Filtrate (g)	Filtrate Volume (m ³)
0	0	0
8	100	1.002E-04
15	122	1.223E-04
20	134	1.343E-04
30	155	1.553E-04
40	172	1.724E-04
50	187	1.874E-04
60	201	2.014E-04
70	215	2.155E-04
80	227	2.275E-04
90	238	2.385E-04
120	269	2.696E-04
150	296	2.967E-04
180	320	3.207E-04
210	342	3.428E-04
240	362	3.628E-04
270	380	3.808E-04
300	399	3.999E-04
330	416	4.169E-04
360	432	4.330E-04
390	447	4.480E-04
420	463	4.640E-04
450	477	4.781E-04
480	490	4.911E-04
510	504	5.051E-04
540	517	5.182E-04
570	530	5.312E-04
600	542	5.432E-04
630	554	5.552E-04
660	566	5.673E-04
690	578	5.793E-04
720	589	5.903E-04
750	600	6.013E-04

TABLE E.23 : Result of Planar Filtration Experiment E.4.5 (continued)

Time (s)	Mass of Filtrate (g)	Filtrate Volume (m ³)
780	611	6.124E-04
810	622	6.234E-04
840	632	6.334E-04
870	642.5	6.439E-04
900	653	6.545E-04
930	662	6.635E-04
960	672	6.735E-04
990	682	6.835E-04
1020	692	6.935E-04
1050	701	7.026E-04
1080	710	7.116E-04
1110	719.5	7.211E-04
1140	728.5	7.301E-04
1170	737.5	7.391E-04
1200	746	7.477E-04
1230	755	7.567E-04
1260	763.5	7.652E-04
1290	772	7.737E-04
1320	780	7.817E-04
1350	788.5	7.903E-04
1380	797	7.988E-04
1410	805	8.068E-04
1440	813	8.148E-04
1470	821	8.228E-04
1500	828	8.299E-04

Mass wet cake : 129.38 g

Measured cake thickness : 7 mm

Mass dry cake : 26.45 g

Calculated cake thickness : 6.94 mm

Average cake dry solids concentration : 0.2044 m/m

E.4.6 Experiment E.4.6

Date : 28/1/97

Filtration pressure : 400 kPa

Filtration time : 30 minutes

TABLE E.24 : Result of Planar Filtration Experiment E.4.6

Time (s)	Mass of Filtrate (g)	Filtrate Volume (m ³)
0	0	0
9	100	1.002E-04
25	150	1.503E-04
30	163	1.634E-04
50	199	1.994E-04
60	214	2.145E-04
70	228	2.285E-04
80	242	2.425E-04
90	254	2.546E-04
110	277	2.776E-04
120	287	2.876E-04
150	315	3.157E-04
180	341	3.418E-04
210	365	3.658E-04
240	386	3.869E-04
270	406	4.069E-04
300	425	4.259E-04
330	444	4.450E-04
360	461	4.620E-04
390	478	4.791E-04
420	494	4.951E-04
450	509	5.101E-04
480	523	5.242E-04
510	538	5.392E-04
540	551.6	5.528E-04
570	565.6	5.669E-04
600	578.7	5.800E-04
630	591.5	5.928E-04
660	603.5	6.048E-04
690	616	6.174E-04
720	627.7	6.291E-04
750	639.8	6.412E-04
780	651.1	6.526E-04

TABLE E.24 : Result of Planar Filtration Experiment E.4.6 (continued)

Time (s)	Mass of Filtrate (g)	Filtrate Volume (m ³)
810	662.2	6.637E-04
840	673	6.745E-04
870	684	6.855E-04
900	694.5	6.961E-04
930	705	7.066E-04
960	715.3	7.169E-04
990	725.3	7.269E-04
1020	735.5	7.371E-04
1050	745.1	7.468E-04
1080	755	7.567E-04
1110	764.4	7.661E-04
1140	773.6	7.753E-04
1170	783.2	7.850E-04
1200	792.6	7.944E-04
1230	801.5	8.033E-04
1260	810.4	8.122E-04
1290	819.4	8.212E-04
1320	828.2	8.301E-04
1350	836.6	8.385E-04
1380	845.2	8.471E-04
1410	853.5	8.554E-04
1440	861.7	8.636E-04
1470	870	8.719E-04
1500	878	8.800E-04
1530	886.1	8.881E-04
1560	894.3	8.963E-04
1590	902	9.040E-04
1620	909.7	9.117E-04
1650	918	9.201E-04
1680	925.4	9.275E-04
1710	932.8	9.349E-04
1740	940.7	9.428E-04
1770	948.1	9.502E-04
1800	955.7	9.578E-04

Mass wet cake : 151.80 g

Measured cake thickness : 8 mm

Mass dry cake : 29.93 g

Calculated cake thickness : 8.12 mm

Average cake dry solids concentration : 0.1972 m/m

Appendix F

Results of Full-Scale Tubular Filter Press Experiments

F.1 TUBULAR FILTER PRESS SPECIFICATIONS

Number of tubes per curtain : 13
 Number of curtains : 2
 Tube internal diameter : 63 mm
 Tube length : 2.338 m
 Filtration area : 12.03 m²
 Tube volume : 0.1895 m³
 Reject manifold volume : 0.04376 m³

F.2 RESULTS OF TESTS AT HIGH FEED SOLIDS CONCENTRATION

F.2.1 Test F.1

Date : 26/9/96
 Time : 15:00
 Approximate operating pressure : 300 kPa
 Limiting filtrate flow rate timer setting : 8.5 s/l
 Feed solids concentration : 28.6 kg/m³
 Tube filling time (visual) : 90 s
 Tube filling time (volume) : 108 s
 Tube filling time (pressure) : 88 s

TABLE F.1 : Result of Tubular Filter Press Experiment F.1

Time (s)	Gauge Pressure (kPa)	Time (s)	Feed Volume (l)	Time (s)	Applied Pressure (kPa)	Time (s)	Filtrate Volume (l)
0	0	0	0	0	36	0	0
11	40	28	48	6	56	22	45
33	40	54	112	28	96	54	101
63	40	80	177	34	126	82	133
88	60	110	238	40	156	110	151
94	80	142	294	49	196	140	167
116	120	170	326	58	226	171	182

TABLE F.1 : Result of Tubular Filter Press Experiment F.1 (continued)

Time (s)	Gauge Pressure (kPa)	Time (s)	Feed Volume (l)	Time (s)	Applied Pressure (kPa)	Time (s)	Filtrate Volume (l)
122	150	198	344	65	256	200	195
128	180	228	360	75	266	228	206
137	220	259	375	97	266	257	218
146	250	288	388	150	266	287	228
153	280	316	399	186	276	316	238
163	290	345	411	2027	276	346	248
185	290	375	421			375	258
238	290	404	431			405	267
274	300	434	441			433	275
2115	300	463	451			462	284
		493	460			493	291
		521	468			522	299
		550	477			551	306
		581	484			581	313
		610	492			610	320
		639	499			639	327
		669	506			668	334
		698	513			698	340
		727	520			727	347
		756	527			759	354
		786	533			786	359
		815	540			815	365
		847	547			845	371
		874	552			874	377
		903	558			903	383
		933	564			933	389
		962	570			962	394
		991	576			991	400
		1021	582			1020	405
		1050	587			1050	411
		1079	593			1079	415
		1108	598			1108	420
		1138	604			1138	425
		1167	608			1167	430
		1196	613			1197	435

TABLE F.1 : Result of Tubular Filter Press Experiment F.1 (continued)

Time (s)	Gauge Pressure (kPa)	Time (s)	Feed Volume (l)	Time (s)	Applied Pressure (kPa)	Time (s)	Filtrate Volume (l)
		962	570			962	394
		991	576			991	400
		1021	582			1020	405
		1050	587			1050	411
		1079	593			1079	415
		1108	598			1108	420
		1138	604			1138	425
		1167	608			1167	430
		1196	613			1197	435
		1226	618			1226	440
		1255	623			1255	445
		1285	628			1285	451
		1314	633			1314	455
		1343	638			1343	460
		1373	644			1372	464
		1402	648			1402	469
		1431	653			1432	473
		1460	657			1463	478
		1490	662			1496	483
		1520	666			1520	486
		1551	671			1548	490
		1584	676			1582	495
		1608	679			1611	499
		1636	683			1637	502
		1670	688			1668	507
		1699	692			1697	511
		1725	695			1727	515
		1756	700			1756	519
		1785	704			1786	523
		1815	708			1816	527
		1844	712			1847	531
		1874	716			1873	535
		1904	720			1906	539
		1935	724			1939	543
		1961	728			1962	546

TABLE F.1 : Result of Tubular Filter Press Experiment F.1 (continued)

Time (s)	Gauge Pressure (kPa)	Time (s)	Feed Volume (ℓ)	Time (s)	Applied Pressure (kPa)	Time (s)	Filtrate Volume (ℓ)
		1994	732			1994	550
		2027	736			2027	554
		2050	739				
		2082	743				
		2115	747				

Filtration time correction : 88 s

Filtrate volume correction : 193 ℓ

Hydrostatic pressure correction : 23530 Pa

Average applied constant pressure : 275.9 kPa

Mass wet cake (bin 2) : 84.58 kg

Mass wet cake (bin 1) : 11.55 kg

Average cake solids concentration (bin 2) : 0.1517 m/m

Average cake solids concentration (bin 2, screened) : 0.2322 m/m

Average cake solids concentration (bin 1) : 0.0378 m/m

Approximate recovered cake dry solids : 11.51 kg

Approximate cake recovery : 67.4 %

Cleaning cycle initiated properly, bulk of cake removed during first two flushes. Due to the amount of cake discharged onto the conveyor, there appeared to be inadequate time for sufficient drainage of the flush fluid, flush fluid reported to the cake collection bin along with the cake. Cake flakes large (approximately 9 - 18 cm²) and approximately 5 mm thick.

F.2.2 Test F.2

Date : 27/9/96

Time : 11:40

Approximate operating pressure : 200 kPa

Limiting filtrate flow rate timer setting : 6 s/ℓ

Feed solids concentration : 26.3 kg/m³

Tube filling time (visual) : 117 s

Tube filling time (volume) : 133 s

Tube filling time (pressure) : 117 s

TABLE F.2 : Result of Tubular Filter Press Experiment F.2

Time (s)	Gauge Pressure (kPa)	Time (s)	Feed Volume (l)	Time (s)	Applied Pressure (kPa)	Time (s)	Filtrate Volume (l)
0	0	0	0	0	27	0	0
18	40	10	11	16	47	11	20
47	40	39	63	23	57	41	68
80	40	69	118	34	77	72	111
107	40	98	170	48	107	99	137
117	50	128	224	60	127	128	155
133	70	158	272	77	157	157	170
140	80	189	315	84	177	187	184
151	100	216	341	195	187	216	197
165	130	245	359	255	192	245	208
177	150	274	374	340	197	276	220
194	180	304	388	729	202	304	230
201	200	333	401	823	207	334	240
312	210	362	412	923	207	362	250
372	215	393	424			393	259
457	220	421	434			423	269
846	225	451	444			453	277
940	230	479	454			483	285
1040	230	510	463			510	292
		540	473			541	300
		570	481			570	307
		600	489			598	313
		627	496			628	320
		658	504			659	328
		687	511			686	334
		715	517			716	340
		745	524			745	348
		776	532			775	354
		803	538			803	361
		833	544			832	367
		862	552			862	373
		892	558			895	380
		920	565			923	386
		949	571				
		979	577				
		1012	584				

TABLE F.2 : Result of Tubular Filter Press Experiment F.2 (continued)

Time (s)	Gauge Pressure (kPa)	Time (s)	Feed Volume (ℓ)	Time (s)	Applied Pressure (kPa)	Time (s)	Filtrate Volume (ℓ)
		1040	590				

Filtration time correction : 117 s

Filtrate volume correction : 204 ℓ

Hydrostatic pressure correction : 23500 Pa

Average applied constant pressure : 196.9 kPa

Mass wet cake (bin 2) : 64.94 kg

Mass wet cake (bin 1) : 17.54 kg

Average cake solids concentration (bin 2) : 0.1244 m/m

Average cake solids concentration (bin 2, screened) : 0.2031 m/m

Average cake solids concentration (bin 1) : 0.0303 m/m

Approximate recovered cake dry solids : 7.18 kg

Approximate cake recovery: 65.4 %

The bulk of the cake was removed during the first two flushes, due to the amount of cake discharged onto the conveyor, there appeared to be inadequate time for sufficient drainage of the flush fluid, flush fluid reported to the cake collection bin along with the cake.

F.2.3 Test F.3

Date : 27/9/96

Time : 13:20

Approximate operating pressure : 200 kPa

Limiting filtrate flow rate timer setting : 8.5 s/ℓ

Feed solids concentration : 27.3 kg/m³

Tube filling time (visual) : 108 s

Tube filling time (volume) : 127 s

Tube filling time (pressure) : 112 s

TABLE F.3 : Result of Tubular Filter Press Experiment F.3

Time (s)	Gauge Pressure (kPa)	Time (s)	Feed Volume (ℓ)	Time (s)	Applied Pressure (kPa)	Time (s)	Filtrate Volume (ℓ)
0	0	0	0	0	36	0	0
19	40	12	13	5	46	21	37

TABLE F.3: Result of Tubular Filter Press Experiment F.3 (continued)

Time (s)	Gauge Pressure (kPa)	Time (s)	Feed Volume (l)	Time (s)	Applied Pressure (kPa)	Time (s)	Filtrate Volume (l)
48	40	42	71	10	56	47	75
82	40	71	128	27	76	76	108
112	60	100	186	32	96	107	127
117	70	133	244	42	116	135	142
122	80	159	282	53	136	165	156
139	100	188	315	58	146	198	170
144	120	219	334	63	156	229	182
154	140	247	349	83	176	253	190
165	160	277	363	214	181	285	202
170	170	310	377	441	186	314	211
175	180	341	389	1064	191	342	220
195	200	365	397	1098	196	370	228
326	205	397	409	1178	186	400	236
553	210	426	418	2119	186	431	245
1176	215	454	427			460	253
1210	220	482	435			488	260
1290	210	512	443			517	267
2231	210	543	452			546	274
		572	460			576	282
		600	467			609	289
		629	474			637	295
		658	481			669	302
		688	489			698	308
		721	496			726	314
		749	502			756	320
		781	509			782	325
		810	515			813	331
		838	521			844	337
		868	527			875	343
		894	532			903	348
		925	538			930	353
		956	544			961	359
		987	550			989	364
		1015	555			1022	370
		1042	560			1051	375
		1073	566			1082	381

TABLE F.3 : Result of Tubular Filter Press Experiment F.3 (continued)

Time (s)	Gauge Pressure (kPa)	Time (s)	Feed Volume (l)	Time (s)	Applied Pressure (kPa)	Time (s)	Filtrate Volume (l)
		1101	571			1105	385
		1134	577			1136	390
		1163	582			1166	394
		1194	588			1194	398
		1217	592			1227	403
		1248	597			1253	407
		1278	601			1286	412
		1306	605			1313	416
		1339	610			1341	420
		1365	614			1375	425
		1398	619			1403	429
		1425	623			1431	433
		1453	627			1457	437
		1487	632			1489	442
		1515	636			1515	446
		1543	640			1551	451
		1569	644			1580	455
		1601	649			1609	459
		1627	653			1638	463
		1663	658			1669	467
		1692	662			1692	470
		1721	666			1729	475
		1750	670			1751	478
		1781	674			1782	482
		1804	677			1819	487
		1841	682			1844	490
		1863	685			1875	494
		1894	689			1898	497
		1931	694			1930	501
		1956	697			1963	505
		1987	701			1989	508
		2010	704			2020	512
		2042	708			2051	516
		2075	712			2075	519
		2101	715			2108	523

TABLE F.3 : Result of Tubular Filter Press Experiment F.3 (continued)

Time (s)	Gauge Pressure (kPa)	Time (s)	Feed Volume (ℓ)	Time (s)	Applied Pressure (kPa)	Time (s)	Filtrate Volume (ℓ)
		2132	719			2119	524
		2163	723				
		2187	726				
		2220	730				
		2231	731				

Filtration time correction : 112 s

Filtrate volume correction : 207 ℓ

Hydrostatic pressure correction : 23510 Pa

Average applied constant pressure : 186.8 kPa

Mass wet cake (bin 2) : 84.43 kg

Mass wet cake (bin 1) : 18.56 kg

Average cake solids concentration (bin 2) : 0.1468 m/m

Average cake solids concentration (bin 2, screened) : 0.2233 m/m

Average cake solids concentration (bin 1) : 0.0306 m/m

Approximate recovered cake dry solids : 11.37 kg

Approximate cake recovery: 73.3 %

No cake recovered by rollers, cake thickness approximately 5 mm.

F.2.4 Test F.4

Date : 30/9/96

Time : 11:17

Approximate operating pressure : 400 kPa

Limiting filtrate flow rate timer setting : 6 s/ℓ

Feed solids concentration : 25.6 kg/m³

Tube filling time (visual) : 115 s

Tube filling time (volume) : 132 s

Tube filling time (pressure) : 124 s

TABLE F.4 : Result of Tubular Filter Press Experiment F.4

Time (s)	Gauge Pressure (kPa)	Time (s)	Feed Volume (l)	Time (s)	Applied Pressure (kPa)	Time (s)	Filtrate Volume (l)
0	0	0	0	0	37	0	0
25	40	19	28	20	47	13	23
53	40	47	81	33	57	42	72
85	40	77	134	55	77	76	125
124	60	108	190	69	97	103	162
144	70	137	241	86	117	131	195
157	80	166	290	93	127	161	224
179	100	200	343	98	137	189	247
193	120	227	380	112	157	218	269
210	140	255	413	127	177	247	287
217	150	285	442	140	197	277	304
222	160	313	465	151	217	308	324
236	180	342	487	166	237	336	341
251	200	371	505	173	247	367	355
264	220	401	522	182	257	396	367
275	240	432	542	195	277	425	379
290	260	460	559	211	297	454	390
297	270	491	573	233	307	483	400
306	280	520	585	261	317	514	411
319	300	549	597	288	327	541	420
335	320	578	608	295	357	573	431
357	330	607	618	317	387	603	441
385	340	638	629	348	377	633	451
412	350	665	638	1988	377	663	460
419	380	697	649			690	468
441	410	727	659			720	476
472	400	757	669			746	483
2112	400	787	678			780	492
		814	686			806	499
		844	694			837	507
		870	701			868	515
		904	710			900	523
		930	717			925	529
		961	725			954	536
		992	733			983	543
		1024	741			1013	550
		1049	747			1044	557
		1078	754			1074	564
		1107	761			1099	569

TABLE F.4 : Result of Tubular Filter Press Experiment F.4 (continued)

Time (s)	Gauge Pressure (kPa)	Time (s)	Feed Volume (l)	Time (s)	Applied Pressure (kPa)	Time (s)	Filtrate Volume (l)
		1137	768			1133	577
		1168	775			1159	583
		1198	782			1190	590
		1223	787			1218	596
		1257	795			1247	602
		1283	801			1276	608
		1314	808			1306	614
		1342	814			1335	620
		1371	820			1366	626
		1400	826			1398	632
		1430	832			1429	638
		1459	838			1456	643
		1490	844			1483	648
		1522	850			1510	653
		1553	856			1542	659
		1580	861			1569	664
		1607	866			1603	670
		1634	871			1631	675
		1666	877			1659	680
		1693	882			1688	685
		1727	888			1721	691
		1755	893			1751	696
		1783	898			1776	700
		1812	903			1805	705
		1845	909			1835	710
		1875	914			1869	716
		1900	918			1893	720
		1929	923			1923	725
		1959	928			1954	730
		1993	934			1988	735
		2017	938				
		2047	943				
		2078	948				
		2112	953				

Filtration time correction : 124 s

Filtrate volume correction : 218 l

Hydrostatic pressure correction : 23490 kPa

Average applied constant pressure : 376.5 kPa

Mass wet cake (bin 2) : 76.59 kg

Mass wet cake (bin 1) : 7.24 kg

Average cake solids concentration (bin 2) : 0.1736 m/m

Average cake solids concentration (bin 2, screened) : 0.256 m/m

Average cake solids concentration (bin 1) : 0.0389 m/m

Approximate recovered cake dry solids : 12.26 kg

Approximate cake recovery: 61.5 %

Rollers were responsible for removing no cake, the bulk of the cake was removed during the second flush.

F.2.5 Test F.5

Date : 30/9/96

Time : 13:55

Approximate operating pressure : 400 kPa

Limiting filtrate flow rate timer setting : 8.5 s/l

Feed solids concentration : 26.9 kg/m³

Tube filling time (visual) : not recorded

Tube filling time (volume) : 113 s

Tube filling time (pressure) : 95 s

TABLE F.5 : Result of Tubular Filter Press Experiment F.5

Time (s)	Gauge Pressure (kPa)	Time (s)	Feed Volume (l)	Time (s)	Applied Pressure (kPa)	Time (s)	Filtrate Volume (l)
0	0	0	0	0	26	0	0
16	40	8	11	9	36	3	6
43	40	37	73	16	46	31	65
74	40	67	137	23	56	65	128
95	50	98	202	38	76	91	169
104	60	126	261	50	86	121	209
111	70	160	324	56	96	150	239
118	80	186	365	60	106	179	263
133	100	216	405	70	126	207	284
145	110	245	435	77	146	236	301
151	120	274	459	84	166	269	318
155	130	302	480	88	176	295	330
165	150	331	497	95	196	325	343
172	170	364	514	102	216	356	356
179	190	390	526	110	236	387	368

TABLE F.5 : Result of Tubular Filter Press Experiment F.5 (continued)

Time (s)	Gauge Pressure (kPa)	Time (s)	Feed Volume (<i>l</i>)	Time (s)	Applied Pressure (kPa)	Time (s)	Filtrate Volume (<i>l</i>)
183	200	420	539	116	256	413	378
190	220	451	552	127	286	444	389
197	240	482	564	133	296	473	399
205	260	508	574	145	316	503	409
211	280	539	585	162	336	531	418
222	310	568	595	172	346	560	427
228	320	598	605	180	356	589	436
240	340	626	614	195	366	620	445
257	360	655	623	212	376	648	453
267	370	684	632	2689	376	678	461
275	380	715	641			708	470
290	390	743	649			738	478
307	400	773	657			774	487
2784	400	803	666			797	493
		833	674			825	500
		869	683			853	507
		892	689			887	515
		920	696			912	521
		948	703			942	528
		982	711			972	535
		1007	717			1005	542
		1037	724			1033	548
		1067	731			1065	555
		1100	738			1093	561
		1128	744			1122	567
		1160	751			1150	573
		1188	757			1180	579
		1217	763			1206	584
		1245	769			1237	590
		1275	775			1268	596
		1301	780			1294	601
		1332	786			1325	607
		1363	792			1357	613
		1389	797			1385	618
		1420	803			1417	624
		1452	809			1445	629
		1480	814			1472	634
		1512	820			1501	639
		1540	825			1529	644

TABLE F.5 : Result of Tubular Filter Press Experiment F.5 (continued)

Time (s)	Gauge Pressure (kPa)	Time (s)	Feed Volume (l)	Time (s)	Applied Pressure (kPa)	Time (s)	Filtrate Volume (l)
		1567	830			1558	649
		1596	835			1593	655
		1624	840			1622	660
		1653	845			1651	665
		1688	851			1681	670
		1717	856			1705	674
		1746	861			1735	679
		1776	866			1766	684
		1800	870			1797	689
		1830	875			1827	694
		1861	880			1853	698
		1892	885			1885	703
		1922	890			1918	708
		1948	894			1945	712
		1980	899			1976	717
		2013	904			2002	721
		2040	908			2035	726
		2071	913			2061	730
		2097	917			2088	734
		2130	922			2121	739
		2156	926			2154	744
		2183	930			2181	748
		2216	935			2207	752
		2249	940			2234	756
		2276	944			2269	761
		2302	948			2300	765
		2329	952			2335	769
		2364	957			2359	773
		2395	961			2387	777
		2430	965			2415	781
		2454	969			2440	785
		2482	973			2475	789
		2510	977			2501	792
		2535	981			2529	796
		2570	985			2562	801
		2596	988			2591	805
		2624	992			2619	809
		2657	997			2649	814
		2686	1001			2677	818

TABLE F.5 : Result of Tubular Filter Press Experiment F.5 (continued)

Time (s)	Gauge Pressure (kPa)	Time (s)	Feed Volume (ℓ)	Time (s)	Applied Pressure (kPa)	Time (s)	Filtrate Volume (ℓ)
		2714	1005			2689	820
		2744	1010				
		2772	1014				
		2784	1016				

Filtration time correction : 95 s

Filtrate volume correction : 196 ℓ

Hydrostatic pressure correction : 23510 Pa

Average applied constant pressure : 376.5 kPa

Mass wet cake (bin 2) : 78.19 kg

Mass wet cake (bin 1) : 6.58 kg

Average cake solids concentration (bin 2) : 0.1927 m/m

Average cake solids concentration (bin 2, screened) : 0.2586 m/m

Average cake solids concentration (bin 1) : not recorded

Approximate recovered cake dry solids : 14.47 kg

Approximate cake recovery: 62 %

Bulk of cake removed during second and third flushes, no cake was removed by the rollers. Cake consisted of large chunks approximately 11 mm in thickness. The average cake dry solids concentration for bin 1 was not recorded so the feed solids concentration was used as the solids concentration of the flush fluid in the calculation of the cake recovery.

F.3 RESULTS OF TESTS AT LOW FEED SOLIDS CONCENTRATION

F.3.1 Test F.6

Date : 2/10/96

Time : 14:30

Approximate operating pressure : 200 kPa

Limiting filtrate flow rate timer setting : 6 s/ℓ

Feed solids concentration : 17.8 kg/m³

Tube filling time (visual) : not recorded

Tube filling time (volume) : 139 s

Tube filling time (pressure) : 116 s

TABLE F.6 : Result of Tubular Filter Press Experiment F.6

Time (s)	Gauge Pressure (kPa)	Time (s)	Feed Volume (l)	Time (s)	Applied Pressure (kPa)	Time (s)	Filtrate Volume (l)
0	0	0	0	0	27	0	0
20	40	14	18	11	37	16	28
50	40	43	68	22	47	47	77
80	40	73	120	32	57	75	114
108	40	102	170	44	67	104	149
116	50	132	222	53	77	137	180
127	60	163	271	67	97	164	200
138	70	191	308	83	117	193	217
148	80	220	343	91	127	223	234
160	90	253	374	101	137	251	250
169	100	280	394	111	147	280	264
183	120	309	411	122	157	311	277
199	140	339	428	136	167	340	289
207	150	367	444	154	172	369	301
217	160	396	458	231	187	400	313
227	170	427	471	287	177	426	323
238	180	456	483	844	192	457	334
252	190	485	495	1384	187	487	345
270	195	516	507	1828	192	516	355
347	210	542	517	2085	192	546	365
403	200	573	528			576	375
960	215	603	539			604	384
1500	210	632	549			634	393
1944	215	662	559			664	402
2201	215	692	569			698	412
		720	578			723	419
		750	587			751	427
		780	596			781	435
		814	606			811	443
		839	613			840	451
		867	621			870	460
		897	629			901	468
		927	637			930	475
		956	645			958	482
		986	654			991	490
		1017	662			1016	496
		1046	669			1049	504
		1074	676			1075	510

TABLE F.6 : Result of Tubular Filter Press Experiment F.6 (continued)

Time (s)	Gauge Pressure (kPa)	Time (s)	Feed Volume (ℓ)	Time (s)	Applied Pressure (kPa)	Time (s)	Filtrate Volume (ℓ)
		1107	684			1107	517
		1132	690			1134	523
		1165	698			1166	530
		1191	704			1193	536
		1223	711			1221	542
		1250	717			1254	549
		1282	724			1282	555
		1309	730			1311	561
		1337	736			1341	567
		1370	743			1372	573
		1398	749			1399	578
		1427	755			1430	584
		1457	761			1457	589
		1488	767			1488	595
		1515	772			1514	600
		1546	778			1546	606
		1573	783			1578	612
		1604	789			1605	617
		1630	794			1633	622
		1662	800			1662	627
		1694	806			1694	633
		1721	811			1721	638
		1749	816			1751	644
		1778	821			1779	649
		1810	827			1812	655
		1837	832			1840	660
		1867	838			1873	666
		1895	843			1901	671
		1928	849			1930	676
		1956	854			1959	681
		1989	860			1989	686
		2017	865			2018	691
		2046	870			2048	696
		2075	875			2072	700
		2105	880			2085	702
		2134	885				
		2164	890				
		2188	894				
		2201	896				

Filtration time correction : 116 s

Filtrate volume correction : 194 ℓ

Hydrostatic pressure correction : 23390 Pa

Average applied constant pressure : 187.4 kPa

Mass wet cake (bin 2) : 51.59 kg

Mass wet cake (bin 1) : 15.14 kg

Average cake solids concentration (bin 2) : 0.1723 m/m

Average cake solids concentration (bin 2, screened) : 0.2222 m/m

Average cake solids concentration (bin 1) : 0.0227 m/m

Approximate recovered cake dry solids : 8.6 kg

Approximate cake recovery: 65.6 %

Bulk of cake removed during first two flushes, rollers removed very small amount of cake. Flush fluid reported to cake collection bin due to insufficient drainage as a result of a greater amount of cake discharged onto the conveyor.

F.3.2 Test F.7

Date : 3/10/96

Time : 11:07

Approximate operating pressure : 300 kPa

Limiting filtrate flow rate timer setting : 6 s/l

Feed solids concentration : 15.3 kg/m³

Tube filling time (visual) : not recorded

Tube filling time (volume) : 134 s

Tube filling time (pressure) : 115 s

TABLE F.7 : Result of Tubular Filter Press Experiment F.7

Time (s)	Gauge Pressure (kPa)	Time (s)	Feed Volume (l)	Time (s)	Applied Pressure (kPa)	Time (s)	Filtrate Volume (l)
0	0	0	0	0	27	0	0
13	40	6	4	16	37	9	16
42	40	35	54	25	47	41	69
71	40	66	109	39	57	67	112
103	40	94	162	51	67	98	157
115	50	124	216	62	77	134	204
131	60	156	269	75	87	157	232
140	70	182	312	82	97	185	265
154	80	213	357	90	107	217	296

TABLE F.7 : Result of Tubular Filter Press Experiment F.7 (continued)

Time (s)	Gauge Pressure (kPa)	Time (s)	Feed Volume (l)	Time (s)	Applied Pressure (kPa)	Time (s)	Filtrate Volume (l)
166	90	249	404	107	127	245	317
177	100	272	432	114	137	275	336
190	110	300	465	125	157	306	354
197	120	332	496	142	177	335	370
205	130	360	517	171	207	362	384
222	150	390	536	174	217	396	401
229	160	421	554	178	227	424	414
240	180	450	570	194	257	450	426
257	200	477	584	199	267	480	439
286	230	511	601	208	277	511	452
289	240	539	614	225	287	541	464
293	250	565	626	251	277	568	475
309	280	595	639	285	282	597	486
314	290	626	652	563	282	631	498
323	300	656	664	587	279	662	509
340	310	683	675	2671	279	691	519
366	300	712	686			717	528
400	305	746	698			745	537
678	305	777	709			776	547
702	302	806	719			804	556
2786	302	832	728			833	565
		860	737			863	574
		891	747			893	583
		919	756			922	591
		948	765			951	600
		978	774			980	608
		1008	783			1012	617
		1037	791			1041	625
		1066	800			1070	633
		1095	808			1097	640
		1127	817			1127	648
		1156	825			1157	656
		1185	833			1193	665
		1212	840			1215	671
		1242	848			1243	678
		1272	856			1276	686
		1308	865			1304	693
		1330	871			1333	700
		1358	878			1366	708

TABLE F.7 : Result of Tubular Filter Press Experiment F.7 (continued)

Time (s)	Gauge Pressure (kPa)	Time (s)	Feed Volume (l)	Time (s)	Applied Pressure (kPa)	Time (s)	Filtrate Volume (l)
		1391	886			1392	714
		1419	893			1422	721
		1448	900			1453	728
		1481	908			1479	734
		1507	914			1510	741
		1537	921			1537	747
		1568	928			1569	754
		1594	934			1597	760
		1625	941			1630	767
		1652	947			1658	773
		1684	954			1686	779
		1712	960			1714	785
		1745	967			1744	791
		1773	973			1777	798
		1801	979			1807	804
		1829	985			1837	810
		1859	991			1861	815
		1892	998			1891	821
		1922	1004			1922	827
		1952	1010			1953	833
		1976	1015			1978	838
		2006	1021			2009	844
		2037	1027			2045	851
		2068	1033			2072	856
		2093	1038			2099	861
		2124	1044			2126	866
		2160	1051			2158	872
		2187	1056			2185	877
		2214	1061			2218	883
		2241	1066			2246	888
		2273	1072			2281	894
		2300	1077			2301	898
		2333	1083			2336	904
		2361	1088			2364	909
		2396	1094			2393	914
		2416	1098			2422	919
		2451	1104			2451	924
		2479	1109			2479	929
		2508	1114			2509	934

TABLE F.7 : Result of Tubular Filter Press Experiment F.7 (continued)

Time (s)	Gauge Pressure (kPa)	Time (s)	Feed Volume (ℓ)	Time (s)	Applied Pressure (kPa)	Time (s)	Filtrate Volume (ℓ)
		2537	1119			2538	939
		2566	1124			2575	945
		2594	1129			2597	949
		2624	1134			2628	954
		2653	1139			2657	959
		2690	1145			2671	961
		2712	1149				
		2743	1154				
		2772	1159				
		2786	1161				

Filtration time correction : 115 s

Filtrate volume correction : 200 ℓ

Hydrostatic pressure correction : 23350 Pa

Average constant applied pressure : 279 kPa

Mass wet cake (bin 2) : 50.2 kg

Mass wet cake (bin 1) : 10.55 kg

Average cake solids concentration (bin 2) : 0.1838 m/m

Average cake solids concentration (bin 2, screened) : 0.2361 m/m

Average cake solids concentration (in 1) : 0.0233 m/m

Approximate recovered cake dry solids : 8.94 kg

Approximate cake recovery: 58.8 %

Bulk of cake removed during first two flushes, some flush fluid carried into cake collection bin during second flush.

F.3.3 Test F.8

Date : 3/10/96

Time : 14:42

Approximate operating pressure : 300 kPa

Limiting filtrate flow rate timer setting : 4.25 s/ℓ

Feed solids concentration : 17.1 kg/m³

Tube filling time (visual) : not recorded

Tube filling time (volume) : 128 s

Tube filling time (pressure) : 110 s

TABLE F.8 : Result of Tubular Filter Press Experiment F.8

Time (s)	Gauge Pressure (kPa)	Time (s)	Feed Volume (l)	Time (s)	Applied Pressure (kPa)	Time (s)	Filtrate Volume (l)
0	0	0	0	0	27	0	0
12	40	4	2	12	37	15	28
40	40	33	53	21	47	43	78
69	40	62	109	29	57	72	123
110	50	91	164	39	67	100	162
122	60	125	227	48	77	131	200
131	70	153	277	55	87	159	229
139	80	182	322	60	97	192	259
149	90	210	361	70	107	218	278
158	100	241	399	77	117	248	297
165	110	269	428	84	127	276	313
170	120	302	458	89	137	305	329
180	130	328	477	95	147	336	345
187	140	358	496	107	167	365	359
194	150	386	512	113	177	394	373
199	160	415	528	120	187	423	386
205	170	446	544	126	197	451	398
217	190	475	558	140	217	482	411
223	200	504	572	146	227	512	423
230	210	533	585	156	237	541	434
236	220	561	597	165	247	571	445
250	240	592	610	175	257	598	455
256	250	622	622	188	267	629	466
266	260	651	633	204	277	658	476
275	270	681	644	1452	277	688	486
285	280	708	654			719	496
298	290	739	665			747	505
314	300	768	675			776	514
1562	300	798	685			806	523
		829	695			835	532
		857	704			866	541
		886	713			893	549
		916	722			924	557
		945	731			954	566
		976	740			984	574
		1003	748			1010	581
		1034	756			1040	589

TABLE F.8 : Result of Tubular Filter Press Experiment F.8 (continued)

Time (s)	Gauge Pressure (kPa)	Time (s)	Feed Volume (ℓ)	Time (s)	Applied Pressure (kPa)	Time (s)	Filtrate Volume (ℓ)
		1064	765			1070	597
		1094	773			1101	605
		1120	780			1133	613
		1150	788			1157	619
		1180	796			1189	627
		1211	804			1218	634
		1243	812			1247	641
		1267	818			1277	648
		1299	826			1311	656
		1328	833			1337	662
		1357	840			1368	669
		1387	847			1394	675
		1421	855			1425	682
		1447	861			1452	688
		1478	868				
		1504	874				
		1535	881				
		1562	887				

Filtration time correction : 110 s

Filtrate volume correction : 199 ℓ

Hydrostatic pressure correction : 23380 Pa

Average constant applied pressure : 276.6 kPa

Mass wet cake (bin 2) : 32.59 kg

Mass wet cake (bin 1) : 5.62 kg

Average cake solids concentration (bin 2) : 0.1913 m/m

Average cake solids concentration (bin 2, screened) : 0.2295 m/m

Average cake solids concentration (bin 1) : 0.026 m/m

Approximate recovered dry solids : 6.08g

Approximate cake recovery: 50 %

Cake recovery as per Test F.7 except less entrained flush fluid due to lower cake volume.

F.3.4 Test F.9

Date : 4/10/96

Time : 10:58

Approximate operating pressure : 400 kPa

Limiting filtrate flow rate timer setting : 6 s/l

Feed solids concentration : 16.1 kg/m³

Tube filling time (visual) : not recorded

Tube filling time (volume) : 131 s

Tube filling time (pressure) : 111 s

TABLE F.9 : Result of Tubular Filter Press Experiment F.9

Time (s)	Gauge Pressure (kPa)	Time (s)	Feed Volume (l)	Time (s)	Applied Pressure (kPa)	Time (s)	Filtrate Volume (l)
0	0	0	0	0	27	0	0
28	40	19	28	12	37	30	53
55	40	49	82	26	47	58	102
83	40	78	137	43	57	85	144
111	50	108	192	53	67	117	188
123	60	141	250	62	77	144	221
137	70	169	299	69	87	173	253
154	80	196	341	82	97	203	282
164	90	228	385	89	107	235	309
173	100	255	418	95	117	262	330
180	110	284	450	101	127	294	353
193	120	314	479	108	137	321	372
200	130	346	506	117	147	353	393
206	140	373	527	125	157	379	410
212	150	405	550	130	167	409	428
219	160	432	569	137	177	437	445
228	170	464	590	158	197	469	463
236	180	490	607	169	207	497	478
241	190	520	625	187	227	528	493
248	200	548	642	196	237	558	506
269	220	580	660	216	257	591	520
280	230	608	675	230	267	618	531
298	250	639	690	249	277	644	542
307	260	669	703	272	287	672	553
327	280	702	717	288	297	703	565
341	290	729	728	303	307	732	576
360	300	755	739	309	317	760	587
383	310	783	750	336	327	790	598
399	320	814	762	353	337	822	609
414	330	843	773	379	347	851	619

TABLE F.9 : Result of Tubular Filter Press Experiment F.9 (continued)

Time (s)	Gauge Pressure (kPa)	Time (s)	Feed Volume (l)	Time (s)	Applied Pressure (kPa)	Time (s)	Filtrate Volume (l)
420	340	871	784	401	357	878	628
447	350	901	795	422	367	908	637
464	360	933	806	437	377	939	646
490	370	962	816	485	387	970	657
512	380	989	825	549	377	999	666
533	390	1019	834	968	367	1027	675
548	400	1050	843	1043	377	1056	684
596	410	1081	854	3449	377	1086	693
660	400	1110	863			1113	701
1079	390	1138	872			1144	710
1154	400	1167	881			1175	719
3560	400	1197	890			1203	727
		1224	898			1232	735
		1255	907			1261	743
		1286	916			1291	751
		1314	924			1320	759
		1343	932			1350	767
		1372	940			1380	775
		1402	948			1407	782
		1431	956			1438	790
		1461	964			1466	797
		1491	972			1498	805
		1518	979			1526	812
		1549	987			1554	819
		1577	994			1584	826
		1609	1002			1613	833
		1637	1009			1642	840
		1665	1016			1672	847
		1695	1023			1704	855
		1724	1030			1730	861
		1753	1037			1760	868
		1783	1044			1794	876
		1815	1052			1825	883
		1841	1058			1848	888
		1871	1065			1880	895
		1905	1073			1912	902
		1936	1080			1941	908
		1959	1085			1968	914
		1991	1092			1998	920

TABLE F.9 : Result of Tubular Filter Press Experiment F.9 (continued)

Time (s)	Gauge Pressure (kPa)	Time (s)	Feed Volume (ℓ)	Time (s)	Applied Pressure (kPa)	Time (s)	Filtrate Volume (ℓ)
		2023	1099			2025	926
		2052	1105			2056	932
		2079	1111			2087	938
		2109	1117			2112	943
		2136	1123			2142	949
		2167	1129			2173	955
		2198	1135			2203	961
		2223	1140			2233	967
		2253	1146			2260	972
		2284	1152			2292	978
		2314	1158			2319	983
		2344	1164			2346	988
		2371	1169			2378	994
		2403	1175			2405	999
		2430	1180			2438	1005
		2457	1185			2465	1010
		2489	1191			2498	1016
		2516	1196			2526	1021
		2549	1202			2553	1026
		2576	1207			2581	1031
		2609	1213			2615	1037
		2637	1218			2642	1042
		2664	1223			2670	1047
		2692	1228			2703	1053
		2726	1234			2730	1058
		2753	1239			2758	1063
		2781	1244			2791	1069
		2814	1250			2819	1074
		2841	1255			2787	1079
		2869	1260			2876	1084
		2902	1266			2910	1090
		2930	1271			2939	1095
		2898	1276			2968	1100
		2987	1281			2997	1105
		3021	1287			3026	1110
		3050	1292			3055	1115
		3079	1297			3085	1120
		3108	1302			3115	1125
		3137	1307			3145	1130

TABLE F.9 : Result of Tubular Filter Press Experiment F.9 (continued)

Time (s)	Gauge Pressure (kPa)	Time (s)	Feed Volume (ℓ)	Time (s)	Applied Pressure (kPa)	Time (s)	Filtrate Volume (ℓ)
		3166	1312			3175	1135
		3196	1317			3205	1140
		3226	1322			3236	1145
		3256	1327			3260	1149
		3286	1332			3291	1154
		3316	1337			3322	1159
		3347	1342			3345	1163
		3371	1346			3375	1168
		3402	1351			3406	1173
		3433	1356			3437	1178
		3456	1360			3449	1180
		3486	1365				
		3517	1370				
		3548	1375				
		3560	1377				

Filtration time correction : 111 s

Filtrate volume correction : 197 ℓ

Hydrostatic pressure correction : 23360 Pa

Average applied constant pressure : 375.9 kPa

Mass wet cake (bin 2) : 58.93 kg

Mass wet cake (bin 1) : 8.58 kg

Average cake solids concentration (bin 2) : 0.2132 m/m

Average cake solids concentration (bin 2, screened) : 0.2655 m/m

Average cake solids concentration (bin 1) : 0.0287 m/m

Approximate recovered cake dry solids : 12.19 kg

Approximate cake recovery: 62.1 %

Bulk of cake removed during first two flushes.

F.3.5 Test F.10

Date : 4/10/96

Time : 14:22

Approximate operating pressure : 400 kPa

Limiting filtrate flow rate timer setting : 4.25 s/ℓ

Feed solids concentration : 15.4 kg/m³

Tube filling time (visual) : not recorded

Tube filling time (volume) : 122 s

Tube filling time (pressure) : 94 s

TABLE F.10 : Result of Tubular Filter Press Experiment F.10

Time (s)	Gauge Pressure (kPa)	Time (s)	Feed Volume (l)	Time (s)	Applied Pressure (kPa)	Time (s)	Filtrate Volume (l)
0	0	0	0	0	27	0	0
33	40	18	30	10	37	13	26
94	50	44	83	22	47	40	78
104	60	76	144	29	57	71	132
116	70	107	205	37	67	99	176
123	80	134	257	48	77	132	222
131	90	165	311	59	87	159	256
142	100	193	355	67	97	189	290
153	110	226	401	76	107	221	323
161	120	253	435	82	117	246	346
170	130	283	469	89	127	274	369
176	140	315	502	95	137	306	393
183	150	340	525	103	147	336	415
189	160	368	548	108	157	362	432
197	170	400	572	116	167	392	451
202	180	430	594	122	177	423	469
210	190	456	611	129	187	451	485
216	200	486	630	136	197	481	501
223	210	517	648	146	207	513	517
230	220	545	664	155	217	541	530
240	230	575	680	163	227	569	543
249	240	607	696	170	237	599	556
257	250	635	709	175	247	628	568
264	260	663	722	181	257	656	580
269	270	693	735	189	267	688	593
275	280	722	747	196	277	719	605
283	290	750	759	201	287	747	616
290	300	782	772	214	297	773	626
295	310	813	784	226	307	803	637
308	320	841	795	237	317	834	648
320	330	867	805	246	327	865	659
331	340	897	816	263	337	894	669
340	350	928	827	282	347	923	679

TABLE F.10 : Result of Tubular Filter Press Experiment F.10 (continued)

Time (s)	Gauge Pressure (kPa)	Time (s)	Feed Volume (l)	Time (s)	Applied Pressure (kPa)	Time (s)	Filtrate Volume (l)
357	360	959	838	302	357	952	688
376	370	988	848	328	367	980	698
396	380	1017	858	369	377	1011	708
422	390	1046	867	419	387	1038	716
463	400	1074	877	496	392	1068	726
513	410	1105	887	577	387	1097	735
590	415	1132	895	814	377	1126	744
671	410	1162	905	2054	377	1156	753
908	400	1191	914			1187	762
2148	400	1220	923			1218	771
		1250	932			1246	779
		1281	941			1273	787
		1312	950			1305	796
		1340	958			1334	804
		1367	966			1363	812
		1399	975			1392	820
		1428	983			1422	828
		1457	991			1455	837
		1486	999			1482	844
		1516	1007			1509	851
		1549	1016			1540	859
		1576	1023			1571	867
		1603	1030			1599	874
		1634	1038			1628	881
		1665	1046			1656	888
		1693	1053			1684	895
		1722	1060			1717	903
		1750	1067			1747	910
		1778	1074			1773	916
		1811	1082			1802	923
		1841	1089			1832	930
		1867	1095			1862	937
		1896	1102			1892	944
		1926	1109			1919	950
		1956	1116			1954	958
		1986	1123			1985	965
		2013	1129			2012	971
		2048	1137			2039	977

TABLE F.10 : Result of Tubular Filter Press Experiment F.10 (continued)

Time (s)	Gauge Pressure (kPa)	Time (s)	Feed Volume (l)	Time (s)	Applied Pressure (kPa)	Time (s)	Filtrate Volume (l)
		2079	1144			2054	980
		2106	1150				
		2133	1156				
		2148	1159				

Filtration time correction : 94 s

Filtrate volume correction : 179 l

Hydrostatic pressure correction : 23360 Pa

Average applied constant pressure : 378 kPa

Mass wet cake (bin 2) : 39.58 kg

Mass wet cake (bin 1) : 5.92 kg

Average cake solids concentration (bin 2) : 0.2141 m/m

Average cake solids concentration (bin 2, screened) : 0.2541 m/m

Average cake solids concentration (bin 1) : 0.0259 m/m

Approximate recovered cake dry solids : 8.29 kg

Approximate cake recovery: 53.4 %

F.4 RESULTS OF TESTS TO DETERMINE MEDIUM RESISTANCE

F.4.1 Test F.11

Date : 1/10/96

Time : 13:40

TABLE F.11 : Result of Test F.11 to determine Medium Resistance

Time (s)	Volume (s)	Time (s)	Gauge Pressure (kPa)	Pressure (kPa)	Medium Resistance (1/m)
0	0	0	0	0	-
16	27	16	40	16.8	-
54	101	54	40	16.8	-
76	144	76	40	16.8	-
107	206	107	50	26.8	1.967E+11
136	261	136	50	26.8	1.967E+11
163	314	163	50	26.8	1.967E+11
192	369	192	50	26.8	1.967E+11
221	425	221	50	26.8	1.967E+11
252	483	252	55	31.8	2.333E+11
280	538	280	55	31.8	2.333E+11

Hydrostatic pressure correction : 23150 Pa

Average flow rate : $1.929 \times 10^{-3} \text{ m}^3/\text{s}$

Cleaning cycle initiated after 300 seconds.

F.4.2 Test F.12

Date : 1/10/96

Time : 14:06

TABLE F.12 : Result of Test F.12 to determine Medium Resistance

Time (s)	Volume (s)	Time (s)	Gauge Pressure (kPa)	Pressure (kPa)	Medium Resistance (l/m)
0	0	0	0	0	-
29	40	36	40	16.8	-
58	97	65	40	16.8	-
87	155	97	40	16.8	-
117	213	154	50	26.8	2.004E+11
147	271	185	50	26.8	2.004E+11
177	329	213	55	31.8	2.377E+11
205	384	243	60	36.8	2.750E+11
234	438	274	60	36.8	2.750E+11
264	493	301	60	36.8	2.750E+11
293	547	330	60	36.8	2.750E+11
323	603	360	65	41.8	3.123E+11
352	655				

Hydrostatic pressure correction : 23150 Pa

Average flow rate : $1.894 \times 10^{-3} \text{ m}^3/\text{s}$

Cleaning cycle initiated after 360 seconds.

F.5 SAMPLE CALCULATIONS

F.5.1 Calculation of Approximate Cake Recovery

The recovered cake that reported to cake collection bin 2 contained flush fluid that had not drained through the conveyor belt and been entrained along with the cake. The correct mass dry cake recovered that does not include the solids from the entrained flush must be calculated to determine the actual cake recovery. The dry solids concentration of the recovered cake was determined by taking a representative sample of cake from bin 2 that included both the cake and the entrained flush fluid. A second cake sample was taken from bin 2, placed on a screen and allowed to drain over a period of time. The dry solids concentration of the screened cake sample therefore represented the dry solids concentration of the cake if drainage on the conveyor had been ideal and no flush fluid has been entrained with the cake. Although the flush fluid originates from the feed tank, the solids concentration of the flush fluid will be greater than the feed solids concentration due to redispersal of the less consolidated outer cake layers during the cake removal process. Cake collection bin 1 was placed directly under the conveyor belt and hence contained some of the flush fluid that had drained through the conveyor. The solids concentration of the flush fluid in bin 1 was therefore a very good approximation of the flush fluid as a whole. From a mass balance over both the total dry and wet mass of cake before and after screening, the actual recovered mass dry solids can be determined from the following expression:

$$\text{actual mass dry cake} = \text{recovered mass dry cake} \left(\frac{C_s}{C_f - C_s} \right) \left(\frac{C_f - C_r}{C_r} \right) \quad (\text{F.1})$$

where C_r = average dry solids concentration of recovered cake, (m/m).
 C_s = average dry solids concentration of screened cake, (m/m).
 C_f = average dry solids concentration of flush fluid, (m/m).

For example for Test F.1:

Mass wet cake (Bin 2) : 84.58 kg

Average cake solids concentration (Bin 2) : 0.1517 m/m

Recovered mass dry cake : $(84.58)(0.1517) = 12.83$ kg

Average cake solids concentration (Bin 2, screened) : 0.2322 m/m

Average cake solids concentration (Bin 1) : 0.0378 m/m

Actual recovered cake dry solids (from Equation F.1) : 11.51 kg

In order to calculate the cake recovery, the total mass of dry cake deposited in the tubes that could theoretically be recovered must be determined. Due to operational constraints, an accurate mass balance over the Tubular Filter Press at the end of the filtration cycle could not be performed in order to determine the mass of dry cake deposited in the tubes. The mass of dry cake deposited in the tubes could be calculated by determining the volume of feed pumped during the filtration cycle (note: this excludes the feed required to fill the tubes and manifolds). From a volume balance, the feed volume will equal the sum of the filtrate volume and cake volume. The exact cake volume is not known, but can be approximated by the actual recovered mass dry solids and the screened cake concentration.

For example for Test F.1:

Mass dry solids recovered from tubes : 11.51 kg

Approximate mass wet cake in tubes : $(11.51)/(0.2322) = 49.55$ kg

Approximate liquid mass in cake : $(49.55 - 11.51) = 38.04$ kg

Approximate cake volume in tubes : $(38.04)/(996.5) + (11.51)/(2314.3) = 0.04315$ m³

Filtrate volume : 0.554 m³

Approximate feed volume : $(0.554 + 0.04315) = 0.5971$ m³

Feed solids concentration : 28.6 kg/m³

Approximate mass dry cake in tubes : $(0.5971)(28.6) = 17.1$ kg

The approximate cake recovery can therefore be calculated. The approximate cake volume determined by the above method will be less than the actual cake volume since it only accounts for the recovered cake volume. Cake recoveries calculated by this method will therefore be slightly elevated.

Approximate cake recovery : $(11.51)/(17.1) = 0.674$

Appendix G

Control and Optimisation Strategy for the Continuous Operation of the Tubular Filter Press

Consider the Tubular Filter Press running continuously with a fixed operating pressure, and fixed limiting plant flux, determined to optimise the dry solids production rate. The initial feed solids concentration of the sludge in the feed tank, operating pressure and limiting flux, will determine the initial plant recovery. Assuming that the feed to the Tubular Filter Press has a constant solids concentration, since the plant recovery is not ideal, the concentration of the sludge in the feed tank will increase slightly as the flush fluid drains back into the feed tank. The mains water used to clean the cake conveyor will dilute the contents of the feed tank slightly, however, under normal operation, the net effect will be an increase in the solids concentration of the feed tank. At the fixed operating pressure, the increase in solids concentration of the sludge in the feed tank, will result in a reduction in the final filtration time when the fixed limiting filtrate flux is reached, for the subsequent filtration cycle. The plant recovery is strongly dependent on the final filtration time, and a decrease in final filtration time will therefore result in a decrease in plant recovery. The decrease in plant recovery will in turn lead to an increase in the solids concentration of the sludge in the feed tank. This effect will propagate, and ultimately lead to shorter filtration times and lower recoveries, until the dilution from the feed sludge at a lower solids concentration, pumped to into the feed tank from the holding tank, and the mains water from the spray valve, is sufficient to offset the concentrating effect of the flush fluid. The Tubular Filter Press will now however, be in an non-optimal, steady state operating regime, associated with low recovery, and hence, a low dry solids production rate. The shorter filtration time, will further decrease the overall dry solids production rate, since a greater percentage of the overall plant operation time, will be spent in the cleaning cycle and not the filtration cycle.

If, however, the plant operation is controlled by fixing the final filtration time, the increase in the solids concentration of the sludge in the feed tank, as a result of flush fluid draining into the feed tank, will result in an increased plant recovery, since the operating pressure and final filtration time are fixed. With each successive filtration cycle, the influence of plant recovery on the feed solids concentration of the feed tank will decrease, the feed solids concentration will reach a constant equilibrium value, and the plant will acquire a favourable steady state operating regime. The use of final filtration time is therefore a far more favourable control parameter than the final filtrate flux.

Due to the non-ideal cake recovery, which is an inherent part of the Tubular Filter Press process, a complex relationship exists between feed tank solids concentration, cake recovery and filtration performance. This is because the feed tank solids concentration, is a partial function of the cake recovery at the end of the filtration cycle, the cake recovery, is in turn a partial function of both the feed tank solids concentration and the overall filtration performance, and the filtration performance, is a partial function of the feed tank solids concentration. Due to this dynamic, even if the external operating parameters are fixed, the Tubular Filter Press will move towards a steady state operating regime which will be different to the operating regime as dictated by the fixed, external operating parameters. In light of steady state operation, in order control the continuous operation of the Tubular Filter Press, and optimise the dry solids production rate, it is therefore not sufficient to base control and optimisation calculations on the initial fixed, external operating parameters, but to determine the steady state operation regime of the Tubular Filter Press, based on the initial fixed, external operating parameters.

In order to successfully control and optimise the Tubular Filter Press, not only do the filtration characteristics of the sludge need to be known, but also the recovery characteristic of the sludge. The true sludge characterisation is therefore required, in addition to an accurate recovery correlation, or plant specific characterisation. In addition, to determine a control strategy for the Tubular Filter Press, the parameters that influence the operation, and hence the control of the Tubular Filter Press, must be identified. With this information, the steady state operation of the Tubular Filter Press can be determined by performing successive, accurate mass balances, over the entire system.

The overall operation of the Tubular Filter Press consists of a filtration cycle followed by a cleaning cycle. The parameters that influence the filtration cycle are, the feed solids concentration, the filtration pressure, and the final filtration time. The concentration of the sludge in the feed tank cannot be controlled directly, as it is dependent on the feed solids concentration to the Tubular Filter Press, which may be variable, and the operation of the Tubular Filter Press itself, in terms of the effects of cake recovery. The concentration of the feed tank may also change during the filtration cycle, when the level switches initiate the raw sludge pump, to fill the feed tank with sludge from the holding tanks. It is assumed that the feed tank is sufficiently large, so that it is filled near the end, or after the filtration cycle. The concentration of the sludge in the feed tank is therefore assumed to remain constant during the course of the filtration. The feed solids concentration is therefore not considered to be a control parameter. The filtration pressure, and the final filtration time can however be easily controlled externally, and are considered to be control parameters.

The parameters that influence the cleaning cycle are, the number of flushes, the flush fluid flow rate, and if and when the roller cleaning carriage is utilised. The cleaning cycle plays an important role in determining the steady state operation of the Tubular Filter Press, as it not only influences the recovery mechanism and

hence cake recovery directly, but also significantly influences the overall mass balance. In addition, both the recovery correlation and the plant specific characterisation, are dependent on the cleaning cycle. It is therefore important that the cleaning cycle be fixed during the normal continuous operation of the Tubular Filter Press, and that it is the same during the continuous normal operation, as it was when the recovery correlation, or plant specific characterisation was determined. The parameters associated with the cleaning cycle are therefore not considered to be control parameters. Other factors are associated with the cleaning cycle, which do not influence cake recovery directly, but may influence the steady state operation of the Tubular Filter Press. Inadequate drainage of the flush fluid along the cake conveyor will influence the overall mass balance, for the purposes of this discussion, it is assumed that drainage along the cake conveyor is ideal. The effect of the addition of mains water to the feed tank from the spray valve during the cleaning cycle, must also be accounted for in the overall mass balance.

There are therefore only two control parameters of any significance, available to the operator, to successfully control and optimise the dry solids production of the Tubular Filter Press. They are the operating pressure, and the final filtration time.

An effective and efficient cleaning cycle is very important to the stable and optimal operation of the Tubular Filter Press. For a particular sludge type, the most efficient cleaning cycle is best determined from practical experience. Within the set number of flushes, all the cake must be effectively removed from the tubes. The flush fluid flow rate, must be set so that it can effectively remove all the cake from the tubes, whilst minimising as much as possible the effects of cake loss, which will result in a poor cake recovery. In addition, the number of flushes utilised, should be sufficient to remove all the cake, however, an unnecessarily large number of flushes will increase the overall tube cleaning time, which will negatively affect the overall dry solids production rate. It is however, critically important that the tubes are cleaned effectively, since the efficiency of the following filtration cycle will be greatly reduced if any cake is left in the tubes. For this reason, the use of the roller cleaning carriage during the final flush is recommended, since the increased shear of the flush fluid through the constricted tubes should effectively remove any remaining cake, whilst allowing the flush flow rate for the preceding flushes to be gentle enough, to reduce cake losses as much as possible. Once the optimum cleaning cycle has been determined, it should be fixed for the normal continuous operation of the Tubular Filter Press. The optimal cleaning cycle may have to be overriden during periods of unstable plant operation if difficulty is experienced in removing the cake from the tubes, the inclusion of the roller cleaning carriage has the added benefit of rigorously cleaning the tubes, should complications such as tube blockages occur.

The Tubular Filter Press should then be operated, initially on a batch basis, over a range of feed solids concentrations, operating pressures, and final filtration times in order to obtain sufficient experimental data to

determine an accurate recovery correlation, or plant specific characterisation, for the particular sludge and the fixed cleaning cycle. Concurrently, the true sludge characterisation should be determined.

With the accurate plant specific characterisation, or recovery correlation, and the true characterisation, the steady state operating regime can be determined for a given initial feed solids concentration, operating pressure, and final filtration time. More importantly, the dry solids production rate can be optimised in terms of the two control variables, the operating pressure, and the final filtration time. For the purposes of this discussion the feed to the Tubular Filter Press is assumed to be have a constant concentration and therefore the Tubular Filter Press will eventually reach steady state operation.

For a given initial feed solids concentration, operating pressure and final filtration time, the true characterisation can be used to determine the average cake concentration and volume of filter cake deposited in the tubes at the end of the filtration cycle, the amount of filtrate produced, and the change in volume of the feed tank. Depending on the approach used, the recovery correlation, or the plant specific characterisation, can be used to determine the cake recovery for the particular operating condition, and hence calculate how much cake will be lost and report to the feed tank with the flush fluid. For example, from the same initial feed solids concentration, operating pressure and final filtration time, the plant specific characterisation can be used to directly determine the average cake dry solids concentration, and volume of the cake, that will be recovered from the tubes. Since the cleaning cycle is fixed, the exact volume of flush fluid pumped during the cleaning cycle will be constant, assuming that slight changes in the viscosity of the flush fluid, due to changes in solids concentration, are not significant. Since drainage is assumed to be ideal, all the flush fluid will return to the feed tank, along with the lost cake, and the mains water from the spray valve. From a mass balance, the new concentration of the sludge in the feed tank can be calculated. Depending on how the plant is operated, the feed tank will be filled to its original volume, determined by the level switches, at the end of the filtration cycle, or just prior to the start of the next filtration cycle. This should be considered when calculating the new concentration of the sludge in the feed tank. Based on the new solids concentration of the sludge in the feed tank, and with the same operating pressure and final filtration time, the procedure can be repeated, until the solids concentration of the sludge in the feed tank reaches an equilibrium value and the plant has reached steady state. The steady state dry solids production rate can then be determined for the particular operating pressure and final filtration time. The steady state dry solids production rate can then be determined in the same manner, over a range of operating pressures and final filtration times, to determine the operating pressure and final filtration time that will optimise the steady state dry solids production rate for the given feed sludge concentration.

The variability of the solids concentration of the feed to the holding tank will depend on the particular application of the Tubular Filter Press. A sudden change in the feed solids concentration will upset the

optimal steady state control of the Tubular Filter Press, the operation may quickly become unstable, and may result in further complications such as tube blockages. The sludge holding tanks should serve to balance any sudden changes in feed solids concentration, so that timely changes can be made to the operational parameters to ensure that the plant will reach the optimal steady state operating regime, based on the new feed solids concentration.

The question of plant control is further complicated if the filtration characteristics of the feed sludge changes. If the sludge characteristics change, then not only does the true characterisation of the sludge, but also the recovery correlation and the plant specific characterisation. If the application of the Tubular Filter Press is such that the filtration characteristics of the sludge are expected to vary, the true characterisation, plant specific characterisation or recovery correlation, which are needed to calculate the optimum steady state operating regime, will have to be updated continuously. By maintaining a window period of filtration data from the Tubular Filter Press, and regressing on the filtration data, the average plant specific characterisation over the window period, can be determined. As the data base for the regression analysis is updated by adding new plant data, the old data at the end of the window period is removed. The expected variability of the sludge characteristics will dictate the length of the window period that is used and how often the plant specific characterisation should be updated. Concurrently, the true sludge characterisation is updated, either by regressing on filtration data obtained from controlled laboratory-scale data, or by conventional laboratory characterisation methods. The sludge holding tanks will also balance any sudden changes in filtration characteristics of the sludge.

Appendix H

Evaluation of Direct Search Technique

The direct search technique employed by the regressive solution procedure is evaluated using pseudo experimental data created by the constant pressure compressible cake filtration model.

H.1 PSEUDO EXPERIMENTAL DATA

The pseudo experimental data for the regression analysis was produced by the computer programme COMPRESS.

H.1.1 Programme Input : COMPRESS

The following input parameters were used in the programme COMPRESS.

H.1.1.1 Physical Properties

Solids density : 2380 kg/m³
 Liquid density : 1000 kg/m³
 Liquid viscosity : 0.001 Pa.s
 Coefficient of earth pressure at rest : 0.5

H.1.1.2 Plant Specifications

Plant geometry : internal cylindrical
 Tube length : 1 m
 Tube internal radius : 0.0125 m
 Number of tubes : 1
 Medium resistance : 5.353 x 10¹⁰ m⁻¹

H.1.1.3 Sludge Characterisation

$K = 6.00 \times 10^{-13} p_{sf}^{-0.5}$	$0 \leq p_s \leq p_{sf}$	(H.1.a)
$K = 6.00 \times 10^{-13} p_s^{-0.5}$	$p_{sf} \leq p_s \leq 3457 \text{ Pa}$	(H.1.b)
$K = 1.80 \times 10^{-10} p_s^{-1.2}$	$p_s \geq 3457 \text{ Pa}$	(H.1.c)
$(1 - \varepsilon) = 0.03 p_{sf}^{0.08}$	$0 \leq p_s \leq p_{sf}$	(H.1.d)
$(1 - \varepsilon) = 0.03 p_s^{0.08}$	$p_{sf} \leq p_s \leq 2380 \text{ Pa}$	(H.1.e)
$(1 - \varepsilon) = 8.00 \times 10^{-3} p_s^{0.25}$	$p_s \geq 2380 \text{ Pa}$	(H.1.f)

H.1.1.4 Calculation Parameters

Numerical integration steps : 150
Cake increment thickness : 0.00025 m
Convergence criterion : 1 Pa

H.1.1.5 Operating Conditions

Feed solids concentration : 30 kg/m³

Four sets of experimental data were created, at two different operating pressures, 100 kPa and 300 kPa, and two different final filtration times, 600 s and 1200 s.

H.1.2 Programme Output : COMPRESS

In addition to the operating data, listed below is the minimum relevant data that is required by the programme REGRESS, for the regression analysis.

H.1.2.1 100 kPa, 600 s

Final filtration volume : 0.002067 m³
Final filtrate flux : 1.8755×10^{-5} m³/m²/s
Cake concentration : 0.17684 m/m
Filtrate volume versus time data : see Table H.1

H.1.2.2 100 kPa, 1200 s

Final filtration volume : 0.002743 m³
Final filtrate flux : 1.1191×10^{-5} m³/m²/s
Cake concentration : 0.18994 m/m
Filtrate volume versus time data : see Table H.1

H.1.2.3 300 kPa, 600 s

Final filtration volume : 0.002374 m³
Final filtrate flux : 2.1877×10^{-5} m³/m²/s
Cake concentration : 0.20020 m/m
Filtrate volume versus time data : see Table H.1

H.1.2.4 300 kPa, 1200 s

Final filtration volume : 0.003173 m³
Final filtrate flux : 1.346×10^{-5} m³/m²/s

Cake concentration : 0.21604 m/m

Filtrate volume versus time data : see Table H.1

TABLE H.1 : Filtrate Volume versus Time Data for Pseudo Experimental Data

$P_0 = 100 \text{ kPa}$		$P_0 = 300 \text{ kPa}$	
Time (s)	Filtrate Volume (m^3)	Time (s)	Filtrate Volume (m^3)
33.2476	0.000539589	33.8211	0.000627717
45.379	0.000626928	46.4784	0.000729516
59.3708	0.000713325	61.1191	0.000830434
75.2219	0.000798802	77.7568	0.000930524
92.9244	0.000883333	96.3891	0.00102973
112.485	0.00096696	117.038	0.00112812
133.893	0.00104965	139.704	0.00122565
157.163	0.00113144	164.413	0.00132239
182.282	0.0012123	191.17	0.00141829
209.274	0.0012923	220.01	0.00151341
238.132	0.00137138	250.938	0.00160773
268.86	0.00144957	283.993	0.00170129
301.482	0.00152689	319.189	0.00179408
335.994	0.00160333	356.586	0.00188617
372.431	0.00167893	396.177	0.00197748
410.78	0.00175364	438.06	0.00206815
451.114	0.00182757	482.257	0.00215815
493.424	0.00190066	528.793	0.00224746
537.708	0.00197289	577.775	0.00233617
584.084	0.0020444	629.264	0.0024243
632.543	0.00211512	683.299	0.00251183
683.132	0.00218507	740.032	0.00259888
735.966	0.00225435	799.546	0.00268545
791.179	0.00232307	861.903	0.00277152
848.549	0.00239089	927.36	0.0028573
908.376	0.00245808	996.024	0.00294277
970.764	0.00252468	1068.09	0.00302801
1035.83	0.00259071	1143.77	0.00311308
1103.67	0.00265616	1200	0.00317315
1174.7	0.00272131		
1200	0.00274337		

H.2 REGRESSION ANALYSIS

The regressive solution procedure developed in Section 3.4, which has been incorporated into the programme REGRESS, is evaluated using the pseudo experimental data.

H.2.1 Programme Input : REGRESS

In addition to the physical properties, plant specifications and pseudo experimental data listed above, the following parameters were used in the programme REGRESS, for the regression analysis.

H.2.1.1 Search Specifications

Reflection coefficient (ζ) : 1.3

Boundary approach limit (ϖ) : 1×10^{-16}

Feasible loop exit number (N_f) : 10

Improvement loop exit number (N_i) : 10

Number of complex replacements (N_r) : 1

Number of replacement attempts (N_a) : 10

Percentage local proximity (P_p) : 10

Maximum standard deviation squared (ζ^2) : 1×10^{-7}

Maximum vertex distance (D_m) : 0.0001

H.2.1.2 Correlation Data

The correlation data over the initial solids compressive pressure range, given by Equation H.1.b and Equation H.1.e, is included in the regression analysis. This data would typically be obtained from settling tests. As a result, the regression analysis will be looking for the correlation parameters in the higher solids compressive pressure range, given by Equations H.1.c and Equation H.1.f, normally obtained from C-P Cell tests, and not a single characterisation equivalent to Equations H.1.

H.2.1.3 Explicit Parameter Bounds

The explicit parameter range given in Table H.2, is very large, ordinarily the explicit parameter bounds would be given more realistic values around where the values of the respective parameters are expected to lie. Due to the inclusion of correlation data in the low solids compressive pressure range, the value of the parameter P_{si} will be fixed to its minimum value as determined by the implicit constraint given by Equation 3.99.

TABLE H.2 : Explicit Bounds of Objective Function Variables for Regression Analysis on Pseudo Experimental Data

Parameter	Minimum	Maximum
F	1×10^{-20}	1×10^{-5}
δ	0	2
B	1×10^{-10}	0.1
β	0	1
psi	0	100

H.2.1.4 Experimental Data

The four pseudo experimental data points listed above were included in the regression analysis. The experimental data was obtained at two different pressures and final filtration times. Under normal circumstances the number of experimental points should be far greater than four.

H.3 RESULTS OF REGRESSION ANALYSIS

Polyhedra direct search strategies, such as the search strategy developed in Section 3.4.1, for the regressive solution procedure can converge slowly and occasionally terminate prematurely. In addition, the search may terminate on a local minimum and not the global minimum. The initial configuration of the complex can also influence the result obtained. As a result, when performing a regression analysis, in order to ensure the consistency of the final result, and also to ensure that the global minimum has been located, several runs should be performed with different initial configurations of the complex. The initial configuration of the complex is determined randomly, therefore by changing the value of the random number generator seed, or the values of the explicit bounds defining the range from which the initial parameter values are selected, the initial configuration of the complex can be changed.

In order to test the robustness of the search strategy, the regression analysis was deliberately performed with the minimum of experimental data and with an extremely large explicit parameter range.

initial complex configuration.

TABLE : H.5 Results of Regression Analysis H.3

Seed : 2	$W_1 = 1, W_2 = 1, W_3 = 0, W_4 = 0$		$\alpha = 9.648$
F	5.7211×10^{-11}	$a(\Delta P_c)$	13.934
δ	1.0833	$a(\varepsilon_{av})$	5.3613
B	0.03	$a(V_f)$	-
β	0.1163	$a(\theta)$	-

During regression H.3, the search did not converge on the global minimum, but on a different local minimum.

The exact form of the objective function can be manipulated by changing the values of the weighting factors of each component of the objective function. The regression analysis above was repeated with the same initial complex configuration, but a slightly different objective function.

TABLE : H.6 Results of Regression Analysis H.4

Seed : 2	$W_1 = 1, W_2 = 2, W_3 = 0, W_4 = 0$		$\alpha = 0.1093$
F	1.7957×10^{-10}	$a(\Delta P_c)$	0.1838
δ	1.1997	$a(\varepsilon_{av})$	0.03473
B	0.00799	$a(V_f)$	-
β	0.2501	$a(\theta)$	-

Increasing the sensitivity of the average cake pressure drop component of the objective function during regression H.4, by doubling the weighting factor, W_2 , the regression analysis found the global minimum directly, whereas previously, with the same random number generator seed, it had not.

Regression H.5 converged on the global minimum directly.

TABLE : H.7 Results of Regression Analysis H.5

Seed : 4	$W_1 = 1, W_2 = 1, W_3 = 0, W_4 = 0$		$\alpha = 0.1093$
F	1.796×10^{-10}	$a(\Delta P_c)$	0.1837
δ	1.1997	$a(\varepsilon_{av})$	0.03479
B	0.00799	$a(V_f)$	-
β	0.2501	$a(\theta)$	-

In order to ensure that the search had indeed converged on local minima during regression H.1 and regression H.3, and had not terminated prematurely, the convergence criteria were reduced by a factor of ten, and the regressions repeated. The results remained the same indicating that the regressions had indeed converged on local minima.

H.3.2 Time Dependent Analysis

During the time dependent analysis, only the filtrate volume and cake thickness components of the objective function are utilised, see Section 3.4.2.2.

Filtrate volume data below 30 seconds, was not included in the regression analysis. The filtrate volume component of the objective function was found to be sensitive at very low filtrate volumes if the difference in the calculated and experimental volumes was large, relative to a small experimental filtrate volume denominator. This sensitivity was found to destabilise the objective function and reduce the efficiency of the regression analysis. The initial filtrate volumes are to a large extent, a function of the medium resistance and the filtration pressure, and not the characteristics of the sludge, therefore in terms of the regression analysis, no important information is lost by excluding the initial filtrate volumes.

TABLE : H.8 Results of Regression Analysis H.6

Seed : 1	$W_1 = 0, W_2 = 0, W_3 = 1, W_4 = 1$		$a = 0.4273$
F	3.6917×10^{-10}	$a(\Delta P_c)$	-
δ	1.2717	$a(\varepsilon_{av})$	-
B	0.005191	$a(V_f)$	0.1456
β	0.29382	$a(\theta)$	0.7089

Regression H.6 was terminated prematurely as the complex had become stuck on a concave region of the objective function or implicit constraints.

TABLE : H.9 Results of Regression Analysis H.7

Seed : 2	$W_1 = 0, W_2 = 0, W_3 = 1, W_4 = 1$		$a = 1.7035$
F	9.6636×10^{-9}	$a(\Delta P_c)$	-
δ	1.5987	$a(\varepsilon_{av})$	-
B	0.00045	$a(V_f)$	0.5899
β	0.53808	$a(\theta)$	2.8171

The direct search technique was developed to overcome this problem by attempting to update the complex by randomly selecting points in both the global and local parameter space, see Section 3.4.1. However, due to the very large global parameter space, defined by the explicit parameter bounds, by nature of probability, it would take a very long time to randomly select suitable points to update the complex. The time dependent analysis appeared prone to becoming stuck on concave regions of the objective function as indicated by the results of regression H.7 and regression H.8, both of which we also terminated prematurely, after becoming stuck on concave regions.

TABLE : H.10 Results of Regression Analysis H.8

Seed : 1	$W_1 = 0, W_2 = 0, W_3 = 1, W_4 = 1$		$\alpha = 1.3017$
F	4.1961×10^{-9}	$\alpha(\Delta P_c)$	-
δ	1.5138	$\alpha(\varepsilon_{av})$	-
B	0.005862	$\alpha(V_f)$	2.4978
β	0.29007	$\alpha(\theta)$	0.1056

In order to illustrate the effectiveness of the direct search technique to free itself from concave regions of the objective function, regression H.8 was repeated with a reduced parameter space as shown in Table H.3.9.

TABLE H.11 : Reduced Objective Function Variable Space for Regression H.9

Parameter	Minimum	Maximum
F	1×10^{-20}	1×10^{-5}
δ	1	1.5
B	1×10^{-10}	0.1
β	0.1	0.4
p_{st}	0	100

TABLE : H.12 Results of Regression Analysis H.9

Seed : 3	$W_1 = 0, W_2 = 0, W_3 = 1, W_4 = 1$		$\alpha = 0.0015$
F	1.7978×10^{-10}	$\alpha(\Delta P_c)$	-
δ	1.1999	$\alpha(\varepsilon_{av})$	-
B	0.008005	$\alpha(V_f)$	0.0008
β	0.24995	$\alpha(\theta)$	0.0022

During regression H.9, the search technique was eventually able to free itself from the concave region and converge on the global minimum.

In light of the fact that experimental data, with the exception of filtrate volume data, can be affected by cake loss, a number of regression analyses were performed utilising filtrate volume data only. It was found that there appears to be no distinct solution, but rather a locus of permeability and porosity correlation parameters that minimises the objective function. The filtrate volume data alone is found to be not sufficient to obtain an accurate true physically characterisation of the sludge.

H.3.3 Combined Analysis

For the combined regression analysis, all four components of the objective function are utilised.

TABLE : H.13 Results of Regression Analysis H.10

Seed : 1	$W_1 = 1, W_2 = 1, W_3 = 1, W_4 = 1$		$a = 0.05823$
F	1.7779×10^{-10}	$a(\Delta P_c)$	0.0302
δ	1.1987	$a(\varepsilon_{av})$	0.1788
B	0.007998	$a(V_f)$	0.0163
β	0.25004	$a(\theta)$	0.0076

TABLE : H.14 Results of Regression Analysis H.11

Seed : 2	$W_1 = 1, W_2 = 1, W_3 = 1, W_4 = 1$		$a = 0.06007$
F	1.7953×10^{-10}	$a(\Delta P_c)$	0.0352
δ	1.1997	$a(\varepsilon_{av})$	0.1848
B	0.007977	$a(V_f)$	0.0091
β	0.25028	$a(\theta)$	0.0112

TABLE : H.15 Results of Regression Analysis H.12

Seed : 3	$W_1 = 1, W_2 = 1, W_3 = 1, W_4 = 1$		$a = 0.40652$
F	1.7769×10^{-10}	$a(\Delta P_c)$	0.7071
δ	1.1987	$a(\varepsilon_{av})$	0.1822
B	0.009718	$a(V_f)$	0.3323
β	0.23113	$a(\theta)$	0.4044

TABLE : H.16 **Results of Regression Analysis H.13**

Seed : 4	$W_1 = 1, W_2 = 1, W_3 = 1, W_4 = 1$		$\alpha = 0.06206$
F	1.7784×10^{-10}	$\alpha(\Delta P_c)$	0.03467
δ	1.1988	$\alpha(\varepsilon_{av})$	0.1877
B	0.00802	$\alpha(V_f)$	0.0159
β	0.24973	$\alpha(S)$	0.0099

With the exception of regression H.12, all converged directly onto the global minimum. Regression H.12 was terminated prematurely as it had got stuck on a concave region of the objective function.

Appendix I

Results of Regression Analysis on Planar and Tubular Filter Press Filtration Data

A time dependent regression analysis was performed on the planar filtration and Tubular Filter Press experimental data in order to obtain a plant specific characterisation for each.

I.1 PROGRAMME INPUT : REGRESS

The physical properties of the sludge at the temperature of 22 °C for the planar filtration experiments, and 27 °C for the Tubular Filter Press experiments are given in Appendix A. The specifications of the planar filtration apparatus are given in Section 4.5, and for the Tubular Filter Press in Appendix F. The medium resistance for the planar filtration apparatus is as determined in Section 5.5.1, and for the Tubular Filter Press as determined in Section 5.6.2.

I.1.1 Search Specifications

Reflection coefficient (ζ) : 1.3
Boundary approach limit (ϖ) : 5×10^{-20}
Feasible loop exit number (N_f) : 5
Improvement loop exit number (N_i) : 5
Number of complex replacements (N_r) : 1
Number of replacement attempts (N_a) : 15
Percentage local proximity (p_p) : 5
Maximum standard deviation squared (ζ^2) : 1×10^{-8}
Maximum vertex distance (D_m) : 1×10^{-5}

I.1.2 Correlation Data

The correlation data over the initial solids compressive pressure range, obtained from the settling tests, and given by Equation 5.7.b and Equation 5.7.g, is included in the regression analysis.

I.1.3 Explicit Parameter Bounds

Based on the values of the correlation parameters obtained from the C-P cell experiments, realistic explicit parameter bounds were set. Due to the inclusion of correlation data in the low solids compressive pressure range, the value of the parameter p_{si} will be fixed to its minimum value as determined by the implicit constraint given by Equation 3.99.

I.1.3.1 Planar Filtration

TABLE I.1 : Explicit Bounds of Objective Function Variables for Regression Analysis on Planar Filtration Data

Parameter	Minimum	Maximum
F	1×10^{-12}	5×10^{-10}
δ	0.9	1.4
B	0.0005	0.01
β	0.25	0.6
p_{si}	0	100

I.1.3.2 Tubular Filter Press

The explicit parameter bounds for the regression analysis on the Tubular Filter Press data was initially as for Table I.1, however, they were adjusted when the results of preliminary regression analyses converged onto some of the explicit bounds.

TABLE I.2 : Explicit Bounds of Objective Function Variables for Regression Analysis on Tubular Filter Press Filtration Data

Parameter	Minimum	Maximum
F	5×10^{-14}	5×10^{-12}
δ	0.5	1
B	0.0001	0.01
β	0.25	0.5
p_{si}	0	100

I.1.4 Experimental Data

I.1.4.1 Planar Filtration

The experimental data utilised for the regression analysis on the planar filtration data is tabulated in Appendix E. Tests E.3.6 and Test E.4.6 were omitted from the regression analysis, because the filtrate volume profiles indicated slightly different filtration behaviour from the other tests, Test E.2.5 was also excluded since the experimental data was incomplete. Filtrate volume data obtained below 30 seconds was also excluded from the regression analysis.

I.1.4.2 Tubular Filter Press

The experimental data utilised for the regression analysis on the Tubular Filter Press data is tabulated in Appendix F. Test F.1 and Test F.7 were omitted from the regression analysis as they exhibited notably different filtration form all the other experiments.

Filtrate volume data during the variable pressure stage of the Tubular Filter Press was excluded from the regression analysis. The programme REGRESS utilises the constant pressure solution procedure to calculate filtration properties with respect to time. As shown in Section 5.8.2, the difference between the calculated filtration properties using the variable pressure solution procedure and the constant pressure solution procedure, was not significant after the initial pressurisation period was over. The use of the constant pressure solution procedure in the regression analysis on filtration data obtained from a plant with an initial variable pressure stage, is therefore not expected to influence the results of the regression analysis significantly, provided filtration data obtained from the initial variable pressure stage of the filtration is not included in the analysis.

The screened average cake dry solids concentrations are included in the regression analysis as they represent the average cake solids concentration of the recovered cake, if drainage on the conveyor belt had been ideal. It would not be possible to obtain an accurate plant specific characterisation if the unscreened average cake dry solids concentrations are used, since the effects of inadequate drainage on the unscreened average cake dry solids concentrations, is variable and extreme. The cake thicknesses for the time dependent analysis are calculated from the filtrate volume and the average cake dry solids concentration.

I.1.5 Calculation Parameters

Numerical integration steps : 150

Cake increment thickness : 0.0001 m

Convergence criterion : 1 Pa

I.2 RESULTS OF REGRESSION ANALYSIS

I.2.1 Planar Filtration

TABLE : I.3 Results of Regression Analysis I.1

Seed : 1	$W_1 = 0, W_2 = 0, W_3 = 1, W_4 = 1$		$a = 5.2732$
F	1.8966×10^{-10}	$a(\Delta P_c)$	-
δ	1.3056	$a(\varepsilon_{av})$	-
B	0.004855	$a(V_f)$	5.8291
β	0.36616	$a(\theta)$	4.7173

TABLE : I.4 Results of Regression Analysis I.2

Seed : 2	$W_1 = 0, W_2 = 0, W_3 = 1, W_4 = 1$		$a = 5.2833$
F	2.1326×10^{-10}	$a(\Delta P_c)$	-
δ	1.3196	$a(\varepsilon_{av})$	-
B	0.005043	$a(V_f)$	5.9023
β	0.36365	$a(\theta)$	4.6642

TABLE : I.5 Results of Regression Analysis I.3

Seed : 3	$W_1 = 0, W_2 = 0, W_3 = 1, W_4 = 1$		$a = 5.2614$
F	1.8411×10^{-10}	$a(\Delta P_c)$	-
δ	1.3024	$a(\varepsilon_{av})$	-
B	0.005631	$a(V_f)$	5.8961
β	0.34948	$a(\theta)$	4.6268

I.2.2 Tubular Filter Press

TABLE : I.6 Results of Regression Analysis I.4

Seed : 1	$W_1 = 0, W_2 = 0, W_3 = 1, W_4 = 1$		$a = 5.3074$
F	3.1649×10^{-13}	$a(\Delta P_c)$	-
δ	0.6471	$a(\varepsilon_{av})$	-
B	0.001586	$a(V_f)$	3.6075
β	0.3972	$a(\theta)$	7.0072

TABLE : I.7 Results of Regression Analysis I.5

Seed : 2	$W_1 = 0, W_2 = 0, W_3 = 1, W_4 = 1$		$a = 5.2654$
F	1.0301×10^{-13}	$a(\Delta P_c)$	-
δ	0.5381	$a(\varepsilon_{av})$	-

B	0.007679	$a(V_f)$	3.6174
β	0.2502	$a(\theta)$	6.9135

TABLE : I.8 Results of Regression Analysis I.6

Seed : 3	$W_1 = 0, W_2 = 0, W_3 = 1, W_4 = 1$		$a = 5.6486$
F	5.6501×10^{-13}	$a(\Delta P_c)$	-
δ	0.7054	$a(\varepsilon_{av})$	-
B	0.000642	$a(V_f)$	3.6199
β	0.4824	$a(\theta)$	7.6772

TABLE : I.9 Results of Regression Analysis I.7

Seed : 4	$W_1 = 0, W_2 = 0, W_3 = 1, W_4 = 1$		$a = 5.1479$
F	1.1226×10^{-13}	$a(\Delta P_c)$	-
δ	0.5455	$a(\varepsilon_{av})$	-
B	0.00318	$a(V_f)$	3.5438
β	0.3285	$a(\theta)$	6.752

pressure and the mass of dry cake deposited. The mass of dry cake deposited is in turn dependent on the filtration pressure, feed solids concentration and the filtration time. The recovery function could then be modelled on these three parameters.

Some work was done in this regard, but was abandoned when the empirical expressions got too complex to be of practical use. The recovery mechanism will be strongly dependent on the physical design of the filtration plant with regard to how the cake is removed and conveyed from the tubes. It is therefore unlikely that a general empirical correlation will be applicable to all plants.

The development of an accurate Recovery function is important since it will enable stable operating regimes to be located and the productivity of the plant to be optimised.

3.8 MODEL IMPLEMENTATION

The relationships detailed in this chapter were incorporated into two Visual C++ programs, COMPRESS and REGRESS. The program COMPRESS implements the predictive solution procedure, and simulates plant performance with given model parameters. The program REGRESS implements the regressive solution procedure, and allows for the estimation of model parameters from measured plant data. The algorithms used by these programs are summarized in the following flowcharts, and are, in outline, the same for the planar and cylindrical cases.

3.8.1 Predictive Solution Procedure (COMPRESS)

Inputs

Operational Parameters: P_o, s_f

Physical Parameters: m_f, r_f, r_s

Plant Parameters: R_m, A (planar) or r_i, l (internal cylindrical)

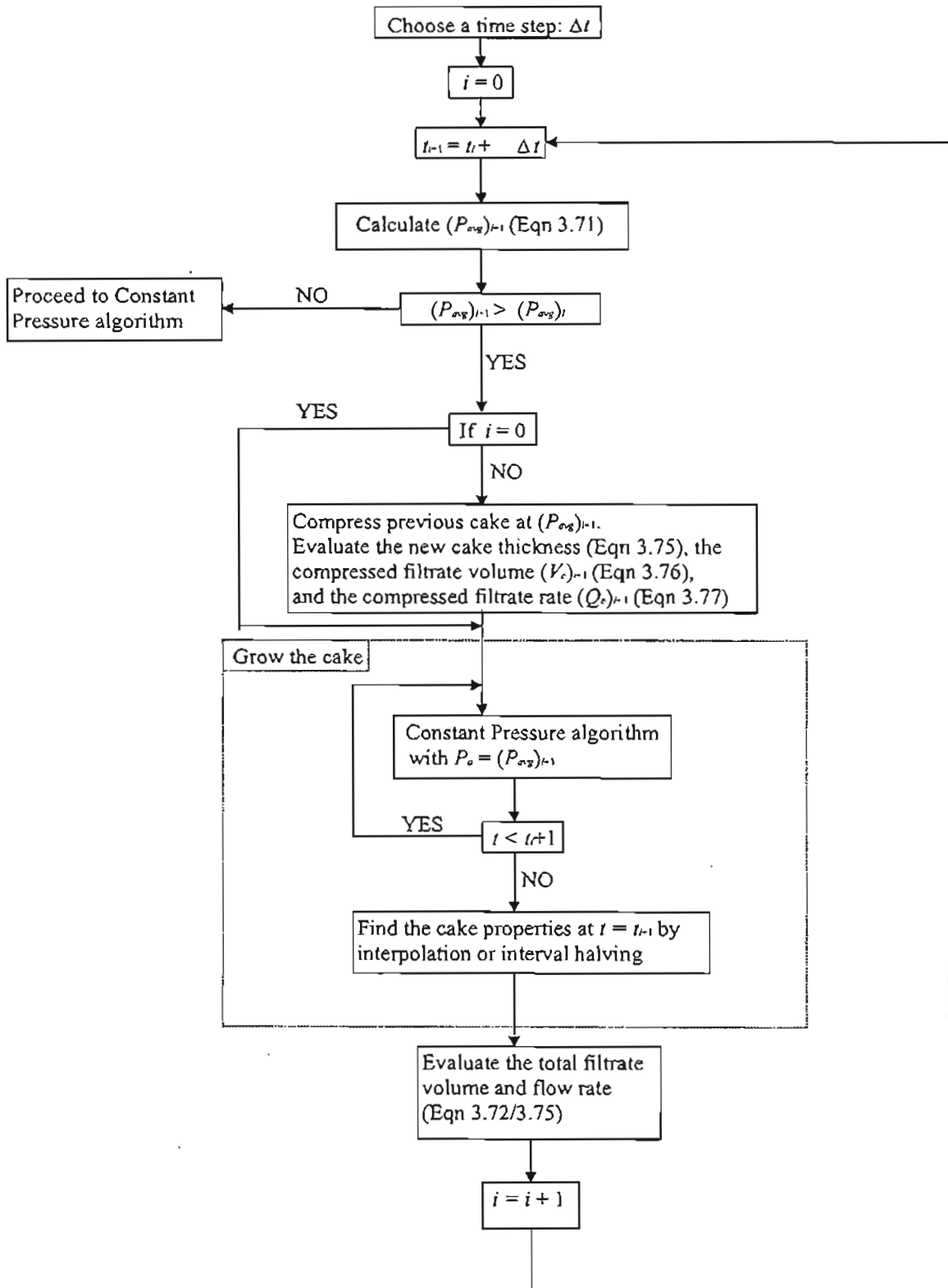
Correlation Parameters: F, d, B, b and A_o, p_{sa} (area contact model)

Outputs

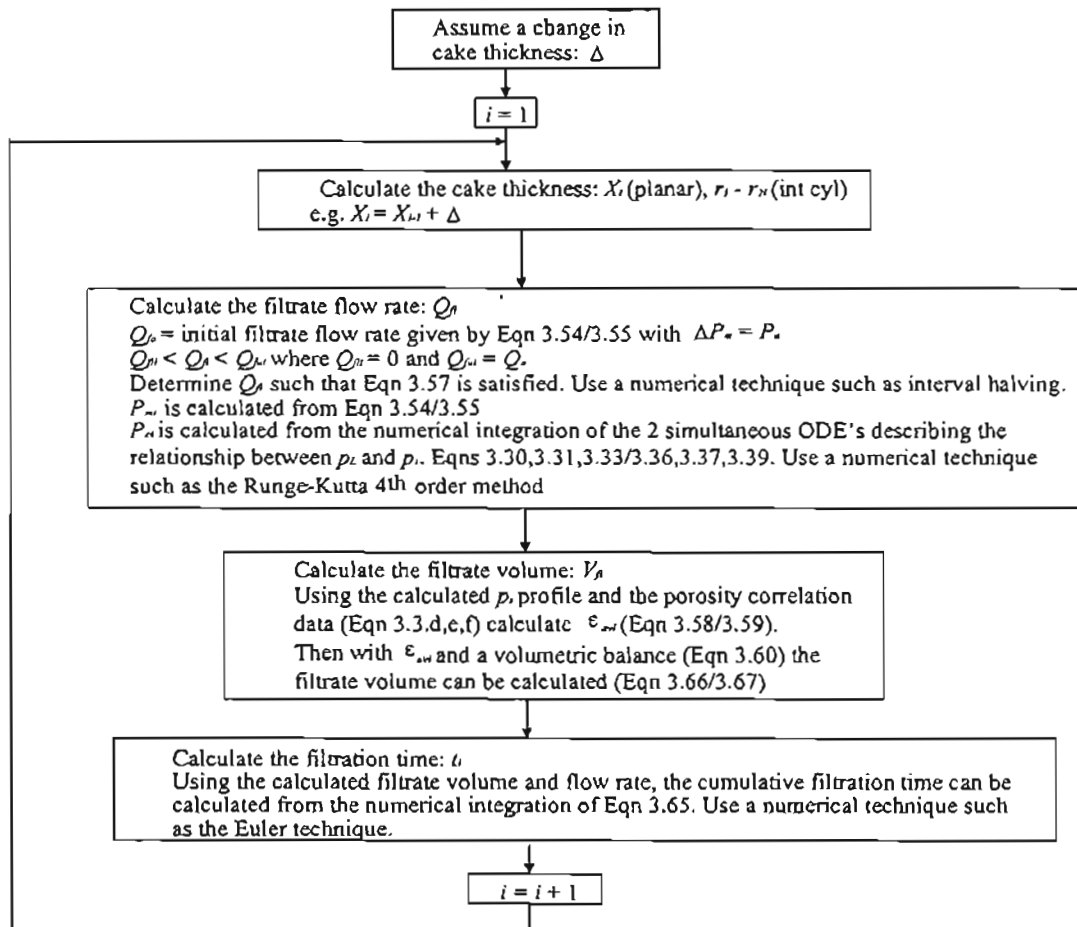
As functions of filtration time:

Q_f, V_f , cake thickness, cake pressure drop, average cake porosity, p_s and p_L profiles

Pseudo Variable Pressure Algorithm



Constant Pressure Algorithm



3.8.2 Regression Procedure (REGRESS)

Inputs

For each experimental point:

Operational Parameters: P_o, s_f

Physical Parameters: m_f, r_f, r_s

Plant Parameters: R_m, A (planar) or r_l, l (internal cylindrical)

Experimental Data: $(Q_f)_{final}, V_f$ versus t , final average cake porosity

Outputs

Correlation Parameters: F, d, B, b and A_o, p_{sa} (area contact model)

For the regressive solution procedure the principle component of the solution algorithm is the direct search technique: the modified complex method, for which a flow chart describing the solution algorithm is given in (Figure 3.7). Within this algorithm, is the calculation of the objective function (Eqn 3.87). The time dependent component (Eqn 3.87.d,e) uses the algorithm for the constant pressure solution procedure (given above) using the assumed set of correlation parameters as determined by the complex method and the specific plant, physical, operational and experimental data for each filtration run included in the analysis. The time

independent component of the objective function (Eqn 3.87.b,c) uses portions of the constant pressure solution algorithm to determine the instantaneous filtration properties. The inputs and outputs for these steps have been discussed in the relevant sections.

Filter Press, namely, tube blockages during the filtration stage, and low cake recoveries during the cleaning stage. The work however, was not applied to a full-scale plant.

In the light of difficulties experienced on the prototype unit, in order to produce a marketable product and obtain effective technology transfer, a full-scale pilot plant was needed for experimental and developmental purposes. The weaknesses that were identified in the design of the prototype unit at H.D. Hill were addressed in the design of the new pilot plant (Pryor and Mullan, 1998). The most significant difference in the new design, was a vertically mounted tube curtain, with tubes of shorter length and larger internal diameter, in order to reduce the potential for tube blockages and to assist in the cake recovery. The pilot plant was built at the Umgeni Water Wiggins Water Works in Durban, and was used to treat the combined sludge from the clarifiers and sand filter backwash. The pilot plant was commissioned in September 1995, and the technology demonstrated at the International Water Supply Association Conference. The performance of new design was also assessed (Pryor and Mullan, 1998). Tube blockages were completely eliminated in the new design, and the performance of the filter was found to be reasonable, producing cake concentrations of 20 to 32 % solids (m/m), and cake recoveries of up to 75 %. It remains to be demonstrated that the pilot-plant can be operated on a continuous basis, and effectively controlled and optimised.

1.2 PROJECT OBJECTIVE

An impediment to the exploitation and commercialisation of the Tubular Filter Press technology, is the lack of a suitable design procedure. The key mechanisms of the process have been identified (Rencken, 1992), however, due to the complexity of the mathematical model, and the rigorous numerical calculations required by the solution procedure, the filtration model has been essentially inaccessible. The filtration model must be therefore be presented in a format so that it can be easily utilised in the development of a suitable design procedure, and so that control and optimisation strategies can be developed for the continuous operation of the Tubular Filter Press, and other constant pressure compressible cake filtration applications.

Rencken (1992), documents standard laboratory characterisation techniques required to obtain the empirical parameters necessary for the filtration model. Although these tests are standard, they still require specialised equipment, are difficult to perform, lengthy, and often prone to failure. In addition, there is doubt as to the accuracy and applicability of characterisations obtained from the non-filtration standard laboratory techniques. A more immediate, reliable and accurate method for determining the empirical parameters is therefore essential to complement the design procedure, and assist in the control and optimisation of the Tubular Filter Press, particularly if the quality of the feed sludge is variable.

The objectives of this project were to :

- Extend or improve upon the constant pressure compressible cake filtration model, predictive solution procedure, and standard laboratory characterisation techniques required to obtain the empirical model parameters, presented in Rencken (1992).
- Incorporate the constant pressure compressible cake filtration model and the associated predictive solution procedure into a user-friendly computer programme that will facilitate the design and optimisation of full-scale plants.
- Develop a regressive solution procedure, and incorporate this procedure into a user-friendly computer programme, that will enable the empirical model parameters, normally obtained from standard laboratory-scale tests, to be obtained from actual filtration data.

1.3 THESIS OUTLINE

The project is introduced in **Chapter 1**, and the objectives for the project are defined. The main findings of the literature survey conducted on constant pressure compressible cake filtration, are summarised in **Chapter 2**. The mathematical filtration model and associated solution procedures are developed, and the experimental theory for constant pressure compressible cake filtration is presented, in **Chapter 3**, along with the relevant literature, which discussed in more detail. The experimental equipment and techniques for the study of compressible cake filtration are detailed in **Chapter 4**. The results of the experimental study are presented and discussed in **Chapter 5**, and the mathematical filtration model and associated solution procedures are evaluated. Conclusions and recommendations are presented in **Chapter 6**.